UNIVERSIDADE DE LISBOA

FACULDADE DE CIÊNCIAS

DEPARTAMENTO DE GEOLOGIA

NEOTECTONICS OF THE SOUTHWEST PORTUGAL MAINLAND: IMPLICATIONS ON THE REGIONAL SEISMIC HAZARD

Paula Cristina dos Santos Marques de Figueiredo

Doutoramento em Geologia
Especialidade em Geodinâmica Interna

2015

UNIVERSIDADE DE LISBOA
FACULDADE DE CIÊNCIAS
DEPARTAMENTO DE GEOLOGIA

NEOTECTONICS OF THE SOUTHWEST PORTUGAL MAINLAND: IMPLICATIONS ON THE REGIONAL SEISMIC HAZARD

Paula Cristina dos Santos Marques de Figueiredo

Tese co-orientada pelo Prof. Doutor João Manuel Lopes Cardoso Cabral (FCUL) e co-orientada pelo Prof. Doutor Thomas K. Rockwell (San Diego Sate University), especialmente elaborada para a obtenção do grau de doutor em Geologia, Especialidade em Geodinâmica Interna

2015

This dissertation should be cited as: Figueiredo, P.M. (2015). Neotectonics of the Southwest Portugal, Mainland: Implications on the regional seismic hazard. Doctoral Dissertation, University of Lisbon, Portugal.

Contents

* Marked annexes are only available in digital version

Acknowledgments

In the first place I would like to acknowledge the financial support that allowed me to conduct this dissertation:

- through the attribution of a Doctoral scholarship from the Fundação para a Ciência e Tecnologia *(SFRH/BD/36892/2007);*

- through the *Research Project "Paleoseismological study of active faults in Mainland Portugal" (PTDC/CTE-GIN/66283/2006), co-financed by FEDER*, that partially supported field studies and Research Project "*Fault Activity and Seismicity Triggered by Ocean Loading in West Iberia*" (PTDC/GEO-GEO/2860/2012) that has supported research during the final stage of this thesis.

Secondly I would like to express my gratitude to my supervisors, Prof. João Cabral and Prof. Thomas Rockwell. Without your guidance and support, this work would not have reached a final stage.

Thirdly, a great number of people contributed somehow for this work:

- to Dr. Ruben Dias, I am grateful for the access to digital topography, aerial photographs and relevant information concerning the field area;
- to Prof. Dr. Fernando Marques, I thank access to aerial photographs, orthophotomaps, digital topography and relevant information concerning the coastal area;
- to Prof. Dr. Pedro Proença e Cunha, I acknowledge the access to the Sedimentology laboratory at Coimbra University, where I pre-processed samples for Optical Stimulated Luminescence dating. I also thank Pedro for processing the same samples in Rizo Laboratory;
- to Prof. Dr. António Martins, I am grateful for his effort and support to accelerate the processing of my samples at the Rizo Laboratory;
- to Prof. Dr. Dylan Rood, I am grateful for the fast processing of the samples for Cosmogenic Nuclide dating, providing access to the results and encouragements;
- to Prof. Dr. Carlos Antunes, the I acknowledge the lend of DGPS –RTK equipment, that allowed me to conduct precise field surveys, fundamental to Chapter 2;
- to Prof. Dr. Maria Conceição Neves, the learning and the support related with the ocean loading effects modeling;
- to Dr. Hector Perea, the multiple discussions about the observations I collected through the years, the suggestions, and the friendship;
- to Ana Nobre Silva, I thank the constant help with the ArcGIS software, and MatLab explanations;
- to Rita Matildes, I am grateful for constant support with the ArcGIS software, specially the innumerous times I need to change "projections systems";

- to Alexandra Oliveira, I acknowledge the access to geological maps, digital topography, numerous papers and documents and the constant support in multiple occasions, the encouragement but especially when ArcGIS was not collaborative enough!
- to Dr. Cristina Lira, I thank the support with MatLab software, namely the codes developed that greatly improved my research during the last stage. I also thank Cristina for teaching me more efficient ways to process data in the ArcGIS;
- to Disepla group, namely through Mónica Ribeiro, the access to their facilities that allowed me to conclude Chapter 4;
- to my San Diego State University colleagues, *i.e.*, the "Rockwell students" for helping me with all the new things and concepts I was not familiar with and for making me feel I was at home. Rebecca Tsang deserves a special acknowledgment for being always so supportive and for sheltering me, each time I needed. Rebecca, you are a great friend!

Special thanks are due and should be highlighted.

To Tom Rockwell and his family, Kim and Morgan (and Gobi), thank you so much for receive me in your home, for including me in your family and for doing all you could to make my stays at San Diego always a pleasure. Tom, you were much more than a supervisor, you are a friend and I owe you and Kim a lot!

To my parents in law, Helena and Jorge, I am gratefull not only for the constant support but also the free access to their home at Lagos, which at a certain point was my main home. Without this home, I wouldn't have conducted the huge amount of field surveys I did, neither to undertake field campaigns involving Lisbon University staff! Thank you so much!

To my parents, Fernanda and Jaime but especially to my father Jaime, for their constant support and motivation, and for their financial support during a large period of this dissertation, when there was not any funding available. I couldn't have made it without you; you are my strength and my support, you are my "foundation stone"!!

To my close family, my four four-legged family, Té, Ki, Bruxa and Duna…. thank you so much for forcing me to take some breaks. For not stopping playing with me, for forcing me to have always room for you by my desk…literally!!! I am grateful for all of you always reminding me the real important things in life.

Finally, but not the least, my special and enormous thank you to my husband, André that has endured my absences, my hassles, my regrets, my despair…. withstood through all the rough moments. I cannot explain with words how much I am grateful to you, how much I am aware that our life was "suspended"… I love you, you are the best person I've met in my life and this should be a conclusion I should add to this dissertation, because you taught me that during this time!

Resumo

A presente tese de doutoramento tem por objectivo o reconhecimento das estruturas neotectónicas presente no Sudoeste Português continental e a sua caracterização sismotectónica de modo a que o conhecimento sismogenético da zona seja mais aprofundado e, consequentemente, a avaliação da perigosidade sísmica para esta zona seja melhorada. Para tal, foi dado particular ênfase na identificação das deformações ocorridas durante o Plistocénico e o Holocénico, e na quantificação das mesmas, de modo a compreender os ciclos de deformação associados às estruturas que evidenciaram actividade sísmica para este período temporal.

Trabalhos anteriores levaram ao reconhecimento de estruturas sismogénicas activas para esta zona, particularmente na região emersa, com actividade reconhecida para o período Pliocénico terminal – Quaternário, embora não tenham sido reconhecidas evidências de sismicidade recente, directamente associadas às estruturas reconhecidas. Do mesmo modo, estudos desenvolvidos durante as últimas 2 décadas, levaram ao reconhecimento de inúmeras estruturas sismogénicas activas localizadas na região imersa, ao largo da Margem Sudoeste Continental. Ambos os reconhecimentos, de estruturas activas na região emersa e imersa próxima, bem como os dados de sismicidade instrumental, sugerem a existência de uma estrutura regional complexa, que se deverá ter desenvolvido a partir do Miocénico terminal, mas cuja componente Plistocénica se encontra pouco caraterizada.

A relação desta estrutura regional com a deformação topográfica regional não se encontrava detalhadamente caracterizada, nomeadamente em relação aos movimentos verticais crustais, que embora estimados não tinham sido reconhecidos para o Plistocénico.

Deste modo, os trabalhos que conduziram à elaboração desta dissertação, tiveram duas linhas principais de investigação que no entanto, se complementaram: uma referente ao estudo e caracterização dos movimentos verticais crustais ocorridos durante o Plistocénico e o Holocénico e outra referente à identificação dos segmentos activos das estruturas sismogénicas presentes na zona de estudo, sua caracterização e quantificação da deformação ocorrida durante o Plistocénico e o Holocénico.

Numa fase inicial de reconhecimento e estudo geral sobre a área relativa ao Sudoeste Português, as várias estruturas previamente reconhecidas e consideradas sismogénicas foram analisadas, não tendo no entanto sido possível reconhecer para todas elas deformação ocorrida no Plio-Plistocénico, quer através de estudos geomorfológicos, quer através de observações directas do traço da falha e de sedimentos deformados. Esta falta de informação sobre deformação quaternária não implica que as estruturas previamente consideradas

sismogénicas não se encontrem activas, mas que os dados existentes não nos permitiram proceder a estudos mais detalhados, que consistem o âmbito principal deste trabalho.

Para proceder aos estudos de movimentação vertical regional, foram consideradas superfícies geomorfológicas talhadas pela acção abrasiva do mar, isto é, plataformas de abrasão marinhas e terraços marinhos, o que nos permitiria assegurar uma informação altimétrica para a génese destes elementos morfológicos. A falta de informação sobre as idades absolutas destas superfícies, bem como a ausência de sedimentos a elas geneticamente associados e a dificuldade na aplicação bem sucedida de métodos geocronológicos que permitissem a obtenção de idades absolutas, levaram a que as superfícies morfológicas fossem objecto de estudo principal, isto é, os terraços marinhos, gerados durante os interglaciários Plistocénicos mais recentes, nomeadamente durante o Estádio Isotópico Marinho (EIM) 5e, que expectavelmente estarão a cotas altimétricas actuais, mais baixas e cuja identificação e relação com as curvas eustáticas do nível médio do mar existentes poderá ser estabelecida de uma forma mais correcta.

Assim, os trabalhos centraram-se principalmente na caraterização detalhada sobre o sistema de falhas São Teotónio – Aljezur – Sinceira eno reconhecimento de terraços marinhos plistocénicos tardio, ao longo de cerca de 140 km de sector litoral: ao longo da costa ocidental a sul do cabo de Sines e ao longo do sector ocidental do barlavento algarvio, desde Sagres até aproximadamente ao Carvoeiro.

No âmbito deste trabalho foram assim caracterizadas várias morfologias pertencentes a terraços marinhos, a maioria das quais não tinha sido referenciada nem descrita em trabalhos anteriores. O reconhecimento de morfologias aplanadas ao longo da faixa litoral, de elementos morfológicos erosivos tais como entalhes basais e cavernas em substracto rochoso, e a presença e associação a estes elementos de sedimentos caracteríscos de ambiente litoral, a diferentes elevações, permitiu inferir que o sector litoral estudado se encontrava em soerguimento tectónico. Foi assim conduzido um levantamento sistemático e caracterização altimétrica detalhada com recurso a DGPS- RTK, deste elementos, para toda a zona de estudo.

A consequente análise destes diversos elementos morfológicos e superfícies aplanadas, que embora existentes em locais diferentes, mas cujas cotas são semelhantes, conduziu à interpretação que para um mesmo nível do mar, as evidências da sua presença, podem variar conforme características hidrodinâmicas locais e com o tipo de substracto rochoso onde estão talhados, tal como sucede para o nível do mar actual. Esta compreensão e comparação com as condições hidrodinâmicas actuais para cada local, permitiu a reconstrução dos terraços marinhos expectáveis para cada local ou na ausência da formação de um terraço, da identificação de marcadores que deveriam existir, em analogia com o actual. Este raciocínio, levou assim à interpretação de alguns dos dados recolhidos como sendo evidências de terraços formados durante o EIM 5, em particular durante 3 picos do nível médio do mar, EIM 5a (aproximadamente 80 mil anos), EIM (aproximadamente 105 mil anos) e EIM 5e (aproximadamente 120 mil anos), tendo este raciocínio sido confirmado numa fase final de redação deste manuscrito com a obtenção da idade de EIM 5c para um dos terraços marinhos estudados.através de datação absoluta por Luminescência Opticamente Estimulada. Com base

no seu posicionamento actual e na posição original conforme estudos noutras áreas de estudo indicam, foi estimada uma taxa de soerguimento tectónica de 0.09 ± 0.001 mm/ano. Esta mesma taxa de soerguimento tectónico é consistente com uma sequência de terraços que continua até cotas mais altas, nomeadamente numa sequência de terraços que é identificável na zona de Sagres, onde uma escadaria de terraços marinhos pode ser seguida desde a cota do mar actual na costa sul até próximo de 130 m de elevação, na zona da plataforma de abrasão regional, muito bem expressada na zona compreendida entre os vértices geodésicos do Mosqueiro e da Torre de Aspa. Um dos terraços pretencente a essa sequência foi estudado e também alvo de datação absoluta (obtida recentemente) através de Nuclídeos Cosmogénicos, indicando de cerca de 2 Milhões de anos, o que corresponde a uma idade mais antiga do que a expectável, e que permitiu estimar uma taxa de soerguimento tectónica na ordem dos 0.04 mm/a, para o início do Plistocénio e provavemente Pliocénico final. Com base nesta idade obtida para um terraço quaternário alto, foi possível calibrar idades para morfologias enquadradas na superfície de abrasão regional, que deverá ser de idade Pliocénica, parcialmente retocada durante a transgressão Plistocénica. Contudo, verifica-se que existe uma variação nas taxas de soerguimento tectónico, em que se regista uma velocidade maior para o Plistocénico mais recente.

Foi igualmente conduzida uma análise morfotectónica sobre as bacias exorreicas que desaguam na costa portuguesa desde o sul da Arrábida, até Vila Real de Santo António, com o objectivo de comparar taxas de movimentação vertical verificadas para o sudoeste português e zonas vizinhas. A análise demonstrou que as taxas de movimentação vertical são superiores para o sector do sudoeste português, sendo inferiores a norte do Cabo de Sines, e a leste da falha de São Marcos – Quarteira. No âmbito desta análise, foi ainda evidenciado que a estrutura São Marcos – Quarteira encontra-se provavelmente activa, e constitui um limite importante na propagação de deformação vertical, que parece ser diferente de ambos os lados desta estrutura.

Para a caracterização do sistema de falhas de São Teotónio – Aljezur – Sinceira, foram efectuados diversos estudos, suportados em reconhecimentos de campo, estudos de geomorfologia detalhada e análises de morfotectónica, de modo a reconhecer os segmentos activos desta estrutura. Embora tenha sido reconhecida deformação ao longo da bacia de São Miguel, para o troço São Teotónio – Odeceixe e ao longo da bacia da Sinceira, a complexidade e dimensão da bacia de Aljezur e a existência de várias estruturas tectónicas bem como de sedimentos potencialmente mais recentes, favoreceu que a generalidade dos estudos para a caracterização do sistema de falhas se tenha centrado na zona de Aljezur-Alfambras. Assim numa fase inicial foram conduzidos estudos de reconhecimento dos traços de falha activa, bem como estudos de prospecção paleosismológica, nomedamente em dois locais ao longo da falha de Aljezur: estes estudos corroboram a presença de uma estrutura activa com componente de desligamento esquerda principal e a migração intra-bacia dos segmentos mais activos da falha, mas não permitiram a individualização de eventos sísmicos que possibilitassem a verificação de um sismo característico para esta estrutura. A localização e confirmação de traços de falha, inferidos pela geomorfologia e não cartografados foi efectuada através de métodos de prospecção geofísica, nomeadamente através de perfis de resistividade eléctrica, que permitiram a definição do prolongamento da falha de Aljezur ao longo da

planície aluvial da Ribeira de Aljezur, o reconhecimento de uma estrutura inferida para o bordo este da mesma planicie aluvial, e a confirmação de uma zona de falha no vale de Framangola. Estudos geomorfológicos ao longo da bacia de Aljezur-Alfambras, permitiram estimar uma taxa de deformação vertical de aproximadamente 0.015 mm/ano para a bacia de Aljezur, durante o Quaternário e uma taxa de deformação horizontal entre 0.09 a 0.16 mm/ano desde 1.5 Ma.

Palavras Chave : *Geomorfologia Tectónica, Terraços Marinhos, Quaternário, Falhas Activas, Sismotectónica, Sudoeste Portugal.*

Abstract

The following doctoral thesis aim is to improve the knowledge on the neotectonic structures present in the southwest Portugal and its characterization seismogenic, so that the assessment of the seismic hazard for this area is improved. As such, a particular emphasis was given towards the recognition of the Plio-Pleistocene deformation and their quantification, in order to understand the seismic cycles associated with the structures that evidenced seismic activity within this time period.

Previous works led to the identification of seismogenic structures for this area, with known activity for the late Plio– Quaternary particularly in the emerged region, although evidences of paleoseismological or historical seismicity directly associated with those structures were not found. Studies developed during the last 2 decades led to the identification of multiple active seismogenic structures located in the off-shore region, along the Southwest Continental Margin. The recognition of active structures, both emerged and submerged, as well as instrumental seismicity data, suggests the existence of a complex regional structure that might have been developed since the late Miocene, but its Plio-Pleistocene component is still poorly characterized.

The relation between this regional structure and the topographical deformation was not adequately characterized, particularly regarding to the crustal vertical movements which despite having been estimated were not adequately recognized and quantified for the late Pleistocene.

As such, the research conducted for the elaboration of this thesis, was divided into two main lines that complemented each other: one referring to the study and characterization of the crustal vertical movements occurred during the Plio-Quaternary, and the other referring to the identification of active segments at the seismogenic structures present within the study area, as well as their characterization and quantification of the deformation occurred during the Plio-Pleistocene.

In an early stage of this research, faults considered as seismogenic in the Southwest of Portugal were surveyed and analyzed in order to identity clear evidence of Plio-Pleistocene activity. However, most of the faults do not evidence a clear Plio- Pleistocene tectonic activity, either through geomorphologic studies or direct observations of the fault trace or deformed sediments. This absence of expression for Plio-Pleistocene tectonic activity does not imply that these faults are not active, but that the available data would not favor a more detailed study, which will constitute the main scope of this work. A fault stood out from all the faults present at the study area, which was the São Teotónio-Aljezur-Sinceira fault system, which exhibits a clear geomorphic expression at the regional, and that reason we have focus our research at this regional structure.

In order to conduct a regional vertical movement study, we have recognized several marine terraces for a coastal sector of circa 140 km length, through a detailed field survey and

thorough coastal morphology analyses based on high resolution digital topography, which has allowed us to identify a sequence from marine terraces, from late Pleistocene to early Pleistocene/ late Pliocene.

Several morphologies belonging to marine terraces were thereby characterized in the scope of this work; most of them had not been yet referenced nor described in previous works. Recognition of flattened surfaces along the coastline, of erosive morphological elements such as notches and sea caves, as well as sediments in association with these elements of coastal environment at different elevations, allowed to confirm that the study region was been uplifted. Thus, a systematic survey, with a DGPS- RTK, was conducted leading to the build-up of detailed elevation characterization for these elements, for all the field area.

Analysis of distinct morphological elements and flattened surfaces, widely present at different locations, but some with similar elevations, led to the interpretation that for the same sea level, distinct morphological elements elevations can vary within a range according to local hydrodynamic characteristics and bedrock lithologies as is the case for the modern sea level, where inner edges elevations fluctuate within an elevation range. This comprehension and comparison with the modern analog enable the recognition of morphological elements that are also recognized in nowadays sea level, when a marine terrace is not been trimmed at the sea level elevation.

As such, this reasoning allowed the recognition of some lower elevation terraces, which were interpreted as formed during MIS 5, particularly for 3 peaks. MIS 5a (approximately 80 ka), MIS 5c (approximately 105 ka) and MIS 5e (approximately 120 ka). Recently, a MIS 5c was confirmed for a terrace through Optically Stimulated Luminescence geochronology, which all together and based upon its current elevation and the original one as indicated by studies at other locations, an uplift rate of 0.09 ± 0.001 mm/a was estimated. This uplift rate is consistent with a sequence of terraces present in the area, namely at Sagres, where a staircase of marine terraces, can be tracked in the south coast from the current shoreline up to circa 130 m of elevation, at the regional abrasion platform, well expressed in the region of the geodesic marks Mosqueiro and Torre de Aspa. Also recently, a higher terrace was sampled and dated through Cosmogenic Nuclide dating, providing an age of circa 2 Ma. This allow us to estimate an uplift rate for the early Pleistocene/late Pliocene of circa 0.04 mm/a. Based upon this uplift rate, ages were calibrated for higher marine terraces, present at the regional abrasion platform, which should be of Pliocene age, partially reoccupied and re-trimmed during the Pleistocene transgression. It should be noted that there is a change of uplift velocities to the more recent times, where uplift rate are higher for the late Pleistocene when compared with the early Pleistocene.

A morpho-tectonic analysis was also conducted on the coastal basins that outflow into the Atlantic, along the Portuguese coast from south Arrábida, to Vila Real de Santo António, aiming to compare rates of vertical motions for the Portuguese southwest and neighboring areas. The analysis showed that the rates of the vertical motions are higher for the Portuguese southwest sector, and comparatively lower to the north of Cabo de Sines, and to the east of São Marcos -Quarteira fault. In the scope of this analysis, a São Marcos -Quarteira fault activity

is highlighted, and it is suggested, that this structure constitutes an important border to the regional vertical motion, which appears to be different on both sides of the structure.

Concerning the characterization of the Teotónio -Aljezur -Sinceira fault system, several studies were conducted, based upon field recognition, geomorphology studies and morpho - tectonic analysis, in order to recognize the active segments of this structure. Although deformation was recognized along the São Miguel basin, for the Teotónio -Odeceixe section and along the Sinceira basin, the complexity and dimension of the Aljezur-Alfambras basin, and the existence of several tectonic structures as well as potentially younger sediments, favored that generally the studies for the characterization of this fault system were centered in the Aljezur-Alfambras basin. Thus, in an initial stage, paleoseismological studies were conducted, namely at two locations along the Aljezur fault, which corroborate the presence of an active left-lateral strike-slip fault strand as well as a internal-basin migration (or propagation) of the most active segments of the fault, but were not sufficient to individualize seismic events, which would enable the characterization of the "characteristic earthquake" for this structure. The localization and confirmation of active fault strands , inferred through geomorphology and not previously mapped was accomplished through geophysical exploration methods, namely through geoelectric resistivity tomography profiles, which enabled the definition of the projection of the Aljezur fault along the Ribeira de Aljezur alluvial plain, the recognition of an inferred structure along the east side of the same alluvial plain, and the confirmation of a fault zone at the Framangola valley. Geomorphological studies along the Aljezur basin enabled to estimate a vertical displacement rate of circa 0.015 mm/year, during Quaternary and a horizontal displacement ranging from 0.09 to 0.16 mm/year, since the last 1.5 Ma.

Keywords: *Tectonic Geomorphology, Marine Terraces, Quaternary, Active Faults, Seismotectonic, Southwest Portugal.*

Chapter 1

General Introduction

1.1 Motivation

Portugal is one of the more earthquake-prone countries in Europe although destructives earthquakes are infrequent. In fact, destructive earthquakes are not as frequent as at other European countries, such as Italy or Greece; however large magnitude historical earthquakes did occur and the largest historical tsunami for the Atlantic Ocean and one of the world largest was generated off-shore Portugal.

The seismogenic structures present in Portugal have sizes capable to generate moderate to large magnitude earthquakes, as has been inferred by historical seismicity and was evidenced by paleoseismological studies at the Vilariça Fault, northeast Portugal, where a few paleo earthquakes larger than Mw 7 were recognized (Rockwell *et al*., 2009).

Two regions with high seismic hazard in Portugal mainland stand out, due to the occurrence of historical seismicity and its social and economic impacts in the Portuguese society,: one corresponding to the Lower Tagus Valley region, where Lisbon, the Portuguese capital, is located and where local and distant earthquakes have generated high intensities each 200 to 250 years. The other high seismic hazard region corresponds to Algarve, the south Portugal region where frequent historic earthquakes were felt. With the implementation of a national seismograph network start during early XX century, the instrumental seismicity starts to be recorded corroborating the predominance of seismicity occurrence for the Algarve region, along the onshore and also along the offshore.

Despite this consciousness of an earthquake susceptibility, which is rooted into the Portuguese people knowledge, little is known about which faults have been responsible for the historical seismicity or even about the faults behavior.

It has been defined that the neotectonic activity in Portugal mainland refers to the tectonic activity that occurred during the Quaternary, i.e., after the Piacenzian, approximately for the last 2.6 Ma (Cabral, 1995; Cabral, 2012). The selection of this period of time was defined considering that after intense Alpine orogeny phases during the Miocene it followed a relative quiet tectonic stage during the Pliocene, which ceased probably in the late Pliocene, when tectonic activity evidences restarted (Cabral, 1995 and references therein, p.25).

The definition of this period of time to define Neotectonics in Portugal is not directly supported on information about regional stress field modifications, but rather considering regional evidences of changes since late Pliocene on the type of sediments for some areas and in geomorphology, namely an increase of drainage incision, probably as consequence of a late Pliocene setting of an Atlantic exorheic system.

Previous studies have identified tectonic structures which evidence Pliocene-Pleistocene deformation along onshore Southwest Portugal (Cabral, 1995; Dias, 2001), but in those studies, no paleoseismic events were ever identified along the active structures or a detailed quaternary deformation analysis was ever conducted for the region. In this way it has not been possible so far to investigate fluctuations or variations of regional deformation rates through time and space, which would enable an analysis of how regional stress could have been accommodated and released, and eventually investigate possible active structure interactions.

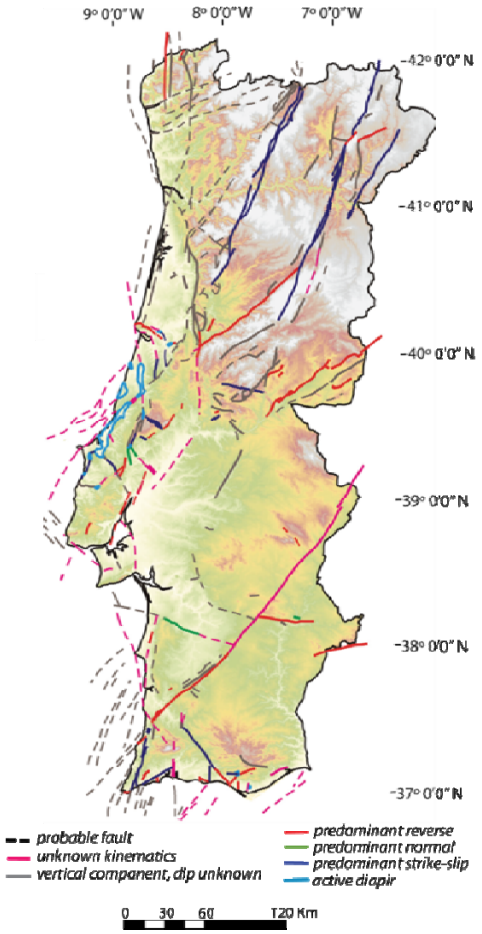

Figure 1.1 – Main neotectonic structures overlapping hypsometric map of Portugal Mainland. Adapted from Cabral (2012).

These analyses although not fundamental to elaborate a seismic hazard map for the region, are a strong complement for the understanding of seismogenic structures behavior and consequently contribute to further understanding of the seismic cycles and characteristic earthquakes for this region.

At the neighboring oceanic area, the Southwest Iberia offshore region, several structures with Plio-Pleistocene deformation were recognized (Bartolomé *et al*., 2012; Gràcia *et al*., 2003; Gutsher *et al*., 2012; Terrinha *et al*., 2003, 2009; Zitellini *et al*., 2001, 2004, 2009) and interpreted as capable of generating moderate to infrequent but large magnitude seismicity, such as the 1755 Mw > 8 (Abe, 1979; Baptista et al. 1998; Johnston, 1996) or the 1969 7.8 Mw (Fukao, 1973) earthquakes.

Those structures were recognized during several campaigns aiming to investigate the plate boundary between Eurasia and Nubia along the Gulf of Cadiz region: the observations corroborated the existence of a complex plate boundary, recognizing several active structures with dimensions suitable for the generation of large magnitude earthquakes and possible tsunami generation and confirming their significance for the regional seismic hazard. The relevance of these studies has been reinforced by the recent worldwide occurrence of very large earthquakes on subduction zones, with generation of large tsunamis, both causing large economical and social impact, as the Indian Ocean, 2004, and the Tohoku, 2011, events.

The 1755 Mw > 8 and the 1969 7.8 Mw earthquakes are the more significant seismic events for the study region having been generated along offshore structures, which is also where instrumental seismicity is better expressed. However, the known active structures located in the onshore region also pose a significant seismic hazard for the local population, despite their smaller dimensions. No record of historical earthquakes with surface rupture or evidence of Holocene deformation was ever recognized for any of them, which could also probably indicate long seismic cycles. Some of these structures are inferred to extend towards the offshore though the degree of activity for these fault strands is less understood. The probable offshore extension of the active faults should be better accessed, not only because it may signify an increase on the size of the rupture area during an earthquake, but also because it diminishes the proximity to larger structures located in the offshore which could be a factor for fault stress interaction. The characterization of these extensions was not conducted in this thesis, although efforts were made to recognize Plio-Pleistocene deformation along the coastal sector where these structures should cross. For some regional analysis, namely for the estimation of the maximum earthquake magnitudes based on the faults segments length, these extensions were also considered.

A fundamental input for the characterization of the quaternary deformation is the age of the sediments or of morphological surfaces present in the vicinity of the active structures and therefore likely to be faulted or in any way affected by the faults. Unfortunately, for the region investigated in this thesis, no absolute ages for the quaternary sediments or surfaces were previously known, although ages have been inferred by correlation with older sediments. The lack of absolute ages for the deformed sediments or morphological surfaces increases the error associated to the calculation of deformation rates, as well as it conditions the characterization of how recent the deformation could be. In our opinion, this is a fundamental matter that should be addressed. In the scope of this thesis, efforts were made to estimate and quantify absolute ages for the Quaternary sediments and morphologic surfaces: fundamental constrains for this task are the lack of available sediments at target sampling

sites, selection of the adequate geochronology method according with the inferred age and by last, the funding available.

1.2 Study Area

The area studied in this thesis is located in the southwest region of mainland Portugal which corresponds simultaneously to the southwest of the Iberian Peninsula. This region corresponds to the continental region in the vicinity of the Southwest Iberian Margin and it is the emerged region of mainland Portugal closest to the plate boundary between Eurasia (Iberia) and Nubia.

The selection of the study area was conditioned by the existence of relevant Pliocene-Pleistocene structures and geomorphic features, and of late Pleistocene to Holocene markers that would enable the recognition of tectonic deformation and its characterization. Thus, the structures that were initially considered as potential targets to investigate tectonic activity are the São Teotónio-Aljezur- Sinceira Fault system, the southern segment of the Alentejo-Placencia Fault, the Barão de São João Fault and the Portimão Fault (Fig. 1.2 and 1.6).

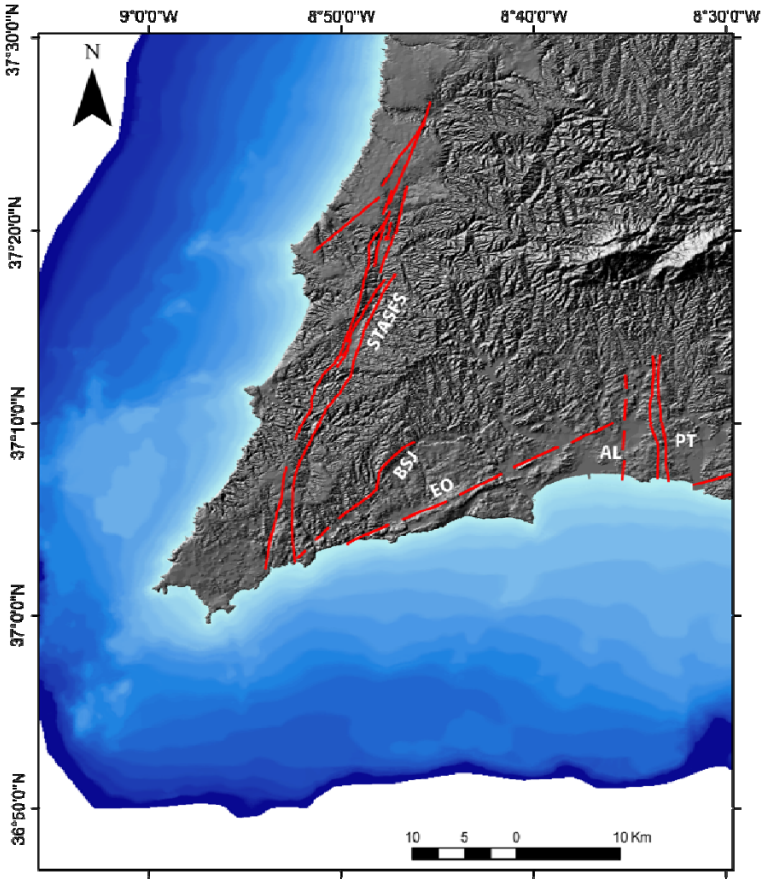

Figure 1.2 - São Teotónio–Aljezur–Sinceira fault system (STASFS) and other main Plio-Pleistocene faults like Barão de São João (BSJ), Espiche-Odiáxere (EO), Alvor (AL) and Portimão (PT) overlapping an ASTER shaded relief DTM. Bathymetric information until 200 m depth also included (adapted from Dias, 2001).

Likewise, the coastal section in this region was also selected as an optimal area to investigate not only the existence of late Pleistocene and older marine terraces, but also to search for vertical deformations of Holocene coastal markers that could be related with historical earthquakes, such as the 1755 or older unknown large magnitude paleo earthquakes.

A target area was thus defined, whose geographic limits are approximately south of parallel 37°30'' North and west of meridian 8° 30'' West (Fig.1.3).

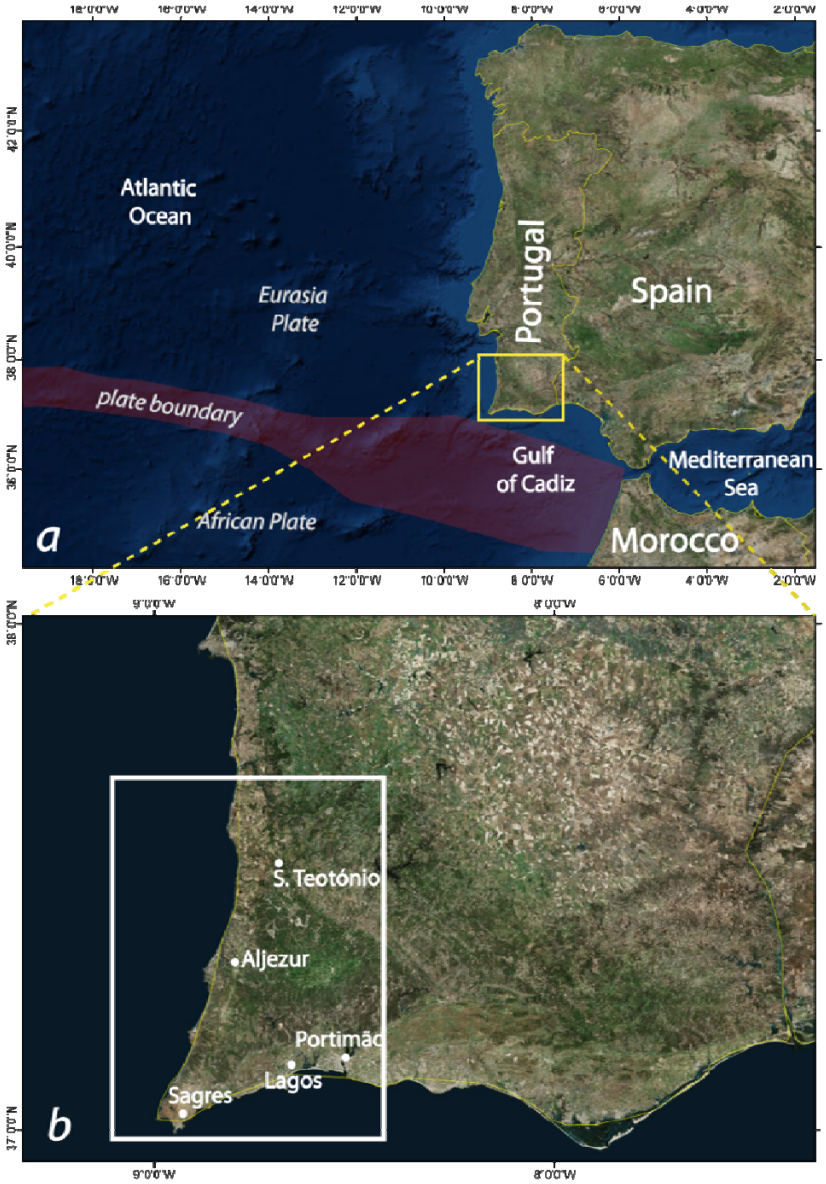

Figure 1.3 – Localization of the study area, highlighted by the white frame in (b). (a) Global setting of the study area, located along the South of Portugal, close to the Eurasia-Nubia plate boundary,: the Atlantic section of the plate boundary is highlighted ; (b) inset of (a) with the geographic limits of the study area, marked by the while frame. Main villages' locations are indicated as well. Images are taken from World Imagery available through ArcGIS (©ESRI) based upon SPOT imagery.

1.2.1 Brief Geological Setting

The selected study area can be roughly divided into two sub-regions according to its geodynamic evolution and geology: a western and northern sub-region, corresponding essentially to the Palaeozoic South Portuguese Zone and a southern sub-region corresponding to the Mesozoic and Cenozoic Algarve basins (Fig. 1.4). A brief geological characterization about these two sub-regions and its evolution is next presented:

Western sub-region

The western sub-region comprises mainly Paleozoic rocks of the South Portuguese Zone of the Hercynian Massif, predominantly formed by Carboniferous continental shelf and oceanic sediments, which were deformed and metamorphosed during the Pangea continent formation. It is composed by several tectono–stratigraphic domains, where Variscan orogeny deformation phases did express differently. The tectono-stratigraphic domains present in the study region are the Southwest Portuguese Sector and the Baixo Alentejo Flysch Group, both exhibiting a lower metamorphism grade. Southwest Portuguese Sector is characterized by metamorphosed siliceous fine sediments, as clayish schists, shales, greywacke and quartzites, and it comprises the Tercenas Formation (late Devonian- early Caboniferous) and the early Carboniferous Carrapateira Group (Quebradas, Murração and Bordalete Formations). The Baixo Alentejo Flysch Group is represented in the study area by the Brejeira Formation which is described as a sequence of turbidites metamorphosed as greywackes and quatzites. In this western sub-region also outcrop remains of a Mesozoic basin, referred to as the "Carrapateira outlier", characterized by basic volcanic rocks, Triassic marls and limestone from the Silves Complex and Jurassic limestone, exhibiting similarities with outcrops in the Telheiro- Sagres area located southward and already belonging to the southern sub-region;

Southern sub-region

- The southern sub-region corresponds mainly to the Algarve Mesozoic and Cenozoic basins. The Mesozoic sedimentary basin infilling is characterized by a few volcanic sedimentary events, sandstones, marls and limestone. It corresponds to one of the western Iberia Mesozoic basins that were generated during the extensional stages that led to the opening of the Atlantic Ocean, west of Iberia, and the opening of the Tethys Sea, to the south. These extensional stages can be differentiated between the western and the southern sub-regions: along the western region the extension was oriented E-W to WNW-ESE, developing N-S to NE-SW faults, while at the southern region an early stage of extension was oriented NW-SE to N-S, developing NE-SW to E-W fragile structures. The oldest units are of Triassic age, characterized by intercalations of volcanic sedimentary units and sandstones, related to early phases of extension. Sedimentation of limestone and marls begins during the Jurassic, with local lithological variability reflecting distinct depositional environments. Starting from the Lower Jurassic (Lias), as a consequence of a continuous Nubia sinistral movement towards Eurasia (with Iberia), which induced a transcurrent and transtensive regime, with lithosphere stretching and the development of pull-apart sub-basins: a western one, to the west of Sinceira structure, a central one, from Budens to Lagoa, characterized by a structural high and

therefore less deep, and an eastern one, from Lagoa eastward to Tavira (Manupella, 1992). At the study area, only the western sub-basin and the shallower basin of Budens-Lagoa are present. During the Jurassic and the Cretaceous, the Algarve basin depocenter gradually moved eastward, promoting ticker units to the east and the absence of the Upper Cretaceous units to the west (Manupella, 1992).

An igneous massif of late Cretaceous age, the Monchique alkaline massif, intrudes the region north of the Algarve basin, and west of the Atlantic coastline. Later, after the development and filling of the Mesozoic basins, starting in the late Cretaceous, the Nubia plate changed the trajectory towards Iberia, from a SW to NE direction in late Cretaceous to a S to N direction during the Paleogene, and induced a rotation of Iberia promoting a change from a transtensive to a compressive regime. This change of tectonic setting lead to the deformation of the Mesozoic sediments and the generation of relief, which also resulted in a sedimentation hiatus between Cretaceous and Paleogene units (Terrinha, 1998; Roque, 2007; Terrinha *et al*., 2013).

Figure 1.4 – Algarve Basin Geological Map. 1-Holocene,2-Pleistocene, 3- Pliocene, 4-Niocene, 5- Paleogene, 6- Cretacic, 7- Jurassic, 8- Triassic/Hetangian, 9- Monchique alkaline complex, 10- Paleozoic, 11- dykes, 12- faults (adapted from Oliveira et al, 1992 in Terrinha et al., 2007)

The Algarve Cenozoic basin is located mostly offshore. Onshore it almost exclusively comprises Neogene sediments which are generally thin, present along all the study area though often in discontinuous outcrops, although better expressed at that area along the southern sub-region, where the units thickness is larger; Miocene marine sediments are present mainly along the southern area, although remains are preserved inside tectonic basins along the western sub-region. Pliocene and Quaternary sediments are also present along all the study area, associated to marine terraces or fluvial systems, as well as forming cemented carbonate aeolianite units. A detailed analysis and descriptive characterization for the study area, focusing on the tectonic stages, their evolution and timing, can be consulted in two

doctoral theses, one focused in the Mesozoic evolution by Terrinha (1998) and another one addressing the Pliocene- Quaternary tectonic activity by Dias (2002).

A brief description was presented and although details have not been presented here, it should be mentioned that the study region at the southwest of Portugal has been subjected through distinct times to the evolution of the plate boundary between Africa and Eurasia, sometimes as part of Nubia, but mostly as part of Eurasia. This favours a regional structural complexity, that is also expressed through the complexity of the nowadays plate boundary section at the Gulf of Cadiz, that reflects the long term interaction between Iberia and Nubia, where structures with different geometries and tectonic styles, mainly thrust and strike-slip, have interacted at different scales through time (Duarte *et al*., 2011). Ribeiro *et al*. (1996) proposed that a change from a passive Atlantic margin to an active one might be already in course, offshore Portugal, to what it was called an incipient subduction process. This theory was further detailed in Ribeiro (2002) and later resumed by Duarte *et al*. (2013) which proposed that the South Iberia Margin, i.e. the continuation of the study region to the offshore, might be favourable for a nucleation cell of a subduction zone, assuming a propagation of the convergence localized along the Gibraltar Arc and the Mediterranean belt towards the Gulf of Cadiz (Fig.1.5).

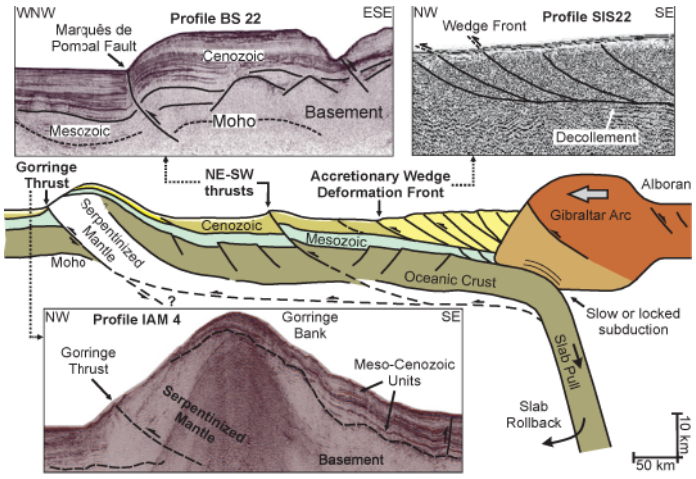

Figure 1.5 – Crustal sections interpretations from the Southwest Iberia Margin and Gibraltar Arc according to Duarte et al., 2013: westward Gibraltar Arc main active structures along the Gulf of Cadiz and Southwest Iberia margin are depicted (adapted from Duarte et al.2013)

Strain in the study area and the Gulf of Cadiz results from WNW-ESE oblique convergence between Iberia and Nubia. at a rate of 4-5 mm/yr (Fernandes *et al.*, 2007, Nocquet *et al*., 2004, Serpelloni *et al.* 2007; Stich *et al*., 2006)This Iberia-Nubia plate convergence corresponds to the plates interaction at the eastern section of Eurasia-Nubia plate boundary in the Atlantic Ocean.

The Eurasia-Nubia plate boundary along the Atlantic Ocean is described by three distinct sections: a western one, from the Mid-Atlantic Ridge eastwards, characterized by a WNW-ESE

transtensional fault zone (the Terceira leaky transform), a central section corresponding to the roughly E-W 400 km-long right-lateral Gloria transform fault (Laughton & Whitmarsh, 1972), and a third eastern section, crossing the Tore Madeira into the Gulf of Cadiz region. In the vicinity of the Gorringe Bank area, the plate boundary evolves from a discrete localised boundary to a more complex and diffuse plate boundary (Sartori *et al*., 1994), where deformation is distributed along a zone a few hundred kilometres in width, through several structures (Fig. 1.6).

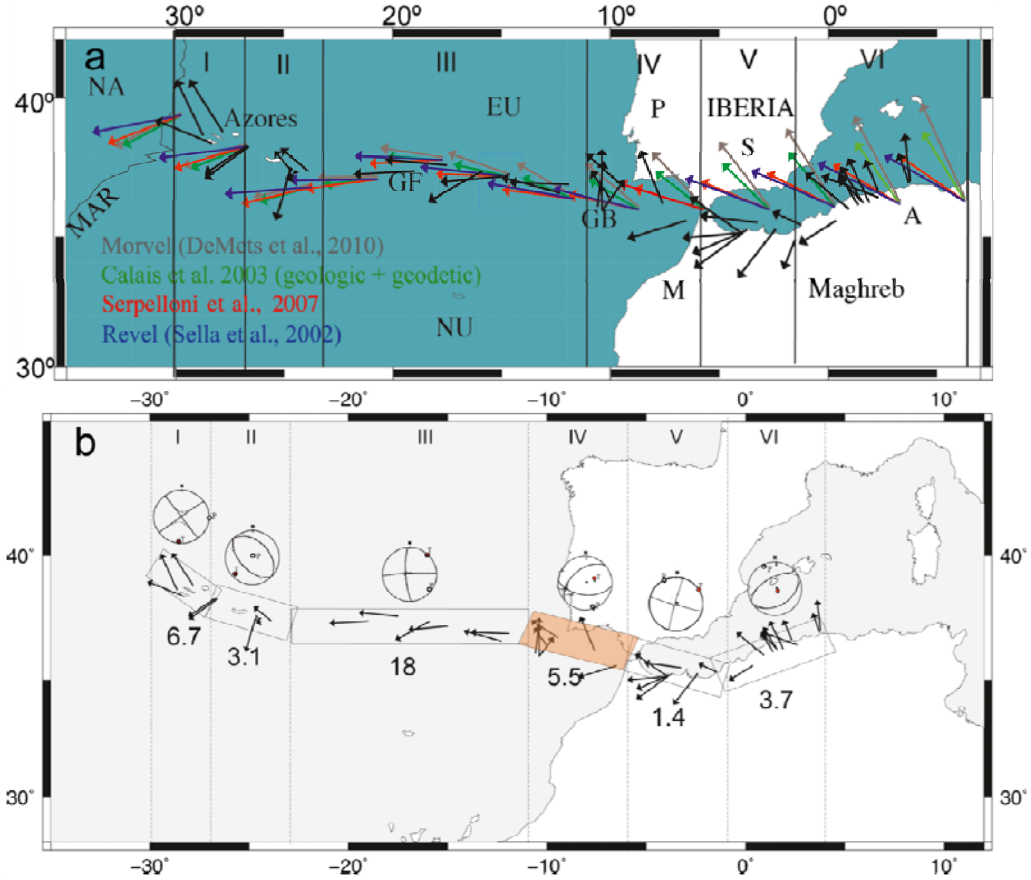

Figure 1.6 –Eurasia-Nubia plate boundary along the Atlantic and western Mediterranean areas: in this figure it is depicted distinct plate boundary sectors, according to Bezzeghoud et al. (2014). (a) Kinematic velocities estimated from several authors in colours grey (De Mets et al., 2010, green (Calais et al., 2003), red (Serpelloni et al., 2007), blue (Sella et al., 2002) and in black slip vectors estimated from seismicity (Bezzeghoud et al., 2014); (b) based upon shallow seismicity data, slip velocities, total seismic moment tensor and horizontal projections of the slip vectors. For the Southwest Iberia Margin and Gulf of Cadiz sector, which is highlighted, the calculated slip velocity is 5.5 mm/yr.

The Iberia-Nubia interaction along the Gulf of Cadiz section is estimated from GPS data as a WNW-ESE convergence at a rate of 4-5 mm/yr, whereas geological models although referring to a similar rate indicate a NW-SE convergence for the last 3 Ma (DeMets *et al*., 1994; 2010).

In order to recognize active structures and seismogenic sources for this area and to better understand the primary tectonic elements of this region of diffuse deformation, several

geophysical, bathymetrical and geological studies were undertaken during the past two decades (Bartolomé *et al*., 2012; Gràcia *et al*., 2003; Gutsher *et al*., 2012; Terrinha *et al*., 2003, 2009; Zitellini *et al*., 2001, 2004, 2009).

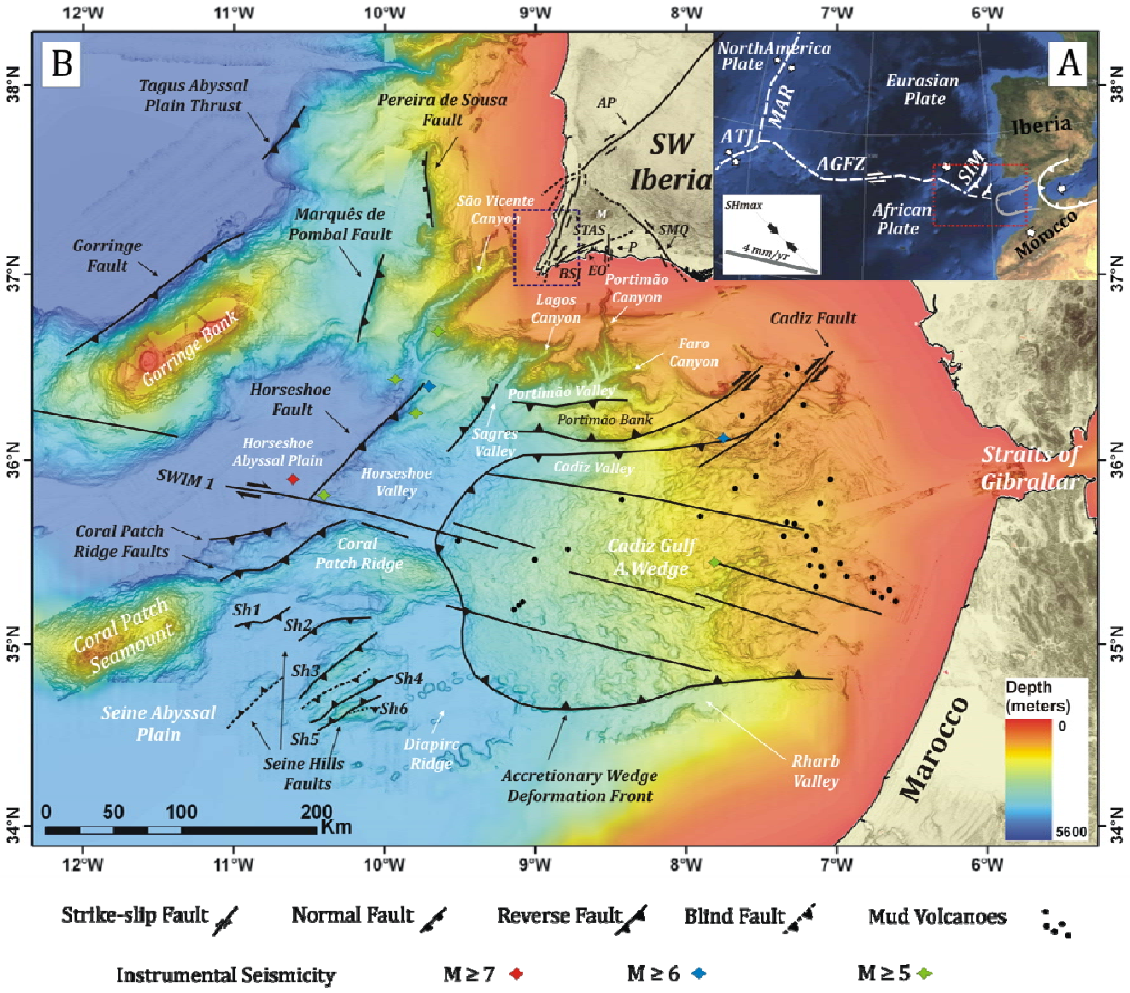

Figure 1.7 – Main active structures and morphological features in the Southwest Iberia region (according to Rosas et al. 2012, and Martínez-Loriente et al. 2013, for the offshore, and Dias, 2001, for the onshore) and their localization regarding the Eurasia – Nubia plate boundary. (A): Schematic Eurasia- Africa Plate boundary for the region and localization of figure 1 MAR - Mid - Atlantic Ridge; ATJ- Azores Triple Junction; AGFZ – Azores Gloria fault zone; SIM – Southwest Iberian Margin (adapted from Duarte et al, 2013); (B) Offshore structures identified in the map; onshore structures : AP – Alentejo- Placencia Fault; STAS – São Teotónio-Aljezur-Sinceira Fault System; BSJ – Barão de São João Fault; EO – Espiche –Odiáxere Fault; P – Portimão Fault; SMQ – São Marcos-Quarteira Fault. The area studied in this work is delimited by the dashed line (adapted from Rosas et al., 2012, in Figueiredo et al, 2013).

These studies led to the recognition of previously unknown relevant submarine active structures, such as the Marquês de Pombal and Horseshoe NNE-SSW to NE-SW thrust faults at the northwest and the Coral Patch Ridge and the Seine Hills thrust faults at the southwest of Gulf of Cadiz, some with significant morphological expression, or as the roughly WNW-ESE SWIM (Southwest Iberia Margin) faults, or even as the E-W trending Portimão Bank faults. Interference between the NNE-SSW to NE-SW thrust system and the WNW- ESE dextral strike-

slip fault system was also identified in this margin (Duarte *et al*., 2011, Rosas *et al*. 2012) (Fig.1.7).

At the onshore region, several faults with evidence of Pliocene and Quaternary activity were previously recognized (Feio, 1951; Pereira, 1990; Cabral, 1995; Dias, 2001), mainly through geomorphologic analyses and evidences of Plio-Pleistocene sediments deformation.

The most relevant of the Pliocene-Pleistocene structures in the study region is the NNE-SSW 50 km long São Teotónio–Aljezur–Sinceira left-lateral fault system (STASFS) (Fig. 1.2). This fault zone extends north towards the southwestern section of the Alentejo-Plasencia fault (Cabral, 1995, Villamor *et al*., 2012), though their spatial and temporal relationships are still not clear from the available data. STASFS trends parallel to the western coast, and presents a geometry which is similar to the main active structures along the Southwest Portuguese margin; simultaneously is also the closest active brittle structure located inland. It has been suggested that the STASFS probably extends southward along the southern continental shelf, through an inferred Jurassic structure (Terrinha, 1998; Lopes, 2002; Roque, 2007; Dias *et al.,* 2010 in ANPC), which would add another possible 50 km to its length. This extension is based upon submarine geomorphology interpretation, instrumental seismicity alignment and post-Miocene (?) deformation evidences recognized at some oil industry seismic lines, but there is no unequivocal evidence to correlate the inland fault system with the morphological features inferred as the fault extension in the offshore, and little characterization for this possible Offshore structure was conducted or its degree of activity accessed.

The STASFS fault zone deforms a regional abrasion platform that is ca. 10 km wide, considered to be originally of late Miocene age, and that has been reoccupied and re-trimmed by the sea during the Pliocene and the early Pleistocene, implying that the capping sediments should be of Pliocene and Pleistocene ages. Dias (2001) estimated a slip-rate of ca. 0.03-0.06 mm/yr for this fault system based on the vertical offset of morphological features, but as slip on this structure is inferred to be primarily strike-slip these values should be a minimum estimate. Plio-Pleistocene geomorphic deformation seems to be more evident along the northern segments of the STASFS, near Aljezur whereas along the southern segments, south of Sinceira basin, there is little evidence for significant Plio-Pleistocene vertical deformation. This could be due to a modification of the fault system, which towards the south splays into several minor faults. In fact, several parallel faults, trending NNE-SSW to N-S do exist in the local Mesozoic limestone bedrock south of Sinceira, along the coastal section (Martinhal–Zavial) where the STASFS should intersect the coastline. These structures seemed to have promoted the development of karst pits, which are filled with Plio-Pleistocene sands (Faro-Quarteira Sands). The spatial distribution and elongated shape of those karst features suggest a structural control by a previous structural fabric on the karst development (Dias & Cabral, 2002).

Other structures with Pliocene-Pleistocene tectonic activity for the study region are the NE-SW Barão de São João, the ENE-WSW Espiche-Odiáxere fault and the N-S Lagos and Alvor structures. However all of these structures do not evidence significant deformation during the

Pleistocene and are considered to have low activity rates, less than 0.1 mm/yr (Dias, 2001) (Fig. 1.2).

Summarizing, the regional complex tectonic framework that resulted from the Variscan and Alpine orogenies structural control can be simplified and described as predominantly organized into three large brittle structures systems:

i) structures with a N-S to NNE-SSW direction;
ii) structures with a NW-SE direction;
iii) Structures with a E-W to WNW-ESE direction;

The structures with a N-S to a NNE-SSW (sometimes NE-SW) direction are present mostly along the western Algarve Basin and at the Hercynian South Portuguese Zone along the western coastline, being the most relevant of them the São Teotónio – Aljezur – Sinceira Fault system and the Portimão Fault: the direction of these structures may reflect a structural heritage from the extensional stages during the early Mesozoic, when several structures with similar direction were generated. These NNE-SSW structures evidence a Quaternary left lateral strike-slip kinematics, with a minor, commonly reverse, vertical motion component; the kinematics for the Portimão fault is not fully understood. In the Offshore, these N-S to NNE-SSW structures are also very well expressed by the Marquês de Pombal and Horseshoe NNE-SSW to NE-SW thrust faults or even the distant Coral Patch Ridge and the Seine Hills thrust faults at the southwest of Gulf of Cadiz.

The NW-SE structures are less frequent and commonly evidence right lateral strike-slip: inland the more expressive of these is the São Marcos-Quarteira fault, which is located about 100 km to the east of the study area. Their Quaternary activity, although recognized, is poorly understood.

Finally, the WNW-ESE ENE to E-W structures are present inland along the western Algarve Basin and despite their geomorphologic expression and visibility in the satellite imagery, they do not evidence a significant Quaternary activity and furthermore seem displaced by N-S to NNE-SSW structures (Dias, 2001). At the Offshore, WNW-ESE to E-W structures are also present as the Portimão Bank thrusts or the important SWIM faults which correspond to a 400 km length dextral strike-slip system that is likely to evidence Late Pleistocene to Holocene activity (Bartolomé *et al*., 2012) and that were interpreted as main structures to accommodate the nowadays plate boundary convergence at this region.

Interference between structures has been interpreted, not only inland, but also in the Offshore between the NNE-SSW to NE-SW thrust systems and the WNW-ESE dextral strike-slip system (Duarte *et al*., 2011, Rosas *et al*. 2012).

1.2.2 Brief Geomorphology Description

The foundations of the regional geomorphology were established decades ago by Mariano Feio (1951) who conducted a large study, predominantly focusing on the morphology and geology of the landscape of Lower Alentejo and Algarve regions, i.e. the Portuguese territory approximately south of parallel 38° N. That study defined the major elements for the landscape of the region, describing them. Later studies were conducted on smaller areas at the

vicinity or along the study area, focusing on parts of Feio's work, like the geomorphologic study of Pereira (1990), or from a geological perspective Cabral (1995), Pimentel (1997), Moura (1998) and Dias (2001). The geomorphic components defined by Feio (1951) in the Southwest Portuguese landscape can be described as:

- An internal peneplain, poorly preserved at the top of interfluves of a rough morphology, which is almost not possible to identify along the study area;
- A western littoral plateau, which consists in a regional flat surface extending from the coastline towards the foothill of internal reliefs, with variable lengths from 5 to 15 km, interpreted as a regional platform of marine genesis;
- The Monchique Igneous Mountain, an inselberg that stands out from the internal peneplain;
- And a southern sector, carved into limestones and sandstones from the Algarve basin, which shares some similarities with the western littoral plateau along its coastal area.

The western littoral plateau, commonly called as the regional "littoral platform" (Pereira, 1990; Cabral, 1995), can be segmented into distinct sectors according to sedimentary differences of overlying deposits, elevation of sea cliffs and surface dip, from the north to the south (Pereira, 1990). This platform has been assumed as older than late Miocene but younger than the Quaternary (Feio. 1951), since Pleistocene marine terraces are interpreted to be cut into it. However, there is no absolute age or fossils known for these sediments or surfaces and consequently its age is an open question: how old and how many times this flat surface have been trimmed. The age of this morphological element, and if it has been re-trimmed through time is a key to understand vertical crustal movements for the region.

South of São Teotónio, the regional plateau is deformed by the São Teotónio-Aljezur-Sinceira Fault system, which generated the development of five small tectonic basins. These tectonic basins are narrow, elongated depressions along this flat surface, and are important morphological elements in the landscape. From the north to the south, these basins are respectively São Miguel, along the Baiona fault segment, Aljezur and Alfambras, along the Nova Castelãs, Aljezur and Alfambras fault segments, and the minor basins of Sinceira and Pedralva, along the Sinceira fault segment. These basins are orientated approximately NNE-SSW to N-S and generally their elevation is in the order of some tens of meters lower than the regional platform. It has not been demonstrated so far that this difference in elevation is exclusively due to tectonic displacement or also to erosion, although the basins are controlled by faults. Also, the timing of this deformation is a matter of debate, since no absolute ages are available either for the sediments present on the platform nor for the sediments located inside the basins; an exception is for Miocene limestones that are preserved in the lower sequences of the Aljezur and Alfambras basins.

The Monchique Igneous Mountain, that reaches elevations of 900 m, is surrounded by remains of an older erosion surface, ranging from circa 300 to 400 m elevation probably of upper Miocene-lower Pliocene (?) age ranging from and, towards the coastline, the morphology presents a staircase of surfaces lower than 300 to 250 m that probably correspond to marine terraces of Pliocene age, poorly preserved and highly dissected.

Along the southern sector of the study area, the landscape shows structural reliefs controlled by the structure of the Mesozoic sedimentary units, such as cuestas. Closer to the coastline there are marine terraces cut into the Mesozoic basement and several types of karst morphologies are widespread, most of them filled with sands from Pliocene to Pleistocene age. These karst forms can be large, and the sediment infilling is frequently deformed as a consequence of the karst development (Dias & Cabral, 2002).

As referred, several Marine terraces, probably from Pleistocene age, have been recognized along the coastal area, cut into the littoral platform or located lower along the seacliffs (Feio, 1949, 1951; Pereira, 1990; Cabral, 1995; Dias, 2001). However, despite some ages were inferred by those authors, there is no absolute age control or any correspondence to Marine Isotope Stages, interglacial or glacial periods was proposed.

1.2.3 Regional Seismicity

1.2.3.1 Instrumental Seismicity

The seismicity in the study region is not easily characterized and it its correlation with the tectonic structures evidencing Plio-Pleistocene deformation is not clear. Most of the regional significant seismicity is located in the Offshore, along the Gulf of Cadiz and Southwest Iberian Margin, as for examples the already referred (> 8 Mw) 1755 earthquake, the 7.8 Mw 1969 even tor the more recent events in 2003 (5.3 Mw), 2007 (5.9 Mw) and 2009 (5.5 Mw) (Custódio et al., 2012; Pro et al., 2013). Very likely other large magnitude historical earthquakes were generated in this offshore region, such as the 382 A.D event (Brito, 1597; Mendonça, 1758). Although there are no records of relevant historical earthquake unequivocally interpreted as generated inland, less frequent and lower magnitude seismicity also occurs onshore.

In the study region the instrumental seismicity can thus be described as being of low to moderate magnitude with a diffuse distribution (Carrilho *et al*., 2004; Carrilho, 2005), make difficult its correlation with the known active tectonic structures, as it will be further discussed. The majority of the regional instrumental seismicity occurs in the Offshore, where it is broadly distributed, rather than being aligned along a discrete plate boundary. Inland, instrumental seismicity also presents a scattered distribution, except for the area of the Monchique Igneous Massif which evidences an anomalous concentration of seismicity. Regional seismicity occurs at depths generally shallower than 40 km, although occurrence of seismicity for the 40-60 km depth interval is also registered (Custódio ., 2012 and references within). For the study area, the occurrence of shallow seismicity, i.e. seismicity with hypocenters located in the first 10 km depth, is less frequent than the remaining seismicity (Fig.1.8). This deeper seismicity altogether with its scattered distribution (which cannot be associated with any tectonic structure or morphological alignment in the surface), and the poorly constrained geometry of the Plio-Pleistocene active structures at depth, contribute for a poor interpretation of the seismic activity and do not favour any correlation with the regional known active tectonic structures nor any evidence of unrecognized active structures.

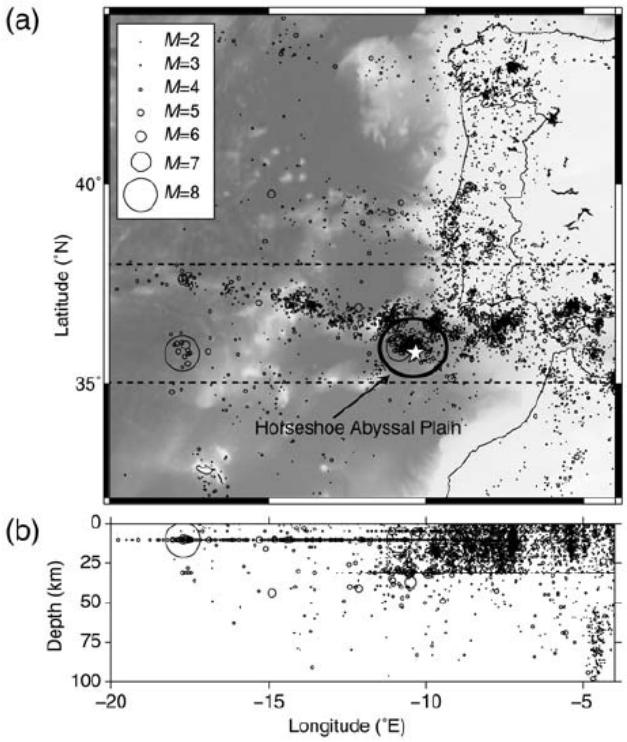

Figure 1.8 – Regional seismicity for the Southwest Iberia and Gulf of Cadiz. The star corresponds to the 2007, Mw 5.9 event. Adapted from Custódio et al. (2012).

An Ocean-Bottom Seismometer (OBS) campaign was undertaken at the northern Gulf of Cadiz, near to the study region, for 11 months (from August 2007 to July 2008), with the goal to characterize seismicity and correlate it with the active structures. Survey results demonstrated that seismicity extends deeper than 40 km, concentrating at 50-55 km depth (Geissler *et al*, 2010). Furthermore, three major clusters of earthquakes were recognized coinciding with the location of the three larger instrumental earthquakes for the region, the 28th February 1969 (Mw~7.9), the 12th February 2007 (Mw 5.9), and the 17th December 2009 (Mw 5.5) events (Silva *et al*., 2010).

Recently, a denser broadband seismic network was installed inland covering all the Portuguese territory in the scope of research project WILAS, carrying out a survey for a period of 2 years from 2010 to 2012 (Custódio *et al*., 2014). One of the main goals was to enable a better location for the events occurred during that period and consequently improving the correlation with the active structures. Unfortunately, for the study area and despite the improvement of the instrumental seismicity localization, the seismicity that occurred during the survey had generally deep hypocenters which did not favour an expected improvement towards a correlation with the known regional active structures (Fig.1.9).

The survey results however corroborated the area with an anomalous concentration of instrumental seismicity located at the cretaceous Igneous Massif of Monchique. This seismicity is characterized by having low magnitude and deeper hypocenters and it has not been directly related with any Pliocene-Pleistocene tectonic structures or geomorphic structural element:

the understanding and interpretation of this seismicity is not clear and has not been conducted in the scope of this thesis.

A small number of focal mechanisms are available for both the onshore and Offshore regions (Fig 1.10); analyses of the focal mechanisms indicate a predominance of thrust and strike-slip faulting, with some normal faulting also present locally in the Offshore (Borges et al., 2001; Bezzeghoud & Borges, 2003; Stich *et al*., 2010 and references within). However, based upon these focal mechanisms there are no clear geographical domains evidencing distinct faulting type, but rather a spatial mixing of variable types of faulting which probably reflects strain adjustments on distinctly trending structures, corroborating the complex tectonic framework of this region.

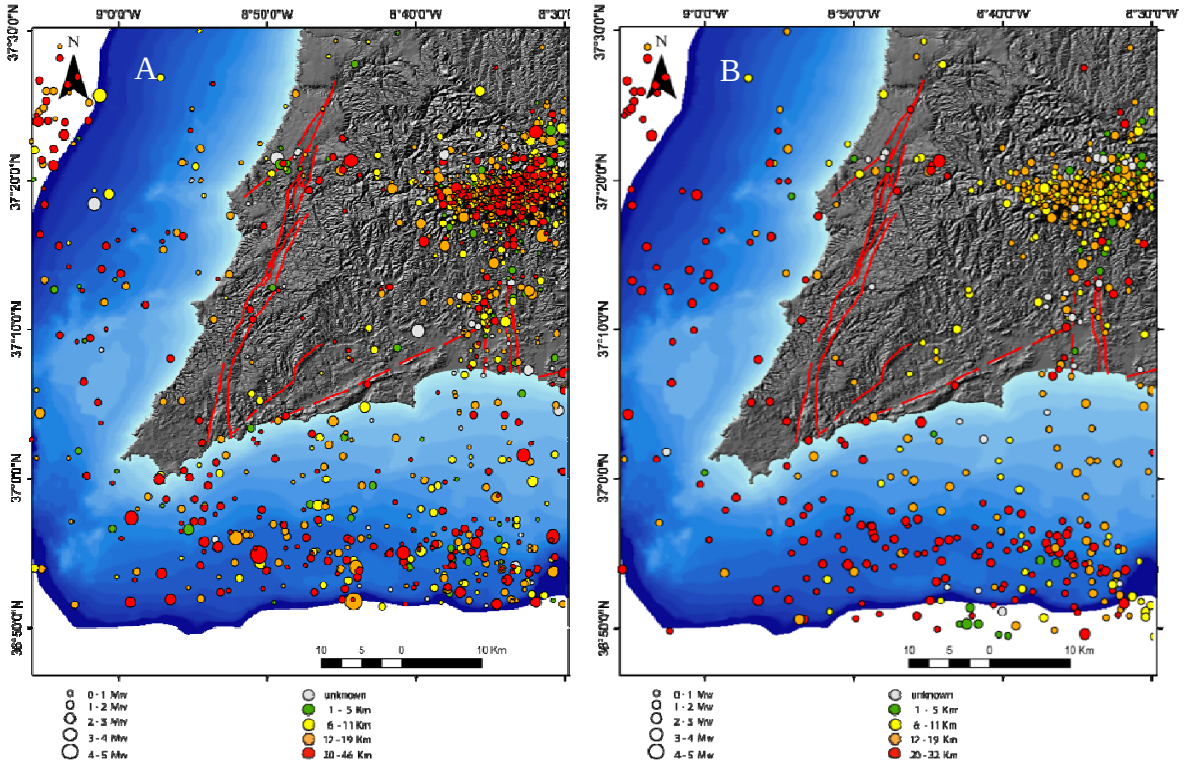

Figure 1.9 – Instrumental seismicity at the study area for the period 1961-2013 (A) and for the period 2009- 2013 (B) including the WILAS project database. Notice that in B the seismicity at the Monchique Igneous Mountain is less deeper (12-19 km) than for the period 1961-2013 (A) and that the STASFS evidences rare instrumental seismicity.(courtesy of the WILAS project team for which we are grateful).

An exception however concerns the above mentioned OBS survey where, for the three recognized seismicity clusters (Silva *et al*., 2010), focal mechanism analysis indicates thrusting at the Marquês de Pombal fault region, and strike slip associated with the SWIM fault system in the Horseshoe abyssal plain (Bartolomé *et al*. 2012), which is also consistent with the focal mechanism inferred for the Mw 5.9, 2007 earthquake by Custódio and co-authors (2012).

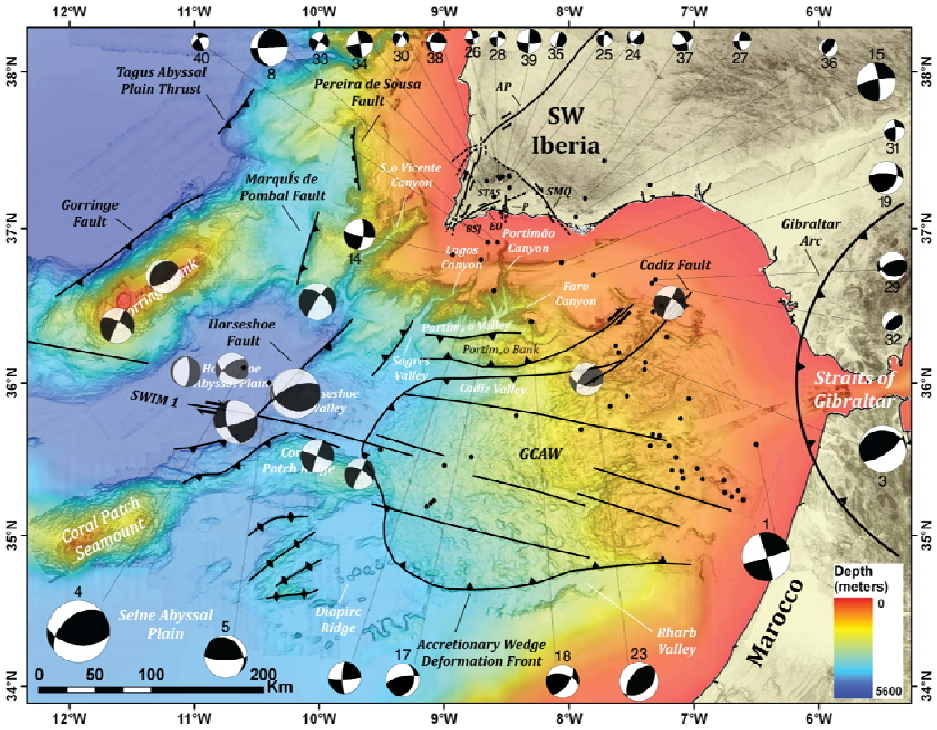

Figure 1.10 – Focal mechanisms for the SW Iberia and Gulf of Cadiz region, and main regional active tectonic structures; onshore focal mechanisms from Borges et al. (2001) and Offshore focal mechanisms from Borges et al. (2001) and Sticht al. (2006). Background map from Figueiredo et al. (2013) adapted from Dias (2001), Rosas et al. (2012) and Martínez-Loriente et al. (2013).

1.2.3.2 Historical Seismicity

The regional tectonic structures evidencing Pliocene-Pleistocene activity have low activity rates and consequently it is expected long periods of seismic quiescence for each structure. Long periods of seismic quiescence, i.e. long seismic return periods, also mean that it is possible that none of the existent active structures has ruptured during the Holocene. Indeed, no historical seismicity with surface rupture inland is known for the past 2500 years, which is the period of time corresponding to the Carthaginian, Roman and Arabic and Modern occupations, and that would likely provide us historical accounts.

However, regional historical seismicity is known and has been interpreted as essentially been generated along the seismogenic sources located in the Offshore, either located in the nearshore or more distant. From those, the largest and one of the best known historical

earthquakes of all is the November 1st 1755 earthquake and tsunami (estimated ≥ Mw 8), known as the Lisbon Earthquake. This major event not only affected a large region as generated a profound effect in the Human perception on earthquakes, initiating several philosophical, religious and scientific assays. Other large historical and paleo-earthquakes generated in the Gulf of Cadiz were also recognized by the identification of correlative tsunami deposits (Baptista *et al*., 2009) and turbidites (Gràcia *et al*., 2010), suggesting a 1300-1800 yr recurrence interval for a regional earthquake (most likely triggered in the Offshore) with magnitude larger than 8.

Having stated that, it seems reasonable to assume that moderate to large magnitude regional seismicity is primarily generated along the offshore and that generation of moderate to large magnitude onshore, although possible, is infrequent and has not occurred during the historical period.

Nevertheless, we consider possible that some seismicity may have been generated by onshore tectonic structures during the historical period, but either with magnitudes lesser than 5.5 to 6 Mw or with higher magnitudes but with deeper hypocenters, since they lack references and no surface rupture was ever described or identified. For some historical events, descriptions suggest high intensities as well as apparent topographic changes; in those cases, efforts were conducted to recognize recent topographic deformation in the landscape, but no unequivocal evidence of primarily deformation due to a surface rupture was recognized.

A significant constraint when analysing historical seismicity descriptions is that for older events the availability and access to the original reports is limited, which questions and limits an unbiased seismogenic interpretation of the provided earthquake information. Another constraint is the possibility of misinterpretations of the high intensities due to the geographical distribution of information which is highly dependent on the type and distribution of settlements, fortifications, harbours or monasteries. A logical assumption when interpreting historical seismicity is that if descriptions for an historical event are well scattered along a region with no localised high intensity, this probably means a more distant source, whereas if the descriptions of strong shacking are more restricted to a particular site, then this probably means that such specific site is close to the likely source of that historical event.

Historical seismicity for the Algarve region has been described since millennia, as a result of being an earthquake prone region and occupied for several civilizations. Several compilations have been written through times which were extensively researched, especially in an effort to recognise events that might be equivalent to the 1755 Lisbon earthquake.

In the next table (Table 1.1) we present the more significant regional earthquakes based upon a bibliographical study, presenting also for each events a likely source location and the available references from where the information was obtained, namely Oliveira (1986) which is a compilation of the historical seismicity database:

Date	***Damage reports Location***	***Source Location***	***References***
IV century B.C or III century B.C	Lagos, maybe other Phoenicians or Carthaginians sites like Tavira	Unknown, likely to be located in the offshore	*Cardoso, 1997; Silva, 2007*
33 B.C	All Portuguese coast	Offshore	*Rodriguez, 1932*
60-63 A.D.	Portugal and North Iberia, tsunami	Offshore	*Brito, 1597; Oliveira, 1986; Barata et al., 1989*
382 A.D	Several locations at SW Portugal, near shore island destruction	Offshore, Gulf of Cadiz	*Brito, 1597; Mendonça, 1758; Oliveira, 1986*
1009 A.D.	South of Portugal	Offshore, Gulf of Cadiz	*Rodriguez, 1932; Oliveira, 1986, Costa et al., 2007*
29-Jun-1033		Offshore, Gulf of Cadiz	*Abranches, 1877; Rodriguez, 1932; Oliveira, 1986; Costa et al., 2007*
22-Feb-1309	South Portugal, Lisbon	Offshore, Gulf of Cadiz	*Oliveira, 1986: Costa et al., 2007*
1353	Silves, village destroyed		*Oliveira, 1986;*
24-Aug-1356	South Portugal, Lisbon; long lasting shaking (15 minutes)	Offshore, Gulf of Cadiz	*Oliveira, 1986; Costa et al., 2007*
18-Jun-1366	Silves, Loulé, Lisbon	Offshore?? On-shore?? South Portugal	*Costa et al., 2007*
Nov- 1587	Loulé, village destroyed	Offshore?? On-shore	*Rodriguez, 1932; Oliveira, 1986*
06-Mar-1719	Portimão high damaged, duration 3-4 minutes (felt in Lisbon)	Offshore?? near shore? Gulf of Cadiz	*Oliveira, 1986*
27-Dec-1722	Tavira destroyed	Offshore south Portugal coast	*Mendonça, 1758; Lopes, 1841; Oliveira, 1986; Baptista et al., 2007*
2-Feb-1734	South Portugal, shaking but no destruction	Offshore?? On-shore?? South Portugal	*Oliveira, 1986*
6-Oct-1736	South Portugal, long lasting shaking	Offshore, Gulf of Cadiz	*Oliveira, 1986*
25-Oct-1739	South Portugal, 2 shakes with destruction	Offshore?? On-shore?? South Portugal	*Oliveira, 1986*
01-Nov-1755	Portugal, Spain and Morocco, Transatlantic tsunami	Offshore, Gulf of Cadiz	*Mendonça, 1758; Oliveira, 1986*

1756-1757	Multiple events, probably aftershocks from the 1755, either offshore or onshore		*Mendonça, 1758;Oliveira, 1986, Lopes, 1842*
31-Mar-1761	Portugal, tsunami, considered a relevant event after the 1755 one.	??	*Oliveira, 1986*
12-Apr-1777	Several shakings felt South Portugal	Offshore, Gulf of Cadiz	*Oliveira, 1986*
12-Jan-1856	Tavira, Loulé, Faro large damage at building and underground noises, several shakings (also felt at Lisbon)	Onshore? Offshore near coast?	*Oliveira, 1986*

Table 1.1 – Compilation of the most significant historical earthquakes with high intensities felt in Algarve region, from available sources.

Unquestionably, the most significant earthquake in the region was the November 1st 1755 event, which is frequently compared with a subduction-like earthquake. It produced great destruction in Portugal, Spain and Morocco, especially in the coastal regions, and was felt thousands of kilometres away throughout Europe. Furthermore, it generated the only transatlantic tsunami observed to date (Baptista *et a*l. 1998a).

From all the historical earthquakes compiled, we emphasize the 382 A.D. event, which description includes references to the destruction of islands located offshore Sagres, i.e. immediately offshore the study area. The overall description for this event is however doubtful since it mentions a damage area from the Atlantic towards the Mediterranean and including the Middle East (Palestine), which is certainly consequence of over interpretation. It is still an interesting earthquake to bear in mind, and to consider when searching for evidences of Holocene deformation. Another probable earthquake, is an event not included in any historical seismicity compilation, but that may have occurred during the second half of the IV century B.C. or during the III century B.C.. After an early Phoenician occupation during centuries VIII and VII B.C., Lagos seemed to have been destroyed by an earthquake (Cardoso, 1997), which led to its abandonment favouring a Carthaginian occupation or conquest during the III century B.C.. Evidences of intense destruction followed by the abandonment of the city during the late IV century B.C. are also present at Balsa (Silva, 2007), that corresponds nowadays to the city of Tavira. Although the timing of this destruction has been interpreted has the consequence of the Phoenician falling and Carthaginian raising, it is nonetheless possible that the destruction could correspond to a regional large earthquake; however this still needs to be investigated and confirmed.

In the earthquake compilation presented in Table 1.1 we also consider that some of the events could refer to seismicity triggered along inland fault segments, namely in the area Tavira-Loulé and also Portimão: in these cases, descriptions indicate very localized intensities, although not enough to discriminate details and exclude an offshore epicentral area.

In spite of all the efforts, there is not a consensus about the likely seismogenic source(s) for the 1755 large magnitude earthquake for the following reasons:

- 1) the size of several of the recognized active structures is not sufficient to generate the seismic moment needed for an Mw > 8 event, except for the Gorringe Bank (Johnston, 1996), Gibraltar Arc (Gutscher *et al*., 2006) or SWIM fault system (Bartolomé *et al*., 2012);

- 2) according to the tsunami travel time and numerical modelling, most authors agree that the main source should be located to the southwest of Portugal, at the Southwest Margin where different sources have been considered, such as the Marquês de Pombal and Horseshoe fault zones (Baptista *et al*, 1996; Baptista *et al*. 1998b; Baptista *et al*. 2009), so this excludes the Gibraltar Arc fault system as a main tsunamigenic source (Gutscher *et al*., 2006);

- 3) the SWIM fault system, the largest structure in the zone, is not an adequate structure for a tsunami generation due to its strike-slip kinematics;

- 4) the Gorringe Bank thrust system, according to Santos *et al*. (2009), based upon different interpretations of the historical descriptions and different numerical models, could be the main source for the event;

5) It is broadly accepted that more than one structure likely ruptured during this event, contributing to the total Mw > 8, not only due to the size of the probable structures but also to the reports which describe three distinct and sequential shocks (Mendonça, 1758; Pereira, 1919; Fonseca, 2005).

Despite all the discussion, the Marquês de Pombal thrust is commonly considered one of the more suitable candidates for the generation of the tsunami (Baptista *et al*., 2009), and is therefore assumed to have ruptured in 1755 together with other faults, such as the Horseshoe thrust, thereby producing a complex rupture (Grácia et al., 2003). There is no clear evidence of surface faulting for the Marquês de Pombal thrust that could be unequivocally attributed to the 1755 event, although detailed studies with side scan sonar reveal a large translational landslide and debris flow with an age circa 230 yr B.P. (Vizcaino et al., 2006) which were associated to this seismic event, and may be covering some of the superficial deformation. An older landslide deposit dated to circa 2300 yr BP was also recognized, suggesting a cyclicality that could be associated with the fault activity.

Whatever was the main seismogenic source, the 1755 large earthquake is closely associated with the southwest Portuguese continental margin, and corresponds to the largest earthquake felt in the study area.

A relevant question to address in the scope of this dissertation is if the 1755 earthquake generated any vertical motion along the South Portugal coastline. If so, this would indicate that a seismogenic structure with an historical rupture may cause or contribute to the inferred Plio-Pleistocene vertical motion for the area (Cabral, 1995; Dias, 2001; Figueiredo et al., 2013). In fact historical descriptions complemented and enriched with the parish surveys ordered by the Portugal minister Marquês de Pombal, provide information about some coastal changes and near coast navigability modifications, but no clear information concerning sea level markers referred. One major difficulty to access changes of the relative sea level is due probably to the tsunami impact that has not only destroyed all major structures such as

harbours, but has certainly covered many areas with debris and deposits along the coast. Andrade (1990) suggested a co-seismic subsidence of a section of Ria Formosa lagoon for the 1755 earthquake which facilitated the overwash of the barrier system by the tsunami that followed the seismic event, and later a post-seismic uplift based upon raised high tide marsh markers. Equivalent However, for the study area, no relationship between the earthquake and vertical motions was ever recognized.

1.3 Objectives of the Present Work

The research conducted for the achievement of this thesis aims the recognition and characterization of the more recent deformation along the neotectonic structures located in Southwest Portugal and the implications for the south Portugal regional seismic hazard knowledge.

With this purpose, two main research lines were pursued:

- a main research line focused on the characterization of the most recent deformation, especially through the recognition of active fault strands and evaluation of their quaternary deformation rates;
- another research line, complementary to the recognition of the Quaternary fault strands, intended to identify and quantify Quaternary crustal vertical movements in the study region.

Both research lines aimed at recognizing the most recent deformation present in Southwest Portugal, in order to access not only Quaternary regional deformation rates, but also to characterize their evolution since the Pliocene.

Several steps were conducted in order to facilitate the research progress, enabling secondary research goals, namely:

- A morphotectonic analysis along the structures with Plio-Pleistocene activity, through the application of several morphotectonic parameters to constrain local areas where deformation is expressed in the landscape and to compare rates of activity;
- Paleoseismological trenches for recognition and detailed analysis of paleo-earthquakes, their timing, their characterization and how the deformation reached the surface, assess their magnitude and infer fault behavior;
- Identification of the active segments along the S. Teotónio-Aljezur-Sinceira fault zone;
- Identification of Pleistocene and Holocene markers, such as sediments and soils, or geomorphic markers such as drainages or terraces to constrain the regional tectonic deformation. For this goal, it was expected that geochronology methods could be applied, such as Optically Stimulated Luminescence (OSL), Cosmogenic Radionuclide or Carbon 14.
- Identification of Late Pleistocene marine terraces in particular, their mapping and recognition of their inner edge elevation, namely the terraces corresponding to the last interglacial MIS 5;

- Identification of older Pleistocene to Pliocene marine terraces, their mapping and recognition of their inner edge elevation;
- Dating of marine terraces sediments or surfaces, through geochronology methods, such as Optically Stimulated Luminescence (OSL) or Cosmogenic radionuclide;
- Evaluation of crustal vertical movements rates through time;
- Analysis of historical seismicity descriptions, namely the coastal area descriptions in order to recognize recent deformation in the Holocene abrasion platform or sea cliff;
- Investigate eventual vertical motions related with historical seismicity, such as the 382 A.D. or the 1755 events;
- Investigate superficial deformation related with high intensities sites, according with historical descriptions.

For all the structures present in the study area, the rates of tectonic activity are low. However, some of the structures are more likely to provide a large spectrum of information which overall will gather better conditions for a detailed analysis and study about the degree of activity of a fault and its behavior.

Preliminary geology and morphological studies followed by field surveys suggested that the structures present in the study area with a stronger evidence of Plio-Pleistocene activity and that simultaneously would provide the best conditions for this study were the fault segments belonging to the São Teotónio-Aljezur-Sinceira fault system, which were then considered the primary target in the present work.

Other structures to be investigated were the Alentejo-Placencia fault along the littoral platform and also its relationship with the São Teotónio-Aljezur-Sinceira fault system, the Barão de São João fault, the Espiche fault and the Portimão fault.

To study the vertical movements, our primary targets were the lower marine terraces, besides the recognition of higher marine terraces cut into the littoral platform. In both cases, the objective was to produce a map of the marine terraces in the study region, from the western coastline to the southern coastline, to evaluate if the rates of vertical movements vary in time and how are they distributed in space. This study was conducted along the entire coastline of the study area, approximately for a length of 120 Km.

1.4 Outline of the Thesis

This thesis is organized in chapters that were prepared to be submitted as papers to scientific journals, covering several approaches which were undertaken to achieve the aims proposed:

- Chapter 1 corresponds to the presentation of the motivation and goals behind this study, and presents a brief description of the study area and regional seismicity. It also presents the thesis outline;

- Chapter 2 is already published as *Figueiredo, P.M., Cabral, J. and Rockwell, T.K. 2013. Recognition of Pleistocene marine terraces in the Southwest of Portugal (Iberian*

Peninsula): Evidences of regional Quaternary uplift. Annals of Geophysics, Vol.56, n.6, Special Issue Earthquake Geology, S0672, doi:10.4401/ag-6276 and refers to the characterization of the lower marine terraces present in the study area, which were interpreted as Late Pleistocene in age, allowing an estimation of an uplift rate for the region, for the Late Pleistocene;

- Chapter 3 corresponds to a paper in preparation and refers to the culminant regional abrasion platform where older marine terraces should be preserved. A listing of the sites where some marine terraces remains were identified is presented, and preliminary results of absolute ages for those sediments are also presented. It is also presented a preliminary map of the marine terraces interpretation for this region;

- Chapter 4 corresponds to a paper under submission to a scientific journal and refers to the morpho-tectonic analysis conducted along coastal drainage basins, south of the latitude of Lisbon. This analysis provided a support to compare vertical movements rates inferred for the southwest region with the eastern region of Algarve and the coastal area immediately north of the study area;

- Chapter 5 has been presented mostly at conferences and meetings, and it is under preparation to be submitted to a scientific journal in the scope of tectonics. In this chapter is it presented the work conducted to recognize paleoseismic events and to investigate the active strands along fault zones, both tasks were not previously undertaken. Geophysical exploration techniques are also presented as a tool to recognize, evaluate widths and constrain localization of active fault strands. Based upon recognized tectonic morphologies and inferred ages for the deformed sediments and paleosoils, quaternary deformation rates are presented for the Aljezur basin active fault strands;

- Chapter 6 corresponds to a paper in preparation to a scientific journal in the scope of tectonic geomorphology and refers to the morpho-tectonic study of Aljezur basin and the regional abrasion platform that is in the vicinity of the Aljezur basin. Several poorly preserved surfaces were recognized, but absolute ages are not available for them, which limits the understanding of the deformation timings;

- Chapter 7 concerns the seismotectonics of the STASFS and main active structures considered in this dissertation and presents an evaluation of the likely maximum magnitudes expected and estimated recurrence periods, based upon empirical relationships and fault characteristics;

- Finally Chapter 8 concludes this dissertation, presenting as well additional information which was obtained during the last stage of this study and has not been included in the remaining chapters. It presents a discussion about the knowledge development

due to new data presented and also discusses research lines that should be pursued in the future.

Chapter 2 and 3 are strongly connected, since both refer to marine tTerraces present int the study region, and are interpreted as uplifted. Chapter 2 is focused in late Pleistocene morphologies and sediments whereas Chapter 3 is focused in older morphologies, probably Pleistocene to older ones. The availability and quality of the available data for the lower, younger terraces are distinct than for the higher, older terraces, which influenced the type of field survey, data acquisition and processing, therefore resulting in two separated manuscripts.

Chapter 4 is fundamentally a geomorphologic analysis based upon basins that outflow directly to the Atlantic Ocean, in an effort to identify anomalous areas that might be related with tectonic deformation at a regional scale. Results allow establishing a comparison between the study region and immediately neighboring areas, concluding that at the study region vertical movements uplift rates are apparently higher than northwards and eastwards, and establishing a link with Chapters 2 and 3.

Chapter 5 and 6 are related in the sense that both investigate tectonic deformation related with the São Teotónio-Aljezur-Sinceira Fault system. Chapter 6 presents the results of a thorough morpho-tectonic study, investigating all possible effects of subtle deformation at the landscape along the Nova Castelã, Aljezur and Alfambras active segments of the São Teotónio-Aljezur- Sinceira Fault system. Chapter 5 is focused on the active fault segments identification and recognition of deformation and, when possible, its quantification.

Chapter 7 presents a seismotectonic analysis and presents information based upon the results of Chapters 2, 4, 5 and 6 to be applied in the regional seismic hazards analysis.

Chapter 2

Recognition of Pleistocene Marine Terraces in the Southwest of Portugal (Iberian Peninsula): Evidences of regional Quaternary uplift

Published as: Figueiredo, P.M., Cabral, J. and Rockwell, T.K. 2013. Recognition of Pleistocene marine terraces in the Southwest of Portugal (Iberian Peninsula): Evidences of regional Quaternary uplift. Annals of Geophysics, Vol.56, n.6, Special Issue Earthquake Geology, S0672, doi:10.4401/ag-6276 .

Abstract:

Southwest mainland Portugal is located close to the Eurasia-Nubia plate boundary and is characterized by moderate seismicity, although strong events have occurred, as in 1755 (Mw≥8), 1969, (Mw 7.9), and more recently in 2007 (Mw 5.9) and 2009 (Mw 5.5), all located in the offshore. No historical earthquakes with onshore rupture are known for this region. At the coastline, high sea cliffs, incised drainages, emergent marine abrasion platforms and paleo sea cliffs indicate that this region is undergoing uplift, although no morphological features were found that could be unequivocally associated with the 1755 mega earthquake.

To better understand the recent tectonic activity in this sector of Iberia, it is necessary not only to analyze active structures on land, but also to search for evidence for deformation that may relate to inferred offshore active structures. We thus conducted a study of marine terraces along the coastline to identify regional vertical crustal motions. Several poorly preserved surfaces with thin sedimentary deposits, comprising old beach sediments, were recognized at elevations starting at 2 m elevation and rising inland up to a regional abrasion platform situated at about 120 m a.s.l.. We identified distinct paleo sea level references at several locations at consistent elevations. This terrace sequence is likely Late Pleistocene in age, with individual platforms correlative to MIS 5 high stands and is coherent with a long-term slow uplift of the littoral zone for the southwest of Portugal. Although dating of discrete platforms is an ongoing and difficult task, preliminary correlations of paleo-shoreline elevations suggest that the uplift rate is in the range of 0.1-0.2 mm/yr.

Keywords*: Marine terraces, Coastal geomorphology, MIS 5, Pleistocene, Uplift, Active Tectonics, Portugal*

2.1 Introduction

The littoral section of southwest Portugal corresponds to the onshore area located close to the main known regional offshore active structures and also to the inferred source area of the 1755 earthquake Mw ≥ 8 (estimated Mw 8.7 by Johnston, 1996, or 8.5±0.3, updated by Martínez et al., 2004).

Vertical movements for the southwestern Portuguese coastal region were previously recognized as the result of a Pliocene-Pleistocene long term uplift (Feio, 1951), and the first attempt to quantify the vertical rate was conducted by Cabral (1995) who estimated it to be in the range of 0.1 to 0.2 mm/yr, using an assumed Pliocene or Pleistocene age for the displaced geological markers. However, the ages of sediments were not fully constrained nor were any late Pleistocene interglacial marine terraces recognized, meaning that there was not enough control on the variability of vertical motions through time. Furthermore, no relationship was established between the observed vertical motions and active crustal structures. In what concerns the last major regional tectonic event, the 1755 earthquake, there aren't any references of littoral vertical motion associated with the earthquake in the historical accounts for the studied area, so it is unknown if there were any co-seismic effects, and if so which kind. Following the same reasoning, no recent vertical motions associated with other large historical earthquakes known for the region (such as 382 AD) or paleo-earthquakes are described or were identified.

In order to understand the vertical crustal motions in this region, and to better constrain the younger movements, detailed field surveys were conducted along both the western and southern coastlines for recognizing and mapping paleo sea level features and correlative beach deposits (marine terraces) that could be associated with specific global eustatic high stands (Marine Isotopic Stage - MIS stages). With this aim, a 60 km-long section along the western coastline and a 40 km-long section along the southern coastline were mapped for terrace remnants and surveyed for precise elevation. Two specific high-priority targets were delineated: one was the recognition of geological evidences of recent vertical movements along the coastline that might be associated with historical seismicity, namely with the 1755 earthquake, and the second was the recognition of the last interglacial (MIS 5e) marine terrace, which is expected to be locally preserved and emergent, even if the uplift rate is very low, because the terrace was cut at about 6 m above modern sea level.

2.2 Regional Setting

Southwest mainland Portugal is located close to the Eurasia-Nubia plate boundary. This plate boundary can be differentiated into three distinct zones: one, a western segment, starting at the Mid-Atlantic Ridge and characterized by a transtensional WNW-ESE fault zone, the Terceira leaky transform. This zone continues eastward to a second segment, the Gloria fault, a 400 km-long right-lateral transform fault that trends roughly E-W (Laughton *et al*., 1972). Approaching the Gorringe Bank area, this linear boundary evolves to a third zone, a more complex and diffuse plate boundary (Sartori *et al*., 1994), with deformation being

distributed among several structures that span a zone up to a few hundred kilometres in width at the Gulf of Cadiz (Figure 2.1).

Several geophysical and geological studies have been undertaken during the past two decades to better understand this area of diffuse deformation, and the primary tectonic elements of this region (*e.g.* Bartolomé *et al*., 2012; Gràcia *et al*., 2003a, 2003b; Gutscher *et al*., 2012; Terrinha *et al*., 2003, 2009; Zitellini *et al*., 2001, 2004, 2009). This has allowed the recognition of previously unknown relevant active structures, with some of them showing significant morphological expression, such as the Marquês de Pombal and Horseshoe thrust faults, each with conspicuous scarps that trend NNE-SSW to NE-SW. Structures in the Gulf of Cadiz trending E-W, such as those bounding the Portimão Bank (also named in some references as Gualdaquilvir Bank), and trending WNW-ESE named the Southwest Iberia Margin (SWIM) faults, which are expressed as very long lineaments in the sea floor and interpreted as strike slip faults (Zittellini *et a*l., 2009; Duarte *et al*., 2011, Bartolomé *et al*., 2012). More recently Martínez-Loriente *et al*. (2013) demonstrated that south of the SWIM faults, in the Coral Patch Ridge and Seine Hills areas at the south Gulf of Cadiz region, active NE-SW thrusts (such as North Coral Patch Ridge and South Coral Ridge faults, Seine Hill 1 and 6 faults) and WNW-ESE dextral strike slip faults (such as Lineament South and Strike slip 1 faults) deform the Holocene sedimentary unit and are therefore active structures.

The structural complexity in the Gulf of Cadiz area is the result of the long term interaction between Iberia and Nubia, where structures with different geometries and tectonic styles, mainly thrust and strike-slip, have interacted at different scales through time (Duarte *et al*., 2011, Duarte *et al*, 2013, Martínez-Loriente et al. 2013). Geodetic data along with analysis of focal mechanisms indicate ongoing WNW-ESE Iberia-Nubia convergence at a rate of 4-5 mm/yr (Fernandes *et al.*, 2007, Nocquet and Calais, 2004, Serpelloni *et al.* 2007; Stich *et al*., 2006), while geological models for the last 3 Ma point to a NW-SE convergence at roughly the same velocity (DeMets *et al*., 1994; 2010). Ribeiro (2002) suggested the occurrence of sinistral rotation of the maximum horizontal compressive stress in southwest Iberia since the Pleistocene, although changes in the on-going deformation in this region are a matter of debate (Cunha *et al.*, 2012).

The Southwest Portuguese Margin is located in the northwest sector of the Gulf of Cadiz, and is characterized by NNE-SSW to NE-SW striking thrust systems, such as the previously referred Marquês de Pombal, Horseshoe and Gorringe Bank faults. Some of these structures in this sector extend onshore, such as Alentejo-Placencia fault system (Pereira and Alves, 2013) where a minor sinistral strike-slip component has been recognized offshore and the São Teotónio–Aljezur–Sinceira fault system (Terrinha, 1998; Lopes, 2002), where a sinistral component was also recognized but inland.

The regional instrumental seismicity corroborates the occurrence of diffuse deformation: seismicity is moderate, frequently shallower than 40 km and broadly distributed and focal mechanisms are dominantly thrust and strike-slip (Carrilho *et al*, 2004; Carrilho, 2005, Stich *et al*., 2010). An Ocean Bottom Seismometer (OBS) campaign undertaken in the study region for

11 months (from August 2007 to July 2008) showed that seismicity extends deeper than 40 km, concentrating in this time period at a depth of 50-55 km (Geissler *et al*, 2010), corresponding to three major clusters of earthquakes that occurred in areas coinciding with the location of the three larger instrumental earthquakes for the region (Silva *et al*., 2010): the 28th February 1969 (Mw~7.9), the 12th February 2007 (Mw 5.9), and the 17th December 2009 (Mw 5.5) events. The focal mechanisms calculated for the three major earthquake clusters and for the OBS survey also reveal different deformation behaviours, indicating thrusting at the

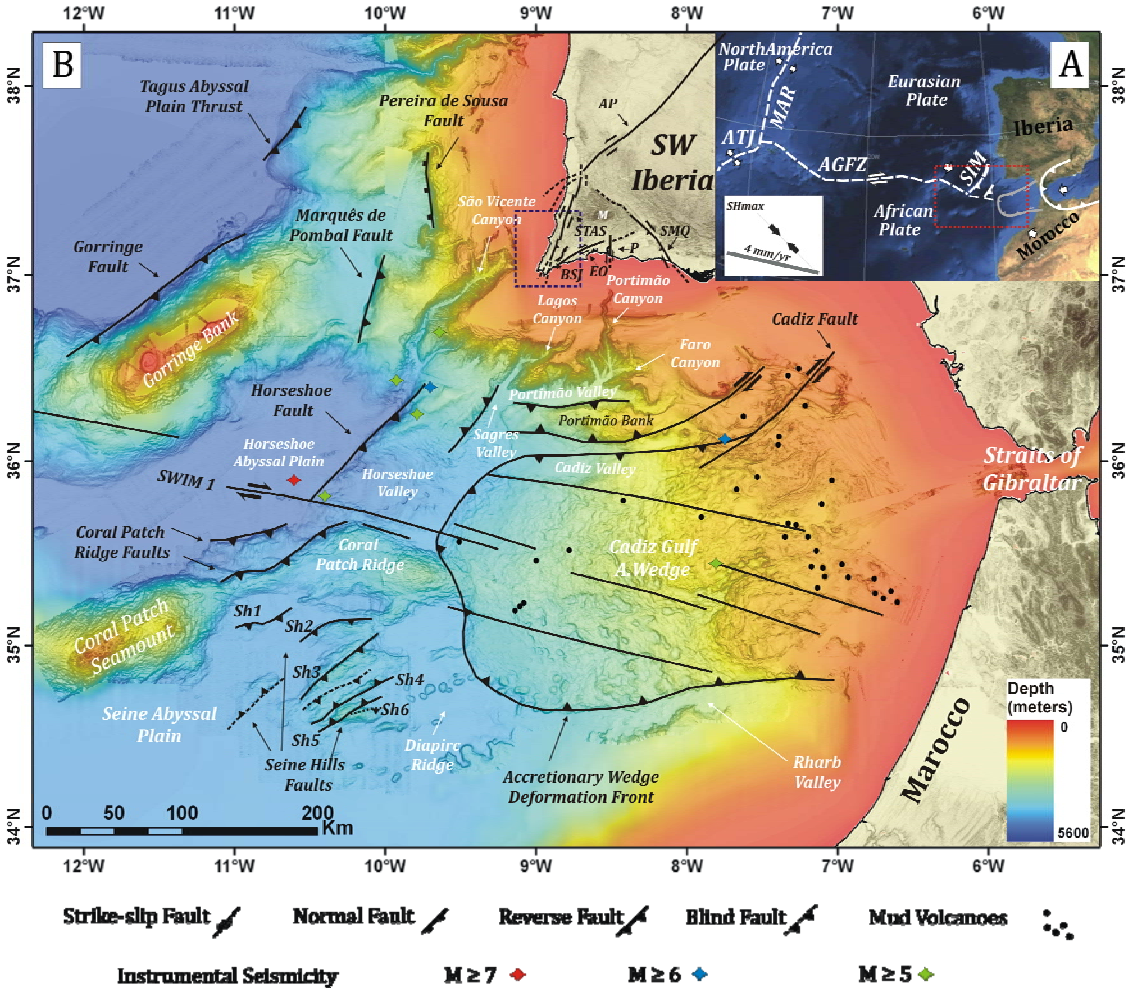

Figure 2.1 – Main active structures and morphological features in the Southwest Iberia region (according with Rosas et al. 2012 and Martínez-Loriente et al. 2013 for the offshore and Dias, 2001 for the onshore) and their localization regarding the Eurasia – Africa plate boundary. (A): Schematic Eurasia- Africa Plate boundary for the region and localization of figure 1 MAR - Mid - Atlantic Ridge; ATJ- Azores triple Junction; AGFZ – Azores Gloria fault zone; SIM – Southwest Iberian Margin (adapted from Duarte et al, 2013); (B) Off-shore structures identified in the map; inland structures : AP – Alentejo- Placencia Fault; STAS – São Teotónio-Aljezur-Sinceira Fault System; BSJ – Barão de São João Fault; EO – Espiche –Odiáxere Fault; P – Portimão Fault; SMQ – São Marcos-Quarteira Fault. The area studied in this work is delimited by the dashed line (adapted from Rosas et al., 2012).

Marquês de Pombal fault region, and strike slip associated with the SWIM fault system in the Horseshoe plain (Bartolomé *et al*. 2012), consistent with the location and focal mechanism of the Mw 5.9, 2007 earthquake (Custódio *et al*., 2012).

Despite the tendency for the occurrence of moderate levels of seismicity, large earthquakes were generated in this area, such as the November 1st 1755 earthquake and tsunami and the Mw 7.9 1969 earthquake (Zittelini *et al*., 2009 and references within). Large historical and paleo-earthquakes generated in the Gulf of Cadiz were also recognized by the identification of correlative tsunami deposits (Baptista *et al*., 2009) and turbidites (Gràcia *et al*., 2010), suggesting a 1300-1800 yr recurrence interval for a regional earthquake with magnitude larger than 8.

The Marquês de Pombal fault is usually considered one of the best candidates for the generation of the 1755 tsunami (Baptista *et al*., 2009), and is therefore assumed to have ruptured in 1755 together with other faults, thereby producing a complex rupture. If so, the 1755 Mw > 8 event is likely closely associated with the southwest Portuguese continental margin.

Several faults with evidence of Pliocene and Quaternary activity have been previously recognized onshore southwest Portugal (Feio, 1951; Pereira, 1990; Cabral, 1995; Dias, 2001; Dias and Cabral, 2002), mainly through geomorphologic analyses. The majority of the active structures in this region trend NNE-SSW to ENE – WSW, though N-S to NW-SE faults are also present (Barão de São João, Espiche and Portimão faults), are mostly less than 20 km long, and show predominantly reverse and strike-slip component. Historical seismicity is known for the past 2000 years (due to Roman and Arab occupations) (Brito, 1597; Lopes, 1842), however no Holocene fault surface rupture was ever recognized. The active faults that are recognized have low activity rates, less than 0.1 mm/yr (Dias, 2001; Dias and Cabral, 2002), and therefore long periods of seismic quiescence are expected. Instrumental seismicity is usually of low magnitude, diffuse and hard to correlate with the known Quaternary structures (Carrilho *et al*., 2004; Carrilho, 2005).

The most representative of such active structures in the study region is the NNE-SSW, sub-vertical,50 km long São Teotónio–Aljezur–Sinceira left-lateral fault system (STASFS). This fault zone extends north towards the southwestern section of the Alentejo-Plasencia fault (Cabral, 1995, Villamor *et al*., 2012), though their spatial and temporal relationships are still not clear from the available data. STASFS trends parallel to the western coast, corresponding to the nearest known inland active brittle structure that may be related to the ongoing plate boundary deformation observed in the offshore. This fault zone deforms a ca.10 km wide regional abrasion platform that is considered to be originally of late Miocene age, and which has been reoccupied or recut during the Pliocene and the Pleistocene, implying that the capping sediments are of Quaternary age. Dias (2001) estimated a slip-rate of ca. 0.03-0.06 mm/yr for this fault zone, based on the vertical offset of morphological features. However, considering that the sense of slip on this structure is probably mainly strike-slip, those vertical separation values are likely a minimum estimate. Some authors suggest that the STASFS extends to the offshore, towards the south or southwest (Lopes, 2002; Terrinha, 1998; Roque,

2007), but there is no unequivocal evidence to correlate the inland fault system with the morphological features inferred as the fault extension in the offshore. Detailed geomorphologic and paleoseismological studies along the STASFS (Figueiredo *et al.*, 2011; Figueiredo *et al*. in prep.) indicate that its southern sector (south of Sinceira basin) does not show evidence of significant Plio-Pleistocene deformation, the fault system probably having splayed into several minor faults. In fact, several parallel faults do exist in the local Mesozoic limestone bedrock, promoting the development of karst pits, which are filled with Plio-Pleistocene sands (Faro-Quarteira sands) along the coastal section (Martinhal–Zavial) where the STASFS should intersect the coastline. The spatial distribution and elongated shape of those karst features suggest a structural control by a previous structural fabric on the karst development (Dias and Cabral, 2002).

2.3 The Southwest Portugal Coastal Geomorphology

The southwestern Portuguese littoral can be sub-divided in two distinct coastlines types: the first is the NNE-SSW oriented, west facing coastline which is directly exposed to the Atlantic swells, whereas the second is the ENE-WSW trending southern coast of Portugal (Figure 2). The N-S section of coast is exemplified by steep cliffs developed in highly deformed Paleozoic schist and greywacke bedrock. The modern abrasion platform is narrow, around 300 m in width based on topographic and bathymetric maps (I.G.E.O.E. and I.H.), and the littoral zone is dominated by a rocky-shore environment, with coarse clastic sediments and thin sandy

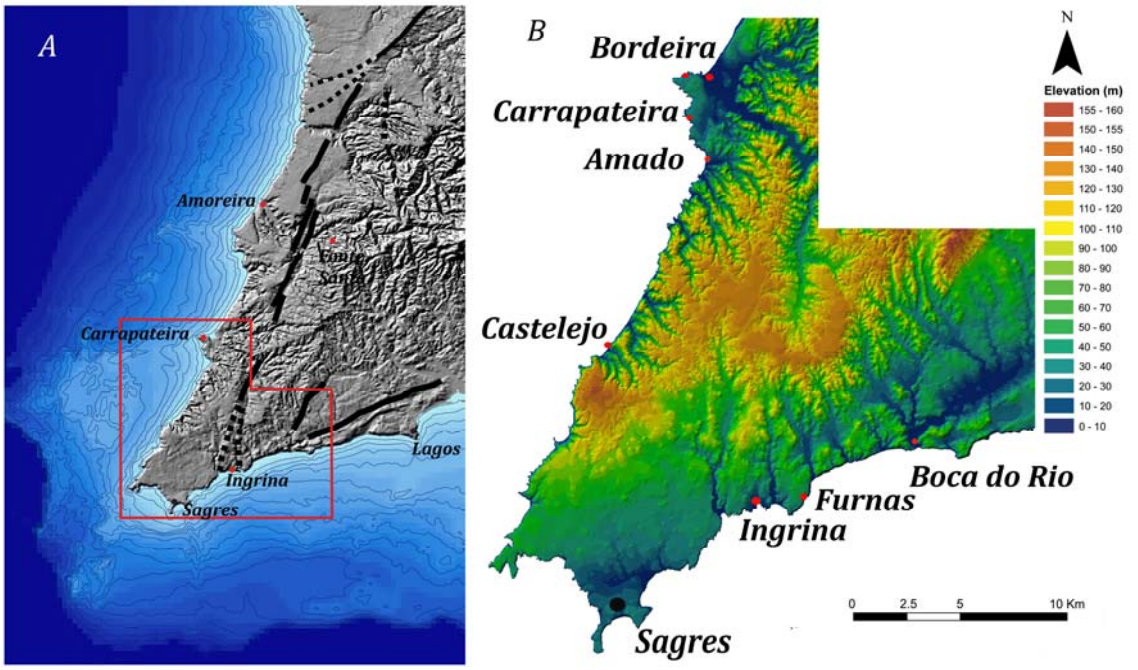

Figure 2.2 - Digital terrain model of southwestern Portugal: (A): Regional Geomorphology with main active structures Shaded relief (SRTM) and continental shelf bathymetry (0 to 200 m depth, contour lines, each 10 m (IH); (B) Digital Terrain Model from the study area, (IGEOE topographic data). Red dots indicate marine terrace locations, black dots correspond to toponymy.

beaches present at the mouths of the main drainages and in sheltered areas, or along some linear coastal segments that locally reach some kilometers in length, but less than a few tens to a few hundred meters in width. Cliffs have steep slopes, and towards the south increase their height, reaching circa 130 m in elevation. Several narrow and deeply incised creeks hanging along the cliffs are also recognized. These creeks contrast with larger fluvial drainages that have broad alluvial filled valleys, which are frequent along the Portuguese coastline in general and also in this sector.

Mass movements are common, favoured by the bedrock structure. An exception exists along this coastline in the Carrapateira area (Figures 2, 7 and 8), where the bedrock is composed of Jurassic limestone in the Alentejo Basin (a N-S elongated Mesozoic basin generated from the Atlantic extension; Pereira & Alves, 2011). This coastal section, with cliffs reaching only 40 m, is cut on less deformed Mesozoic bedrock where karst development has taken place and there are fewer mass movements.

Cliff retreat along the western coastline varies substantially according to lithology and local structure geometry, with present rates ranging from 2.5 to 11 m/ka in the Paleozoic schistose bedrock, to as low as 1 m/ka in the Jurassic limestone, based on 50 years of observations (Marques, 1997). Andrade *et al*. (2002) have calculated that the average wave energy input for a representative site along this coastline (Monte Clérigo) reaches 40 to 45 kWm^{-1}/yr, which is significantly higher than at a sheltered location along a south facing coastal zone near Lisbon, where a value of only 6 kWm^{-1}/yr was inferred using the same methodology, corroborating that the wave energy input along the SW coastline is significantly high.

The approximately E-W oriented southern coastline is developed on Mesozoic limestones in the west and on marls to sandy Miocene sediments towards the east. This difference in lithology, and the consequent resulting morphology, lead to an irregular and lower coastline with cliff heights reaching 50-60 m at Sagres in the west, and decreasing eastward to heights of about 20-30 m. Karstic features are common and sink holes are usually filled with sands. The modern abrasion platform is slightly broader here than along the N-S coastline, also increasing in width eastward. This coastline is sheltered from north and west Atlantic swells, but more exposed to the southwest and southeast ones. Sandy beaches are common, mostly in sheltered areas in the west, but are continuously present towards the east, where dune systems also exist. Historical cliff retreat rates also vary significantly along this coastline, ranging from 0.9 m/ka in the Ingrina–Furnas sector to about 16 m/ka at Boca do Rio–Salema (Marques, 1997) (Figure 2). In the Carrapateira area, the limestone promontory in the west coast, coastal morphology exhibits similarities with that along the southern coastline, and retreat rates are similar to the Ingrina-Furnas sector.

Inland, the most significant geomorphologic feature corresponds to a broad regional abrasion platform cut across the Paleozoic schists. This surface is particularly well represented along the western coast, north of Sagres, where it reaches an elevation of 120–130 m. Capping beach sediments are absent in this sector of the platform, although scattered rounded quartz pebbles are commonly present. No geochronologic information is available for this surface,

although the platform has been considered as possibly late Miocene in age, and reoccupied and re-trimmed during Pliocene and Pleistocene times (Feio, 1951; Pereira, 1990; Dias, 2001). It is likely that during the Plio-Quaternary, an abrasion platform was cut across older Miocene sediments, thereby developing a younger erosional abrasion platform, where Miocene sediments could be sparsely preserved beneath Plio-Quaternary capping sediments.

The highest surface with cover sediments, assumed to be marine or fluvio-marine, is present at Fonte Santa (Figure 2), located 15 km inland at an elevation of about 350 m. According to Feio (1951), these sediments are correlative of a high "summit-plain" which corresponds to a remnant of a Pliocene planation morphology that surrounds Mount Monchique, a Cretaceous igneous massif that reaches 900 m in elevation and is considered an *inselberg*. These marine-like sediments are overlain by aeolianites that are strongly consolidated by iron and manganese oxides and considered to be Pliocene in age (Manupella *et al.,* 1992), again implying that all lower terraces have been refreshed or re-cut after this time.

Towards the southeast, the regional erosion surface transitions to several discrete surfaces cut into the Mesozoic sandstone, marl and limestone bedrock of the Algarve Basin (Pereira, 1990), which may actually correspond to a sequence of closely spaced, poorly preserved, middle Pleistocene marine terraces. This is very similar to the middle Pleistocene Linda Vista terrace set of southern California, which transitions from a very broad (>10 km) abrasion surface at San Diego to a sequence of discrete, narrow (50-200 m-wide) marine terraces northward towards Los Angeles, primarily as a function of bedrock resistance to erosion (Kern and Rockwell, 1992).

2.4 Identification of References For Characterizing Vertical Movements

2.4.1 The Present Reference

The present tidal range in Portugal is meso-tidal within a 2 to 4 m maximum range, and with the maximum high-tide at circa 2 m m.s.l. For characterization of the elevation of the modern wave-cut platform and associated beach deposits in this region, one must take into account this tidal range, as most terrace cutting likely occurs during storms at high tide. As expected, other features in this area, such as notches and sea caves, will also reflect this tidal range and present larger dimensions (Wziatek *et al.*, 2011) than equivalent features that form in regions of micro-tidal ranges, such as in the Mediterranean Sea, and their mean elevation fluctuates within the tidal range. The coastline is frequently hit by storms generated at long distances in the Atlantic (Costa *et al.*, 2001), and the wave energy during such storms is commonly quite high, resulting in the formation of storm benches and storm notches. The shoreline angle elevation reflects not only the tidal range, the wave energy impact, and the bedrock resistance, but also the smaller scale coastal physiography (if it is a bay or an exposed cliff) and, therefore, the shoreline angle elevation fluctuates within a range up to a few meters from the mean sea level (Wright, 1970). Assuming that the resulting effect from all these variables has not changed significantly since the Pleistocene, it is therefore crucial to understand the local modern processes involved in the development of a wave-cut abrasion platform, along

with the cliff and beach system, to properly interpret the past and correctly interpret the elevations of paleo features. We discuss this further below in the section on field interpretations.

As referred above, in this work we will focus on the surfaces and features associated with sea-level that we expect to be the youngest, or attributable to recent vertical movements. Secondly, we discuss observations that pertain to a possible uplift or subsidence signal associated with historical seismicity.

2.5 Recognition of Paleo Marine Terraces

The morphological recognition of paleo marine terraces follows the nomenclature of Bradley and Griggs (1976). According to these authors, most platforms can be described as having three different segments: an offshore or outer edge segment with a generally low gradient, a near-shore segment, with an intermediate gradient, and a shoreline segment characterized by a steeper gradient adjacent to the inner edge at the paleo-shoreline. Thus, a single marine terrace can exhibit these different surface segments, and distinct morphological elements, all generated with the sea at the same level. This differentiation may vary locally, especially with lithology resistance, wave energy incidence and coastal morphology. In the present study we infer the original elevation of the platform segments and of other morphological elements based upon the elevation of their modern analogues.

Paleo sea level features related to past sea level high stands, such as raised marine terraces, are present along the western and the southern coastlines, albeit in a discontinuous pattern. In general, the marine terraces or wave-cut platforms are poorly preserved, beach sediments are mostly eroded and, locally, younger aeolianites cover the entire morphology, making it difficult to recognize the terraces and to distinguish them from other features. Along the cliffs in the Paleozoic schists, lower elevation features that are expected to be correlated with the late interglacial (MIS 5) are mostly absent, since they have been mostly or completely removed by the Holocene transgression and erosion. In areas of limestone cliffs, which are even more resistant to erosion, paleo sea level features at lower elevations are better represented, although they are still poorly preserved in most areas. To understand the regional marine terrace patterns and to establish a regional sequence, consistent observations from several sites are needed, along with their tentative correlations. We will present a brief description of the mentioned sites, describing each of the recognized surfaces, and discuss their inferred ages later.

For detailed geomorphological analyses, topographic surveys were conducted using a DGPS – RTK (Leica GPS1200), with a vertical error smaller than 10 cm. All elevations presented correspond to elevations above mean sea level.

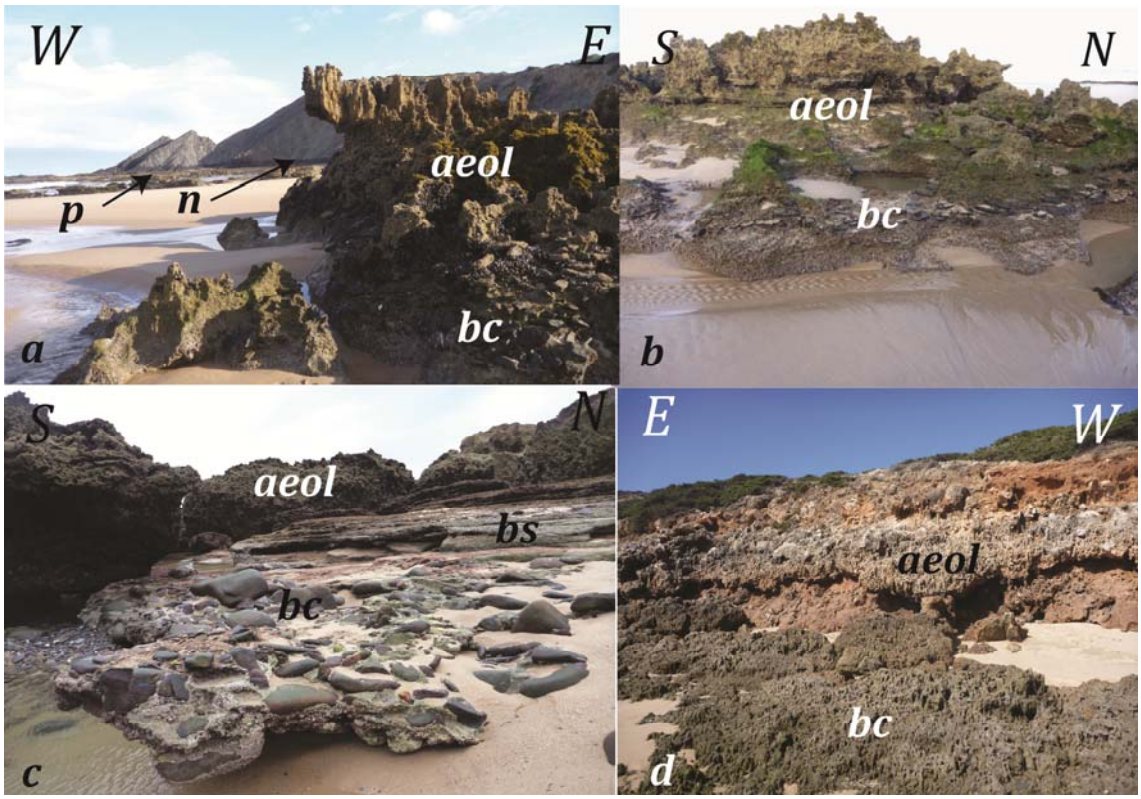

Figure 2.3 – The modern abrasion platform is reoccupying an older one at several sites in the southwest Portuguese coastline. All of these sites share the same sedimentary sequence, and the paleo-shorelines are at the same elevation. a) Perspective at Amoreira beach; in the background the abrasion platform is cut into schists. Overlying the abrasion platform (p), now reoccupied by the nowadays sea level are basal coarser sediments (bc) and aeolianites (aeol), with a notch (n) developed at the back edge. b) Another perspective from Amoreira beach, aeolianites (aeol) on top of basal coarser sediments (bc). c) Castelejo beach, coarser basal sediment (bc), interbedded with medium to fine sand, overlying an abrasion platform (not visible in this image, covered by modern beach sand) and underlying aeolianites (aeol); d) Bordeira beach, basal coarser sediments (bc), underlying several aeolianite (aeol) units.

2.5.1 Ingrina Beach

Located along the southern coastline (Figures 2 and 4), the Ingrina beach is located in a small and confined bay, 200 m in width and 300 m in length, cut into Jurassic limestone. At this site, several surfaces are interpreted as paleo wave-cut platforms, and are preserved in a sequence along with their respective paleo-sea cliffs. The modern wave-cut platform, T0, is developed at the infra-tidal, tidal, and supra tidal zone, and is mostly recognized in the submarine section and during very low tides. The beach has fine to medium sand, and the inner edge is usually covered by beach and aeolian sediments at an elevation of about 2 to 3 m (white line in figure 4).

A bench at 3-4 m elevation corresponds to the modern storm boulder accumulation. At a sheltered section along the eastern side of the bay, paleo sea caves and a possible level of

bioerosion, inferred by the presence of round borings that develop perpendicular to the surface and are assumed to be *Lithophaga* borings, occurs at 2.8 to 3.8 m. No correlative sediments are preserved at this elevation.

A well-preserved bedrock surface at 6 to 8 m elevation is recognized primarily along the western side of the bay. Although this surface is very well preserved, it shows a scarce sedimentary cover. The elevation of the shoreline or inner-edge varies from 6 to 7 m along the southern, ocean-ward section of this surface, and reaches a maximum elevation of 8 m at the cuspate landward back-edge of the bay, similar to the modern shoreline. We refer to this terrace as T1 (blue line in figure 4).

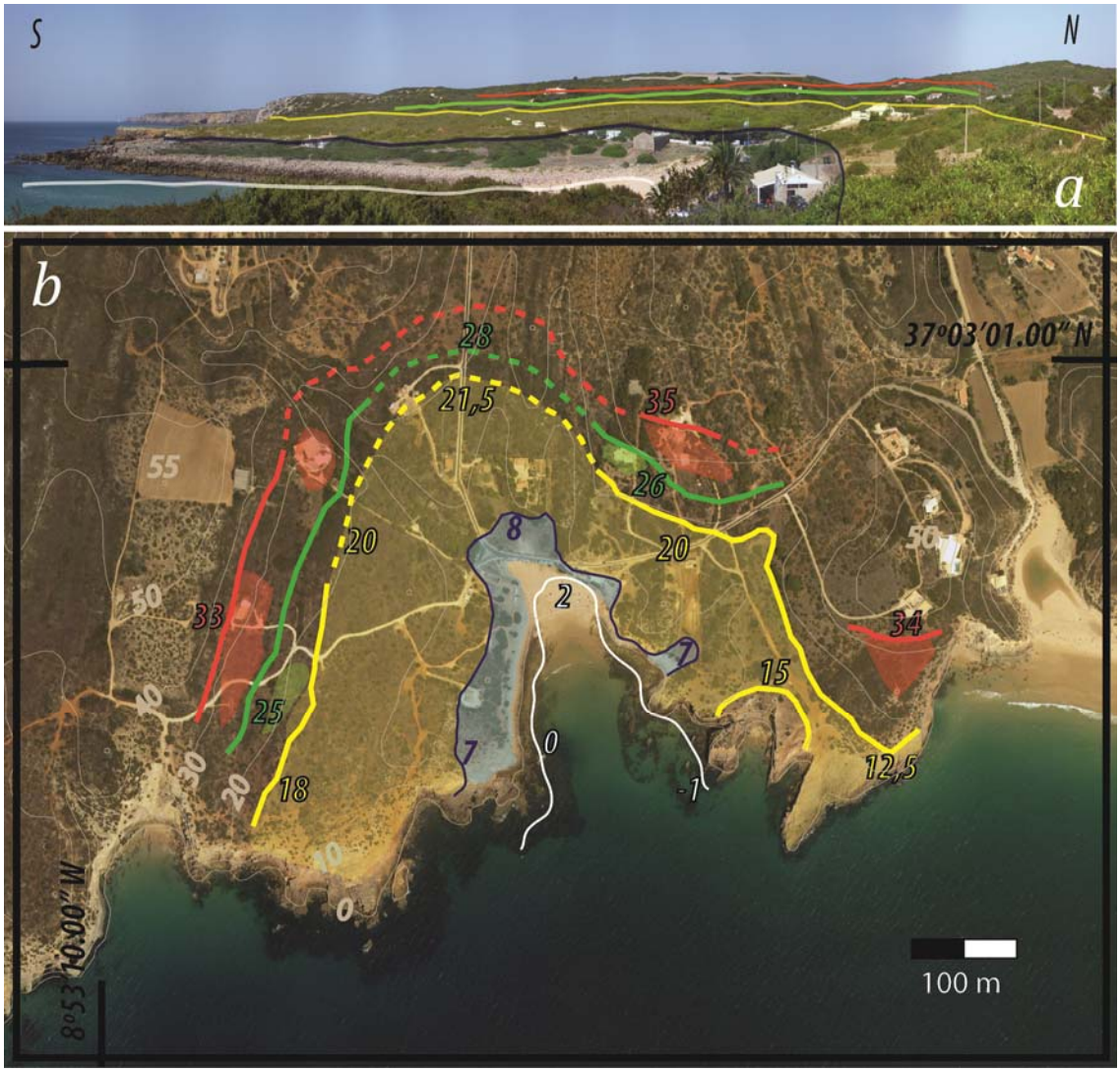

Figure 2.4 – Map identifying the marine terrace at the Ingrina site. a) Panoramic view from east and terrace perspective. b) Inner edge and terrace map. Terraces are mapped in transparent colors and the inner edges in solid line when visible and dashed line when inferred. White – T0 (modern); blue – T1; yellow – T2; green – T3; red – T4. Inner edges elevations in meters are provided. Topography contours lines each 10 m.

Another surface cut into the limestone bedrock at circa 12 m elevation is a striking feature at Ingrina, and it is visible mainly along small spurs on both sides of the bay. This surface expressed along the spurs is generally flat or shows a low gradient, and smoothly ramps up to a higher elevation farther inside the bay, ranging then between 12 m and 16 m elevation. It has pedogenic carbonate locally capping the abrasion surface along with locally preserved cemented littoral sediments. Sandy sediments are scarcely preserved (except where cemented by carbonate), but round quartz pebbles are scattered ubiquitously on the surface. Another surface is present at elevations ranging from 16 to 18 m, gently rising to an internal section where an inner-edge is recognized at 20-21 m. Along the inner-edge or paleo-shoreline, conglomerates of quartz pebbles testify to the presence of the paleo-beach face. No sediments were identified above this level, but scattered quartz pebbles are preserved.

We have interpreted these 3 surfaces as morphological segments of a single wave-cut platform. In general, the surface ramps up towards inland as three distinct morphologic sections: a generally flat or low-gradient section near the outer-edge that ranges between about 12 m and 16 m elevation; a moderately sloping middle section at circa 16-18 m elevation, and a higher more steeply sloping surface that ramps up to the inner-edge of the terrace at 21 m elevation.

Collectively, we designate this sequence as T2, or the second emergent marine terrace at Ingrina. The inner-edge, or shoreline angle, which is locally buried by colluvium, reaches maximum elevations of 20-21 m near the shoreward cuspate part of the paleo-bay, similar to the modern shoreline, which reaches its maximum elevation at the shoreward inner-edge of the bay (green line in figure 4).

Higher surfaces, which correspond to older marine terraces, are also recognized at Ingrina, inferred from slope changes at about 26 m, 33 m, 37 m and 45 m, but further work is needed to adequately identify shorelines, characterize their elevations and their degree of preservation. Nevertheless, their presence, along with the well-preserved terraces at 8 m and 21 m (figure 9), and the higher broad abrasion surfaces at elevations higher than 100 m, indicate long-term uplift of a rising coastline.

2.5.2 Furnas

At Furnas, located in the southern coastline 2 km east of Ingrina and 10 km to the southeast of Castelejo beach (presented in 4.2.3), a narrow raised bench at 2 m elevation is present at the base of a 40 m-high cliff (Figure 2 and 5). Additionally, at this site, there are two levels of sea caves and associated beach sediments at different elevations that we interpret as additional evidence for the presence of the terrace T1 along the southern coast.

Of note at this location is that the modern sea cave notch is actively being cut at about 3 m below m.s.l., probably because this is along a prominent section of the coast and inner edges tend to be lower at promontories; and also because locally the rock could be more resistant to erosion due to its hardness. Thus, paleo-sea level features need to be interpreted according to this relative reference frame.

The raised bench corresponds to a terrace highlighted by a narrow abrasion platform and a sea cave/notch at 2 m, and another sea cave/notch at about 3.8 m elevation (Figure 5). Both sea caves/notches are filled with cemented coarse marine sediments, with cobles ranging from 5 to tens of centimeters (Figure 5b). A cemented sand deposit with marine shells (mussels) is present, covering the coarser sediments, at elevations ranging from 2 m to 4 m. This sand deposit has a depositional shape comparable to a fan, and may be interpreted as a small paleo surge channel. The sands with marine shells indicate a submarine proximity to a paleo beach and a likely paleo intertidal environment presently at the ~4 m elevation. These features are approximately 5-7 m above their modern counterparts, so we infer these to correlate to the T1 terrace surface at Ingrina, which is at a comparable elevation above its modern counterpart.

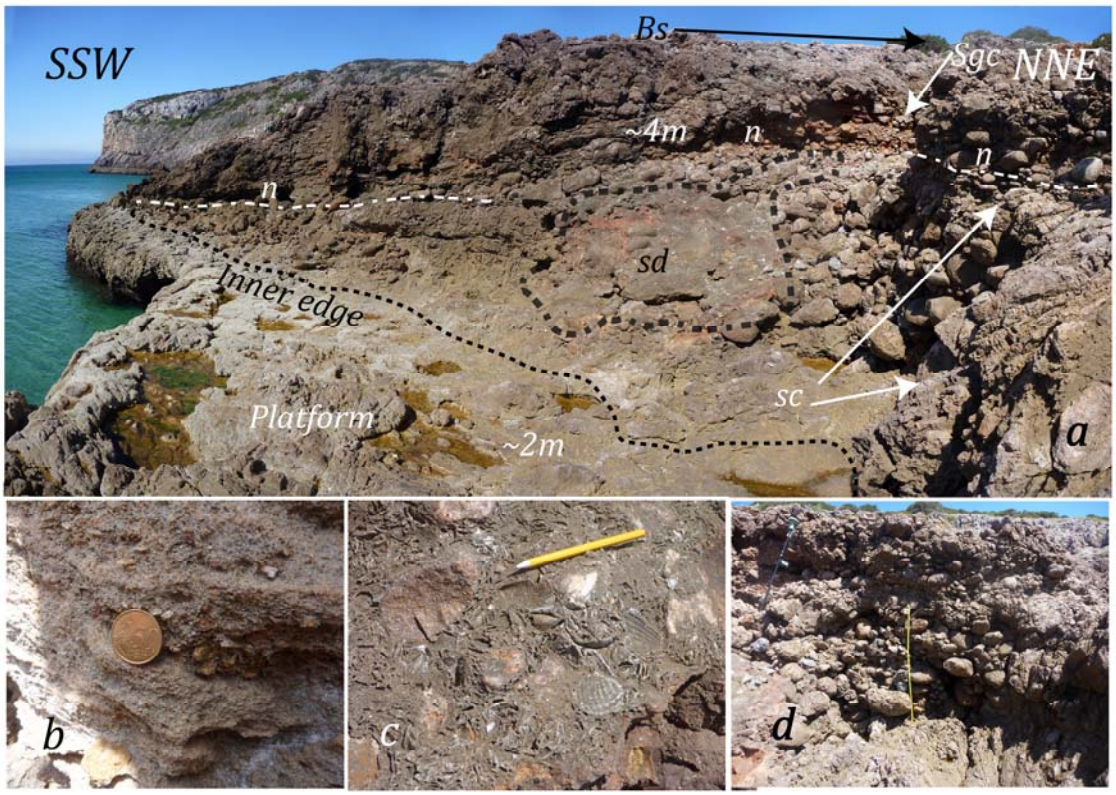

Figure 2.5 - Marine terrace at Furnas site. Location is given in Figure 2. a) Perspective of the terrace: An abrasion platform and an inner edge are recognized at ~2 m elevation; a notch level (~4m elevation) and sea cave (between ~4 and ~2 m elevation) are also indicated; A small surge channel (Sgc) is identified, suggesting that the sand deposit (sd) that covers the coarser deposits is correlated with the beach sand deposit (Bs) present at ~8 m elevation. b) detail of beach sand unit; c) detail of sand deposit; d) sea cave filled by coarse deposits.

Remains of beach deposits with small pebbles, shells and cross bedding are also preserved at 8 m elevation (figure 5c) and probably correspond to a paleo beach in the mouth of the paleo surge channel that is present here. For now, we correlate these marine remnants with the highest T1 terrace elements at the Ingrina site.

In summary, the modern shoreline notch at Furnas is located at about 3 m below sea level, and there are elevated notches at 2-4 m, indicating 5-7 m of relative difference for exposed rock erosional features. At the mouth of a small surge channel, littoral depositional features are preserved up to about 8 m. Together, we interpret these features to represent different littoral elements of the same sea level high stand and correlate all of these with the T1 marine terrace at Ingrina.

2.5.3 Castelejo

Castelejo site is located in the western coastline at the base of a 120 m high cliff (Figures 2, 3c and 6). At Castelejo beach we only recognized one surface, which was referred by previous authors (Pereira, 1990, Cabral, 1995, Dias, 2001). This surface corresponds to a wave-cut platform cut into the Paleozoic schistose bedrock at 1.5 to 2 m elevation: the modern abrasion platform is therefore essentially reoccupying and retrimming an older surface, as evidenced by the preservation of a wave-cut platform locally capped by sediments. Overlying the abrasion platform, there are two conglomeratic layers separated by a thin beach sand layer (Figueiredo *et al.*, 2010; 2011) overlain by strongly cemented aeolianites. Equivalent remnants of this surface and the capping sediments are also preserved at the Amoreira and Bordeira beach sites, also along the western coastline, 15 and 30 km farther north, respectively (Figure 3).

The upper unit, the aeolianite sequence, contains several paleosols and colluvial units (Figure 6), and therefore probably represents multiple periods of deposition on top of a paleo marine terrace and against a paleo-cliff during the late Pleistocene. The sequence is outcropping as a residual relief located 75 to 100 m seawards of the present active cliff. Marques (1997) calculated a maximum cliff retreat of 0.017 m/yr for this specific location based on a 50 year period of observations. This rate is consistent with the average Holocene rate of cliff retreat for the last 4500-6000 years, when Holocene sea level stabilized. This observation also corroborates that the modern wave–cut platform has retrimmed an older one and has extended it inland.

Considering ages from other carbonate aeolianites from Portuguese coastal areas (Moniz, 1992; Pereira and Angelucci, 2004; Soares *et al*., 2006; Prudêncio *et al*., 2007), we assume that the consolidated aeolianites are most probably related with the last stages of the Würm glaciation (~MIS 4-3), or with the Last Glacial Maximum (~MIS 2) and consequently, the underlying beach sediments and platform should be older and possibly correlative of the MIS 5, most likely the last sub-stage, MIS 5a.

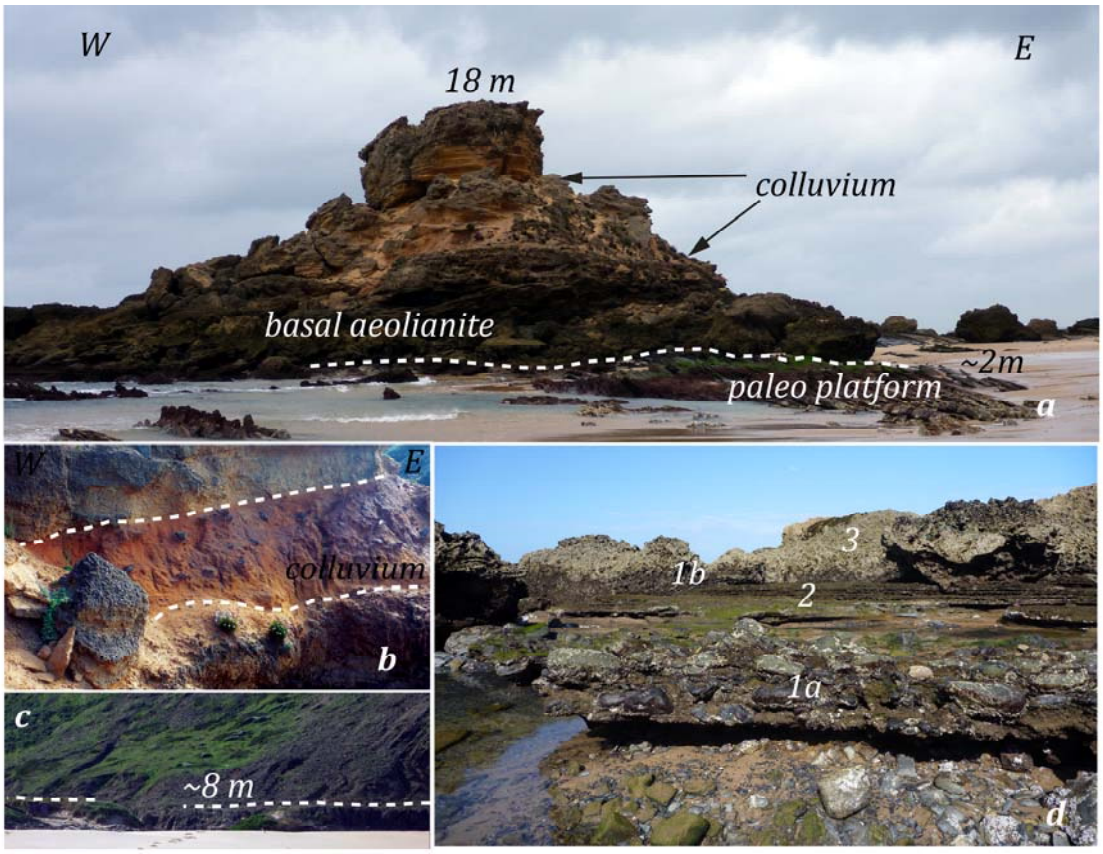

Figure 2.6 - Marine terraces at the Castelejo site. Location is given in Figure 2. a) Perspective of the aeolianites unit which lays on top of a paleo wave-cut platform; b) Detail of a colluvium wedge with soil development inter bedded with aeolianites. c) fluvial terrace at 8m; d) Sedimentary sequence on top of the paleo platform: 1a- basal coarser unit; 2- sandy beach unit; 1b- upper coarser unit; 3- aeolianites.

Close to the beach, a small canyon cut into the schistose bedrock is incised in a flat erosional surface at 7-8 m elevation, which we assume to be a fluvial terrace that should be located very close to the mouth of this drainage. The base level correlated with this surface is likely to correspond to the sea level position that has generated T1. We conclude that this fluvial terrace should correspond to the final section of this canyon, located near the shore, and most likely re-activated during the Holocene transgression and cliff retreat, and re-incised to its actual position (Figure 6c).

We consider that the recognized abrasion surface may correspond to a lower (seaward) section of the terrace T1, and the fluvial terrace as secondary evidence for a higher inner edge elevation, and so we tentatively correlate it to the T1 surface at the Furnas and Ingrina sites.

2.5.4 Carrapateira

Carrapateira is located 10 km north of Castelejo beach, and is a promontory cut into Mesozoic (mainly Jurassic) limestones along the west coast (Figure 2). Because the cliff retreat

rate in the western coast is slower in this area (Marques, 1997) than in the rest of the western coast, it is expected to be a reasonably good site to preserve T1 and T2 terraces. Plus, it presents lithological and morphological similarities with the southern coast and is therefore the ideal site along the western coastline to compare with the marine terraces identified along the southern coastline. However, because the west coast is more exposed to high energy waves than the southern coast, resulting in a broader zone of wave erosion, T1 along this section is poorly preserved and generally difficult to survey. Paleo features, such as raised notches, raised marine sediments, and inner edges were recognized in a discontinuous pattern along a 3 km long section of coast. Locally, at the cliff base, remains of small spurs at about 12 m elevation are present that provide additional evidence of a raised abrasion platform.

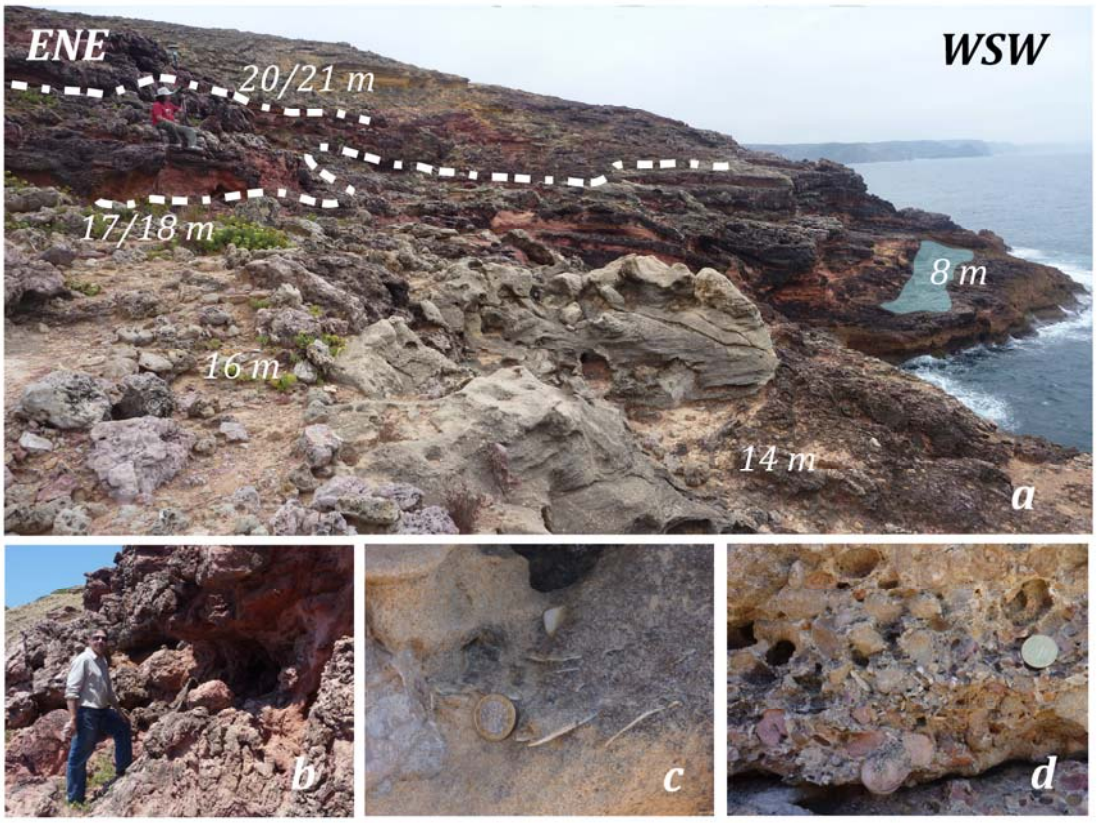

Figure 2.7 - Panoramic view of Carrapateira, southern section Carrapateira site: a) T2 terrace perspective ; b) notch at 20/21 m elevation c) detail of beach sand with imbricate shells; d) basal section of the sedimentary T2 sequence, laying on top of the wave-cut platform with coarser sediments at 14 m elevation.

Along the south section of Carrapateira, the outer-edge of a poorly expressed, narrow wave-cut platform with irregular morphology is exposed in a cliff face at 13-14 m elevation. This surface is covered by coarse, round pebbles and sandy beach sediments, confirming its marine origin (Figure 7). The irregularity of the wave cut rock surface probably indicates that these are surge channels, similar to those present at many sections of the modern coast. In the same vicinity and at generally similar elevations, paleo-sea caves were also identified. The wave-cut platform ramps up to 17-19 m elevation where a thin layer of beach sediments and

cemented aeolianites are also present. Notches and sea caves were also recognized at these higher elevations, which generally are larger than the ones at about 14 m elevation.

At the northern section of the promontory (Figure 8), the 13–14 m surface is substantially eroded, but the 17-19 m surface is very well represented and may reach a width of 20 m to 30 m, likely to correspond to a marine terrace tread area, *i.e.,* to a near-shore zone of marine abrasion. It is locally covered by cemented, gray to white aeolianites. This flat surface evolves into a smooth ramp to a slightly higher section where the inner-edge is well defined at 21 m elevation. We interpret these elements as sections of a marine terrace, and correlate this terrace with the T2 at the Ingrina site, which has similar surfaces and an inner-edge at similar elevations (figure 9). Other higher surfaces with inner-edges at about 26 m and 33 m were also recognized at Carrapateira promontory, which culminates in a higher, flat well-formed surface at about 40 m elevation that is capped by paleo and modern aeolianites, similar to what was identified at Ingrina site, but as mentioned earlier, they will not be interpreted in this work.

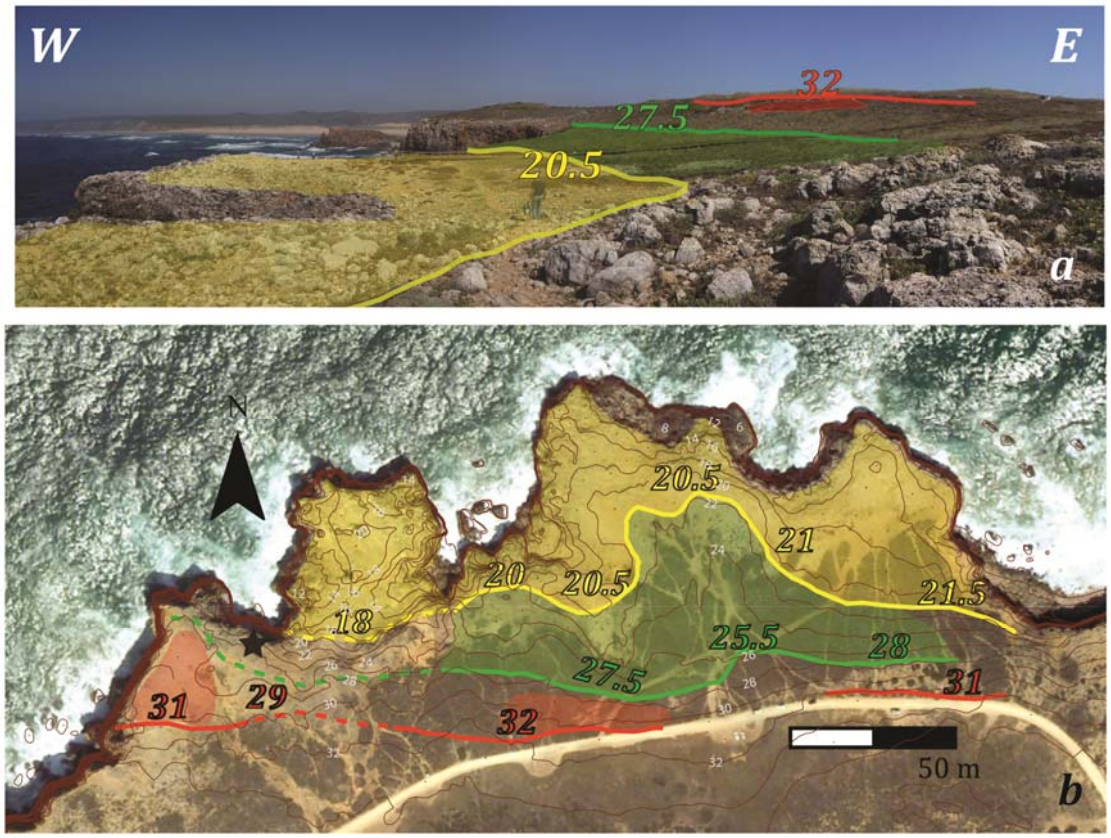

Figure 2.8 - Panoramic view of Carrapateira, northern section Carrapateira site, showing the northern section of the promontory. Marine terrace mapping: a) panoramic view and terrace perspective (site where picture was taken marked by "star" at b); b) inner edge and terrace map. For each terrace, the inner edge is mapped, solid line when visible, dashed line when inferred; Yellow – T2; Green – T3; Red – T4. Inner edge elevations are provided in meters. T3 and T4 are not discussed in detail in this work.

As mentioned above, the T1 terrace along the Carrapateira site is very difficult to recognize. Two benches were identified at elevations of 4 m and 8 m, but both are covered by large

boulders that were likely deposited by high energy events (storms and/or tsunamis). However, at Bordeira beach, immediately north of Carrapateira promontory, cemented beach sediments composed of rounded schist pebbles cover a wave-cut platform cut into the Paleozoic bedrock, and are in turn overlain by cemented aeolianites, similarly to what is observed at the Castelejo site (Figure 3d), so we considered this deposit as likely to be correlative of Castelejo terrace and therefore representative of the T1 terrace. This outcrop is usually buried by the modern beach sand and exposed only during extreme storm events.

2.6 Historical Seismicity and Coastal Deformation

Southwest Portugal has not experienced any significant earthquakes generated by inland active structures for at least as long as there are historical records, that is, in the past 2000 years. However, this region has been affected by several large earthquakes generated from off-shore sources, the most significant being the 1st November, 1755 event. Other relevant historical earthquakes have also been reported for this region, such as the 382 AD (Brito, 1597) earthquake, referenced to have caused the submersion of three islands offshore of Sagres, but descriptions also suggest a macroseismic area extending along all of the Mediterranean coast, including Palestine, so the reliability of such reports is dubious.

There is still no consensus about what structure or structures were the sources for the 1755 earthquake, which was a complex earthquake with three distinct periods of shaking that are considered as sub-events and that possibly reflect a complex rupture pattern with rupture of multiple faults. Several structures are considered as plausible major candidates to have ruptured, such as the Marquês de Pombal, Horseshoe or Gorringe Bank faults. Considering their size, geometry, kinematic characteristics and distance to the shore, it is expected that along the coastline the crust would not suffer any significant vertical deformation. However, if some other fault located closer to the shoreline ruptured in this complex earthquake, some vertical movement may actually have occurred along the coastal region.

Despite all of the detailed descriptions about the 1755 earthquake and resulting effects at many places in southern Portugal, there is no specific mention or known description of relative sea level changes along this southwestern shoreline. This may be partially due to the fact that within 15 to 20 minutes after the earthquake, the coastal area was hit by a large tsunami, which destroyed all of the anthropogenic structures such as harbors, wharfs and other structures, so that people lost all sea level reference frames. Further, the tsunami was so powerful that it generated a large flood and debris field that may have masked any subtle changes. The only relevant report concerns the mention to a harbor at Aljezur, located about 5 km inland from the coast, which connected with the ocean through a deep river channel. Descriptions from a few years after the earthquake reported a decrease of the navigable depth of the channel (Lopes, 1842). However, at the mouth of this river, at Amoreira beach, no vertical change was identified in the Holocene sea level references (T0 in this work), so that a plausible explanation is that the river may have silted up due to the numerous landslides reported in the region as a result of the earthquake.

Hidson *et al*. (1999), based on foraminifera and ostracod assemblages from the sedimentary fill sequence of a fluvial valley at Boca do Rio, located near the southern coastline (Figure 2), inferred an abrupt change from a marine to a brackish environment in this valley at about 1800 to 1300 years ago. They interpreted this change as a consequence of the development of a sand dune barrier, which may have isolated the fluvial valley. However this environmental change may also be the consequence of a minor uplift event, preventing the ocean water from penetrating inland. Koortekas and Dawson (2007) in their study of the 1755 tsunami, also studied a sedimentary fill near the coast at Sagres, 12 km to the west of Boca do Rio, and corroborate a change from a marine to a brackish environment, about 1700 years ago. In fact, a large earthquake is inferred for the area in 382 AD, as mentioned above, so an associated vertical deformation is an open hypothesis. Koortekas and Dawson (2007) also inferred that after the 1755 earthquake and tsunami, this area was subjected to dryer and higher elevation depositional conditions, suggesting that minor uplift might have occurred.

2.7 Discussion

2.7.1 Marine Terraces Correlation

T1 is the lowest terrace recognized in the region (Figure 9). We identified distinct sections or segments for this single terrace at elevations starting from 1.5–2 m for the outer flat section, up to an inner edge at about 8 m elevation, with a similar morphology to the modern marine terrace. We recognized T1 in the west coast at Amoreira, Bordeira, Castelejo and in the south coast at Ingrina and Furnas, at consistent elevations.

T2 is the second terrace present in this region (Figure 9), and correlative sections of this terrace were identified along the west coast at Carrapateira, and along the south coast at Ingrina, exclusively in areas with limestone bedrock. These are areas which are more resistant to erosion and preserved from modern cliff retreat. We have identified the inner edge of this terrace at a consistent elevation of about 21 m.

The best-preserved terrace sequence is at the Ingrina site (Figure 4), where several surfaces with multiple marine features are interpreted as a complete sequence of two marine terraces with shore-line angles at elevations of 8 m and 21-22 m, respectively. At this site, paleo sea cliffs and remains of surfaces with inner edges at about 26 m, 33 m, 37 m and 45 m were also recognized, but details of these surfaces will not be described in this work. Ingrina is the key site for the interpretation of the regional marine terraces sequence for this region, as the terraces are well-preserved and morphologically exposed. We interpret their ages to range from late to middle Pleistocene, and this interpretation is corroborated by the presence of similar surfaces with the same elevations at other locations along the Southwest Portuguese coast, such as at the Furnas, Castelejo and Carrapateira sites (Figures 5, 6, 7and 8).

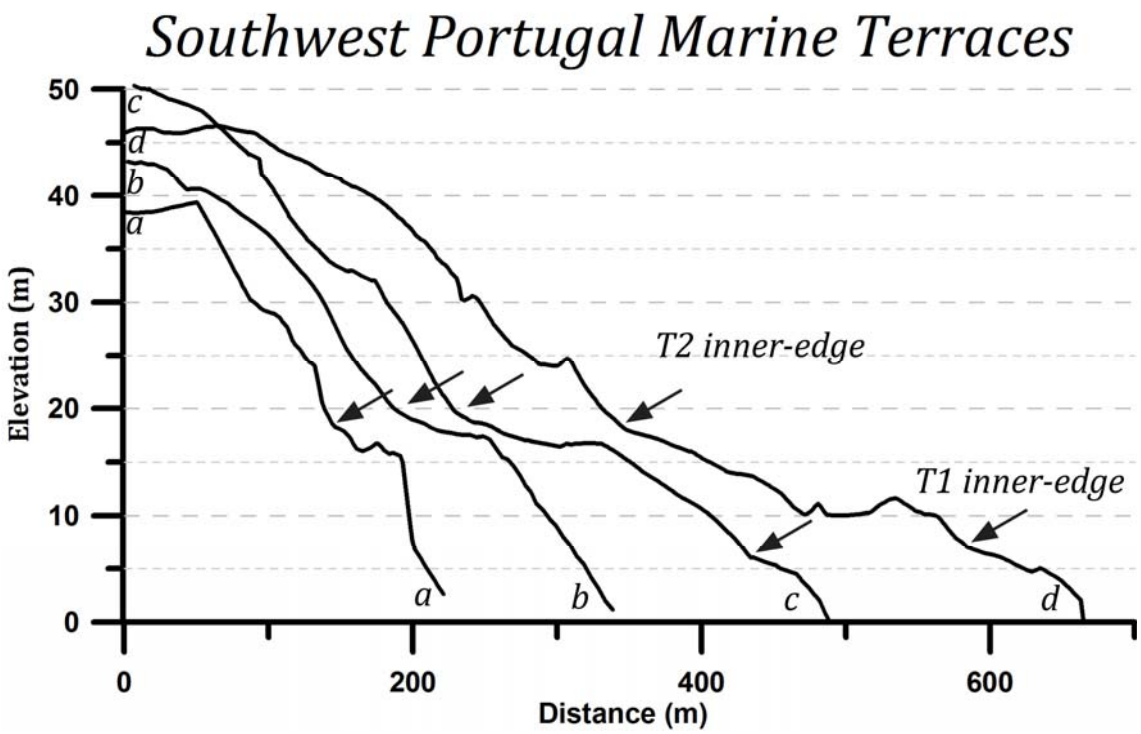

Figure 2.9 – Southwest Portugal marine terraces topographic section profiles, surveyed with GPS- RTK: (a) North Carrapateira; (b) South Carrapateira; (c) Eastern Ingrina; (d) Western Ingrina. T2 inner edges are visible in all profiles at equivalent elevations and T1 inner edges are only visible at Ingrina profiles, due to erosion at Carrapateira.

2.7.2 Terrace Ages and Interglacial Interpretation

During the Pleistocene climatic oscillations, sea level fluctuated between low stands (glacial times) and high stands (interglacial times). Only one of the sea level high stands during the past 130 ka is interpreted to have been higher than current mean sea level, which was during the beginning of the last interglacial period, i.e. the MIS 5e (or MIS 5.5), the oldest of the 3 peaks (5a, 5c, and 5e) of interglacial MIS 5 (Shackleton & Opdyke, 1973, Bloom *et al*., 1974, Siddall *et al*, 2006) (Figure 10). This higher peak was also a long lasting one, starting from about 128 ka to 116 ka (Muhs *et al*, 1994; Muhs *et al*. 2002a), so it should have generated a broad wave-cut platform and marine terrace.

Several studies have been concerned with the elevations of MIS 5e marine terrace features, and their corresponding age, at different locations around the world. The eustatic sea level at the time of MIS 5e has been estimated to be in the range of +2 to +9 m (Hearty *et al*., 2007; Sidall *et al*., 2006; Pedoja *et al*., 2011) with a high probability to have reach +6.6 m (Kopp *et al*., 2009). These compilations have been derived from many sources and regions, implying the application of various geochronological methods to distinct paleo-sea features at different latitudes and in distinct coastal environments. This is discussed by Dutton *et al*. (2012), who also discuss the impact of glacial–hydro-isostatic processes induced by the weight of large ice sheets and water volume changes in the ocean basin promoting deformations in the earth surface, and consequently influencing the positions of the paleo-shorelines. These

deformations occur with different intensity and rate according to their geographical proximity to the ice sheets and also with different timing accordingly with the ice sheet melting time and hydro-isostatic processes. Dutton *et al*. (2012) state that for MIS 5e, the relative sea level was not the same for everywhere on Earth, as the sea level response would not be synchronous, and consequently MIS 5e could have distinct time frames and different elevations for areas according to different glacial–isostatic responses to the ice sheets weight. Rockwell *et al*. (1989) commented about the correlation between paleo sea level references at near equatorial locations such as Barbados and New Guinea and their own observations for the southwest Californian and northwest Mexican coastline at middle latitudes, suggesting a worldwide variation in the relative sea-level of some meters, which if not taken into account then would have an implication on the estimating of vertical motions on a slowly rising coastline, such as Portugal.

In this work, we will primarily consider the MIS 5 sea level references for regions with oceanic rocky coasts at equivalent latitudes that are expected to be similar to the southwest Portuguese coast (Rockwell *et al*., 1994, Muhs *et al*. 1994; 2002b). Thus, we will consider a eustatic sea level reference of +4 to +6 m for the MIS 5e (Rockwell *et al*., 1989; 1994; Muhs *et al*., 2002b), of -2 to -4 m for MIS 5a (80 ka) and of zero to -2 m for MIS 5c (105 ka).

Due to global observations that indicate sea level was 4-10 m above the present mean sea level during the MIS 5e, we expect not only a broad wave-cut platform to have been generated, but also that the corresponding paleo morphology would be emergent, unless the coastal region of Portugal is significantly subsiding. Previous vertical motions studies conducted in Portugal have suggested that this area has been subjected to uplift since the Pliocene, although with a low rate of less than 0.2 mm/ a (Cabral, 1995). It is therefore expected that the more recent interglacial marine terraces should be at least locally preserved, and at elevations that are now higher than elevations at which they were originally formed. It is also expected that they should be well represented and preserved, unless the Holocene erosion rates are sufficiently high so as to have removed all lower terraces. Although the latter is clearly the case in some areas, the presence of significantly elevated marine terraces to 360 m (Fonte Santa), along with the deeply incised canyons and valleys in the Algarve region all support coastal emergence. Thus, the presence of the MIS 5e terrace is expected to be preserved in SW Portugal, albeit only locally.

We have recognized two low terraces that are reasonably well preserved at four locations along the southwestern coast of Portugal, the T1 and T2 terraces with inner edge elevations at 8 m and 21 m, respectively. Comparing these two terraces, the one which has a broader expression is the T2 terrace, where it was possible to us to identified 3 distinct sub-sections, interpreted as morphological segments of a single wave-cut platform. Also, T1 seems to have been cut into the T2 terrace. With this reasoning, we infer that T2 likely corresponds to MIS 5e and that T1 would then correspond to MIS 5c or MIS 5a.

MIS 5c corresponds to a very short peak at 103-105 ka, which may have later been reoccupied by the longer MIS 5a highstand at 80 ka. Thus, the 5c terrace level is commonly not distinguishable from the 5a terrace for regions of low uplift rate, as it has most commonly

been cut out (Hanson *et al*., 1994; Muhs *et al*. 1994; 2002b, Kern and Rockwell, 1992; Rockwell *et al*., 1994). We therefore infer that T1 should correspond to the MIS 5a highstand, and that T1 terrace likely reoccupied or cut out the slightly older MIS 5c terrace section, which is not preserved.

Another factor that tentatively supports the correlation of the T1 and T2 levels to the MIS 5a and 5e global highstands is that their elevations and spacing are nearly identical to the well-dated MIS 5a and 5e terraces at localities in central and southern California (Hanson *et al*., 1994; Muhs *et al*., 2002, Kern & Rockwell, 1992) northern Baja California, Mexico (Rockwell *et al*., 1989), and Tangier peninsula, Morocco along the Strait of Gibraltar (Abad *et al*. ,2013). Areas undergoing slightly high rates of uplift show that the elevation difference between these two terraces increases as their respective terrace elevations increase, as would be expected if paleo-sea level were similar (Hanson *et al*., 1994; Rockwell *et al*., 2002).

If our correlation is correct, then T2 has been uplifted approximately 13 m since the last interglacial (21 m minus the modern inner edge elevation (+2m) and minus the assumed +6 m at the time of formation). There are no references for the precise time and duration of the MIS 5e along the Portuguese coast. Data compilation analysis suggest that the last interglacial had an average duration from 130 ±2 ka to 119±2ka (Hearty *et al*.2007and references within). However, as abrasion terraces are cut during the entire length of the highstand, terraces ages should correspond to the end of the interglacial period. Speed and Chang (2004) recognized at Barbados abrasion terraces the latest MIS 5e peak, that lasted from 127 ka to 120 or to 115 ka; Dabrio *et al*. (2010) through a prograding barrier claims a 10± 2 ka duration for a highstand during MIS 5e for the southeast Spain, but without presenting accurate ages for the interval; Muhs *et al*. (2011) through a fossil reef complex at Florida, identifies a peak that has likely started at 127 ka and lasted until 114 ka, but with some uncertainties due to the reef characteristics. However, Muhs *et al.* (2002b), based upon high precision dating of solitary corals from the MIS 5e terrace along the west coast of North America, suggest that the last interglacial peak lasted from ~128 ka to 116 ka (and may have been double peaked). Thus, we considered that is very likely that the last MIS 5e peak lasted until 116ka and we infer the 13 m of uplift occurred after about 116 ka, yielding a long term uplift rate of 0.11 ± 0.01 mm/ a. If sea level had already begun to drop towards the end of MIS 5e time, then this rate will increase accordingly.

The sea level reference for the MIS 5a, relative to the MIS 5e shoreline elevation, was 2 m to 4 m lower than the modern sea level, as determined for abrasion terraces along the west coast of North America (Muhs *et al*., 2002b, 2004).

Taking into consideration this 0.11 ± 0.01 mm/ a for the last 80 ka, we should expect 8 to 10 m of uplift, meaning that the 80 ka zero sea level reference should now stand at an elevation of 6 m to 8 m. Thus, we consider that the T1 inner edge that is present at approximately 8 m elevation correlates to the MIS 5a marine terrace. The lower surface section of T1, recognized mainly at Castelejo and Furnas, with some remains preserved and reoccupied by the modern wave-cut platform and beach, corresponds to the subtidal section of the marine terrace, exposed during MIS 4 and MIS 3, when it was probably covered by aeolianites.

If the southwest of Portugal is rising at this slow rate (Figure 10), we expect that other marine terraces, such as those that correspond to the MIS 7 and MIS 9 highstands, have been uplifted as well. In fact, we have already identified features that might correspond to their inner edges at elevations consistent with this rate, but further work is needed to characterize this sequence.

Additional marine terraces at higher elevations have been also recognized, although they are typically poorly preserved, towards the regional abrasion surface identified at 120 – 130 m elevation, which should be middle Pleistocene in age. Further work is needed, especially to constrain the age of the sediments and the age of the erosional surfaces when sediments are not present, to properly assess the long-term rates of vertical motion.

2.7.3 Historical Seismicity and Marine Terrace Vertical Deformation

Efforts were made to identify co-seismic evidence of large earthquakes that have affected this area, but no irrefutable evidence was found. Assuming the uplift rate for this area is 0.11 ± 0.01 mm/ a as inferred, we would only expect a little more than 1 m of uplift for the entire Holocene, meaning that either the source (or sources) that are responsible for this vertical motion have long quiescence periods and have not ruptured since the modern sea level stabilized or that the resulting effects were so small, centimetric to decimetric scale, that they would not be differentiable in a high energy mesotidal environment coast such as SW Portugal.

It is possible that a small vertical motion has been identified through interpretation of abrupt changes in the sedimentary fills of two fluvial valleys near the coastline (Boca do Rio and Martinhal, at Sagres), and that this may have happened twice, once following the 382 AD earthquake and again following the 1755 earthquake. However, it is also possible that these environmental changes were partially due to the local perturbations caused by the tsunami flooding, local landsliding, or for other reasons.

The closest large active structure known in this region is the Marquês de Pombal thrust, a 70 km long structure located circa 100 km west-southwest from Sagres, and motion on this fault is not likely to have produced vertical motions at the coastline. Thus, if there was any vertical motion associated with these two historical earthquakes, it is likely to have been generated by a more local, currently unknown source.

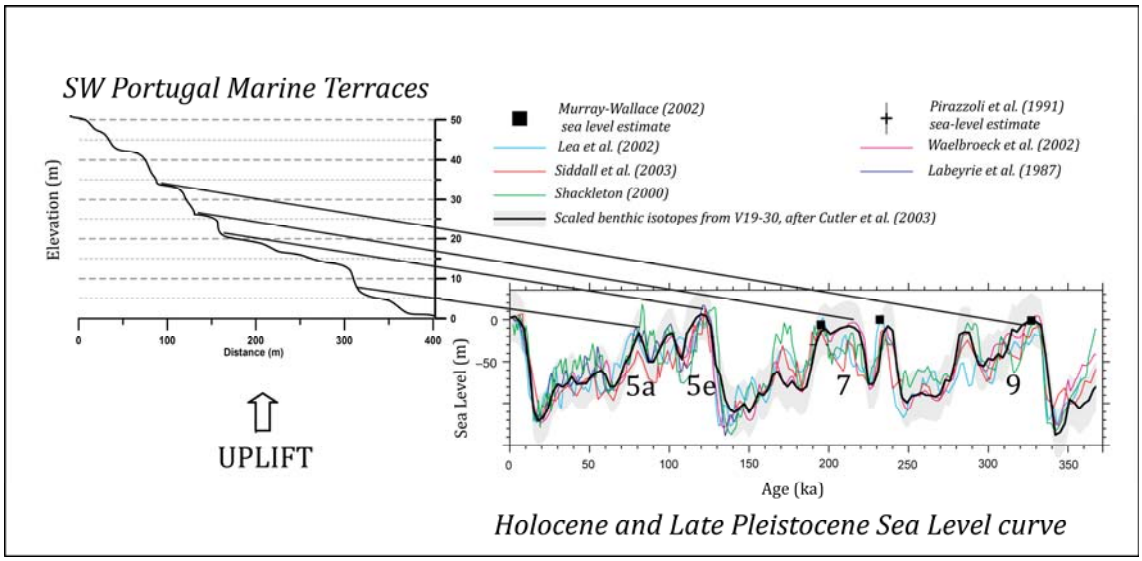

Figure 2.10 – Schematic Southwest Portugal marine terraces correlation with paleo-sea level estimates compiled from different studies: MIS 5a, MIS 5e, MIS 7, MIS 9 interglacials are identified (adapted from Siddall et al., 2006).

2.8 Conclusions

We recognize several marine terraces along the southwest Portuguese coastline, with the lower two (T1 and T2) probably correlating to abrasion terraces cut during the last interglacial period of relative sea level highs (MIS 5). These two terraces were surveyed, and corresponding paleo sea level features were identified. Considering that the MIS 5e marine terrace should be the higher and better preserved of the two, we assumed that it corresponds to T2. If correct, this implies an uplift rate of 0.11 ± 0.01 mm/ a, which also corroborates the T1 marine terrace as the result of the MIS 5a marine high stand. A sequence of higher marine terraces is present, although they are poorly preserved, towards the higher regional abrasion surface, which according with to this rate, should be Middle Pleistocene in age (1 to 1,2 Ma).

This section of the Portuguese coastline is rising at rates not recognized for other regions in south Portugal, suggesting that an unknown local tectonic source be responsible for the long-term uplift of this region.

Acknowledgements : *This work was funded by Fundação da Ciência e Tecnologia, through a PhD scholarship (SFRH/BD/36892/2007) attributed to Paula Marques Figueiredo and Research Project "Paleoseismological study of active faults in Mainland Portugal" (PTDC/CTE-GIN/66283/2006), co-financed by FEDER. The authors also are thankful to Filipe Rosas for providing figure 1 and to Hector Perea whose comments significantly improved this manuscript.*

Chapter 3

The Plio-Pleistocene regional abrasion platform in the Southwest of Portugal (Iberian Peninsula) as evidence of regional uplift

(This chapter is presented in a paper format since it is being prepared to be submitted to a science journal, and it is still in preparation)

Figueiredo, Paula M. (1, 2), Rockwell, Thomas K. (3), Cabral, J. (1,2), Cunha, P. (4), Rood, D. (5)

Abstract:

A large regional elevated surface in the southwest of Portugal corresponds to an extensive marine abrasion platform (Feio, 1951; Pereira, 1990) forming a relevant geomorphologic element along the southwest coastal zone. This regional surface can be as wide as 10 km and is recognizable over circa 100 km along the coast and it is compound by a sequence of spatially close marine terraces generally poorly preserved and with scarce sediments. Its genesis is interpreted as a polygenic surface likely having begun to form during the Miocene, and re-trimmed during Pliocene and Pleistocene times, as evidenced by marine terrace remnants. The elevation of this regional surface varies between 40 m to circa 160 m, providing evidence for regional uplift. The surface itself is also displaced by the São Teotónio – Aljezur - Sinceira fault system, a NNE-SSW left – lateral 50 Km long active tectonic structure, which downthrows the erosional surface into several tectonic basins. The recognition of Pliocene and Pleistocene marine terraces is fundamental not only to evaluate how much Pliocene and Pleistocene marine transgressions extended inland, but as a way to understand the regional Plio-Pleistocene deformation, namely the regional uplift rates and activity rate of the São Teotónio–Aljezur-Sinceira fault system. Several marine terraces are here presented, one of which, with an inner-edge at about 80 m, provided an age of 2.0 Ma +0.3/-0.2, allowing to estimate an uplift rate in the range of 0.03 to 0.04 mm/a in the Southwest region for the early Pleistocene. Recent OSL ages for a lower marine terrace indicate an age of circa 110 ka for beach sand underlying an aeolianites with an age of circa 90 ka, suggesting that the marine terrace corresponds to MIS 5c. If that the case, then this is evidence for a higher uplift rate during late Pleistocene, meaning that the uplift rate has increased through time.

3.1 Introduction. The Regional Surface

The more significant geomorphologic element throughout the coastal zone of Southwest Portugal is a wide and flat surface trending parallel to the coastline, with slopes ranging

between 0.5 to 1,5 % and a width that varies from 5 to 15 km along a length of approximately 100 km (Feio, 1951). This abrasion platform is frequently covered by a thin cap of sediments, typically sands often with interbedded coarser sands and finer silty sands, which are never more than a few meters thick. The bedrock, which corresponds mostly to Paleozoic rocks from the South Portuguese Zone of the Iberian Variscan Massif, is eroded and is occasionally overlapped by a coarse deposit with sub-rounded blocks followed by well sorted sands, which have been interpreted as a beach deposit sequence. The presence of sediments is pervasive in the northern area whereas southward, sediments are scarce, poorly preserved and sediment remnants are evidenced by scarce rounded quartz pebbles overlaying directly the bedrock. The elevation of this surface is considered not to exceed 150 m (Feio, 1951) although elevation gradually increases towards the south similarly to the sea cliffs height which varies from less than 10 meters height south of Sines but reach 130 m at the Vila do Bispo area at the south. The drainage incision is also higher towards the south, which together with the increase of elevation and decrease of sediments thickness suggests a southwards increase in the regional uplift rates. Towards the southeast, at the Sagres area, the regional erosional abrasion platform transitions to several discrete surfaces cut into the Mesozoic sandstone, marl and limestone bedrock of the Algarve Basin (Pereira, 1990), which may actually correspond to a sequence of closely spaced, poorly preserved, Pleistocene marine terraces.

The regional abrasion platform is deformed by the NNE-SSW left – lateral São Teotónio-Aljezur-Sinceira strike slip active fault system (STASFS), with a length of approximately 50 km, which downthrows the regional abrasion platform into several narrow tectonic basins, namely (from the north to the south) the São Miguel, Aljezur, Alfambras, Pedralva and Sinceira basins. These tectonic basins have in general some kilometers in length and a width of some hundreds of meters, and contain inside sediments dating from the Miocene to the Quaternary: some of the sediments that are preserved inside the tectonic basins, as the Miocene carbonate sediments in the Aljezur basin which date from the Burdigalian to the Tortonian (Pais *et al*., 2012) have a marine genesis and are inferred to be displaced from an older abrasion platform.

A detailed characterization of the regional abrasion platform was conducted a few decades ago by Pereira (1990), who divided this geomorphologic element into three distinct sectors (Fig 3.1):

- A northwestern abrasion platform, north of Odeceixe, called the “Vila Nova de Milfontes sector”;
- A southwestern abrasion platform, south of Odeceixe towards Telheiro near Sagres, called the “Arrifana sector”;
- And a southerly abrasion platform, approximately from Telheiro towards Lagos called “Meridional littoral platform”.

The present study was conducted along the “Arrifana sector” and part of the “Meridional littoral platform” of Pereira (op. cit.) which correspond approximately to an area covering the Aljezur and Vila do Bispo municipalities: for this area we were granted a high resolution digital topography at the 1/10,000 scale which allowed us to conduct detailed morphologic analyses

complementary to the extensive field surveys. We denominate this region as the Aljezur-Vila do Bispo region.

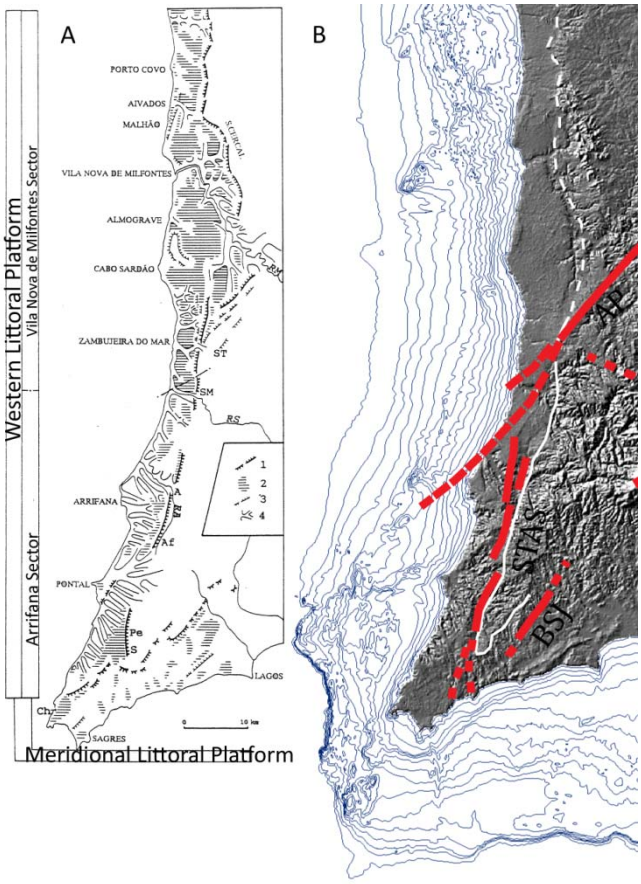

Figure 3.1 – Regional Abrasion Platform along the southwest Portugal coastline.. (A)- Characterization and sector division according with Pereira (1990) is also included 1- Littoral Platform inneredge; 2- areas with slope ≤1°; 3- slope changes in the littoral platform and aligned with the relief Carregousal- São Teotónio; 4- littoral platform indentation (adapted from Pereira, 1990); (B) Shaded relief map for the southwest Portugal overlaid by major active structures, marked by red line and regional inneredge, drawn with line: AP – Alentejo Placencia fault; STAS- São Teotónio- Aljezur- Sinceira fault system; BSJ – Barão de São João fault.

In this region, the regional abrasion platform generally exhibits a very smooth topography with a slope varying from 4 to 7%, except for the circa ~130 m surface in the vicinity of Vila do Bispo-Sagres , which exhibits a slope lower than 1% (Fig. 3.2). The abrasion platform extends inland gently increasing in elevation from the coastline, where elevations vary from 90 to 120 m, towards the interior at a higher altitude paleo-shoreline. The shoreline angle, which was previously described at circa 200 m in elevation (Feio, 1951; Pereira, 1990; Dias, 2001) is difficult to recognize at this elevation due to the strong drainage incision that has partially erased its expression.

Fig. 3.2- Regional abrasion platform in the Sagres vinicity, view from south of the Castelejo beach towards the north. Here, sea cliffs have a height of circa 130 m. It is possible to observe the wide flat surface corresponding to the abrasion platform. At Castelejo beach, remnants of a marine terrace overlaid by sequences of consolidated aeolianites is reoccupied by the nowadays sea level. Very incised creeks, form valleys that were partially covered by Holocene, MIS 2 and MIS 3 aeolianites.

Field surveys and geomorphologic analyses evidenced a distinct change of slope from a lower smoother topography towards a higher, rough topography, at circa 160 m elevation, which we assume to correspond to the regional inner-edge for the abrasion platform (Fig. 3.3). This is consistent with changes in the cover sediments at the elevations close to 160 m: medium grain sands with quartz pebbles inferred to be beach or marine sands, although sparse and weathered, can be continuously tracked from 155-160 m elevation towards lower elevations (~100 m) adjacent to the coastline. Nevertheless, sediments are present at elevations higher than 160 m until about 190-200 m NE of Aljezur, which we interpreted as corresponding to aeolianites that are locally interbedded with alluvium deposits. Both observations suggest that the shoreline angle elevation for this regional abrasion platform is effectively close to 160 m.

At the regional abrasion platform of the Aljezur-Vila do Bispo region, sediments are frequently absent or occur as poorly preserved thin remnants of beach deposits consisting of sands with rounded quartz pebbles along what are probably marine terraces remnants. Our interpretation of the regional abrasion platform morphology is that it corresponds to a sequence of closely spaced marine terraces. The individual inner edge for each of these marine terraces is generally difficult to track, since it has been smoothened and locally eroded through time. The elevation difference between successive terraces seems to be small in most cases, which all together makes it additionally difficult to separate individual terraces. Nevertheless, detailed field surveys and high resolution digital topography allowed us to detect individual marine terraces, although frequently it was not possible to map their inner and fore edges.

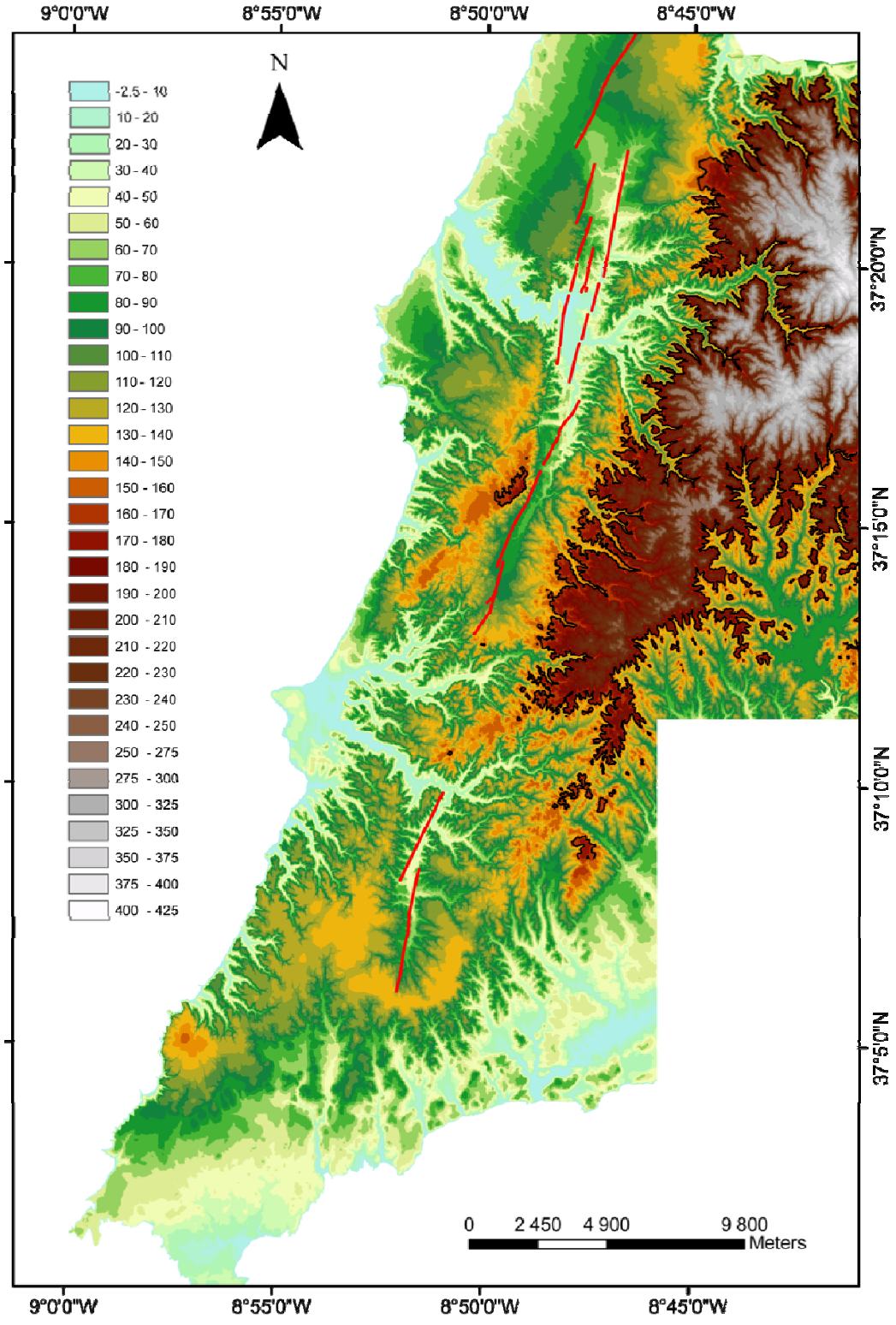

Fig.3.3 – Hipsometric map of Aljezur and Vila do Bispo municipalities areas, based upon 1/10.000 digital topography. Elevation intervals legend is included in the image. The black line represents the 160 m elevation, which we assume as corresponding approximadetely to the regional abrasion platform inneredge. The known active traces of São Teotónio-Aljezur-Sinceira fault system are mapped as red lines.

Despite the difficulty to individualize marine terraces along much of the regional abrasion surface, distinct flat surfaces are present which, when within a constant elevation interval and with remains of marine sediments, where interpreted as marine terraces trimmed (or re-trimmed) during the same sea-level position. Among these flat surfaces, the larger one corresponds to a surface at height of circa 130 m, best expressed north of Sagres, close to Vila do Bispo village and along the west block of STASFS, especially aside the Aljezur and Alfambras basins. This 130 m high surface seems to be displaced by the STASFS Aljezur and Sinceira fault segments.

The age assumed for this regional abrasion platform is likely to be late Pliocene to early Pleistocene, although its genesis and development has been interpreted as polygenic with re-trimming probably since the Miocene as a consequence of several episodes of marine transgression, either related with eustatic sea level fluctuations or related with tectonic deformation. Miocene carbonate sediments are preserved inside the tectonic basins, and were not found on the abrasion platform, although it is possible that remnants of Miocene sandy deposits may also be present on it. In the study region remnants of marine sediments commonly overly a very flat abrasion surface trimmed on Paleozoic bedrock which is locally at elevations close to 90-100 m. A thick argillic paleosol rich in ilite, characteristic of temperate xeric soils, typically occurs on the Paleozoic bedrock beneath the marine cover. The presence of this thick soil indicates that after the trimming of the Paleozoic bedrock there was a period of marine regression and subaerial exposure under conditions of minor erosion, promoting the soil profile development, followed by another marine transgression that deposited younger marine sands that overlaid it.

Our interpretation is that a Piacenzian trangression related to a eustatic high-stand re-trimmed a previous erosion platform inferred to be Miocene by the marine sediments of this age that overlie it, and finally, during the Pleistocene interglacial periods, the Pliocene abrasion platform was re-occupied and Pleistocene terraces were built on it.

Consolidated sand dunes are frequently present covering the Pleistocene marine terraces, namely close to Aljezur, Carrapateira, Castelejo and Sagres areas, inferred to correspond to late Pleistocene sea level lowstands younger than the MIS 5. Some of these dunes were dated with C14 which provided ages ranging from 35 -36 ka cal BP for the Castelejo and Telheiro sites. A younger dune generation, with ages ranging from 19 to 23 ka cal BP, was also identified at Sagres and Castelejo (Martins, 2014), having been interpreted as belonging to MIS 3 and likely also to MIS 2. Holocenes dunes are present generally close to the sea level, although some are present at the top of the sea cliffs but without being consolidated. There are no ages available for the consolidated aeolianites at Carrapateira, neither for the thick sequence of consolidated aeolianites at Monte Clérigo, close to the Aljezur River mouth

There are no ages available for the regional abrasion platform sediments or surfaces, except for the Miocene sediments preserved in the tectonic basins. The ages of the abrasion surfaces and of the overlaying remnants of marine sediments have been inferred by correlation with equivalent sediments or surfaces at other regions in Portugal and Spain.

However, these regions may not have been subjected to the same deformation and vertical motion rates, and therefore their marine surfaces may not be suitable for a proper correlation.

3.2 The Marine Terraces

A detailed geomorphologic analysis was conducted along with field surveys aiming to recognize marine terraces along the regional abrasion platform. Frequently, marine terraces correspond to erosional features, where sediments are absence and evidences of inner-edges are scarce. We conducted this survey along the entire field area, and the height of remnants of sediments and of morphological features were measured with GPS-RTK survey equipment (Leica 1200 series) which provided us precise elevation with errors in the centimeter range. Distinct surfaces were recognized within the Aljezur area and further south, at the Vila do Bispo area with similar elevations.

At the Aljezur area we recognized a break in slope from a lower smoother topography to a higher and rougher morphology at circa 160 m, which we have assume to correspond to the regional inner-edge for the regional abrasion platform. This feature is not present southward, at the Vila do Bispo, since the landscape here has elevations lower than 160 m (Fig. 3.3).

Rising above the abrasion platform there are some isolated reliefs with elevations higher than the inferred inner-edge, as at Valinhos, near Aljezur, that reaches 180 m, or at Torre de Aspa, near Sagres, that reaches 154 m. Both elevations lack marine sediments, and present a thin soil profile, with some angular blocks at the surface probably resulting from the physical weathering of the schist bedrock. At Torre da Aspa site, a lower surface was recognized inserted on this higher morphology. We interpret these observations as evidences to consider those higher morphological features as residual reliefs.

At the Aljezur area, an approximately E-W transect west of Alfambras towards the shoreline allowed to recognize most of the marine terraces evidences for the Aljezur area. West of Alfambras, at circa 160 m, there is a poorly preserved very thin cap of sand with rounded quartz pebbles as residual coarser sediment, which is covered by an iron cap. From approximately 150 m to 140 m height, a yellowish sandy unit with red streaks, generally medium to coarse grained, is frequently present never exceeding circa 0.5 m thickness, and it is interpreted as marine sands. Towards the top, the sand becomes finer and enriched in iron with pebbles and cobbles from consolidated fine sandy unit with iron oxide cement. Remnants of this unit enriched in iron are widely scattered and occasional larger blocks probably still in situ are present. It was not possible to differentiate this unit as aeolian or marine sand. Evidences of an iron enrichment episode or episodes are frequently present affecting sediments or weathering the bedrock at elevations close to 150 m.

Sands are present mainly below 135 m, where a thin cap of marine sands, generally medium size, occasionally with sedimentary structures is covering a trimmed surface in the Paleozoic schist and greywackes. Locally, underlying the sands and overlying the Paleozoic basement, there is a level of cobbles of quartzite, quartz and greywacke. Less frequent are thin lens of silty sand, generally white to yellowish in color, generally interbedded within sandy layers. At this transect, these sandy layers can be identified until a height of approximately 130

m but are not preserved at lower elevations due to the short distance (less than a 1 km) to the coastline which favors a strong incision of the creeks.

At the regional abrasion platform in Vila do Bispo area there aren't elevations higher than approximately 140 m and the higher and more relevant surface corresponds to a flat surface at 120-130 m height with a slope < 1%, that reaches 10 km in length and can be as wide as 3 km. Similarly to the Aljezur area, where the 130 m surface bypasses the southern Alfambras tectonic basin, this surface also bypasses the Sinceira tectonic basin. On this surface is not possible to differentiate morphological elements belonging to marine terraces, but along this surface there are marine sediments very similar to those at Aljezur, at similar elevations. Towards the eastern side, at about 135 m, near Lagoa de Budens, a sequence is identified overlying the greywacke bedrock: a lower layer of cobbles followed by a sandy layer with clay and mica, underlying yellowish medium sand to fine gravel. This sequence is covered by a layer rich in iron concretions. The thickness of this deposit is variable, but it can reach more than one meter. Towards the west, at Mosqueiro, the sediments are now more homogeneous, and are characterized by fine to medium sands, fairly sorted, with some silt and clay, where occasionally some cross bedding can be identified. This deposit can reach a few meters in thickness which decreases towards the west, namely towards elevations reaching a height of 120 m to 130 m where the surface is now covered by a thin cap of sand and where abundant rounded pebbles of quartz are present.

From circa 110 m elevations, there is a differentiation between the area of Vila do Bispo-Sagres and the one close to Aljezur. At the south, at the Vila do Bispo area, the terraces are highly indented by the steep creeks and are not as preserved as the higher 120-130 m surface. Sediments are almost absent, and there is no soil profile, frequently the bedrock is exposed. Sparse round pebbles of quartz are frequent, some with an elongated shape, similar to almonds.

Close to Aljezur, terraces at circa 110 m elevation have remnants of marine sediments preserved, some with a thin soil profile, and a coarser layer with cobles is widely spread as a residual sediment. The same differentiation is also recognized for the 100 m surface, wherein sediments are not present at the Vila do Bispo area, and along Aljezur, specially at north of Aljezur a thin cover of marine sand is frequently present.

Approximately from 90/95 m to lower elevations, it is possible to identify small indentations in the abrasion surface, which we have interpreted as younger marine terraces embedded in the regional abrasion platform. Those marine terraces are not continuous, and generally do not extend much in area, but they frequently preserve marine sands. The distribution of those younger marine terraces it also varies within the study area.

At approximately 95 m elevation, north of Carrapateira, beach sediments are present, although very weathered. Near this site, no sediments were recognized at the regional abrasion surface, except here. The sediments correspond to beach sand, cemented by iron oxide.

In the Vila do Bispo- Sagres region, at Telheiro (Fig.3.4) a terrace trimmed in the Triassic bedrock is preserved with a thick sedimentary sequence, from the base to the top:

- Coarse basal deposit, generally less than 0.5 m thick, with frequent boulders ranging 20 cm in size, sub rounded to angular, from the Triassic bedrock, Paleozoic greywacke and some rare carbonate, with a matrix of coarse sand;
- Layer of round pebbles , mainly white quartz, size approximately less than 3 cm, interpreted as a beach sand;
- Sand, orange in color, generally of medium size with some coarser layers, rounded grains of quartz, rare feldspar. Finer sand units with some silt and mica, are present but rare. This unit evidences some fracturation;
- Another sandy unit, light brown in color, rare mica but silty matrix, interpreted as aeolianites, on which it is developed a paleo soil;

Figure 3.4- Marine terrace at Telheiro, circa 75 m elevation. (A) Basal coarse deposit at Telheiro beach; (B) General perspective of the marine terrace, it is visible the sedimentary sequence at the aeolianites at the top; (C) marine sands partially covered with consolidated aeolianites.

It is not clear the position of the inneredge for this terrace, which is partially covered by aeolianites. An elevation of circa 80 m is inferred, based upon field surveys and detailed morphological analysis.

Recently, this terrace was sampled for Cosmogenic Nuclide dating, and a preliminary result was obtained (Fig.3.5). Quartz clasts from the basal unit were collected for 26 Al and 10 Be, providing an age o2.0 Ma +0.3/-0.2, which combined with the inneredge of circa 80 m, allow us to estimate an uplift rate of 0.04 ±0.004 mm/a, for the early Pleistocene.

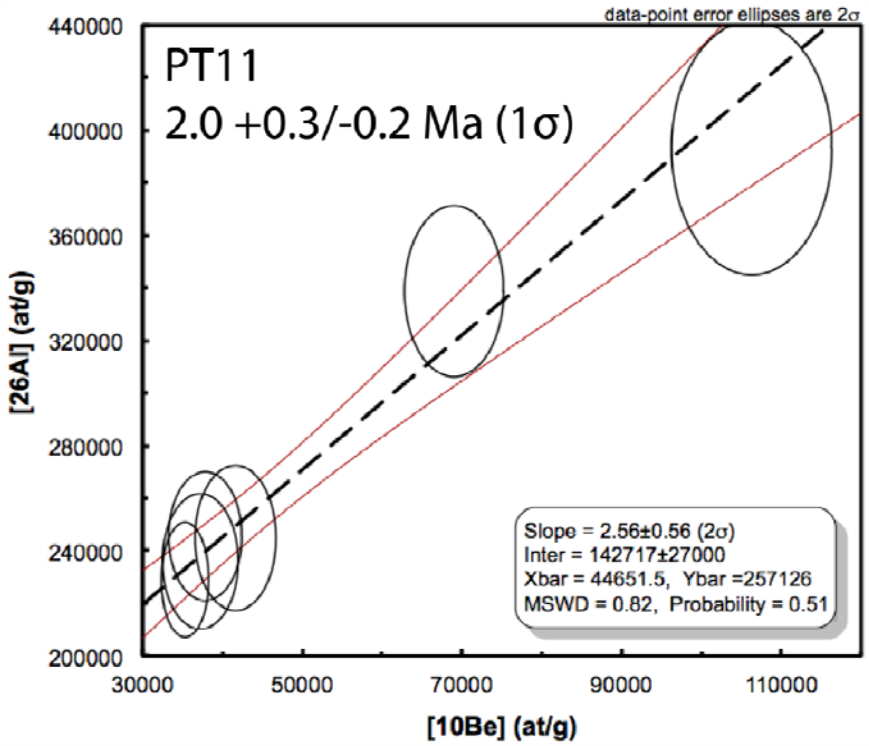

Figure 3.5 – PT11 (Telheiro site) preliminary results for cosmogenic nuclide dating.

Other terraces at elevations ranging to 75- 80 m elevation were recognized north of Carrapateira, however at those other locations, no sediment is preserved like in Telheiro. Evidence for marine terraces is the abundant quartz rounded pebbles and at one site, a line of sub rounded allochthonous boulders was recognized and inferred as related with a paleo coastline.

An elevation at which several marine terraces were recognized, most of them with a thick sedimentary deposit is the 50-60 m elevation, especially along the coastal section Monte Clérigo-Carrapateira (Fig.3.6). Here, deposits of sand, overlying a basal coarse deposit are identified, and the sediment characterization reveals many similarities with the Telheiro terrace, further south. Sands are also orange in color, medium to coarse sands, interbedded with lens of coarser sand.

One hypothesis, to justify that these terraces deposits are better preserved along this coastal sections, is that these terraces are partially covered by consolidated aeolianites, which could have preserved them from erosion.

Figure 3.5 – (A) Perspective from the coastal section, with the steep sea cliff and at the top, at the regional abrasion platform, remnants of a marine terrace at circa 55 m elevation; (B) the basal coarse layer underlying the terrace sediments and overlaying the Paleozoic; (C) marine sands with coarser layers.

Occasionally, when the bedrock corresponds to carbonate lithologies, karsts are developed favoring the preservation of sediments due to the infilling of the karst

morphologies. We assume that the infilling of these karst features should be of Pleistocene, assuming that these features were submerged during the early to middle Pleistocene.

Additional marine terraces at lower elevations are also present. A wide surface is present at Carrapateira promontory at circa 40-45 m elevation, as well as at Sagres region. This surface is only present at carbonate bedrock, probably because the ones trimmed at the Paleozoic schist bedrock promoted the fast retreat of the sea cliffs and the destruction of the uplifted marine terraces. There are no ages for these terraces, nonetheless we believe it is reasonable to assume that it should have been trimmed (or re-trimmed) during middle to late Pleistocene.

Uplift rates for the late Pleistocene have been presented for the region, assuming the presence of MIS 5 marine terraces, and an rate of 0.11 ±0.01 mm/ a was inferred (Figueiredo *et al.*, 2013). However this study did not include absolute ages that supported that reasoning. Recently, we collected 3 samples to date through OSL (Optically Stimulated Luminescence) sediments from a marine terrace at Castelejo beach.

At Castelejo site, a terrace at circa 1.5 to 2 m elevation is been reoccupied by the modern

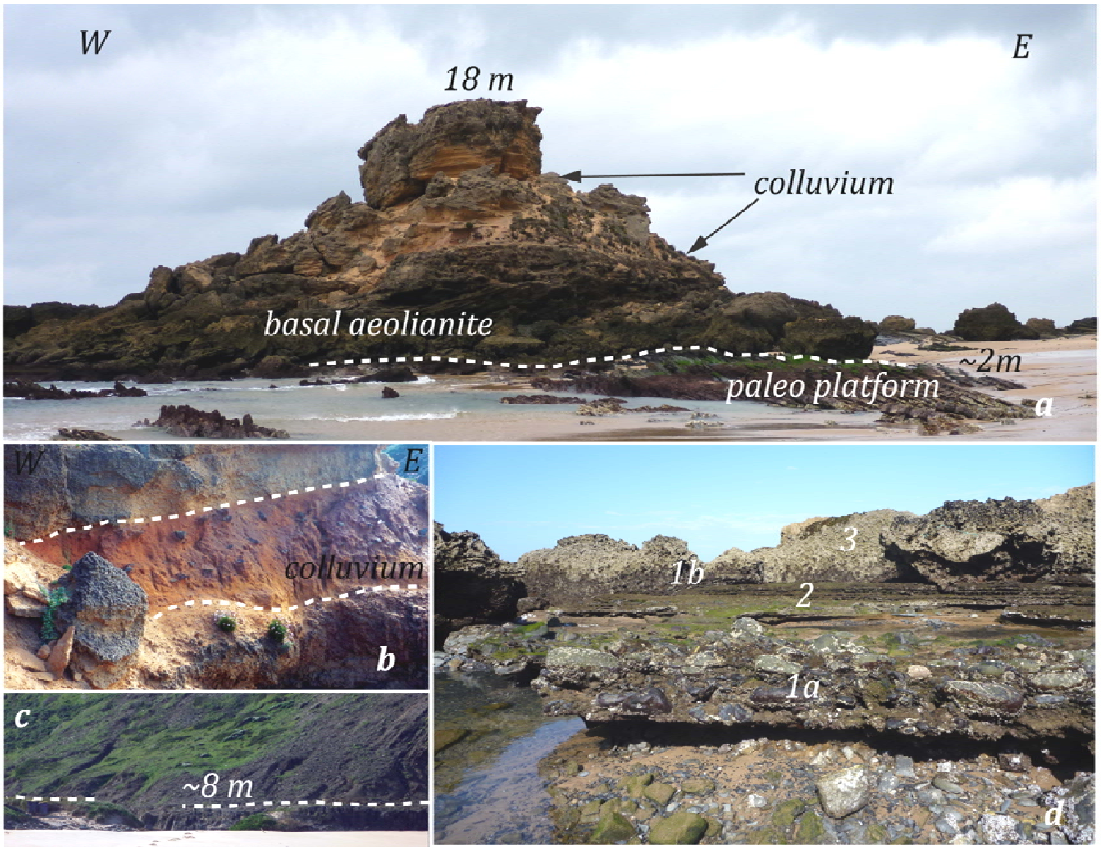

Figure 3.6 - Marine terraces at the Castelejo site. 2. a) Perspective of the aeolianites unit which lays on top of a paleo wave-cut platform; b) Detail of a colluvium wedge with soil development inter bedded with aeolianites. c) fluvial terrace at 8m; d) Sedimentary sequence on top of the paleo platform: 1a- basal coarser unit; 2- sandy beach unit; 1b- upper coarser unit; 3- aeolianites.

abrasion platform, which is essentially reoccupying and retrimming an older surface, as evidenced by the preservation of a wave-cut platform locally capped by sediments.

Overlying the abrasion platform, there are two conglomeratic layers separated by a thin beach sand layer overlain by strongly cemented aeolianites (Fig. 3.6).The top of these aeolianites was recently dated by C14, which provided an age of circa 35 ka cal BP. In order to constrain the age of this terrace samples were collected at the thin sand layer and at the base of the aeolianites.

We have collected two samples in the sandy layer interbedded with the coarser unit (layer 2 in Fig. 3.6 d) and one sample in the basal aeolianites.

For the selection of the site to collect samples for OSL, we followed a careful selection in order to avoid contamination of the sediment by secondary minerals. The sediment outcrop was excavated in order to remove the superficial layer exposed to the light and weathering, and an lightproof metal tube was inserted into the sediment, following the bedding or the sedimentary structure, in order to collect grains deposited at the approximate same period of time. Samples of the sediment were also collected to measure water content percentages. Then, the samples were prepared for the luminescence analyses, at a laboratory at Coimbra University with darkroom conditions, with the following procedure: the sediment was carefully removed from the tube, and from the sediment that was collected in the central section of the tube samples were sieved with water in order to individualize the fractions of 180 and 250 mm grain size, which were then subjected to HCl (at 10%) and H2O2 (at 10%) solutions in order to remove the carbonates and the organic matter. Samples were then dried and the quartz and silicates fraction was separated from the K-fedspar enriched fraction, through differential flotation in a heavy liquid solution of sodium polytungstate (with a density of 2.58 g/cm^3): K-feldspar has a density lower than 2.58 g/cm^3 and quartz and silicates have a density higher than 2.58 g/cm^3. The fraction of quartz and silicates was then subjected to a solution of HF (40%) during 60 minutes in order to obtain the quartz and the K-feldspar fraction was also subjected to a solution of HF (10%) during 20 minutes to remove the outer layers and clean the grains. Finally, both fractions were subjected to an HCl (10%) solution in order to remove remaining fluorides.

The next step was conducted at Risø, in the Nordic Laboratory for Luminesce Dating, Denmark. Results indicated that:

- The thin sandy layer was dated through the pIRIR method, measurements made in K-feldspar (both 18 aliquots), and the two samples provided ages of 112 ±7 ka and 110 ± 5 ka;
- The basal aeolianites dated through OSL with the quartz fraction, providing an age of 84 ±6 ka, while the K-feldspar through the pIRIR provided an age of 98 ±6 ka.

The age of the sand beach should be in the range of 110-112 ka, which was covered by aeolianites with an age of circa 80-90 ka. This strongly suggest that this terrace might correspond to the highstand MIS 5c, and that the aeolianites were deposited during the lowstand of MIS 5b. The eustatic sea level for the MIS 5c is less constrained than for the MIS 5e or even the MIS 5a, but it is know that MIS 5c was a lower highstand than MIS 5e, then this confirms that the terrace T2 identified by Figueiredo *et al*. (2013), with an inneredge of 21 m should be MIS 5e.

Due to the little constrain in MIS 5c eustatic sea level, we choose to estimated the uplift rate using T2 references of Figueiredo *et al*., (2013). The eustatic sea level for the MIS 5e has been estimated as to be in the range of +2 to +9 m (Hearty *et al*., 2007; Sidall *et al*., 2006; Pedoja *et al*., 2011) with a high probability to have reach +6.6 m (Kopp *et al*., 2009). Assuming that the MIS 5e may have reached +9m elevation, then T2 has been uplifted approximately 10 m since the last interglacial (21 m minus the modern inner edge elevation (+2m) and minus the assumed +9 m at the time of formation). If we assume that the eustatic sea level was +6.6 m, then we may infer a maximum of 12.4 m of uplift (21 m minus the modern inner edge elevation (+2m) and minus the assumed +6.6 m at the time of formation). The MIS 5e highstand started to recede circa 119-116 ka (Muhs *et al.*, 2002b; Muhs *et al*., 2011).

Considering a total of 9 m of uplift (or 12.4 m if we consider the initial MIS 5e position at +6.6m) during the last 119-116 ka, we calculate an uplift rate of 0.08 mm/a (or a maximum of 0.1 mm/a), corresponding to a mean uplift rate of 0.09 ± 0.001 mm/a.

We have now two uplift rates for the region:

- One, calculated through a early Pleistocene marine terrace, which is 0.04 ±0.004 mm/a;
- And another one, calculated through a late Pleistocene marine terrace and aeolianites, which is 0.09 ± 0.001 mm/a.

Both uplift rates are within the same range of magnitude, both are lesser than 1 mm/a, however the rate calculated for the late Pleistocene is about twice the rate calculated for the early Pleistocene, which points to a change in the vertical deformation velocity during Pleistocene, at the Southwest Portugal..

3.3 Driving Mechanisms for the Uplift

The uplift at the southwest Portugal, is not completely understood. Although, the region is located close to a plate boundary, this region seems to be uplift at faster rates than other regions at south Portugal. This evidence is supported by the deeply incised drainage, by the absence of sediments compared with eastern south Portugal, or even with regions immediately to the North. Southwest Portugal also exhibits sea cliffs higher than at other locations.

An immediate reasoning is to assume that the active faults recognized in the past decades in the Southwest Portuguese Margin could be promoting the uplift along this region. However, those faults, like the Marquês de Pombal, are located at a distance that would not condition any vertical motion for the inland region.

Other hypothesis is to assume that the vertical motion could be promoted by buckling due to large scale flexure of the lithosphere, and for that we would need to access how vertical motions would modify between Southwest Portugal and other: if it is a gentle modification, it could be due to buckling if it is a more sharp transition, then this transition should reflect other mechanism, such as a local tectonic source.

In fact, a local fault could justify the higher uplifts rates that seem not to be present at other regions. This fault is not recognized inland, and consequently must be localised along the offshore. As previously said, in order to have a constrain in the vertical motion inland, it needs to be located close to the coastline or having a very low dip in order to have a large area of rupture.

Several studies have been conducted during the past decades, and multiple seismic lines and other geophysical methods have investigated a large area along the Southwest Portuguese Margin, nevertheless studies along the continental shelf were never conducted.

From a simple analysis of the southwest Portugal continental shelf, it immediately stand out that the western continental shelf is shorter and with higher slopes than the southern one (Fig. 3.7). Although many studies need to be conducted and the quality of the data is very poor, it is possible to detect a variation along the bathymetrical lines, which seems to be structural and not due to slopes controlled by the eustatic fluctuations during the Pleistocene. Taken this into account, we considered that this could be evidence for a structure located along the continental shelf, and if so, then it should be active because it is deforming the continental shelf topography and can also be responsible for the ongoing uplift.

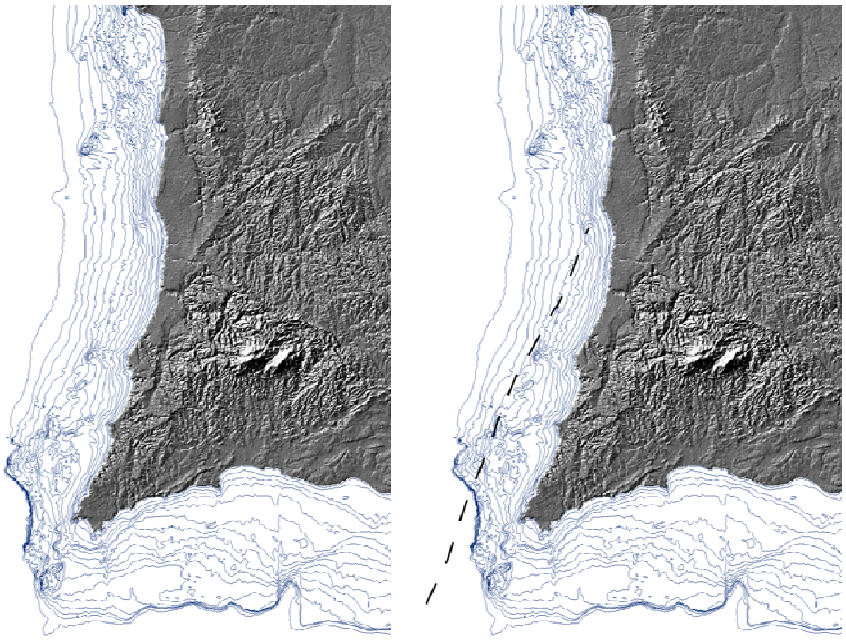

Figure 3.7 -Shaded relief of Southwest Portugal and bathymetry for the 200 m depth.

We have estimated this fault as having circa 70 km length, with a NE-SW to NNE-SSW direction, and we considered that it should correspond to a thrust, probably a blind thrust.

3.4 Conclusions

The regional abrasion platform is composed by a sequence of marine terraces, present in a non-continuous way, but punctually preserved. We have obtained absolutes ages for two marine terraces, through 2 distinct geochronology methods: a lower marine terrace was dated

using OSL and OSL-iRIRI, providing an age of 110-112 ±6 ka and a aeolianites overlying the marine terrace with an age of 80-80 ka, which allow us to confirm that this marine terrace is of MIS 5c, and consequently identify the previous MIS 5e, which allowed us to calculate an uplift rate of of 0.09 ± 0.001 mm/a, for the late Pleistocene.

A higher marine terrace with an inneredge assumed to be at circa 80 m elevation was dated through the Cosmogenic Nuclide geochronology method, providing us an age of 2.0 +0.2/-0.2, which led us to calculate an uplift rate of 0.04 ±0.004 mm/a.

This is evidence for a regional uplift, which may not have a constant rate for all Pleistocene. Finally, we consider that it is very likely that a unrecognized structure located in the nearshore could be promoting the uplift along the southwest Portugal.

Chapter 4

Southwest Iberia Coastal Streams: Morphotectonic and drainage analysis to decode active tectonics and vertical movements

In submission as: Figueiredo, P.M., Rockwell, T.K., Cabral, J. and Lira, C., Southwest Iberia Coastal Streams: Morphotectonics and drainage analysis to decode active tectonics and vertical movements. Geomorphology

Abstract:

About 80 exorheic basins along 460 km of the Portuguese coastline south of the latitude of Lisbon were analysed through geomorphic indexes in order to evaluate local and regional tectonic activity. The two main purposes in this study are: 1) to identify Quaternary deformation along tectonic structures that are presumed to be active; and 2) to evaluate uplift or subsidence rates along this coastline. Geomorphic indexes used in this study are stream channel sinuosity (*S*), basin relief ratio (*Rh*), elongation (Re), basin shape ratio (Bs), valley floor width to height ratio (V_f), basin asymmetry factor (AF), drainage hypsometric analysis, and the stream-length gradient index (SL), and we propose a new index, the terminal basin shape index (TBS). Analysis of results led to the identification of active surface deformation, confirming that the São Teotónio-Aljezur- Sinceira Fault System is a significant regionally active structure, as is the São Marcos Quarteira fault and other minor, but likely active structures. Differential uplift rates along the western and southern Portuguese coastline south of Lisbon are recognized with these indices and agree with marine terrace observations, with the highest uplift rate in the southwest sector (0.11±0.01 mm/a) being 2 a 3 times higher than neighbouring regions (minimum 0.03 mm/a).

Keywords: coastal basins, morphotectonics, quantitative geomorphology, uplift, Portugal

4.1 Introduction

Analysis of geomorphologic parameters is a valid approach to recognize, evaluate, describe and quantify landform modifications through time, even for long periods such as thousands to millions of years (Bull, 2007, 2009; Keller and Rockwell, 1984; Keller and Pinter, 1996). Landforms evolve as a consequence of geomorphic processes that are ultimately controlled by major factors, such as climate, topography, lithology and tectonics. Tectonic

activity may play a direct control in the formation and evolution of a landscape, as for example along active faults or tilted and folded surfaces, but also indirectly through tectonic plate motions, where topography and lithology are controlled by geodynamic conditions (Bull, 2007, 2009). Tectonic activity for this study has been investigated through qualitative and quantitative geomorphic analyses: while qualitative analyses are more related with description of landforms and their geometry and spatial distribution, quantitative geomorphic analyses focus on the detail characterization of geomorphic features through measurement of various geomorphic parameters. Both types of analyses can be undertaken through the application of geomorphic indexes, which are used as tools to characterize the landforms and geomorphic features, and to recognize deformation related to active tectonic deformation. Geomorphic indexes have been applied successfully in many studies (Bull, 1977, 1978, 2007, 2009; Bull and McFadden, 1977; Hare *et al.*, 1985; Rockwell *et al.*, 1985; Merritts *et al.*, 1989, 1994; Ramírez-Herrera, 1998; Wakabayashi *et al.*, 2001; Chen *et al.*, 2003; Silva *et al.*, 2003; Snyder *et al.*, 2003; Troiani *et al.*, 2008; Pedrera *et al.*, 2009; Peréz-Peña *et al.*, 2010; Azañon *et al.*, 2012; Giaconia *et al.*, 2012, among many others), even for areas with low to moderate tectonic rates (Silva *et al.*, 2003, Pedrera *et al.*, 2009). However, special care is required to select the appropriate indexes, taking into consideration the tectonic source and the other factors that control local and regional geomorphic processes (Bull, 2007, 2009; Keller and Rockwell, 1984).

In order to investigate the long term Quaternary deformation either associated directly with recognized active structures, or with large amplitude deformations at a regional scale, and also to evaluate local and regional vertical deformation, we have applied a set of geomorphic indexes to drainage basins. With this aim, the majority of the exorheic basins south of the latitude of Lisbon, *i.e.* south of the Tagus River basin, were selected, making for a total of 78 drainage basins along 460 kilometres of coastline length.

To conduct an adequate morphotectonic analysis and obtain reliable results, the selection of applicable geomorphic indexes was done by taking into consideration the type of tectonic structure and other factors that may control geomorphic processes, such as climate and geology. For the entire study area, the climate is classified as Cs “temperate with dry or hot summer” according to the Köppen - Geiger classification, and average total annual precipitation is between 600 and 1000 mm (Iberian Climate Atlas, 2011), whereby we assume that all of the basins analyzed are subjected to relatively equal conditions. Similarly, we also consider that during the Pleistocene, conditions should have been more or less similar for the entire area, albeit different than today (Desprat *et al.*, 2007, Rodrigues *et al.*, 2011).

Geomorphic indexes were equally applied for all of the basins, independent of the absence or presence of local structures. The applied indexes that refer to basin shape are the basin relief ratio, elongation ratio and basin asymmetry factor. Stream channel sinuosity was also applied to test the channels responses to the presence of local structures, and to evaluate base level changes. Valley floor width to height ratio, which is an index formulated to apply to mountain fronts that respond to base level changes that result from the activity of mountain front structures, was in our case applied to the coastline as a tool to investigate valley floor width to height ratio responses to sea-level changes and regional uplift. Stream-length (SL)

gradient indices were calculated and SL maps were produced to detect abrupt stream power modifications that are either controlled by local or regional active tectonics. Finally, drainage hypsometric analysis was conducted to evaluate modifications in basins hypsometry.

Depending on the coastline orientation, drainage basins were grouped into four sectors based on the bedrock geology and inferred uplift rates, so as to facilitate the geomorphic analysis and interpretation (Figure 4.1).

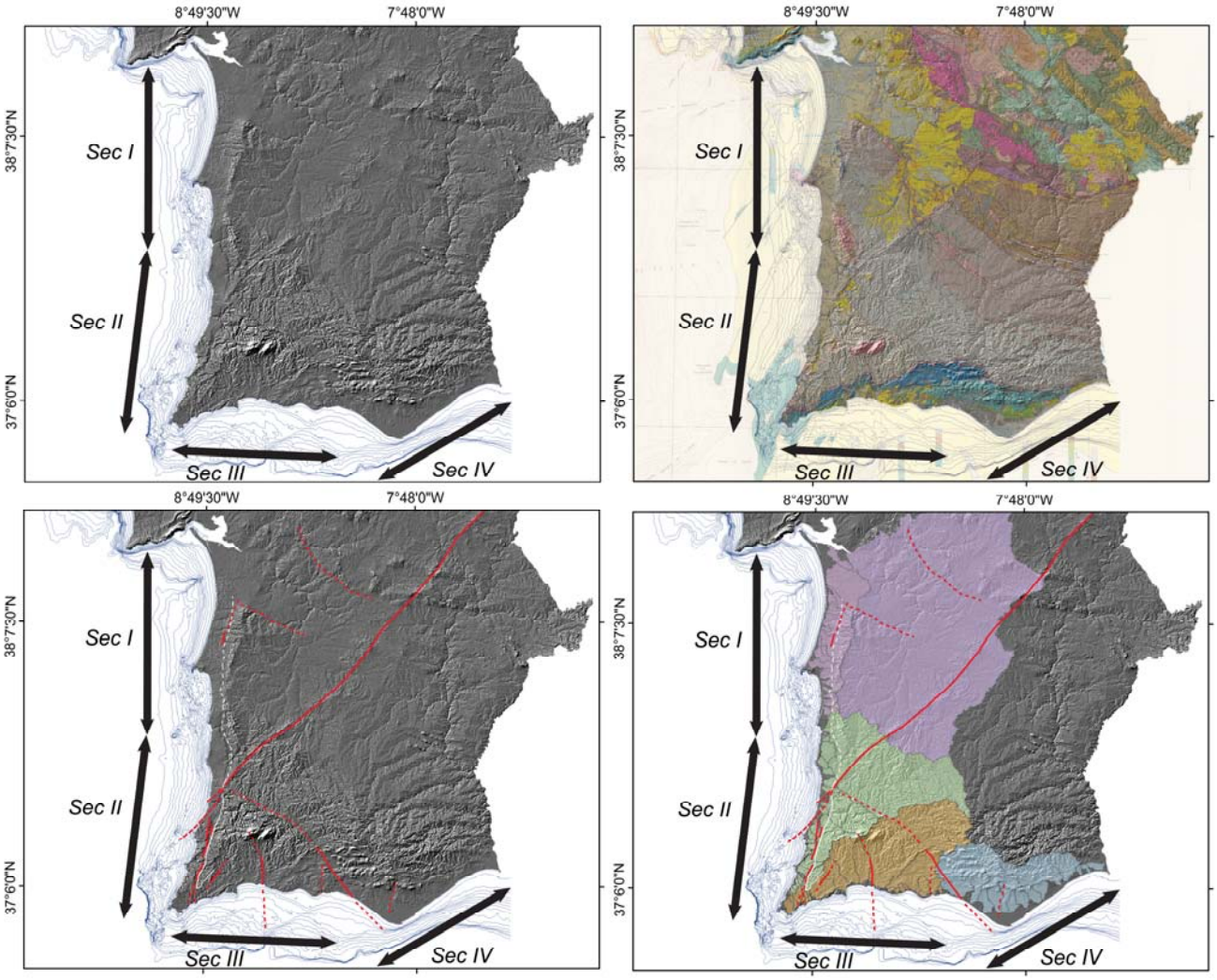

Figure 4.1 - Sectors defined for this study with several information: up left, shaded relief with bathymetrical curves until 200 m depth; up right, geological map 1/500.000 scale overlapping a shaded relief map; down left, shaded relief with the main active structures present in the study area; down right, coastal basins defined foe each sector overlapping shaded relief with the main active structures present in the study area.

4.2 Regional Setting and Structures

The southwest Iberia region corresponds to the southern mainland Portugal territory, and it is the emergent Iberian region closest to the Eurasia - Africa plate boundary. Offshore

Portugal, along the South Iberian Margin and Gulf of Cadiz, several active structures partially accommodate the convergence between the Iberian (Eurasia) and Nubian (Africa) plates (Figure 4.2). This plate boundary region, with moderate to low tectonic rates (Fernandes *et al*., 2007; Nocquet and Calais, 2004; Serpelloni *et al*., 2007, Stich *et al.,* 2006) and diffuse deformation, is characterized by moderate seismicity (Carrilho *et al*. 2004, Geissler *et al*. 2010) that occasionally generates large earthquakes, such as the Mw 7.9 1969 Horseshoe Abyssal plain earthquake (Zittelini *et al*., 2009 and references within) and the November 1st 1755 Lisbon earthquake and tsunami (estimated ≥ Mw 8). Large offshore historical and paleo-earthquakes were also recognized by the identification of correlative tsunami deposits (Baptista *et al*., 2009) and turbidites (Gràcia *et al*., 2010), indicating a high probability for the occurrence of large regional earthquakes with a 1300-1800 yr recurrence interval.

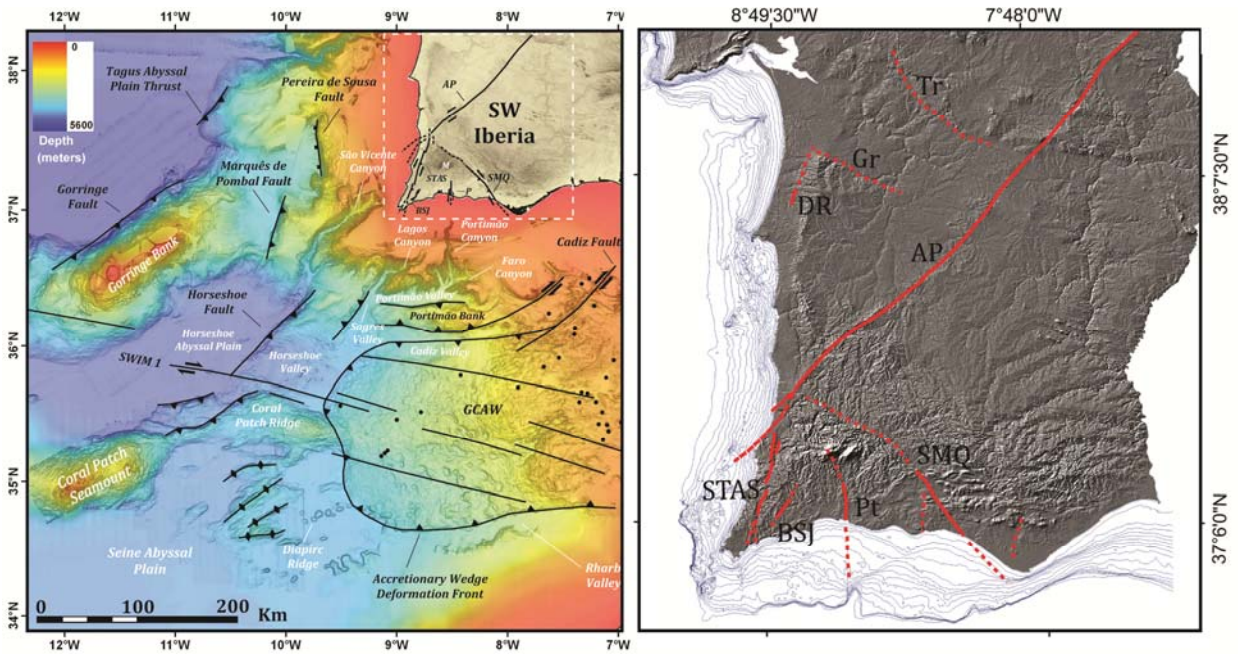

Figure 4.2 - Main active structures and morphological features in the Southwest Iberia region (adapted from Rosas et al. 2012 and Martínez-Loriente et al. 2013 for the offshore and Cabral, 1995 and Dias, 2001 for the onshore). Main tectonic structures and geomorphic elements located at the Off-shore are identified in the map; inland structures mapped upon a shaded relief base : Tr – Torrão Fault, Gr – Grândola Fault, DR – Deixa-o-Resto Fault, AP – Alentejo-Placencia Fault; STAS – São Teotónio-Aljezur-Sinceira Fault System; BSJ – Barão de São João Fault; Pt – Portimão Fault; SMQ – São Marcos-Quarteira Fault.

Inland, in southern Portugal, several structures with Pliocene and Quaternary activity are present (Feio, 1951; Cabral, 1995; Dias *et al.*, 2002), albeit with low activity rates that are generally less than 0.1 mm/yr (Dias, 2001). Major structures in the western region are the Alentejo-Plasensia fault (APF), also known as the Messejana fault (Feio, 1951; Pereira, 1990; Cabral, 1995; Villamor *et al.*, 2012), the São Teotónio – Aljezur- Sinceira Fault System (STASFS),

(Pereira, 1990; Cabral, 1995; Dias, 2001; Figueiredo *et al.*, 2011), the Portimão fault (PF) and the São Marcos Quarteira fault (SMQ) (Dias, 2001, Dias and Cabral, 2002) (Figure 4.1).

The Alentejo-Plasensia fault is the longest tectonic structure in Iberia, with a length greater than 500 km, extending from Placencia, Spain in the northeast to Odemira, Portugal in the southwest, plus an off-shore prolongation farther to the southwest (Pereira *et al.*, 2013). This structure has experienced a complex evolution since the late Variscan orogeny, expressing different kinematics through the subsequent deformation phases. During the Tertiary and Quaternary, several pull-apart basins filled with Miocene and younger sediment attests to a primarily left lateral strike-slip sense of motion. In general, this fault averages a long-term slip rate of about 0.05 mm/a (Villamor *et al.*, 2012), and it is believed that the APF segments in SW Portugal were more active than the northeastern segments (Cabral, 1995), especially during Pliocene to early Quaternary time. For about 20 km of the western Portuguese coastline, near Odemira, the APF inflects towards the south, crossing the coastline and extending to the offshore where it is recognized in oil industry seismic lines; offshore, the fault zone is interpreted to have experienced a complex evolution during the Mesozoic related to the Iberian rifting phases (Pereira *et al.*, 2013), but its Quaternary behaviour is less understood. Exposures of the fault zone along coastal cliffs show evidence for a wide fault zone that has likely experienced a complex history, with several fault splays exhibiting various modes of motion, including normal faulting, reverse faulting, right lateral and left lateral displacements. However, no Quaternary markers are obviously deformed, suggesting that if any Quaternary deformation has occurred, it is likely horizontal in nature with essentially no vertical motion, making it difficult to track in the poorly consolidated cover sediments (primarily eolian sands) and in the geomorphology.

The São Teotónio – Aljezur- Sinceira Fault System (STASFS) corresponds to a NNE-SSW left-lateral strike-slip fault system with four small pull-apart basins along it, filled with Miocene to Quaternary sediments, and cut by several Pleistocene fluvial terraces. A large regional surface corresponding to a marine abrasion platform that is about 10 km wide, and that was probably re-trimmed during Pliocene and Pleistocene times, as evidenced by marine terrace remains, is displaced by the STASFS: a section of the regional surface drops into the structural depressions at the pull-apart basins, suggesting that STASFS has been active during the Pleistocene. A vertical tectonic slip rate of 0.03-0.06 mm/a, based on vertical post-Pliocene displacements, has been estimated by Dias (2001). However, as the main slip on these structures is likely strike-slip, this slip rate estimate is a minimum.

Efforts to recognize and quantify Quaternary deformation along the STASFS (Figueiredo *et al.*, 2011; Figueiredo *et al.*, 2013) suggest that the fault segments have distinctly different tectonic rates: the southern Sinceira segment of the Sinceira-Pedralva fault has small basins that do not exhibit evidence for significant Quaternary motion, whereas the Alfambras and Aljezur segments do exhibit evidence for vertical and strike-slip motion, probably during the Middle to Late Pleistocene.

Based mainly on observations of submarine geomorphology, Terrinha *et al.* (2013 and references therein) considerer the STASFS to extend into the offshore; however, no certain evidence for Quaternary activity has been observed at the coastline.

The Portimão fault is an N-S striking vertical structure that is about 15 km in length onshore, and extends into the offshore for at least another 40 km, partially controlling the Portimão canyon in the continental shelf. It corresponds to a structure that probably evolved after the late Variscan, and played an important role during the Mesozoic. Plio-Quaternary activity on this fault is recognized but poorly understood, and a left-lateral sense of motion is inferred inland (Dias, 2001) while a right lateral sense of slip associated with normal faulting is recognized along some segments in the offshore (Terrinha *et al.*, 2009). The recent recognition of a sequence of middle to late Pleistocene marine terraces (Figueiredo *et al.*, 2013) has allowed correlation of marine terrace elevations across both fault blocks, and no significant elevation change was recognized. If correct, this implies that this fault has not experienced significant vertical motion during the late Pleistocene, although we cannot preclude some horizontal displacement.

The São Marcos Quarteira fault (SMQF) corresponds to a NW-SE structure that is recognized onshore for about 40 km along a transect between São Marcos da Serra and Quarteira. The fault zone extends into the offshore for at least another 60 km at the Diogo Cão Trench, SE of Faro (Terrinha *et al.*, 2013). This fault is a primary structure for southern Portugal, and has played a significant role in the development of the Algarve Mesozoic basin, as well as later during the Cenozoic. It exhibited a normal sense of motion during the Triassic, with relative subsidence on the eastern block for the remaining Mesozoic. Later, during a basin inversion phase, the fault behaved as a "barrier for deformation" that is expressed by an increase in folding and faulting along the eastern block (Terrinha, 1998), and less deformation at the western block. During the Miocene, sedimentation was also controlled by this structure, as Lower and Middle Miocene sediments (Lagos-Portimão Formation) are predominantly present to the west while Upper Miocene sediments (Cacela Formation) are predominant to the east. Plio-Quaternary activity has been recognized inland as reverse faulting (Dias, 2001) near Boliqueime, although the fault zone is expressed as a broad and very complex zone of deformation, with several structures that exhibit different kinematics.

A probable northern extension of the S. Marcos-Quarteira fault may correspond to the Mesquita fault, which is morphologically express by a break in slope that is interpreted as a probable fault scarp, and which partially coincides with a ridge of Devonian quartzite. This northern segment, which corresponds to a strong lineament in the landscape, is poorly understood, as no major fault has been recognized in the field, although it is believed that the lithologic contact between the highly deformed Carboniferous greywackes of the Mira Formation and Devonian schist and quartzites from the Brejeira Formation may have partially absorbed some deformation. Feio (1951, p.324) argues that this "scarp" may be a fault scarp, and that the fault might be located in the Carboniferous bedrock and has since retreated towards the Devonian quartzites. No Quaternary activity has yet been recognized along this inferred structure, and no alluvial fans have yet been recognized suggesting no differential

vertical motions. However, southwest of the Mesquita fault, very large boulders of quartzite cap a 200 m surface and associated underlying sands that are inferred to be early Pleistocene-aged sediments (Calabrian stage). In turn, these relationships are interpreted as a consequence of the Mesquita relief rejuvenation that probably occurred during Late Pliocene to Early Pleistocene time (Feio, 1951, p.424). Offshore of southern Portugal, the closest active structures are at distances greater than 100 km, and include the NNE-SSW striking Marquês de Pombal thrust, the NNW-SSW striking Horseshoe fault, the Pereira de Sousa normal fault, and the roughly E-W striking Portimão Bank thrust (Terrinha *et al.*, 2009)

Northward, structures such as the Grândola Fault, an onshore normal fault that strikes WNW-ESE for about 30 km and is likely to extend into the onshore for an additional 35 km (Cabral, 1995; Pimentel, 1997), and the NNE-SSW striking, east-side-up Deixa-O-Resto reverse fault (Ribeiro *et al.*, 1993), exhibit evidence for Late Pliocene to early Pleistocene activity but overall their Quaternary tectonic activity is poorly understood. Offshore structures along the northern section of the studied area are also present, such as the Sines fault (Alves *et al.*, 2003; Pereira *et al.*, 2011).

Vertical deformation rates for mainland Portugal are inferred from hypsometric analysis of the landscape and correlation with Pleistocene marine abrasion surfaces with inferred ages, resulting in regional uplift at a rate of 0.1 to 0.2 mm/a, depending on uncertainty of the surface ages (Cabral, 1995). Figueiredo *et al.* (2013) estimated an uplift rate of 0.11 ± 0.01 mm/a for the southwestern Portugal region, based on the elevations of late Pleistocene marine terraces, which is probably a higher rate than that to the north towards the Tagus Valley.

In summary, active tectonic structures in southwestern Iberia exhibit low rates of deformation, and are probably associated with long periods of seismic quiescence. The instrumental seismicity is usually of low magnitude, diffuse and hard to correlate with known Quaternary structures (Carrilho *et al*., 2004; Carrilho, 2005). No historical earthquakes with surface rupture are known for this region for at least the past 2000 years, and paleoseismic studies have not succeeded to demonstrate Holocene surface faulting (Figueiredo *et al.*, 2011).

4.3 Methodology

Coastal streams along the Portuguese coastline south of the latitude of Lisbon were analyzed using a set of geomorphic indices, with the purpose of inferring relative tectonic activity. Our topographic database was generated using the ASTER Global Digital Elevation Model (ASTER GDEM), v2, with 30 m spatial resolution, produced jointly by METI (Ministry of Economy, Trade and Industry of Japan) and NASA (GDEM data can be downloaded from e.g. Japan Space System webpage http://ww.jspacesystems.or.jp/ersdac/GDEM/E/index.html). This data was, whenever possible, complemented with digital topography 1/10.000 scale, both processed with ArcGIS software (©ESRI). Geological maps and orthophotomaps from the Portuguese surveys were also integrated in the database to provide lithological and structural

information the morphotectonic interpretation. For the hypsometric studies of basins, we used CalHypso, a free-ware ArcGIS extension (Pérez-Peña *et al*., 2009a).

4.4 Database Organization

The study area was divided in fours sectors according to average coastline orientation, bedrock geology, the presence of primary tectonic structures, inferred uplift rates and slight changes in the geomorphology. A code was established for the basins identification, according with their relative position plus indicative if the basins outflow along the west coast or along the south coast. Basins were numbered, utilizing Arabic numerals according with their mouth position along the coastline, along the west coast starting at the north towards the south and along the south coast starting at the west towards the east: an extra code was added to this ordination, code "w" for west coast and code "s" for south coast basins. An exception was made for Sado basin, which code is "Sado" due to its very large size and regional meaning. As previously explained, the analysis was conducted along exorheic basins, south of the latitude of Lisbon, i.e. south of the Tagus River basin.

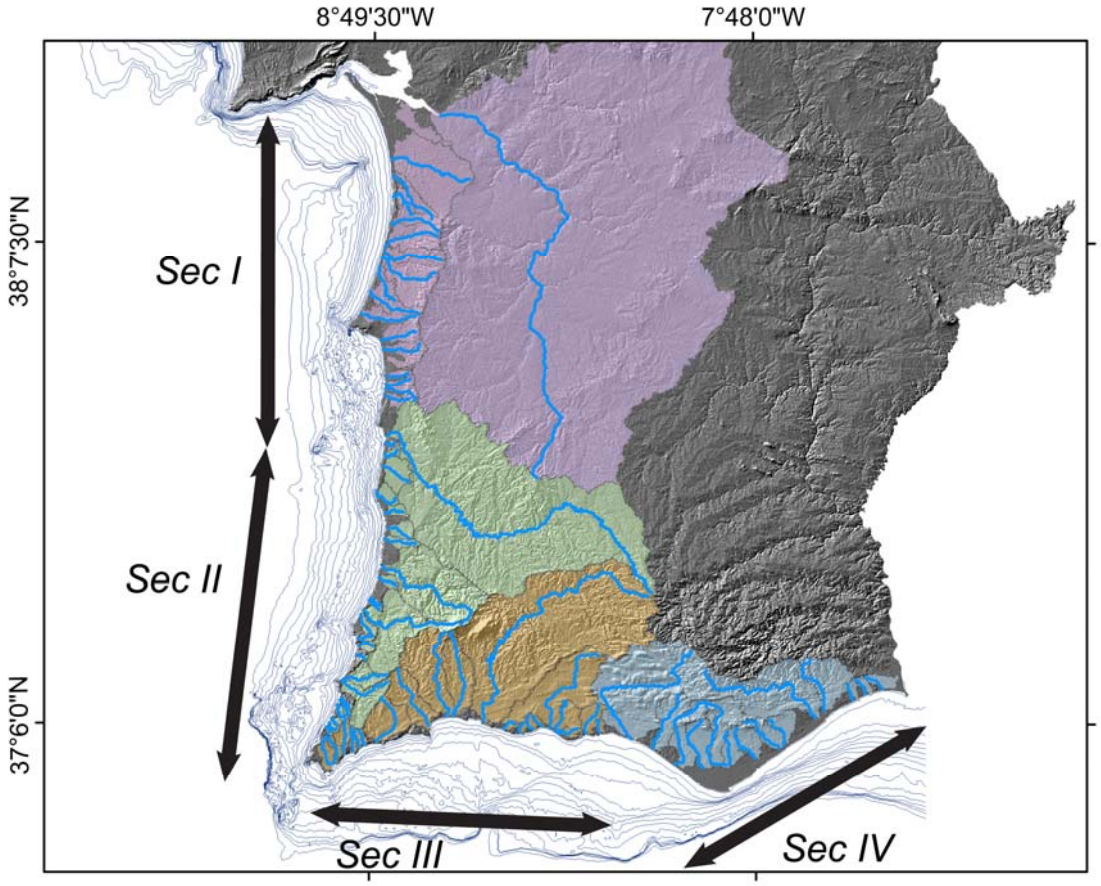

Figure 4.3 – Basins area and main channels defined for each sector, each sector with the same colour, overlapping a shaded relief map.

The southern coastline is mostly developed in Mesozoic and Cenozoic limestone, marl and sandstone, whereas the western coastline is mostly developed in Paleozoic shale, schist and

greywacke, with only scattered areas underlain by Mesozoic limestones or Cenozoic marl and sandstone. Sectors are referred to with roman numerals (I – IV) (Figure 4.3).

Sector I corresponds to the northern section of the western coastline, starting south of the Sado River estuary southward towards the Mira River mouth for about 120 km of coast. Within this sector, we analysed 17 coastal drainages plus the Sado River; the Sado River is highlighted because it is a large basin of about 6270 Km^2. The coastline is generally low in elevation, with abundant sand dune fields and common large lagoons. Small cliffs, where present, are mostly eroded into eolian sand, except for the area near Porto-Covo and the Mira River, where 20 to 40 m-high cliffs are carved into Paleozoic schist.

Sector II corresponds to the southern section of the western coastline, starting at the Mira River mouth southward towards Cape São Vicente, where the coastline inflects and shifts to an east-west orientation. This sector is the longest at 136 Km in length, along which we defined 24 coastal drainages. The boundary with sector I was selected considering the Mira River, which is the second largest drainage along the western coast of Portugal, and its spatial relationship with the Alentejo - Plasensia Fault. There are also changes in the morphology of the coastline in this area. Along this sector, cliffs are always present, mostly carved into Paleozoic rocks, except at Carrapateira and Cape São Vicente where cliffs are carved into Jurassic and Cretaceous limestone units. Cliff heights gradually increase from the Mira River (20 to 40m) towards the south, where they reach about 130 m elevation near Castelejo beach (Torre da Aspa, 154 m), decreasing only in the areas of Mesozoic bedrock. Drainage valleys may be wide, if the drainages are large at the regional scale and have large beaches with dune systems developed at their mouths; no coastal lagoons are present but there are a few salt marshes present, such as at Amoreira and Bordeira beaches. In contrast, smaller drainages and coastal creeks are deeply incised (the “barrancos” as they are called in Portugal) with narrow valleys, and some of them exhibit hanging valleys at various elevations.

The southern coastline was divided into another 2 sectors, westerly (III) and easterly (IV) according to the geology, and because of the presence of a major structure, the São Marcos – Quarteira Fault. Thus, sector III corresponds to the section of the south coastline extending eastward about 113 km from Cape São Vicente to the São Marcos Quarteira Fault zone, whereas sector IV extends from that area an additional 92 Km to the Spanish border, which is coincident with the mouth of the Guadiana River, which is not considered in this analysis. In sectors III and IV, 20 and 14 basins were defined, respectively. Sector III cliffs are higher in the area of Cape São Vicente (50 to 60 m) to Lagos, where cliffs locally reach 80 m elevation at Figueira-Salema and 110 m at Atalaia near Luz beach. Eastward from Lagos, the bedrock changes to Miocene marl and limestone, and the coastal landscape becomes dominated by karst forms, stacks and arches. Cliffs are smoother along sector IV, and are generally lower than 40 m in elevation. Drainages are generally incised, and large beaches with dune systems are develop at the mouths of the larger drainages, sometimes with marshes, as at Alvor, Armação de Pêra, Salgados and Quarteira.

Sector IV typically exhibits a degraded and smoothed landscape, carved into Miocene through Quaternary marl and sandstone. The main littoral feature is Ria Formosa, which corresponds to a system of coastal barriers and lagoons that extend for approximately 55 km of coastline. Ria Formosa has a triangular shape with two spits (Ancão and Cacela), and five sandy barrier islands (Barreta, Culatra, Armona, Tavira and Cabanas) and communicates with the ocean through six inlets, five of them natural. Seven of the studied drainages drain to it (São Lourenço, Seco, Marim, Mosqueiros, Gilão, Almargem and Cacela river basins), and cliffs in general are lower than 30 m in height and valleys are wide.

The highest regional geomorphologic features are the Monchique and Caldeirão Mountains, rising from the regional 300 to 400 m plateau to 900 m in Monchique, the highest peak in the region, and 600m in Caldeirão. Drainages that head in these areas of relatively high relief, are long with a higher relief ratio, and exhibit similarly long, graded profiles that don't appear to reflect regional base level adjustments. Specifically, those basins are 26w, 30w, 9s and 10s for Monchique Mountain, and 18w and 11s (western) and 21s and 30s (eastern) for Caldeirão Mountain.

4.5 Tectonic Geomorphic Indexes

4.5.1 Stream Channel Sinuosity (*S*)

The sinuosity of a given drainage (S) is defined by the ratio of the channel length (Ch_l) and the length of the straight line defined by the channel endpoints (Ch_{sl}), which is generally assumed as equivalent to the valley length,

$$S = \frac{Ch_l}{Ch_{sl}} \tag{1}$$

or the sum of the sinuosity of several reaches along the channel, which is the more correct way to measure the sinuosity of a channel,

$$S = \sum_{i=1}^{n} \frac{Ch_l}{Ch_{sl}} / n \tag{2}$$

Schumm (1963) defined sinuosity (P) as:

$$P = 3.5 \times \left(\frac{W}{D}\right)^{-0.27} \tag{3}$$

where W and D correspond to the width and depth of the channel, which by themselves are a function of bedload size and, consequently, also sinuosity.

A channel is considered straight if S is lower than 1.5, and meandering if higher; however this value has no mechanical or geomorphologic significance. Meandering is a channel's mechanism to dissipate energy, thereby increasing resistance to flow. In order to maintain an equilibrium profile, the laterally channel erodes the banks of the channel, increasing the

sediment supply but also the channel length, which both contribute to the reduction of the channel slope. Causes for meandering may have various origins, such as crossing different bedrock lithologies, climatic events that provide a large discharge or a large sediment supply, or meandering could be related to tectonic forcing or the lack thereof. When a channel is subjected to tectonic activity, its equilibrium profile can be disturbed, which can induce changes in channel sinuosity. In general, one response (feedback) for a channel's increase in slope is to meander, thereby decreasing its average slope and re-approach a graded condition. An alternative response is to incise to compensate for the steeper section, also resulting in a decrease in average channel slope, with the difference in response a function of various thresholds within the system. Changes in sinuosity have been shown to occur downstream of an uplifted area or upstream of a subsided area (Ouchi, 1985; Schumm *et al.*, 2000). In general, upstream of an uplifted area and downstream of an area of subsidence typically favors the development of flooded areas, braided channels, high width/depth channel ratios and ultimately in aggradation. In contrast, areas that are downstream of a region or zone of uplift and upstream of areas of subsidence area commonly exhibit bank erosion, decreases in flooding, low width/ depth channel ratios, and an increase in channel sinuosity. In this work, channel sinuosity was computed using Hawth's Analysis tools for ArcGIS (Beyer, 2004).

4.5.2 Basin Relief Ratio (*Rh*)

Basin relief ratio (Schumm, 1956) is defined as the ratio between the amplitude of the elevation of a basin ΔE (elevation difference of the lowest and the highest point of a basin) and the longest length of the basin parallel to the principal drainage channel, L. This ratio is dimensionless and measures the average gradient of a basin.

$$Rh = \frac{\Delta E}{L} \tag{4}$$

High values are characteristic of basins with resistant lithologies or hilly areas, while low values are associated with basins with less resistant rocks or smoother, gentler topography. Although this parameter is not assuredly correlated with tectonics, it may provide comparisons between basins with similar lithologies, climate and drainage evolution, and therefore may indicated the influence of tectonic aberrations.

4.5.3 Valley Floor Width to Height Ratio (V_f)

This geomorphic index enables the differentiation of narrow V-shaped valleys from broader U-shaped valleys, which is an indicator of relative base level fall. The Valley floor width to height ratio (V_f) was defined (Bull and McFadden, 1977) as:

$$V_f = \frac{V_{fw}}{[(E_{ld} - E_{sc}) + (E_{rd} - E_{sc})] / 2} \tag{5}$$

with V_{fw} being the valley floor width, E_{ld} and E_{rd} being the left and right elevations of the valley divides, respectively, and E_{sc} being the stream channel elevation, all measured at a certain basin or channel location relative to the drainage divide.

Small V_f ratios correspond to narrow V-shaped valleys and are interpreted as an indicator of rapid incision and/or uplift. In contrast, high ratios correspond to broad, generally U-shaped valleys that indicate valley widening and divide lowering, suggesting that degradation or denudation processes are the more significant in the landscape. The selection of the measurement locations implies taking into account the tectonic source likely to be promoting the geomorphologic response, but also the size of the drainage basins and associated lithologies. In a region with the same uplift rate, distinctly different lithologies should promote different V_f ratios, with higher ratios for the more resistant rocks. V_f ratios are measured at a given distance upstream from the tectonic source, which can be a constant distance or a fix basin-position coordinate (Bull, 2007).

In this work, we have measured V_f ratios at basin coordinate position of 0.9, *i.e.* at a basin location 10% upstream from the drainage mouth. We have chosen such criteria rather than a fixed distance, taking into account the variability of the basins size and the bedrock lithologies at a regional scale. Our aim is to analyze base-level modifications, which should be primarily related with the Pleistocene sea-level variations and Holocene coastal processes.

Elevations of valley floors and divide surfaces were extracted from the digital topography, and valley widths were measured from georeferenced orthophotomaps at a 1: 10.000 scale (IGeoE).

4.5.4 Basin Asymmetry Factor (AF)

The Asymmetry factor (AF) was developed to detect tectonic tilting transverse to the average flow direction of the basin (Hare and Gardner, 1985), and is calculated as a ratio between the areas to the right (Ar) of the main channel (according with the downstream flow direction) and the total basin area (At),

$$AF = \frac{A_r}{A_t} \times 100 \quad (6)$$

Under equivalent rock resistant lithologies, rock structural patterns, topography and a stable tectonic setting, a drainage basin is likely to evolve to a symmetrical geometry. If the basin is symmetrical, the index would be close to 50%. However, in the presence of tectonic forcing that promotes tilting that is transverse to the sense of the main channel flow, AF would have values significantly different than 50%. In cases where tilting is systematically in one transverse direction, AF is expected to be consistently higher than 50%.

4.5.5 Drainage Hypsometric Analysis

A hypsometric curve corresponds to an empirical cumulative distribution function, plotted as elevation versus the basin area, which describes the distribution of elevation within the

basin (Strahler, 1952). The Hypsometric Integral (HI) is a first order derivative of this function, and corresponds to the area below the hypsometric curve. This can be calculated as:

$$HI = \frac{E_{me} - E_{min}}{E_{max} - E_{min}} \quad (7)$$

where E_{me}, E_{max} and E_{min} are, respectively, the mean, maximum and minimum elevations within the basin (Pike and Wilson, 1971).

The shapes of the hypsometric curvature and the HI values were interpreted by Strahler (1952) as indicators of basin evolutionary stages, assuming the Davisian geomorphology cycle (Davis, 1899). Although the concept of stage, as professed by Davis, is no longer generally accepted, there are still useful observations that can be made from this type of analysis. Nevertheless, Strahler considered hypsometric curves and HI values to be differentiated into three basin categories: (1) basins with a convex shape that are assumed to represent the disequilibrium stage that corresponds to a youthful evolutionary stage; these generally have high HI values. (2) Basins that have HI values near 0.5 and an S- shaped curve are considered to be near equilibrium and represent a mature stage. Finally, a third (3) shape, referred to as the Monadnock stage, is considered to be the "old age" stage with a subdued landscape that exhibits relief remnants that will eventually be eroded; these basins have a concave shape with HI values that are greatly inferior to 0.5. However, it was later noticed that the hypsometric curve and HI values do not relate directly with the evolutionary state of the basin, but rather with several other factors such as the topological shape of the basin, local and regional lithology, bifurcation of stream channels, tectonic forcing, and denudation rates (Ohmori, 1993; Willgoose and Hancock, 1998; Luo, 2000, Pérez-Peña *et al.*, 2009, 2010; Cheng *et al.*, 2012 and many others). This implies that for the same region, distinct basins could be affected differently, and despite equivalent ages, might have different hypsometric curve shapes. In this manner, for tectonically active areas, interpretation of these results that are exclusively based upon the age and evolutionary model assumptions are likely misleading and should be cross correlated with other parameters.

For this study, hypsometric curves and their statistical moments were computed using the "open source" CalHypso extension for ArcGIS (ESRI) developed by Pérez-Peña *et al.* (2009a).

4.5.6 Stream-Length Gradient Index (SL)

The Stream-Length index (Hack, 1973) corresponds to stream power relationships (Bull, 1979) and hydraulic variables that directly relate to the capacity of sediment load and bed erosion of a stream. Stream power is proportional to channel slope and discharge. Hack considered the length of the channel as a proxy for discharge and analysed the product of the slope of a given reach of a channel and the channel length upstream from the midpoint of the reach to the drainage divide. This is the Stream – Length index (SL), defined as,

$$SL = \frac{\Delta E}{\Delta L} \times L \tag{8}$$

where ΔE is the change in elevation and ΔL the length for a given reach, and L is the horizontal distance from the midpoint of the reach to the drainage divide. SL indices can also be obtained from a semi-logarithmic longitudinal profile (Hack profile), where the gradient index K can be calculated as:

$$K = \frac{(H_1 - H_2)}{(log_e L_2 - log_e L_1)} \tag{9}$$

where H_1 and H_2 are elevations at each end of the reach and L_1 and L_2 are lengths from the source to the end of the reach (Hack, 1973). This semi logarithmic longitudinal profile is named the Hack profile. Most channels profiles have different k values along their profiles, correlating with stream power variations along their length.

The SL index is sensitive to changes in the channel slope, and therefore is applicable as a tool to detect gradient changes that may have originated due to changes in lithologies, topography or tectonic forcing. Along with Hack (1973), many other works have demonstrated this correlation (Keller, 1986; Keller & Rockwell, 1984; Merritts and Vincent, 1989; Chen *et al.*, 2003; Pérez-Peña *et al.*, 2009b). Merritts and Vincent (1989) differentiated between low, intermediate and high uplift rates along the northern California coastline, and pointed out that large channels (high Strahler order) tend to provide less information about vertical deformation, because larger streams more readily adjust their longitudinal profile after changes in base level.

Hack suggested that it is possible to compare different drainages at a regional scale by "...plotting regularly spaced index values on the map..." (1973, p.427). According to that assumption, SL maps were produced that initially had channel information extracted directly from printed topographic maps (Keller and Pinter, 1996 and references therein), and more recently with data extracted from digital topography (Chen *et al.*, 2003, Troiani *et al.*, 2008; Pérez-Peña *et al.*, 2009b).

SL index value comparisons for channels with different lengths has been questioned by some authors, as SL index values are directly correlated with channel length (Seeber and Gornitz, 1983; Harrison *et al.*, 1997; Chen *et al.*,2003; Pérez-Peña *et al.*, 2009b). It was suggested that a gradient index, K, should be used a normalization factor (Seeber and Gornitz, 1983; Harrison *et al.*, 1997; Chen *et al.*, 2003).

Perez-Peña et al. (2009b) investigated the relationships between K, SL, and stream power to conclude that K is equivalent to the product between the natural logarithm of slope and channel length and can be calculated as:

$$K = \frac{C - h_f}{ln L_c} \tag{10}$$

where C and h_f correspond, respectively, to elevations at the channel head and mouth and L_t is the total length of the channel. This parameter can be applied to either the entire drainage profile or to any reach of it; when it is applied to just a channel reach, it is referred to as k, and when it is applied to the entire profile, it is referred as K.

Those authors also concluded that there is a strong relationship between K and the total stream power, and they proposed K as a parameter to normalize SL index in order to compare channels of different lengths. This resulted in a new index, the SLk index, that has been applied to produce SLk maps within which higher value anomalies appear to correlate well to regions of active tectonics (Pérez-Peña *et al.*, 2009b; Pedrera *et al.*, 2009, Azañon *et al.*, 2012; Giaconia *et al.*, 2012).

In this work, we calculated the SL index with a regularly spaced interval, from which we generated SL maps. The topographic data for the channel profiles in this analysis were originally extracted from a DEM, and later processed to smooth out DEM irregularities. We then extracted the topographic data relative to this equally spaced distance (assumed as the reach length). SL values were calculated for each channel reach, and then plotted in ArcGIS. SL values were interpolated with the Spatial Analyst tool. We have chosen to use a 150 m spacing according to the methods of Pérez-Peña *et al.* (2009b).

4.5.7 Drainage Basin Shape Indexes

Drainage basin planimetric shapes have been analyzed in many studies and for multiple purposes, resulting in the definition of several related indexes. Some of them, such as Basin Circularity, R_c (Miller, 1953 in Hobba, 1972) or Basin Elongation, R_e (Schumm, 1956), were later adapted as the Basin Shape index, B_s (Cannon, 1976 in Ramirez-Herrera, 1998) and have been applied in morphotectonic analyses. From these, the one that is most suitable for our study is the Basin Elongation index. Bull (2009) points out that while elongate basins are characteristic of actively rising topography, circular ones are the result of basin development with divide migration and stream capture. Consequently, elongated basins have been interpreted as indicators of regions of active tectonism whereas circular ones have been interpreted to indicate tectonically inactive areas.

Basin Elongation (R_e) is defined as:

$$R_e = \frac{\emptyset \ Area\ Basin\ circle}{L} \tag{11}$$

where Ø corresponds to the diameter of a circle with the same area as that of the basin, and L is to the distance between the drainage mouth and the most distant point in the basin. The R_e ratio is dimensionless and varies between 0 and 1, with common basin values that range between 0.6 and 1.0 for a wide variety of climatic and lithological conditions. Strahler (1964) defined classes for basin elongation: circular basins have high R_e values that are greater than 0.9, and generally exhibit areas of very low relief. Oval basins have R_e values between 0.8 and 0.9, and exhibit moderate relief, whereas basins with R_e values between 0.8 to 0.6 correspond

to elongated basins with higher relief areas. In general, basins are considered "less elongated" if R_e falls between 0.7 and 0.8 and elongated if R_e is less than 0.7.

A basin might have a section along an active mountain front where incision and downcutting are actively occurring, and consequently, the basin will be more elongated. Conversely, along another less active or inactive section, the basin is expected to widen up and become more circular.

The Basin Shape index (B_s) is a similar parameter, defined as:

$$B_s = \frac{B_l}{B_w} \quad (12)$$

where B_l is the basin length from the mouth to the most distant point along the drainage divide and B_w is the largest basin width measured perpendicularly to B_l.

Commonly, even if basins have a low elongation ratio, basin shapes tend to evolve to a narrower basin width downstream at the mouth, and generally most basins present an inverted "pear" shape. Base level oscillations (*i.e.* sea level oscillations) would induce intermittent incision, favouring the narrowing of the terminal section of the basin, followed by aggradation during periods of sea level rise, which would favour the widening of this section. In this study we propose a modified Bs index, which we named the Terminal Basin Shape index (TBS), which aims to measure and compare the width of the drainage basin that may be an indicator of base level changes. Similar to the valley-floor width to height ratio, the position in a basin where its width is measured has to be selected. Terminal Basin Shape index (TBS) is defined as

$$TBS = \frac{B_{tw}}{B_w} \quad (13)$$

Where B_{tw} corresponds to the terminal basin width at the location selected and B_w is the largest basin width perpendicularly to the main channel stream. For this study and similar to where the V_f ratios are measured, we have measure B_{tw} at a basin coordinate position of 0.9 (10% of the distance from the mouth to the drainage divide), taking into account different sized basins and the bedrock lithologic variability within our study region.

Results

The results obtained for all the indexes are compiled according with the sectors in Table 4.1 for sectors I and II and Table 4.2 for sectors III and IV.

4.2.1. Stream channel sinuosity (*S*)

Sinuosity (S) is generally less than 1.5, indicating that most of the channels are considered straight with the majority of values calculated to fit an interval ranging from 1.15 to 1.4. An

exception is present in sector IV where sinuosity values tend to be higher, with an interval ranging from 1.2 to 1.6. Along sector I, sinuosity is low, and there are no changes of sinuosity along streams, except for drainage 4w which we assume is due to the variations in geology (mainly sand dunes). On the other hand, along sector II, some drainages exhibit a higher sinuosity (18w, 26w and 34w) whereas others have low sinuosity (29w, 31w, 37w and 40w), which is associated with the deeply incised channels. There is a change in sinuosity along channel 18w, which we interpreted as an affect of the Alentejo-Plasensia fault: upstream of the fault trace, sinuosity is greater (1.56) while downstream, sinuosity decreases to 1.35. This decrease in sinuosity downstream for the main channel of basin 18w is interpreted to result from relative subsidence across the Alentejo- Plasensia fault, which is downthrown on the northern block and could correspond to an entrenched older incision. Sector III channels generally exhibit low sinuosities, except for the very long main channel of basins 11s and 16s. These two channels cross the São Marcos Quarteira fault, but there are no significant changes in sinuosity that may be associated with activity on this fault zone. Rather, there is a change in direction of the main channel, which could be interpreted as a consequence of a right strike-slip, but it occurs across a band that is 5 km in width, so is not likely tectonic in origin.

Higher sinuosity channels (1.60 to 1.20) are present along sector IV, which can be interpreted to be related to the bedrock geology. Channels 21s, 25s, 26s and 27s exhibit relatively high sinuosity values, and in the case of channel 21s, there is also a change to lower values where it crosses the São Marcos- Quarteira fault. East of the fault, the main channel of drainage 21s has a sinuosity of 1.50, whereas downstream of the fault, the sinuosity drops to 1.21. We interpreted this change in sinuosity to be more related with the change in channel orientation, as it deflects by about 90^{o}, running parallel to the fault after having crossed it. The sinuosity is, therefore, interpreted to be strongly controlled by the fault.

Sector		Code	Basin area (Km^2)	Main Channel Lenght (Km)	Head Elev. (m)	Morpho indexes							
						Stream Sinuosity	Relief ratio	Elongation ratio	Basin shape	Terminal Basin Shape	Valley-floor width	Asymmetry	Hyps. (HI)
Northwest west coast	I	*sado*	6270.12	126.94	295	1.42	0.002	0.70	1.32	0.43	5.18	70.40	0.33
	I	*1w*	39.47	21.11	66	1.43	0.003	0.34	3.32	0.35	41.00	52.39	0.36
	I	*2w*	217.85	23.24	126	1.18	0.01	0.72	1.35	0.48	8.46	41.83	0.19
	I	*3w*	22.89	16.74	186	1.20	0.01	0.32	4.07	0.22	44.12	45.87	0.31
	I	*4w*	14.22	9.67	86	1.51	0.01	0.44	1.67	0.52	2.31	45.83	0.57
	I	*5w*	33.52	14.18	259	1.22	0.02	0.46	2.39	0.40	2.27	56.93	0.31
	I	*6w*	67.87	15.03	267	1.16	0.02	0.62	1.99	0.55	24.67	35.31	0.34
	I	*7w*	35.56	16.25	262	1.16	0.02	0.41	3.47	0.29	57.65	54.59	0.39
	I	*8w*	114.81	18.64	251	1.39	0.01	0.65	1.19	0.29	17.21	36.30	0.38
	I	*9w*	14.41	11.88	74	1.28	0.01	0.36	3.06	0.29	4.29	61.47	0.41
	I	*10w*	35.19	15.46	235	1.18	0.02	0.43	2.56	0.70	2.38	50.32	0.24
	I	*11w*	30.79	15.44	201	1.15	0.01	0.41	2.74	0.40	4.65	52.54	0.23
	I	*12w*	39.92	10.04	185	1.12	0.02	0.71	1.65	0.37	4.29	61.88	0.36
	I	*13w*	32.55	11.37	178	1.30	0.02	0.57	1.75	0.16	2.67	32.69	0.51
	I	*14w*	7.66	6.28	162	1.12	0.03	0.50	2.96	0.36	2.33	59.29	0.45
	I	*15w*	9.80	7.18	161	1.15	0.02	0.49	2.41	0.32	2.40	36.59	0.54
	I	*16w*	13.21	9.81	239	1.31	0.02	0.42	3.60	0.36	2.18	64.34	0.38
	I	*17w*	13.67	7.66	73	1.17	0.01	0.54	2.04	0.24	3.20	28.64	0.27
aver.			***389.64***	***19.83***	***183.67***	***1.25***	***0.01***	***0.50***	***2.42***	***0.37***	***12.85***	***49.29***	***0.37***
Southwest west coast	II	*18w*	1571.05	115.67	450	1.58	0.00	0.39	2.37	0.35	1.88	54.36	0.32
	II	*19w*	2.76	3.64	57	1.38	0.02	0.52	2.13	0.21	1.67	46.62	0.53
	II	*20w*	5.78	4.66	53	1.33	0.01	0.58	1.40	0.19	5.00	61.92	0.59
	II	*21w*	4.16	8.63	74	1.16	0.01	0.27	0.99	0.42	3.13	47.58	0.53
	II	*22w*	16.12	8.37	70	1.75	0.01	0.54	1.67	0.46	6.00	74.73	0.55
	II	*23w*	12.26	6.23	98	1.32	0.02	0.63	1.91	0.20	1.11	47.87	0.49
	II	*24w*	2.06	7.59	182	1.21	0.02	0.21	1.26	0.23	1.38	58.59	0.47
	II	*25w*	15.50	8.80	192	1.15	0.02	0.50	2.71	0.54	0.49	42.85	0.46
	II	*26w*	256.15	35.44	804	1.54	0.02	0.51	1.77	0.24	2.11	63.29	0.26
	II	*27w*	10.00	5.67	127	1.18	0.02	0.63	1.35	0.32	1.52	50.17	0.54
	II	*28w*	2.33	4.29	98	1.24	0.02	0.40	3.41	0.50	1.83	54.95	0.63
	II	*29w*	2.94	4.05	104	1.09	0.03	0.48	2.80	0.35	0.21	63.04	0.65
	II	*30w*	180.28	30.58	802	1.36	0.03	0.50	1.17	0.18	4.76	39.68	0.19
	II	*31w*	12.40	6.83	129	1.10	0.02	0.58	1.87	0.24	0.78	55.34	0.54
	II	*32w*	5.43	4.52	127	1.12	0.03	0.58	1.91	0.48	0.14	43.65	0.61
	II	*33w*	8.12	4.88	148	1.35	0.03	0.66	1.24	0.24	0.45	33.32	0.53
	II	*34w*	2.87	3.36	131	1.50	0.04	0.57	1.50	0.29	0.26	68.29	0.53
	II	*35w*	33.21	12.70	203	1.20	0.02	0.51	1.61	0.10	2.50	56.85	0.37
	II	*36w*	64.56	14.82	154	1.34	0.01	0.61	2.66	0.23	0.73	22.09	0.41
	II	*37w*	3.15	3.85	112	1.09	0.03	0.52	3.19	0.33	0.57	58.35	0.58
	II	*38w*	4.42	5.50	132	1.23	0.02	0.43	2.77	0.30	0.42	38.44	0.64
	II	*39w*	4.97	4.95	127	1.44	0.03	0.51	2.08	0.36	0.11	55.30	0.67
	II	*40w*	3.83	2.75	99	1.09	0.04	0.80	1.11	0.24	0.36	76.71	0.69
	II	*41w*	3.77	3.53	104	1.39	0.03	0.62	1.84	0.43	0.13	59.71	0.66
	II	*42w*	1.47	2.51	124	1.29	0.05	0.54	2.35	0.38	0.14	71.33	0.64
aver.			***89.18***	***12.55***	***188.04***	***1.30***	***0.02***	***0.52***	***1.96***	***0.31***	***1.51***	***53.80***	***0.52***

Table 4.1 - Compilation of values obtained for all the geomorphic indexes for Sector I (Northwest west coast) and Sector II (Southwest west coast).

4.6.2 Basin Relief Ratio (*Rh*)

Basin Relief ratios are generally low for the entire area, meaning that altimetry is generally low and that the topography is relatively smooth. Drainages flowing from regions of

higher topography, such as Monchique mountain (circa 900m) that is drained by basins 26w, 30w, 9s and 10s, typically exhibit higher relief ratios, although the drainages flowing towards the west coastline have slightly higher ratios. The drainages flowing from the Caldeirão

Sector		Code	Basin area (Km^2)	Main Channel Lenght (Km)	Head Elev. (m)	Morpho indexes							
						Stream Sinuosity	Relief ratio	Elongation ratio	Basin shape	Terminal Basin Shape	Valley-floor width	Asymmetry	Hyps. (HI)
Western South coast	III	1s	19.94	8.51	130	1.26	0.02	0.59	1.86	0.53	2.40	53.63	0.36
	III	2s	10.94	8.76	136	1.26	0.02	0.43	2.94	0.35	1.67	44.64	0.46
	III	3s	20.25	9.09	125	1.09	0.01	0.56	2.21	0.17	1.72	68.73	0.57
	III	4s	7.42	6.57	124	1.08	0.02	0.47	2.51	0.40	1.39	54.81	0.52
	III	5s	6.17	4.97	91	1.10	0.02	0.56	2.46	0.33	0.88	43.96	0.43
	III	6s	4.18	4.65	103	1.10	0.02	0.50	2.57	0.30	0.63	45.92	0.44
	III	7s	76.28	15.66	134	1.41	0.01	0.63	1.00	0.29	3.78	66.36	0.35
	III	8s	84.74	18.06	176	1.16	0.01	0.58	1.98	0.32	18.75	63.22	0.29
	III	9s	159.45	26.89	583	1.33	0.02	0.53	1.54	0.20	28.07	81.97	0.20
	III	10s	95.51	24.62	221	1.21	0.01	0.45	3.00	0.27	36.32	64.28	0.14
	III	11s	976.18	86.50	504	1.75	0.01	0.41	2.22	0.39	14.74	37.11	0.23
	III	12s	4.82	4.46	64	1.29	0.01	0.56	2.42	0.69	1.74	43.27	0.58
	III	13s	4.46	3.36	72	1.22	0.02	0.71	1.44	0.17	5.60	60.60	0.63
	III	14s	7.03	4.91	79	1.24	0.02	0.61	2.03	0.25	2.33	50.74	0.58
	III	15s	3.71	3.71	64	1.10	0.02	0.59	2.42	0.25	1.84	53.67	0.57
	III	16s	208.33	30.51	276	1.48	0.01	0.53	1.27	0.29	12.38	62.26	0.21
	III	17s	28.19	10.34	46	1.41	0.00	0.58	1.70	0.30	25.00	23.36	0.47
	III	18s	8.27	6.82	81	1.37	0.01	0.48	1.55	0.27	40.00	47.55	0.33
	III	19s	27.95	9.40	109	1.25	0.01	0.63	1.54	0.35	2.00	73.19	0.56
	III	20s	4.83	4.32	113	1.22	0.03	0.57	2.15	0.41	2.35	50.20	0.50
aver.			87.93	14.61	161.55	1.27	0.01	0.55	2.04	0.33	10.18	54.47	0.42
Eastern South Coast	IV	21s	411.99	49.79	481	1.99	0.01	0.46	1.05	0.51	34.07	53.94	0.36
	IV	22s	59.91	17.36	293	1.21	0.02	0.50	2.14	0.35	9.26	55.37	0.38
	IV	23s	64.13	23.70	270	1.42	0.01	0.38	4.07	0.75	103.70	49.77	0.30
	IV	24s	51.67	16.90	245	1.44	0.01	0.48	1.60	0.33	4.91	34.28	0.21
	IV	25s	78.83	25.48	307	1.64	0.01	0.39	1.89	0.12	12.65	33.26	0.42
	IV	26s	28.52	10.07	109	1.24	0.01	0.60	1.87	0.47	14.55	59.20	0.17
	IV	27s	33.90	11.91	187	1.38	0.02	0.55	1.54	0.13	18.89	29.78	0.21
	IV	28s	35.67	14.33	184	1.34	0.01	0.47	2.32	0.49	18.75	41.65	0.21
	IV	29s	29.64	9.16	81	1.25	0.01	0.67	1.62	0.12	49.67	28.37	0.27
	IV	30s	222.06	45.87	422	1.55	0.01	0.37	1.74	0.32	7.14	49.51	0.39
	IV	31s	97.17	21.37	330	1.49	0.02	0.52	1.56	0.30	18.92	30.53	0.33
	IV	32s	8.52	5.07	76	1.12	0.01	0.65	2.35	0.43	6.67	68.06	0.48
	IV	33s	8.73	5.31	41	1.25	0.01	0.63	2.16	0.22	3.75	52.25	0.35
	IV	34s	19.93	6.03	31	1.12	0.01	0.84	1.29	0.41	12.00	35.44	0.19
aver.			82.19	18.74	218.36	1.39	0.01	0.54	1.94	0.35	22.49	44.38	0.30

Table 4.2 - Compilation of values obtained for all the geomorphic indexes for Sector III (Western South coast) and Sector IV (Eastern South Coast).

Mountain area that reaches 600m elevation, specifically drainage basins 18w and 11s, 21s, 30s, have Rh ratios that are 2.5 times lower than the ones flowing from the Monchique region. Sector I has an average relief ratio of 0.014, and in general, Rh increases towards the south. The highest relief ratios for the entire study area stand out in the southern part of sector II, especially along the deeply incised smaller drainages (33w, 34w, 40w, 41w and 42w),

with values higher than 0.03. Average Rh ratios for sector II is 0.023, but there is an increase from drainage 24w southwards, with values proximal or higher than the average.

Sector III has an average Rh ratio of 0.015, which is very similar to the average ratio in sector I, and sector III drainages exhibit higher Rh values along its western sub-sector, from drainages 1s to 6s. Lower values are present for sector IV, with an average Rh ratio of 0.012, and this section of coast does not express any significant relief ratios.

4.6.3 Valley Floor Width to Height Ratio (V_f)

The valley floor width to height ratio (V_f) was initially developed to evaluate drainage responses to base-level changes along mountain fronts, and through it, assess their relative degree of active or tectonic base level fall (Bull and McFadden, 1977; Rockwell *et al*., 1985; Silva *et al*., 2003). In our study, there are no active structures along inland mountain fronts, but regional uplift has been recognized (Figueiredo *et al*., 2013), suggesting that a source of regional uplift might be present offshore, but not localized inland. Consequently, an equivalent "mountain-front" could be present in the near offshore, forcing base-levels changes for the coastal basins that are greater than that from sea level fluctuations alone.

Base-level changes are not only promoted by tectonic forcing, but also through a complex combination of sea level oscillations and coastal processes that may favour either aggradation or incision. Coastal aggradation would promote a decrease in power stream, which favours the filling of coastal valleys, and consequently, will result in higher V_f values. In contrast, coastal erosion will result in cliff retreat and, consequently, an increase in stream power and channel slope near the drainage outlet, creating a tendency for a decrease in V_f ratios as a function of their incision rate.

Another condition to take into consideration is that as a consequence of the Pleistocene sea-level oscillations, drainages have been subjected to distinct sea-level positions, which were as low as -120 to -130 m during MIS 2, ranged from -30 to -50 m for MIS 3, or was as high as +6 m during MIS 5e. Present day drainage Vf ratios would then simultaneously reflect their evolution relative to high and low stands and long-term coastal and regional uplift. Smaller drainages, which are more sensitive to base level changes, are more likely to exhibit evidence for adjustments to modern base level or similar late Pleistocene high stands, while larger and probably older drainages would reflect bedrock incision during either the low or high stands. With these assumptions, it is possible to recognize for the same region, larger drainages with larger, broad valleys and smaller drainages with narrow incised valleys, although all of them are likely to be subjected to the same base-level reference and to the same tectonic forcing.

Considering that drainages for the study area have different lengths, and with the goal of comparing the responses of similar basins to base-level changes,V_f was calculated at an equivalent drainage basin position, located at the basin coordinate 0.9, which is 10% upstream from the drainage mouth.

V_f values for the four sectors vary substantially, with the lowest values that are on the order of 0.1 for the smaller, narrow and incised valleys. The highest values may be on the order of several tens to hundreds, and are typically associated with large drainages systems in regions with generally smooth topography, and these valleys exhibit evidence of Holocene aggradation, probably as a consequence of late Quaternary sea level rise.

Sector I is characterized by high V_f values, ranging from 2.4 (drainage 15w) to 57.65, with a mean V_f ratio of 12.85. The highest Vf ratio is associated with drainage 7w, which corresponds to a valley with a coastal lagoon, Santo André. This sector can be sub-divided into two zones, a northern section with the highest values and a southern section with lower ones, although all V_f ratios in sector 1 are higher than in any of the other sectors. This difference is coherent with the geology along the coastline, where the northern zone (north of Sines Cape) is characterized by low, sandy cliffs, large, broad valleys with sand dunes and coastal lagoons, and where the underlying Paleozoic strata are never exposed. In contrast, the southern section of sector 1 is characterized by low cliffs, which are partially carved into the Paleozoic rocks, with the cliff heights increasing towards the south.

Sector II has V_f ratios that range from 0.10 (drainage 39w) to 6 (drainage 22w), with a mean V_f ratio of 1.51, which corresponds to the lowest V_f values of all of the studied sectors. Most values are below 2, except for the section of coast that contains drainages 20w to 22w, and for the large basins (drainages 26w, 30w and 35w) whose valleys were probably incised during Pleistocene lowering of sea level, and subsequently filled during sea level rise. Consequently, these large drainages exhibit broader valley bottoms because they are filled by Holocene sediment (Freitas & Andrade, 2005).

Sector III yielded V_f ratios that range from 0.63 (drainage 6s) to 30.53 (drainage 10s), with a mean V_f ratio of 9.89, and is characterized by generally lower values, except for two stretches with large basins (from drainages 8s to 11s and 16s to 18s). We note that drainages incised into Mesozoic limestone, from drainages 1s to 7s and 19s, the V_f ratio values are low, even for large drainage basins. When the channels are incised into the softer marls and Miocene sandstone bedrock (from drainages 8s to 20s), there is a change in the topography and river valleys are wider and smoother, and typically exhibit high V_f values. It should be noted that V_f values for the wide valleys carved into more resistant limestone in the west (the V_f ratios for drainage 1s and 7s are 2.40 and 3.78, respectively) are significant lower than the V_f values for the broad valleys that incise the Miocene marls (V_f ratios that are typically >12).

Sector IV has the highest V_f values found in all of the study area, ranging from 3.5 (drainage 33s) to 103.70 (drainage 23s), with a mean value of 22.50. V_f analysis shows that all of the basins along sector IV have wider valleys and smoother topography than the other studied sectors, which we interpret to mean that aggradational coastal processes have prevailed. In spite of the several basins and channels that incise the Mesozoic marls and limestone, these lithologies are less resistant than those along sector III. Quaternary sediments are also present (Falésia Sand and Faro-Quarteira Sand) at the coastline, as are Miocene marls, but no clear correlation or trend could be established with the V_f ratio values. The abnormally large V_f ratio associated with basin/drainage 23s could be explained by its configuration and

location: the main channel is carved into Quaternary sediments and it trends oblique to the coastline, it drains into the Ria Formosa Barrier system, and these conditions altogether promote aggradational processes that silt-up the main channel valley.

4.6.4 Drainage Basin Shape Indexes

We have applied several drainage basin shape indices, namely basin elongation (R_e), Basin Shape index (B_s) and the Terminal Basin Shape index (TBS), to evaluate how these parameters vary among the distinct sectors.

The basin shape and basin elongation indices are considered to be related in that both should provide information concerning the elongation of a basin. However, elongation shape provides information on the circularity of a basin, which provides proportion ratios between the ratio of the basins "axis" length versus width. Terminal basin shape intends to indirectly evaluate the shape of the basin towards the outlet, i.e. whether or not the width of the basin shape is narrowing. Higher elongation and lower circularity have been used to interpret areas of higher uplift rates (Ramirez-Herrera, 1998; Bull, 2009) but in fact, these parameters are also controlled by the drainage pattern, as is the TBS index.

We have calculated these parameters for each basin and plotted the values accordingly with their sector to analyze for any variations. Figure 3.4 represents values of R_e versus B_s, and it should be noted than the vertical scale is different for each parameter. High Re values imply a more circular-shaped basin, which would then yield Bs values close to 1. In this manner, in sector I, the Sado, 2w and 8w drainage basins are the least elongated with high Re values and B_s values close to 1. In contrast, some drainages such as 12w, despite having a high Re value, have a B_s value that is around 2 or higher, advocating for their elongated shape: overall this sector has elongated basins with Re and Bs values that average about 0.50 and 2.42. The TBS average value is 0.37, with highest values for drainage basins 10w, 2w, 4w and 6w, and there is a general decrease towards the southern sub-sector suggesting that the basin outlets are narrower.

Sector II has several basins with Bs values around 1, such as drainage basins 21w, 24w, 27w, 30w, 33w and in particular 40w, which also stands out with a high Re value. The northern part of sector II displays congruence between Re and Bs values that vary equally from drainages 18w through 25w, and therefore drainages with higher Re values have high Bs values, and the same is true for the lower values. This means that these basins are always elongated, but wider than the ones in the southern part of section II (except for drainage basin 40w). TBS is also greater in the northern area, especially for drainage basins 21w, 22w, 25w and 28w where mean values (0.33) are closer to the sector I average. For the southern part of sector II, TBS values are lower with an average of 0.30, although drainage basins 32w and 41w exhibit larger values. The average values for BS and Re are 1.96 and 0.52, respectively, with both increasing towards the south, whereas the average value of TBS is 0.31 and decreases southward.

In sector III, drainage basins generally exhibit Bs values that are lower than the Re values, and the Re and Bs values are, in general, more similar among themselves meaning that basin shapes are similar. Drainage basins 7s and 16s have lower Bs values and drainage 10s has a Bs value that is higher than its Re value; these values are corroborated by the extremely elongated shapes of these basins when compared with the remaining drainage basins in sector III. Average values for BS and Re are 2.05 and 0.55 in sector III, with BS values decreasing towards the east and the Re values increasing, which is to say that the drainage basins towards eastward are becoming slightly less elongated. TBS ratios are, in general, low with an average value of 0.33 in sector III, but are higher for drainage basins 1s, 12s and 20s, increasing eastward. Finally, in sector IV, Re, Bs and TBS relationships can be interpreted differently for the western and eastern sub-sectors: drainage basin 23s exhibits anomalous values with high a Bs ratio and a lower Re value, which is the opposite of the remaining drainage basins along this sector. Furthermore, TBS ratios are very high. The western sub-section is strongly outlined by the basins that drain to Ria Formosa (sequence from drainages 23s to 29s), which are the drainages that appear to behave differently.

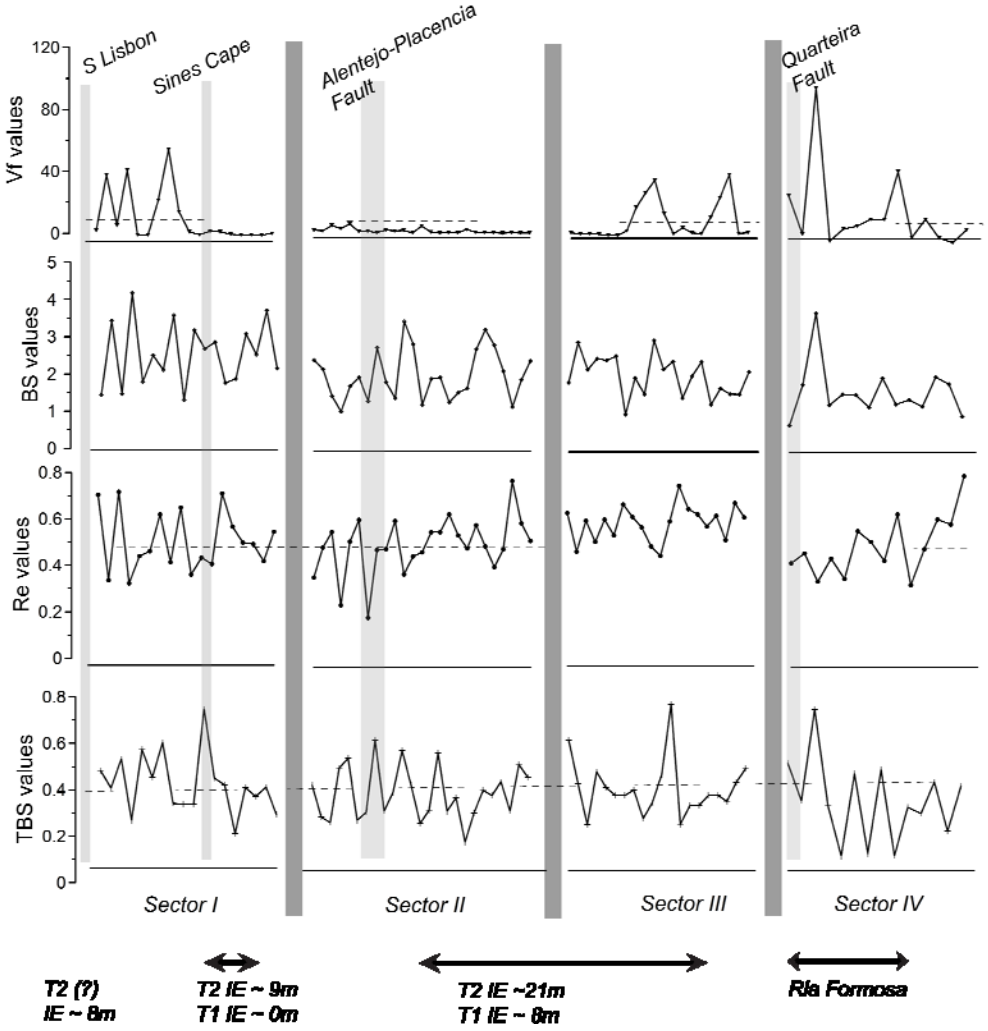

Figure 4.4 – Plots of the results for all the sectors for basin shape indexes and Valley-floor width. Further information relative a geographical reference, main structures and marine terraces inner edges present along the coastline is also included.

So, along this area, the Bs and TBS ratios are greater and Re is smaller than the eastern sub-sector. Average values for sector IV are 1.95 for Bs and 0.35 for TBS, with both decreasing eastward, while Re has an average value of 0.53 and increases eastward.

Overall, the Bs and Re values for the four sectors are very similar, but sector I exhibits higher Bs values whereas Re is lower; In contrast, Re values are higher in sector III. TBS varies in a consistent way, decreasing from sector I to II towards the south along the west coast. Sector III has a similar TBS average than sector II, with increasing ratios in sector IV.

4.6.5 Basin Asymmetry Factor (AF)

We define four classes of basin asymmetry factor values (AF) in order to distinguish the degree of basin asymmetry.

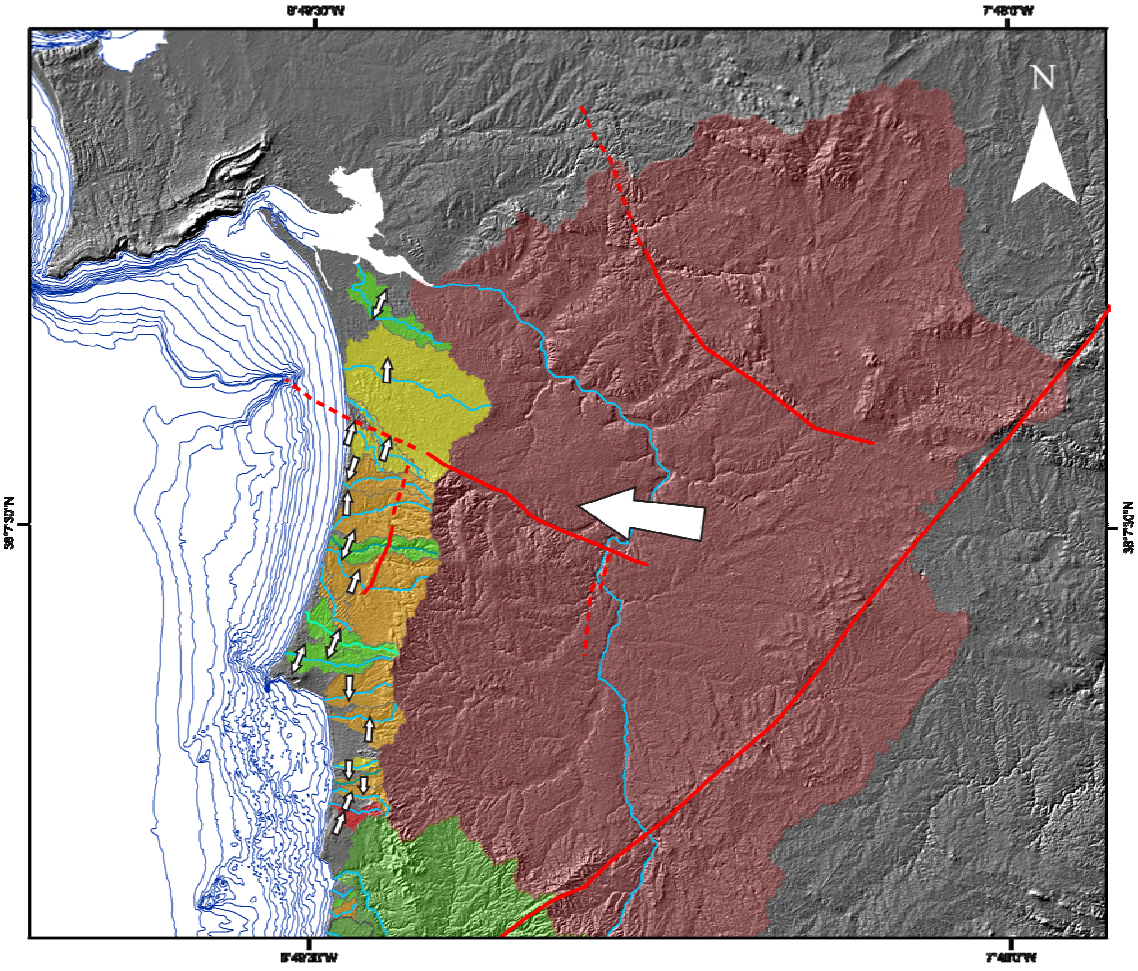

Figure 4.5 – Asymmetry factors calculated for Sector I basins. Main active structures and sense of tilting inferred is also included, overlapping a shaded relief map. Bathymetric lines for each 10 m until 200 m depth.

Class 1 represent symmetrical basins where 45≤AF≤55, whereas class 2 basins are slightly asymmetrical with AF values between 40 and 45 or between 55 and 60. Basins with values

between 30 and 40 or 60 and 70 are “moderately asymmetrical”, whereas class 4 basins are asymmetric with values less than 30 or greater than 70.The majority of the basins in this study are symmetrical or slightly asymmetrical, although some asymmetrical basins can be identified in all 4 sectors.

Sector I basins are generally symmetrical and fall into class 1 or 2, with the exception of Sado basin which is asymmetric and falls into class 4, suggesting a component of regional tilting towards the west or northwest (Figure 3.5). This tilting, which is parallel to the other basins axes, is not recognizable in the other sector I basins, although the minor asymmetries that are observed indicate a tendency for larger south-side basin areas, suggesting that basins may be slightly tilted towards the north or northwest. No correlation with the geology was identified as controlling basin symmetry.

Most basins in sector II are relatively symmetric, and therefore show little or no evidence for regional tilting (Figure 4.6). This is particularly the case for Mira basin (drainage 18w), which is the largest basin in sector II. Drainage basins 26w, 30w and 36w exhibit some asymmetry, which we attribute to the interference generated by active segments of the São Teotónio –Aljezur – Sinceira fault system. The remaining basins do not show any asymmetry, except for drainages 40w and 42w, where AF seems to be controlled by the Paleozoic bedrock schistosity.

Sector III can be sub-divided into two zones: a western zone underlain by Mesozoic bedrock, where basins fall into either class 1 or 2; and an eastern zone from drainage 7s to the east, where basins are moderately asymmetrical (Figure 4.6). In this eastern zone, basins exhibit larger western (right) areas, which may be an indicator of tilting but may also be a consequence of the bedding in the Miocene rocks, which are tilted about 10 º towards the south-southeast. Basins 17s and 19s exhibit evidence for local tilting in opposite directions, suggesting activity on a local antiform that most likely is related to deformation associated with the Albufeira salt diapir, which is considered to have been active in the Quaternary (Dias, 2002).

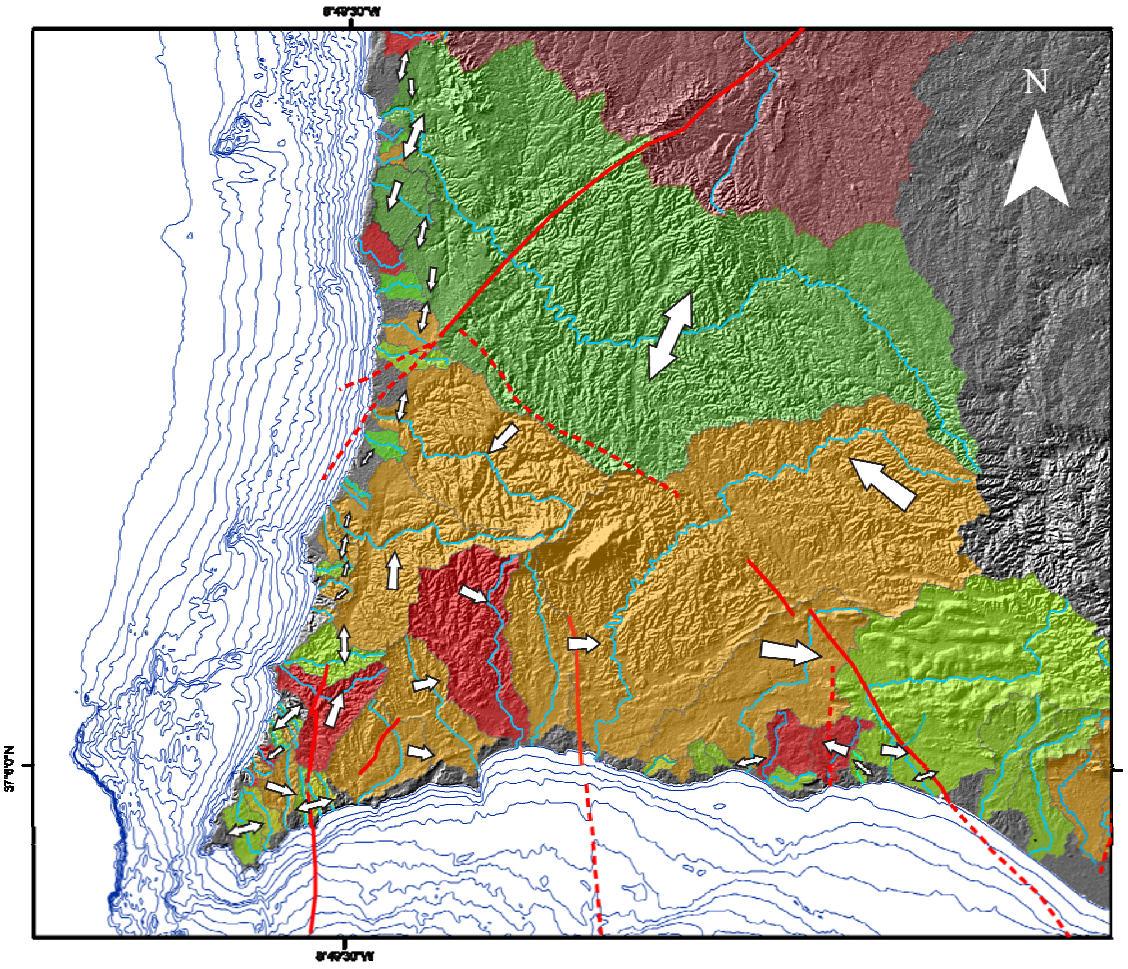

Figure 4.6 - Asymmetry factors calculated for Sector II and III basins. Main active structures and sense of tilting inferred is also included, overlapping a shaded relief map. Bathymetric lines for each 10 m until 200 m depth.

In sector IV, AF values for basins 24s, 25s, 27s, 29s and 31s suggest local tilting towards the west (Figure 3.7). This is not interpreted as a regional tendency because basins 21s through 23s, 26s, 28s and 30s all exhibit symmetry and lie between the slightly asymmetric basins. Thus, the slight asymmetry of some basins may simply reflect local geologic variations rather than actual tilting.

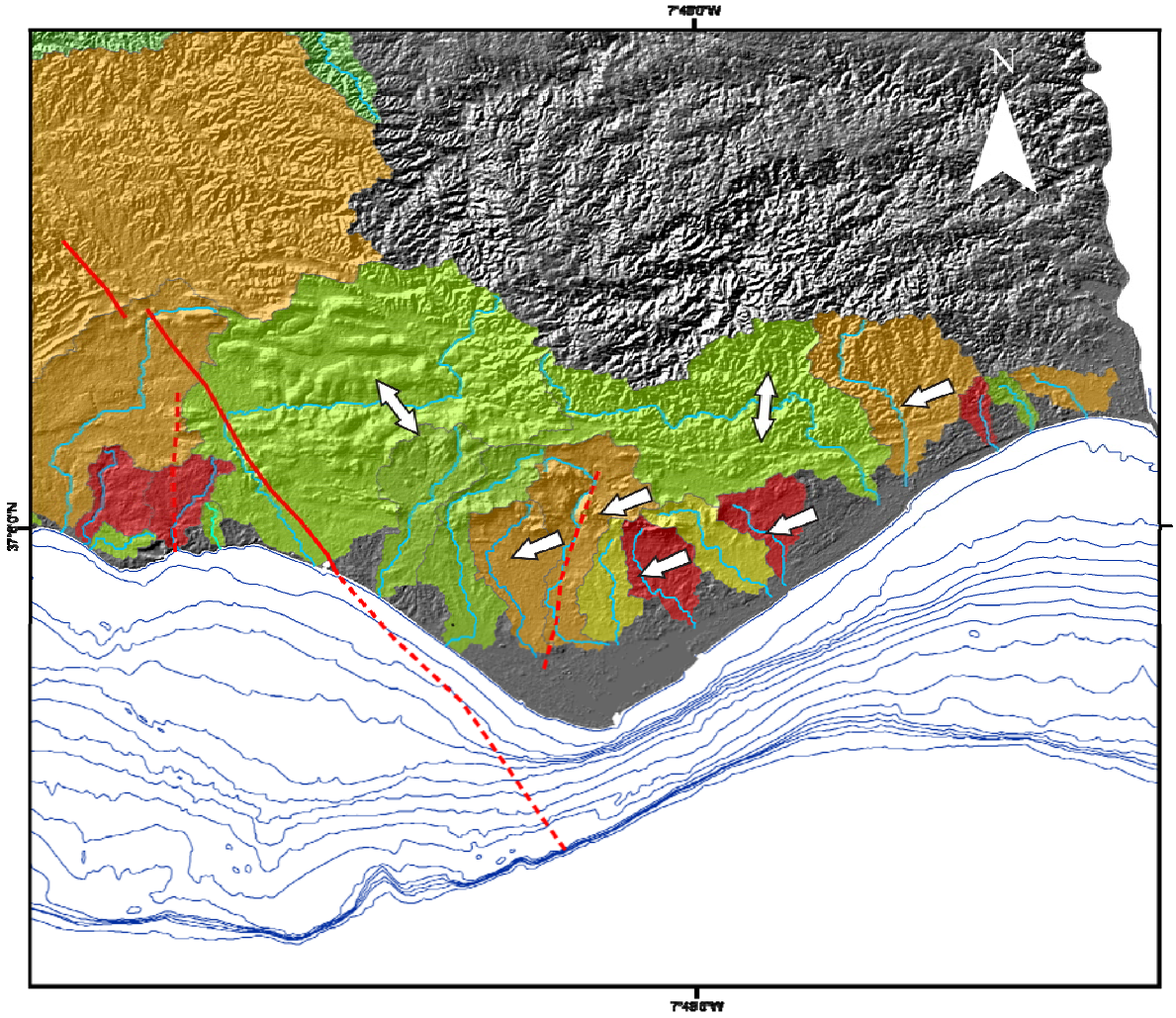

Figure 4.7 - Asymmetry factors calculated for Sector IV basins. Main active structures and sense of tilting inferred is also included, overlapping a shaded relief map. Bathymetric lines for each 10 m until 200 m depth.

4.6.6 Drainage Hypsometric Analysis

Hypsometric curves for all basins were extracted from the digital topography database and their statistical moments calculated through CalHypso ArcGIS extension (Pérez-Peña *et al.*, 2009) and plotted graphically according to their locations (Figure 4.8). To facilitate interpretation of the hypsometric curves, sectors were divided into halves.

4.6.6.1 Hypsometric Curves (HI)

Although hypsometric curves tend to be similar within the same sector, there is also a tendency for the curve shapes to exhibit some characteristic hypsometry for sector II and IV drainages. In these cases, the majority of the basins present exhibit convex and concave shapes, which are interpreted from a Davisian cycle perspective as end members: a rejuvenated landscape and an eroded, low energy landscape.

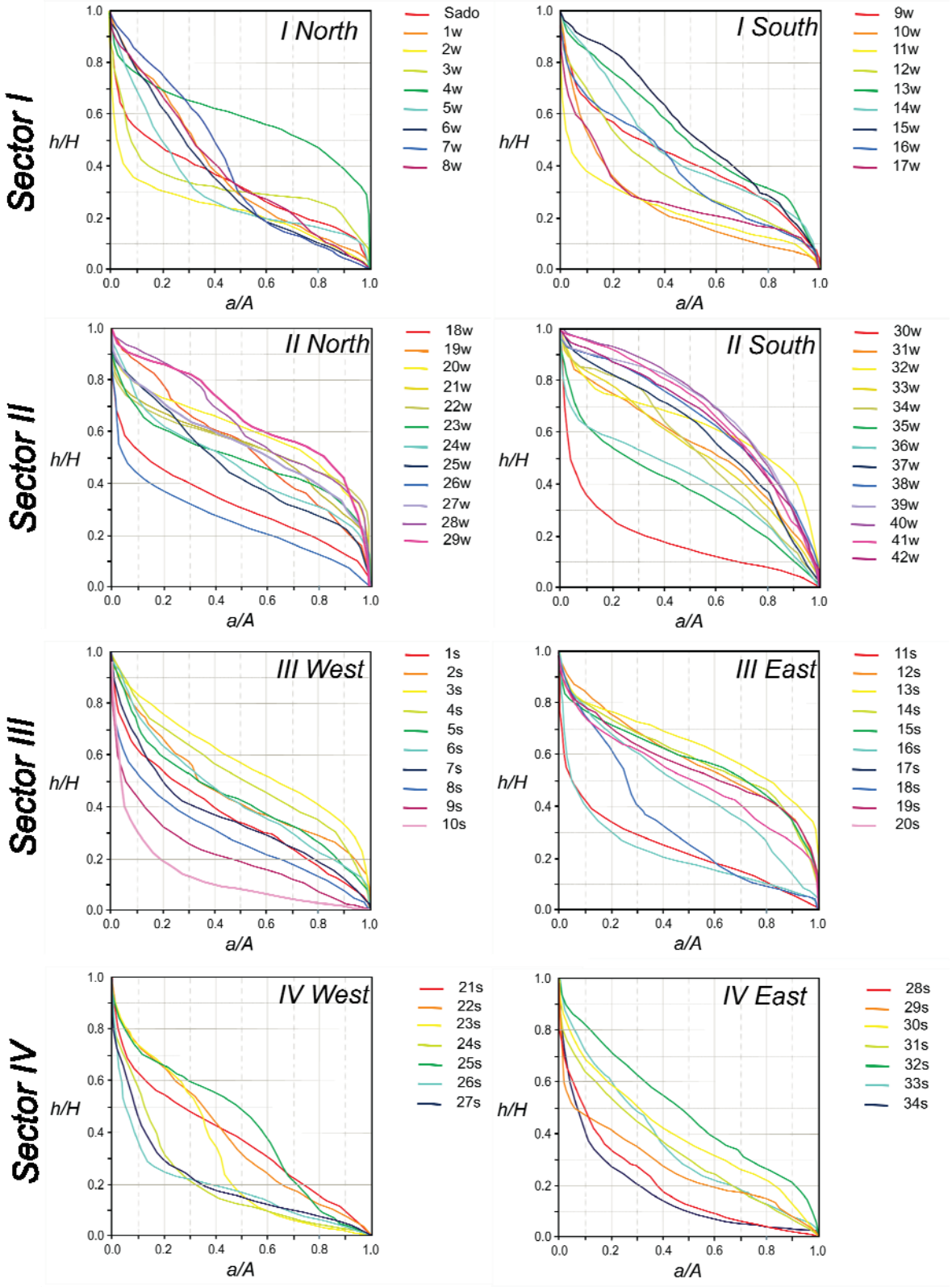

Figure 4.8 - Hypsometric curves for each sector, organized into halves. Legend is included in the figure.

HI values in sector I vary from 0.19 (drainage 2w) to 0.57 (drainage 4w) with a mean of 0.37 (drainages 12w and 1w). In the northern part of sector I, HI curves vary from fairly concave (drainages 2w, 3w) to strongly convex shapes (drainage 4w), while the remaining curves exhibit complex shapes that are slightly concave. Sado basin, the largest basin in sector I as well as the entire study area, exhibits an S-shaped curve, indicating an equilibrium or low energy stage that is consistent with very low or no uplift. The majority of northern sector I drainages have headwater elevations that are greater than 250m, with the exception of drainages 2w, 3w and 4w, which have, respectively, headwater elevations of 126 m, 186m and 86m. This difference in headwater elevation may explain the modification in the HI curve shape for drainage 4w, which should not be understood as evidence for uplift and landscape rejuvenation. Drainage basins 5w to 8w have their headwater elevations at 251 to 267 m, respectively, and have equally sized basins with similar hypsometric curves with a complex shape. Changes in the HI curve slope indicate changes in the topographic distribution within the drainage basin area, indicating elevation intervals, gaps, or accumulations within the basin. Based upon that assumption, we infer for basins 5w to 8w that a large percentage of the basin area that is higher than 50-70 m where there is a topographic break at that elevation is probably related to the change from the Paleozoic bedrock to sandy Plio-Pleistocene sediments.

Towards the southern part of sector I, lower HI Values and concave shapes are present in drainage basins 10w, 11w and 17w. The curves from drainage basins 10w and 11w also suggest a topographic break at about 50-70m elevation, while drainage 17w, located 16km south despite exhibiting a similar HI curve shape, has a headwater elevation of 73m, and consequently, the equivalent topographic break is at about 20m elevation. The remaining drainage basins exhibit complex shapes, but it is still possible to identify in them an area with smoother topography around 50-70m (drainage 14w), a topographic break at about 50m (drainage 13w), and a lower break at about 20 m. Average Hi values for sector I increase from 0.35 in the northern half to 0.39 in the southern half. Within sector I, HI varies from 0.19 (drainage 30w) to 0.69 (drainage 40w), with an overall mean value of 0.53. As previously stated, the majority of the hypsometric curves in sector 1 have convex shapes, although some present complex configurations.

For the entirety of sector II, only three basins exhibit a concave shape, which are drainages 18w, 26w and 30w. These three basins correspond to the largest basins along this sector, and for two of them (drainages 26w and 30w), the drainage headwaters are at about 800 m in elevation, which is exceptional for this sector. Another two relatively large basins, drainages 35w and 36w, exhibit an S-shaped HI curve. For the remaining drainage basins along sector II, drainages 19w to 23w are characterized by headwaters with elevations that are lower than 75 m, while the remaining drainages have higher headwater elevations that average 135 m. In the southern part of sector II, basins associated with drainages 37w through 42w have HI values that are greater than 0.5 and correspond to deeply incised creeks with narrow valleys. A general basin hypsometric curve interpretation for this sector indicates that reliefs higher than about 100-120 m elevation are inherited topography. HI values increases towards the south in sector II, with average values in the north at about 0.50 while to the south, average values are about 0.54.

Along sector III, HI values vary substantially from 0.14 (drainage 10s) to 0.63 (drainage 13s), with a mean HI value of 0.42. Concave HI curve shapes are expressed by drainage basins 9s, 10s, 11s and 16s, which correspond to large basins with headwater elevations that are higher than 220m. Drainage basin 11s, with a headwater elevation of 504m, is the largest drainage that drains to the south coast, and it is the third largest for all the study area. Basins with S-shape curves are present along the western part of sector III, such as drainages 1s, 7s and 8s, and these correspond to well-developed basins with large valleys that are mostly incised into more resistant bedrock composed of Paleozoic schist and Jurassic limestone. The remaining drainages in the western part of sector III, from drainages 2s to 6s, exhibit a slightly convex shape and do not show evidence for remnants of higher relief, which further suggests that most of the area basin is higher than approximately 30 m elevation. The average HI value for this subsection of sector III is 0.45, which is a little greater than the average for the entire sector. From drainage basin 9s towards the east, except for the previously mentioned large basins with concave shapes, the drainages exhibit predominantly convex shapes. These basins have headwater elevations that are typically lower than 100 m, and interpretation of their curves suggest that most of the basin area is higher than 22-25 m elevation. The overall average of the eastern sub-section III is 0.41, implying a decrease in the HI values from the west towards the east.

Finally, for sector IV, the HI curve values vary from 0.17 (drainage 26s) to 0.48 (drainage 32s) with a mean HI value of 0.30. This sector exhibits the lowest HI values of all the areas studied. It is characterized by HI curves with predominantly concave shapes, although a few drainages exhibit complex shapes, such as drainage basins 23s and 25s. These two basins have headwater elevations of about 300 m, and their complex shape is interpreted to be the result of the presence of residual higher relief in the central area of the basin, with incision of the main channel interpreted as an antecedent drainage. For the majority of the basins, headwater elevations are higher than 200m, and basin landscapes are characterized by smooth topography and wide valleys. Drainage basins 23s to 29s flow into Ria Formosa, a system of barriers and coastal lagoons. The western part of sector IV has an average HI value of 0.28, while the eastern part has an average value of 0.34. For the south coast, including HI values from both sectors III and IV, there is a general decrease in values towards the east, with the lowest HI values corresponding to the basins that drain to the Ria Formosa system.

Larger drainage basins typically correspond to regions with a well-integrated drainage network with lower relief over much of the area, generally resulting in a smoothen landscape. The main channels exhibit graded profiles and lower HI values with concave shapes, but this is not always the case for smaller drainages. It has been assumed that higher active tectonic rates are associated with HI values that are greater than 0.5 (Cheng *et al.*,2003). We graphically analyzed how HI values vary for drainage basins with areas smaller than 80 km^2, which represents 63 of the total 77 basins (Fig. 3.9). In this plot, it is easily visible that drainages in sector II and parts of sectors I and III have HI values that are greater than 0.4, and that sector IV and the northern part of sector I have generally lower HI values. It is also possible to infer that basins in sector II have smaller basin areas when compared with the others sectors.

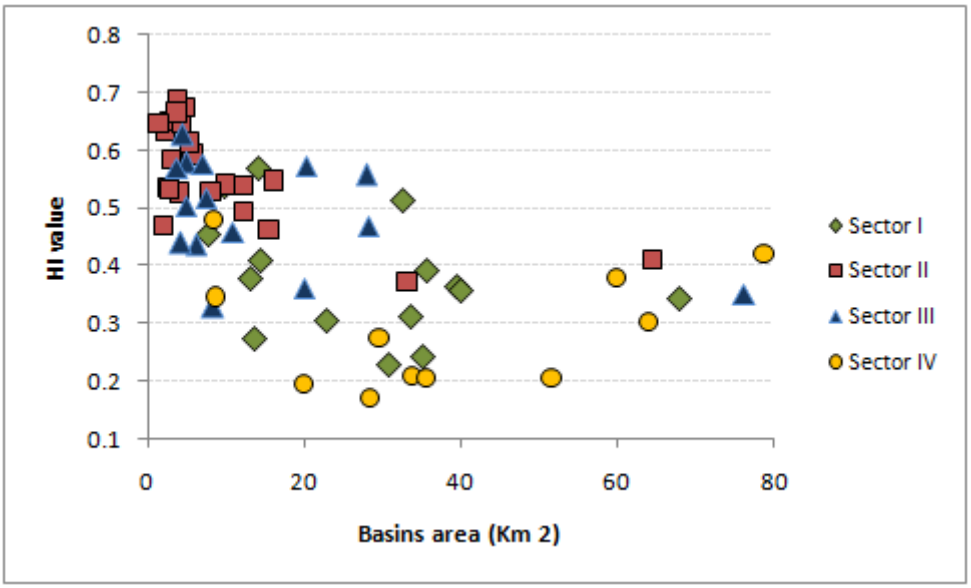

Figure 4.9 – Plot of HI values vs. Basins area. It is visible than sector II basins, have smaller basins and relative higher HI values, suggesting higher uplift rates for this sector.

4.6.7 Stream-Length Gradient Index (SL)

Stream-Length (SL) gradient (Hack, 1973) was calculated for all the basins, and SL maps were produced in order to detect SL anomalies, which may indicate stream power modifications. SL anomalies have been shown to be related to active tectonism as well as passive lithological resistance differences. To produce the maps, SL values for the main channels were calculated each 150 meters, equally distanced, and later plotted on a GIS map. This dataset was then used as a basis for interpolation, using the ArcGIS interpolation tools in the Spatial Analyst Toolbox, with the technique that provided the most reliable results being the Natural Neighbor tool.

SL anomalies for sector I were analysed through two area maps, and are presented separately, due to the very large size of the Sado drainage basin (Figure 4.10). At Sado drainage, two major anomalies stand out: a very strong topographic lineament elongated in the NNW-SWE direction that extends about 50 Km in length, and another lineament in the WNW-ESE direction that extends for a distance of approximately 30 Km. These two features coincide with the Torrão fault and the Grândola fault, respectively. For the remaining coastal drainage basins, a single SL anomaly is identified parallel to the coastline, to which we assigned two hypotheses: one is that the anomaly corresponds to the prolongation of the Deixa-O-Resto fault, and the other is a geomorphologic break between the pre-Quaternary relief along Serra da Grândola and a smooth, flattened surface that probably corresponds to a sequence of Quaternary marine terraces.

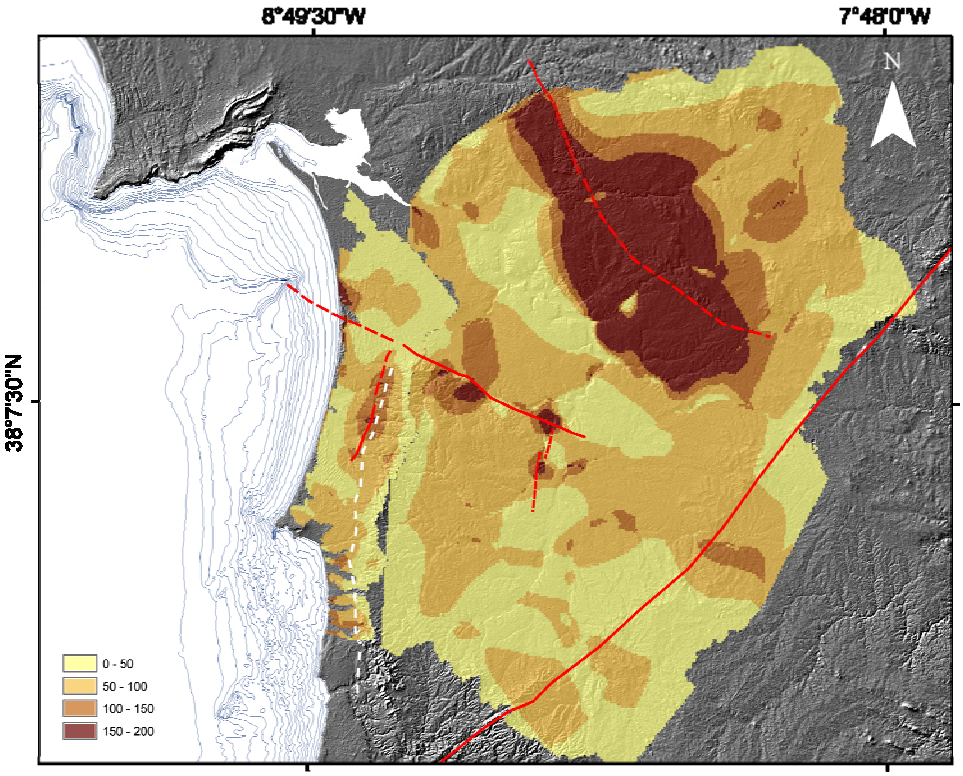

Figure 4.10 – Stream – length map for the Sector I. Main active structures and regional abrasion platform inner edge (white dashed line), overlapping a shaded relief map. Bathymetric lines for each 10 m until 200 m depth.

In sector II, there is a significant contrast between SL values that are higher and lower than 100, with the gradient coincident with the NNE-SSW-striking São Teotónio – Aljezur – Sinceira Fault system. (Figure 4.11) This fault system is also very close to the geomorphologic break in slope between a more incised landscape and a relatively flat, regional surface, which corresponds to an abrasion surface cut during the Pleistocene. The anomaly is not visible along the southern segments of the fault zone, and in the north, the anomaly inflects towards the NE, following the northern segment of the fault system, the Arrifóias graben, and trending parallel and close to the Alentejo – Plasensia fault.

However, despite the anomalous pattern related to the Alentejo – Plasensia fault, it is not as well-expressed as other anomalous trends, which suggests that some drainages that cross the trend may have already adjusted their stream power potential, decreasing it, and consequently graded their profiles. If this is the case, then the Alentejo - Plasensia fault probably has experienced only minor activity during the Quaternary. However, close to the fault trace, there is an anomalous pattern that is visible in drainage basins 24w and 25w, along an area where field observations suggest the presence of several fault branches that are likely to have experienced Pleistocene activity (Figueiredo *et al.*, in prep.). A cluster of higher SL

values are also identified near the coastline, and are interpreted as a consequence of the deeply incised smaller creeks that reflect sea level variations.

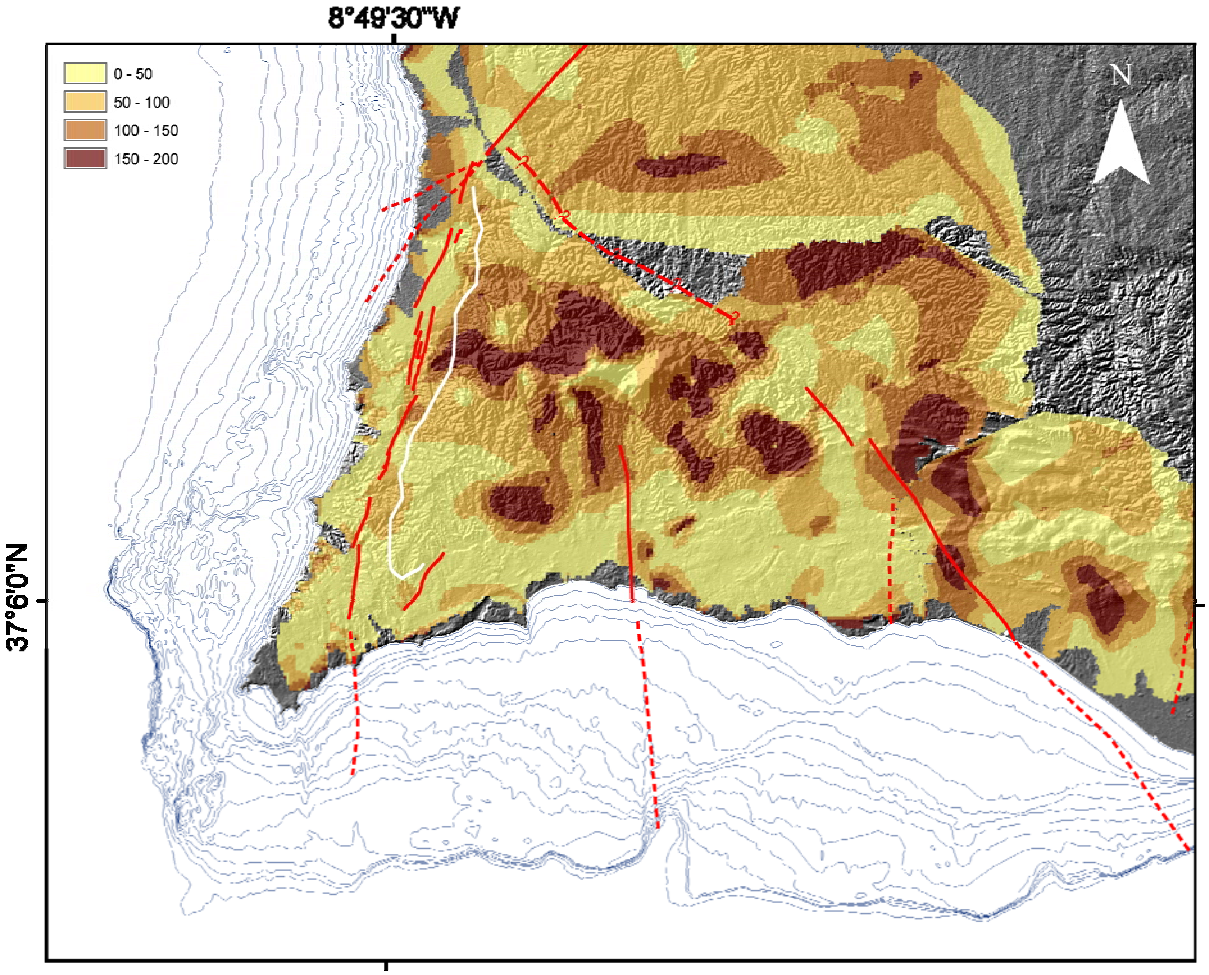

Figure 4.11 - Stream – length map for the Sectors II and III. Main active structures and regional abrasion platform inner edge (white dashed line), overlapping a shaded relief map. Bathymetric lines for each 10 m until 200 m depth.

Sector III was analysed together with the southern area of sector II because it still possible to recognize the effects of the continuation of the São Teotónio – Aljezur – Sinceira fault system into sector III, but the anomaly is now rather smoothed out. Several scattered anomalies in sector III coincide with the borders of a Mezosoic basin, and we therefore interpret them to be related to the distinct lithological resistances to erosion. In these cases, the channels flow from Paleozoic schist and resistant greywacke bedrock into Triassic and Jurassic claystone, sandstone and marl, all of which are softer lithologies. We also observe a 50 km-long NE-SW lineament of scattered anomalies, but they do not correlate with any known active structure. However, they do coincide with several inferred Palaeozoic structures that are probably related to late Variscan orogenic phases.

A NW-SE trending area characterized by lower SL values coincides with a quartzite ridge, which is also the main continental divide that separates drainage basins that flow towards the south from those that flow to the north. Because it corresponds to an area with few incised channels, the SL values are low or almost absent, which may explain the anomalous pattern. However, an important structure for sectors III and IV is the São Marcos- Quarteira fault, which has northern segments that trend parallel to the quartzite ridge, and along which low SL values may suggest a correlation with it (Figure 4.12). Plio-Quaternary tectonic deformation for these northern segments is poorly understood, as the area does not have young sediment cover and no detailed geomorphologic studies have ever been conducted. There is a cluster of three small anomalies near the Portimão fault along the drainage 11s outlet and associated alluvial plain that suggest a greater depth of incision along some of its tributary channels. Because other channels of equivalent order don't exhibit the same SL increment, we interpret this anomaly to be related to neotectonic activity on the Portimão fault.

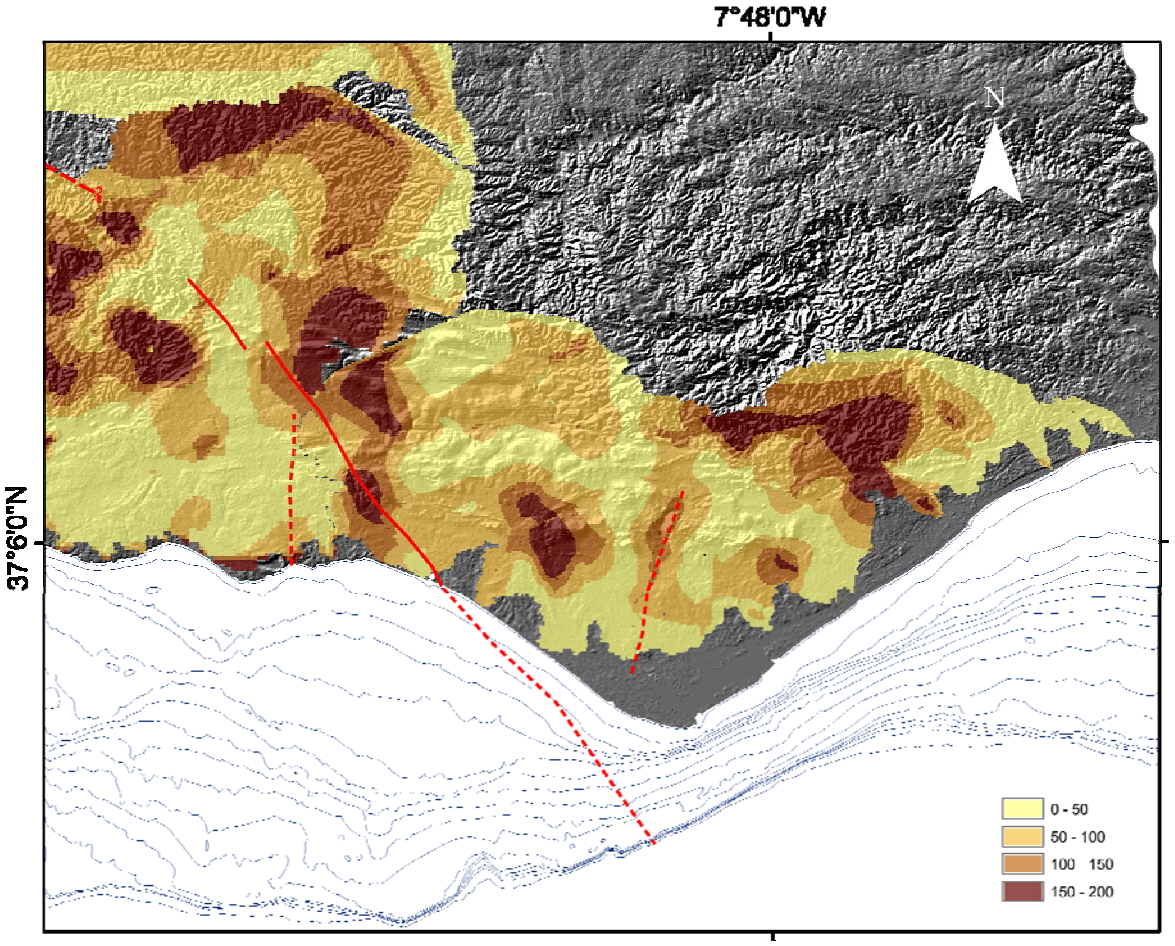

Figure 4.12 - Stream – length map for the Sectors III and IV. Main active structures and regional abrasion platform inner edge (white dashed line), overlapping a shaded relief map. Bathymetric lines for each 10 m until 200 m depth.

The eastern section of the south coastline, sector IV, is similar to sector III in that it exhibits several scattered anomalies that are likely associated with the contact between Mesozoic and younger rocks, with the anomalous values related to the differences in resistance to channel incision. An anomaly is coincident with the southern segment of the São Marcos-Quarteira fault, and another anomaly is present along the NE-SW 20 km-long Carcavai fault. A third anomaly, trending NNE-SSW, is probably related to resistant rocks: drainage basin 23s seems to correspond to an antecedent drainage that crosses through more resistant rocks. However, the southern section of this anomaly also coincides with the location of the Faro fault, which is probably active, although its level and recency of activity are poorly constrained.

4.7 Discussion

The main goal of this study is to analyze, evaluate and compare the effects of tectonic forcing on landscape evolution along the coastal area of southern Portugal. Several geomorphic parameters were applied to coastal drainages along a large area in southern Portugal. As expected, not all of the parameters provided insights in the same way. However, comparisons of the compiled data provide clues that allow us to clarify the impact of tectonic and base level modifications in the development and form of the drainage basin and consequently infer their degree of activity.

In our study, the northernmost sector I exhibits a combination of signals that indicates a different configuration then compared with the other sectors. The Sado drainage basin, which is the largest basin in southern Portugal, has a significant AF that suggests regional tilting towards the west to northwest, which is significant because no other regional tilting was recognized through the AF factor. In general, this area exhibits low basin relief ratios, and the various geomorphic parameters appear to be different between the northern and southern parts of sector I, with Cape Sines being the approximate boundary (*i.e.* approximately at drainage basin 10w). In the northern part of sector I, V_f and TBS ratios are generally high, which suggests either very low vertical motions, subsidence or low rates of coastal retreat. The HI curves are generally concave to complex in shape, the basins exhibit higher R_e values but have variable B_S values, implying that although elongated, some basins are wider. Altogether, these observations are consistent with a relatively stable coastline with little or no long term uplift.

These data contrast with the southern part of sector I, south of Cape Sines, where from drainage basin 11w southward, V_f values decrease significantly and mean TBS values are lower, which we interpreted as an increase in vertical motion , enabling the basins to incise or to preserve incision. HI curves are more concave to linear in shape and HI values are lower. Mean B_S is similar to values to the north, but R_e is higher indicating that the basins are slightly more elongated. Field surveys lead to the recognition of late Pleistocene marine terraces 10 km south of Cape Sines, where the inner edge of the first emergent terrace is at about 9 m in elevation. This lowest terrace is interpreted to be the MIS 5e marine abrasion platform, which

implies a minimum uplift rate close to 0.03 mm/a. North of Cape Sines, no equivalent marine terrace was recognized, but the coastal cliffs are predominantly carved into sand dune deposits along the length of the coast, and an abrasion platform would be difficult to recognize. An abrasion platform carved into Mesozoic limestone is present immediately north of the Sado drainage estuary at Fort Baralha in Arrábida (about 50 km north of Cape Sines) (Regnauld et al., 1995), and is likely the MIS 5e terrace with an inner edge elevation of about 8 m, which would imply an uplift rate similar to near Cape Sines. South of Cape Sines by about 20 km, elevation of the lowest marine terrace gently increases, as suggested by remnants of the lowest terrace at 12 m elevation at Malhão, although no inner-edge was recognized.

Sado basin drainage may have previously flowed out south of its modern mouth, the Sado estuary. Currently, the main channel meets the estuary north of Alcácer do Sal. However, there is evidence that a paleo-drainage course may have existed, probably flowing along Ribeira da Água Cova, Brejos da Carregueira, Vala Real, and Vala do Juncal towards Setúbal canyon, located 20 km south of the modern Sado estuary. This paleo-drainage course is still visible in aerial photographs and Google Earth imagery, but it is filled with late Pleistocene and Holocene (?) dune deposits. It has been suggested that Setúbal canyon is controlled by faults (Gomes, ,2001), with one of them the Grândola Fault, which may extend offshore development of headward erosion of the canyon head, but no direct observations have been able to corroborate this assumption. We then infer that the Sado River may have changed direction due to stream capture by another drainage or that the drainage mouth has migrated to the northeast, possibly as a result of tilting or subsidence towards the northeast.

The SL maps exhibit anomalies within the Sado drainage basin, but there is also a minor anomaly along the remaining drainages. At the Sado drainage, the anomaly is 50 km in length and oriented NW-SE, corresponding to the Torrão fault. Another 20 km-long anomaly is oriented WNW- ESE and corresponds to the Grândola fault, and at the southern tip of this anomaly, it appears to merge with another minor 8 km-long anomaly that is oriented N-S, that corresponds to the Corona fault. Along the coastal area, for the remaining sector I basins, a minor 20 km-long anomaly is oriented NNE-SSW parallel to the coastline and partially corresponds to the mapped trace of the Deixa-o-Resto fault, which has a known surface length of about 8 km. All of these faults are considered to have post-Miocene activity, although Quaternary activity is questionable. Based on a detailed sedimentologic and drainage evolution analysis of the Sado drainage basin, Pimentel (1997) argues that in spite of the significant, 100 meter-high scarp along the Torrão fault, little is understood about its age and that the fault appears to have not experienced any activity for the last 2 Ma (since middle Vilafranquian). The same author suggests that the Grândola fault has experienced some early Pleistocene activity and is probably responsible for minor tilting of Grândola Serra towards the south, but recent geological mapping has been unable to recognize any evidence for Quaternary activity. Pimentel (1997) also concluded that the Sado drainage basin appears to record a differential vertical rate than that inferred for the regional planation surface (p.357) and suggests an uplift rate of 0.05 mm/a rate for Sado drainage basin relative to 0.1 mm/ a for the surrounding landscape.

Results from drainages in Sector II are totally different than those in sector I. Sector II drainages have the highest basin relief ratios of all the study area, particularly south of drainage 23w. Other parameters also show evidence for a change in behavior, suggesting a transition zone in the area covered by drainages 23w to 25 w. In this area, TBS decreases, there are slightly higher V_f values than the average low values of sector II, and R_e and B_S exhibit significant variations to about drainage 25w. Coincidentally, there is also an SL anomaly in this area, especially at the mouths of drainage basins 23w, 24w and 25w, and drainage basin 22w is strongly asymmetrical, indicating a southward tilting. In this area, we have identified remnants of marine terraces that are higher than 20m elevation of unknown age, and there is no evidence that the MIS 5e terrace is preserved. Therefore, we are unable to establish a certain correlation with sector I observations, although we can assert that cliff heights are higher and planar surfaces at the coastline also have higher elevations (35-45 m) when compared with the southern part of sector I, where the fore-edge of the broad, high terrace reaches only to about 25 m elevation. We correlate this anomalous transition area with the Alentejo-Plasensia fault, which west of Odemira near the coast, probably becomes more distributed as it splays into several fault strands, all of which likely have minor displacements. Quaternary activity is hard to recognize because there is no age control for the Quaternary sediments, which are scattered in this region and predominantly correspond to fills along small drainages. We should also emphasize that this area is also at the extension of the probable northern section of the São Marcos-Quarteira fault.

The southern part of sector II, as previously mentioned, has higher relief ratios, lower TBS values, higher mean values of R_e and B_S suggesting more elongated basins. There is an increase in HI values, and the hypsometric curves are predominantly convex. DSK and DKUR are also greater for the southern drainage basins, and the SL map shows an anomaly, which is directly correlated with the São Teotónio – Aljezur – Sinceira fault system. This fault system also controls the asymmetry factor at drainage basins 26w, 30e and 36w, all of which have an anomalous shape that is elongated in the same direction as the fault system. The lower V_f ratios and more elongated basins are typically associated with higher uplift rates (Bull, 2009; Ramirez-Herrera, 1998; Rockwell *et al.*, 1985), and in the case of southwest Portugal, the lower V_f ratios, elongated basins, and lower TBS values are found in the area where there are uplifted late Pleistocene marine terraces (Figueiredo *et al.*, 2013). These authors infer an uplift rate of 0.11 ± 0.01 mm/a based upon the recognition of marine terraces along the southern sub-sector II and western sub-sector III that are correlated to the MIS 5a and 5e high stands, where the inner edge of the MIS 5e terrace was identified at about 21 m elevation. These authors also argue that this late Pleistocene uplift rate may be applicable for the long term, and therefore might correspond to the post-late Pliocene uplift rate. If correct, then the uplift rate substantially increases from sector I southward to sector II. For the southern part of sector II, the convex shape of the HI curves probably reflects not only a higher uplift rate and deep incision below the regional abrasion surface, but it may also reflect a relatively rapid rate of cliff retreat during the last 6000 years, when Holocene sea level rise decelerated and sea level stabilized. At the Castelejo site, consolidated aeolianite units overlie a marine terrace assumed to be 5a in age. These aeolian sands are intercalated with colluvium that is interpreted to have been generated close to a paleo-sea cliff (Figueiredo *et al.*, 2013), and these deposits are now

about 75 to 100 meters from the modern sea cliff. Although we have no age control for the aeolianites, the cliff retreat is contemporaneous of the re-occupation and trimming of the Holocene platform, which started circa 6000 years ago. Consequently, we can roughly estimate the rate of cliff retreat for this period to be 12.5 to 16.7 m/ka. These values are very similar to the maximum values estimated for the past 50 year period at the same location (Marques, 1997), who determined a mean rate of 0.004 m/a and maximum rate of 0.017 m/a.

The western part of sector III exhibits some similarities with southern part of sector II, with lower V_f and TBS values. Along this coastal section, incised and narrow valleys are still present, as are some hanging minor creeks, and according to Marques (1997), mean values of cliff retreat are similar to those identified for southern part of sector II. However, there are no older reference features present along this section of coast to directly evaluate the long-term rate of cliff retreat. Late Pleistocene marine terraces along the western part of sector III have similar elevations to those along the south part of sector II. Low terraces were recognized at several locations along the coastal section of sector III, especially at Ingrina and Furnas (Figueiredo *et al.*, 2013), but also at Lagos, Portimão and Senhora da Rocha, suggesting that most of sector III is subjected to the same uplift rate, at least since the last interglacial. Consequently, we considered the uplift rate for most of sectors II and III to be equivalent.

HI values are high in sector III, with the second highest mean HI value for all the study area. HI curves are S-shaped to convex-shaped, but they are less convex than along the south part of sector II and similar to those in the northern part of sector II. Average R_e and B_S values are slightly higher for sector III when compared with sector II. However, when comparing the south part of sector II with the western part of sector III, we observe equal R_e values with slightly larger B_S values for sector III, suggesting that the bedrock change from schist and greywacke to predominantly limestone may favor wider basins. Basin relief ratios are similar to those in sector I, and are therefore lower than sector II ratios.

Analysis of the basin asymmetry factor of sector III with sector II allows for the possible recognition of regional tilting, because sector II and III drainage basins are oriented roughly perpendicular to each other. In fact, it has been suggested that the regional abrasion surface at about 120 m elevation could be gently tilted towards the south-southeast (Dias and Cabral, 2002). If this is the case, then there may be a recognizable signal with the combined basin asymmetry analysis of both sectors II and III. From our analysis, we do not see evidence of tilting along the 120 m regional abrasion surface, although the AF values do reflect some structural control promoted by São Teotónio – Aljezur –Sinceira fault system, especially at drainage basins 26w, 30w and 36w. However, the southern coastline drainage basins generally exhibit a slight asymmetry that can be interpreted as a gentle tilting towards the SSE, except for the headward part of drainage basin 11s, which exhibits an opposite sense of asymmetry. It should be noted that this distinct asymmetry is located in the eastern block of the São Marcos-Quarteira fault.

Sector IV drainages exhibit some similarities to those of sector I, with the main characteristics being that they have the lowest basin relief ratios, the lowest HI values and the

highest V_f ratios for all of the study area. This indicates that sector IV has an overall smoother landscape, and that drainages are not as incised as much as in sectors II and III. The HI curves have generally concave shapes which also has very low HI values. For basin shape, the average R_e and B_S values are lower than along sector I, and Re increases and Bs decreases towards the east, implying more circular basins to the east. TBS values are lower than along the northern part of sector I, and rise slightly for the area from drainages 23s to 29s, which corresponds to drainage basins that flow towards the Ria Formosa, which again emerges as an anomalous area. In fact, along this area, the AF factor also reflects an anomaly, as drainage basins 24s, 25s, 27s and 29s show evidence for asymmetry that suggest local tilting towards the west. We interpreted this local tilting as possibly related to activity on the São Marcos Quarteira Fault. The SL maps show anomalous values along Faro, which we correlate with the presence of a probable but poorly understood structure mentioned by Dias (2002), and interpreted as a possibly active fault. We emphasize that along the São Marcos Quarteira fault there is no specific high SL anomaly, but rather very low SL values, which implies that the fault has not been active in the late Quaternary, at least in terms of vertical displacement.

Along the southern segment of the São Marcos Quarteira in sector IV, stream-length ratios correspond to the alluvial plain of a very large drainage, and the northern segment in sectors II and III corresponds to a continental divide. We also recognize the straight boundary between drainages 18w and 26w where SL values are consequently very low. However, one striking difference for sector IV is that most of the cliffs are carved into thick Pliocene and Pleistocene sands deposits, the Falésia Sand Formation, the Faro-Quarteira Sand and Gravel, and the Gambelas Sand, whose deposits are more extensive and thick in sector IV than along sector III, where they are discontinuous, thinner, or even absent, except where preserved as karsts filling features. A field survey was conducted in order to search for marine terraces at low elevations, as are present along sectors II and III, but this sector corresponds to a highly urbanized zone where natural forms have been significantly modified at the coastline. Furthermore, a bedrock lithology change from limestone to predominantly weakly lithified sandstone did not allow for the certain recognition of marine terrace forms or sediments in sector IV, comparable with the ones recognized to the west. There is no previous reference to late Pleistocene marine terraces along sector IV, but studies along the Spanish Gulf of Cadiz coastline suggest very low rates of uplift (Zazo *et al.*, 2008) or even subsidence (Zazo *et al.*, 1993).

4.7.1 Characterization of Regional Active Tectonic Classes

Previous morphotectonic studies have applied geomorphic parameters along different tectonic range fronts for a wide range of tectonics rates (Bull, 1977; Rockwell *et al.*, 1985; Silva *et al.*, 2003; Bull, 2007). These studies differentiated the characteristic morphological features and geomorphic ratios for landscapes with different degrees of active tectonic, leading to the definition of tectonic activity classes based upon their field studies. All of these studies have been applied to mountain-fronts and alluvial fans on piedmont areas, and none have been applied to coastal areas. However, we believe that it is possible to apply their observations to our study region, making the necessary adaptations when suitable. Because individual basins

might not reflect a regional tendency, we analyze tectonic activity classes for the four coastal sectors, taking into account their mean observations.

We have already established that for sectors II and III, the uplift rate based on the presence of late Pleistocene marine terraces corresponds to 0.11 ± 0.01 mm/a, which would then be considered as class 2 according to Bull (1977) and Rockwell *et al.* (1985). Studies from Iberia have applied geomorphic parameters slightly differently, so this uplift rate would be considered as moderately active and as a class 1 active tectonic front by Silva *et al.* (2003).

Vf average values for all drainages are greater than 1.5 but less than 5, and are especially low for the southern part of sector II, which may also reflect high rates of coastal retreat, but an overall high rate of stream channel incision. For sector I, we inferred an incremental change in the uplift rate south of Cape Sines, based on changes in the geomorphic parameters of drainage basin. From this, we inferred a low uplift rate of at least 0.03 mm/a for the Cape Sines area and probably the northern part of sector I, which corresponds to a class 3 low active tectonics for Bull (1977) and Rockwell *et al.* (1985), and class 2 moderate tectonic rate for Silva *et al.* (2003). A common association for all the authors is the presence of U shaped valleys and valley floor aggradation, which is a characteristic feature for this sector. For sector IV, we don't have a reliable marker to determine an uplift rate, but we can speculate that it has a similar rate to that along the northern part of sector I, based upon the similarities obtain for all the geomorphic parameters. In this manner, sector IV has probably has an equivalent activity class of 3. It should be noted that while tectonic classes defined for mountain-fronts are applicable whatever the type of fault (*i.e.*, they can be simultaneously applied to normal, reverse or strike-slip faults), but when applied to a coastal landscape, it may be difficult to differentiate between areas of very low uplift, very low subsidence, or a combination between vertical motions and coastal processes.

4.8 Conclusions

Based upon the results obtained for each sector, we interpret that there is a differential vertical rate of motion along the southwest Portuguese coastline, with a higher uplift rate along southern sector II (south of drainage 24w) and sector III. We interpret that this region is probably uplifting as a block because we do not see evidence of regional tilting. We assume that this uplift has been occurring over the long term, and was probably initiated sometime in the Late Pliocene or Early Pleistocene, but that is still to be confirmed as there are no absolute age dates for the sediments or surfaces. This block appears to be limited inland by the São Marcos Quarteira fault, despite exhibiting an apparently low level or rate of tectonic activity during the Quaternary, especially along its southern segment between São Marcos and Quarteira. A possible explanation for the apparently low rate of tectonic activity for this fault is that the deformation may be occurring over a broad fault zone with distributed deformation. In such a case, minor displacements would be difficult to recognize. Channel pattern changes

close to the fault, as well as local tilting towards the fault zone as indicated by several drainage basins in eastern Algarve, are supporting evidence of Quaternary activity.

The Alentejo-Plasensia fault does not exhibit evidence that it provides a significant morphotectonic control for the drainage basins along its trace, although there is a rather subtle and inconsistent suggestion of some tectonic control. This leads to the formulation of two hypothesis: first, that the subtle evidence corresponds to an inherited morphotectonic signal that is possibly Pliocene or early Pleistocene in age, or second, that the fault system evolved to a distributed fault zone with principally a strike-slip sense of displacement where deformation is hard to track through geomorphologic analysis because of the lack of vertical displacement and base level fall.

Along the western coastline, uplift rates seem to decrease northward from south side of the Mira River (drainage basin 18w) to Cape Sines. This northward decrease corresponds with both the Alentejo-Plasensia fault and the northern prolongation of the São Marcos-Quarteira fault, which may correspond to a weaker crustal zone. The eastern Algarve region appears to have a very low uplift rate, and the central Algarve region close to Faro may be tilted towards the west, which would be consistent with a tectonic control generated by the São Marcos Quarteira fault. The Sado drainage basin is interpreted to be tilted towards the WNW – NW, based on the drainage characteristics, and the inflection of the main channel might have occurred during the Quaternary, resulting in the abandonment of the submarine canyon carved into the modern continental shelf. The active structure inland that exhibits the most morphotectonic control is the São Teotónio-Aljezur-Sinceira fault system, which appears to control basin shapes, asymmetries and hypsometry. There are no structures inland that are able to produce the regional uplift signal, nor are there known structures in the offshore that have adequate size or proximity to the coast to be associated with this differential uplift. We therefore speculate on the presence of a previously unknown fault system, located in the near offshore, whose existence and characteristics are yet to be confirmed.

Acknowledgements

This work was funded by Fundação da Ciência e Tecnologia, through a PhD scholarship (SFRH/BD/36892/2007) attributed to Paula Marques Figueiredo and Research Project "Paleoseismological study of active faults in Mainland Portugal" (PTDC/CTE-GIN/66283/2006), co-financed by FEDER. Cristina Lira benefit from a Postdoctoral Contract (SFRH/BPD/81800/2011).

Chapter 5

Recognition of Active fault segments and Paleoseismological studies

Part of this chapter was presented at Conferences and published in their abstracts as .
- Figueiredo, P.M., Cabral, J., Rockwell, T.K. (2010) - *Neotectonics and paleoseismic studies at SW Portugal mainland: The S. Teotónio – Aljezur – Sinceira Fault System, VIII Portuguese Geology Congress, Geosciences On-line Journal, Vol. 11 – n. 8, ISSN 1645-0388*
- Figueiredo, P. M., Cabral, J., Rockwell, T. K. (2011). Plio- PLeistocene Tectonic Activity in the Southwest of Portugal. In: C. Grützner, R. Pérez-López, T. Fernández-Steeger, I. Papanikolaou, K. Reicherter, P.G. Silva and A. Vött (eds.), 2nd INQUA-IGCP 567 International Workshop Proccedings, Vol. 2: Earthquake Geology and Archaeology: Science, Society and Critical facilities: 30-33.

Part of this work is being prepared to be submitted as "Khalil, M.A., Figueiredo, P.M., Santos, F.M., Cabral, J., 2D resistivity tomography as tool to recognize active faulting: the Aljezur faul case study"

5.1 Introduction

The São Teotónio–Aljezur–Sinceira fault system (STASFS) corresponds to the nearest inland brittle structure that may correlate to the ongoing plate boundary deformation in the offshore. It extends NNE-SSW for 50 km, parallel and close to the southwest Portuguese coast (Figure 5.1), and comprises left-lateral strike-slip faults, deforming a large regional abrasion platform ca. 10 km wide, considered of probable late Miocene age, and which was reoccupied during the Pliocene and the Pleistocene. Four small Cenozoic tectonic basins, filled with Miocene to Pleistocene sediments, occur along the STASFS.

Post-Pliocene vertical displacements of up to 100 m may have occurred related to tectonic activity in the STASFS, but generally these only reach a few tens of meters. Dias (2001)

estimated a slip-rate of ca.0.03-0.06 mm/yr, based on the vertical offset of morphological features. However, as the main slip on these structures is strike-slip, those values are a minimum estimative. Dias (2001), taking into account the length of the known fault also estimated a maximum magnitude of Mw 7, an average co-seismic displacement of 1 m and a recurrence period of 19210 - 32017 yr, based upon Wells & Coppersmith empirical relationships.

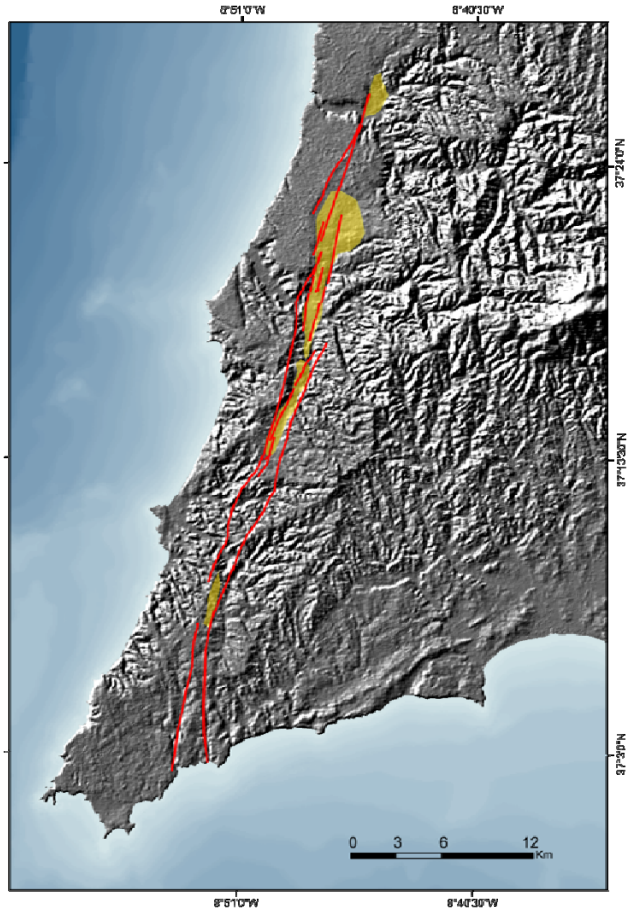

Figure 5.1 - São Teotónio–Aljezur–Sinceira fault system (STASFS) main fault segments overlapping the ASTER shaded refilef. Basins filled with sediments are indicated by the yellow colour. Bathymetric information also included.

No historical ruptures are known for this region, that has been occupied for centuries: this area has evidences of Roman presence and has been occupied since the Islamic conquest of Iberia, about 1500 years ago: Aljezur was an important harbor and military point as well as a religious site, so destruction of the harbor or the castle caused by an earthquake it should be in historical accounts. Since no report for a local earthquake is known for this region, although shaking from distant sources, probably located in the off-shore are occasionally mentioned, we assume than no historical ruptures have occurred along STASFS.

5.2 Data Acquisition

In order to investigate the Holocene ruptures and recognize the most recent fault rupture and also to assess the deformation for a characteristic earthquake, efforts were made in order to identify the active branches of this fault system. Since morphological analyses indicate that landforms better preserved and probably younger were mainly along Aljezur and Alfambras valleys as well as younger sediments, studies aiming to characterized were more focused in that area.

Through detailed geomorphologic and field work studies, several sites were selected in order to recognize Holocene and Late Pleistocene deformation and potentially paleoseismic events: at some of those sites, it was possible to confirm the exact location of the fault zone and the presence of quaternary sediments, or the presence of quaternary paleosoils, that are expected to be use as chronological and spatial markers. At other sites, however, information based upon surface survey was not sufficient to constrain spatially the fault zone, or to confirm the presence of sediments in depth at surfaces that could be trenched. In those cases, we conducted a prospection based on geophysical methods, namely geoelectric resistivity.

5.2.1 The Barranco de Vaca site – Alfambras fault segment

One of the sites were it was possible to recognize the presence of the fault, along the top

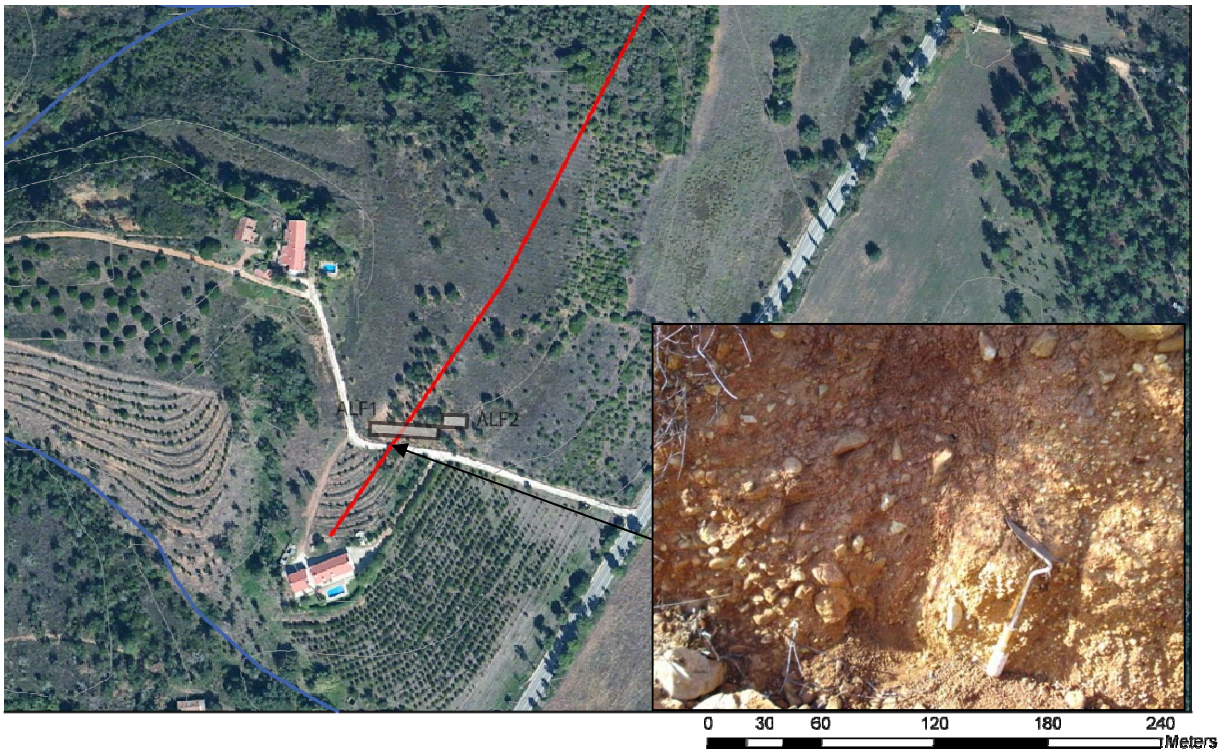

Figure 5.2 - Localization of trenches ALF1 and ALF2 at Barranco da Vaca site. The fault trace is indicated by the red line. The inset presents a detail of the coarse deposit contact with the medium sands is also included in the figure.

of the piedmont, was at Barranco da Vaca, at Alfambras basin, where along the inferred fault trace an anomalous contact between a coarse deposit to the west and medium sands to the east was identified, leading to the opening of two trenches, for detailed investigations (Figure 5.2).

Two trenches with direction E-W were open and the detailed survey of ALF 1 trench was conducted (Figure 5.3), corroborating the presence of a fault zone, that deforms a detritic sequence, probably of fluvial origin that could be related with the main drainage basin. This unit, which is characterized by the repetition of layers or more clayish or sandier, is dragged into the fault zone, where the bedding gradually becomes parallel to the fault zone.

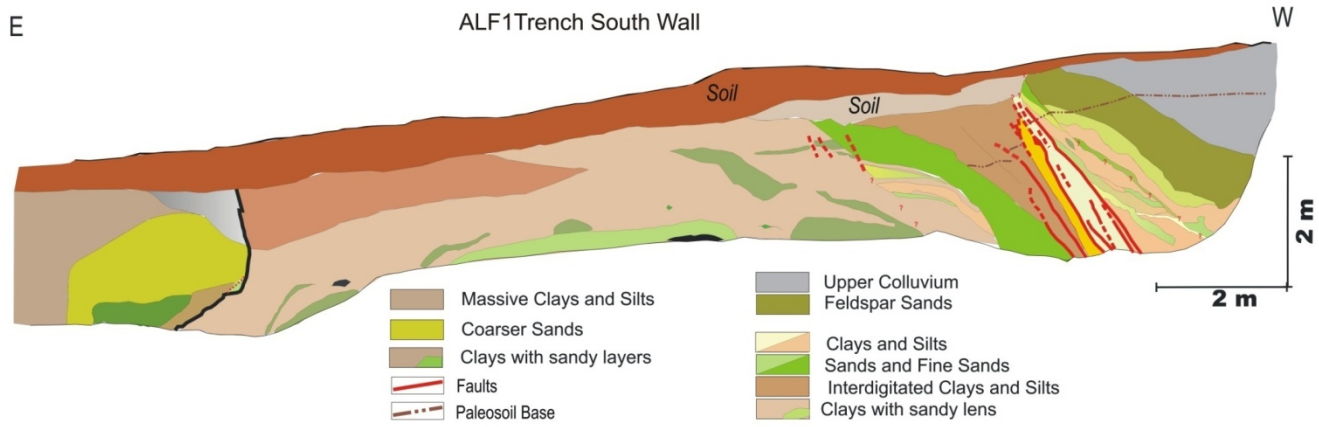

Figure 5.3 - South wall of trench ALF1, located at the Alfambras basin. Description of geology included in the figure.

Above this unit, in an unconformity, is an overlying unit of coarser sediments, characterized as colluviums, which seem also to be deformed, tilted and faulted. All these sediments are younger than the Miocene carbonates, which were recognized only at the base to trench ALF2. Samples for OSL dating were collected to better constrain the ages, but the samples quartz dose-rate were saturated revealing to be too old to be dated.

On the eastern segment of the trench we have interpreted a channel of a drainage, which we assume to correspond to a paleo channel of the Aljezur River. In fact it seems to exist a correlation between active strands of the fault and channel position, which has been inferred for others locations within the Aljezur-Alfambras basin.

A paleosoil profile developed after the sedimentation of the upper unit and developed across the upper unit and the detritic/fluvial unit: a horizon B was recognized and identified as *Alfisoil* crossing the fault, and displaced vertically at a maximum of 1.5 m (Figure 5.4).

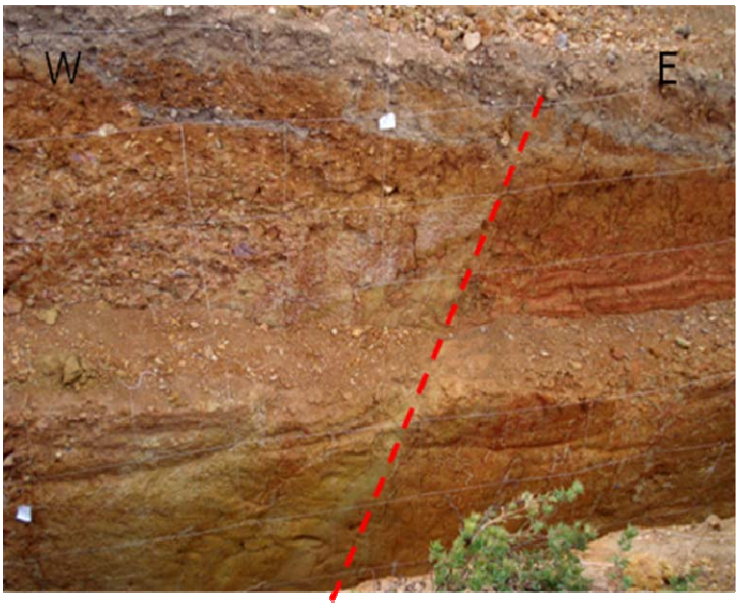

Figure 5.*4 – Detailed of the displaced paleosoil along the north wall.*

We assume the age of this *Alfisoil* as likely Middle to Early Pleistocene, based upon comparisons with other soils, for equivalent latitudes and climate. At this trench it was not possible to recognize individual paleoseismic events, since all the stratigraphy is dragged into the fault zone and the fault strands do not cross each other, and fault planes are essentially disposed mostly parallel between them (Figure 5.5).

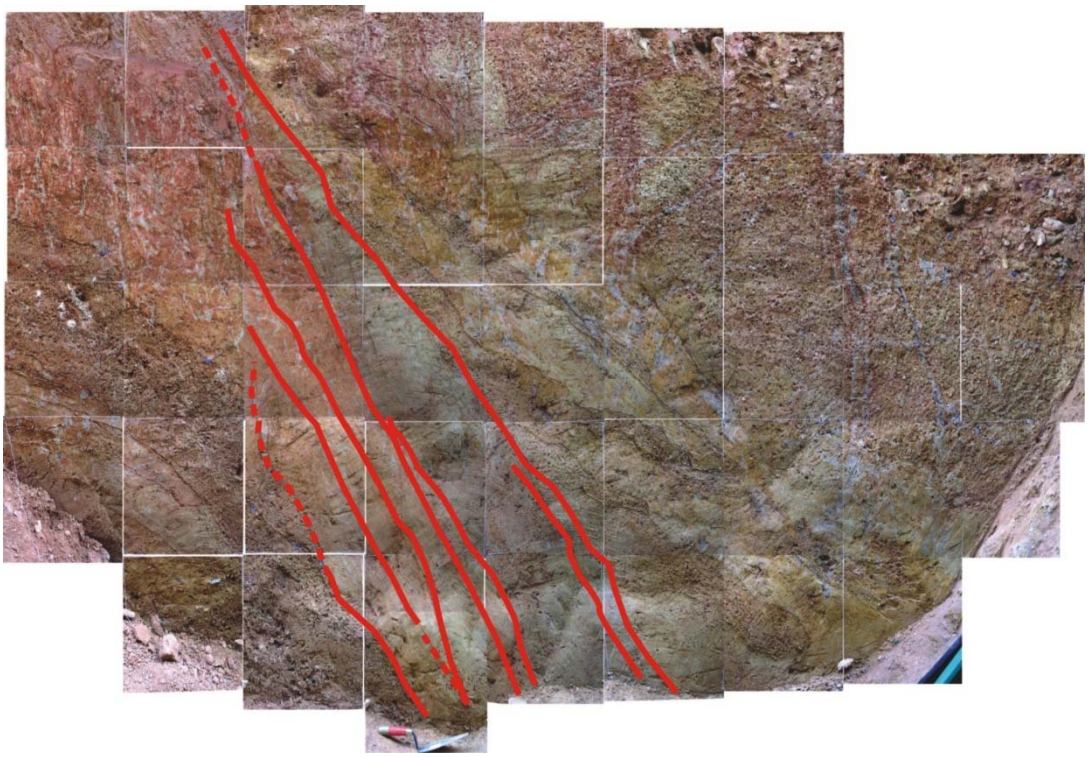

Figure 5.5 – Photo-mosaic of the fault zone at the ALF1 trench South wall. Red lines, mark several of the fault planes.

We saw no unequivocal deformation within the upper soil units; therefore we could not state an obvious correlation between the fault trace and the topography which would imply a more recent activity.

Since this fault is mainly a strike-slip one it was not possible to identify markers to quantify lateral displacement, at the trench, however, the vertical displacement recognized is consistent with a left-lateral fault, with a small pitch to the North, as previously recognized (Cabral, 1995; Dias, 2001)

More paleoseismic sites were selected farther north in the Alfambras and Aljezur basins, where geoelectric tomography profiles up to 50 m depth were obtained corroborating the existence of several fault traces near the topographic surface.

5.2.2 The Framangola site – Alfambras fault segment

The Framangola site (at Alfambras basin) is located at the alluvial plain close to a landform that was interpreted as a shutter ridge. In order to investigate the fault zone and potencial deformation at the Holocene alluvial plain sedimentary sequence, a geoelectric tomography profile was conducted and two trenches were opened at the alluvial plain (Figure 5.6 and 5.7).

Figure 5.6 – Localization of the geoelectric tomography profile and trenches open at Framangola alluvial plain. The fault trace recognized through geomorphology is also indicated. Another fault trace inferred by the geoelectric tomography is indicated by the dashed line.

The geoelectric tomography profile interpretation evidence two areas with strong contract between higher and lower resistivity values (Figure 5.7), located at approximately 35-40 m and 105 – 110 m of the profile. Both these anomalies have a disposition that could be interpreted as related with a fault plane, tilted towards the west, similarly with the fault

expositions that have been recognized. Since the more obvious anomaly was the one corresponding to the position 35- 40 m, which was also coincident with the localization of the fault trace inferred by the geomorphology, and that this location was also the more favoured to have Holocene sediments, a trench was opened in order to investigate the fault presence and sediment deformation.

The trench was then excavated through several alluvial and fluvial sediments, until the paleozoic bedrock. A "step" was recognized at the base of the trench, at the Paleozoic bedrock, which leads us to increase the trench depth in order to investigate if it was fault controlled or if it was paleo topography. Unfortunately, the deep excavations reach the water table, which conditioned the continuity of this trench.

A second trench was later opened in conditions of lower water table, but it was still not enough to safely undertake surveys in the trench. In the second trench a very coarse upper unit was recognized, with blocks with diameter close to a meter and with no evidence of a significant transport. At this coarse unit, archaeological artefacts from the Islamic occupation (that lasted until the XIII century) were found. We interpreted this unit, as likely to be a sort of debris-flow, with a strong input of large boulders from a close source, which lead us to infer to be related with a large or several landslides.

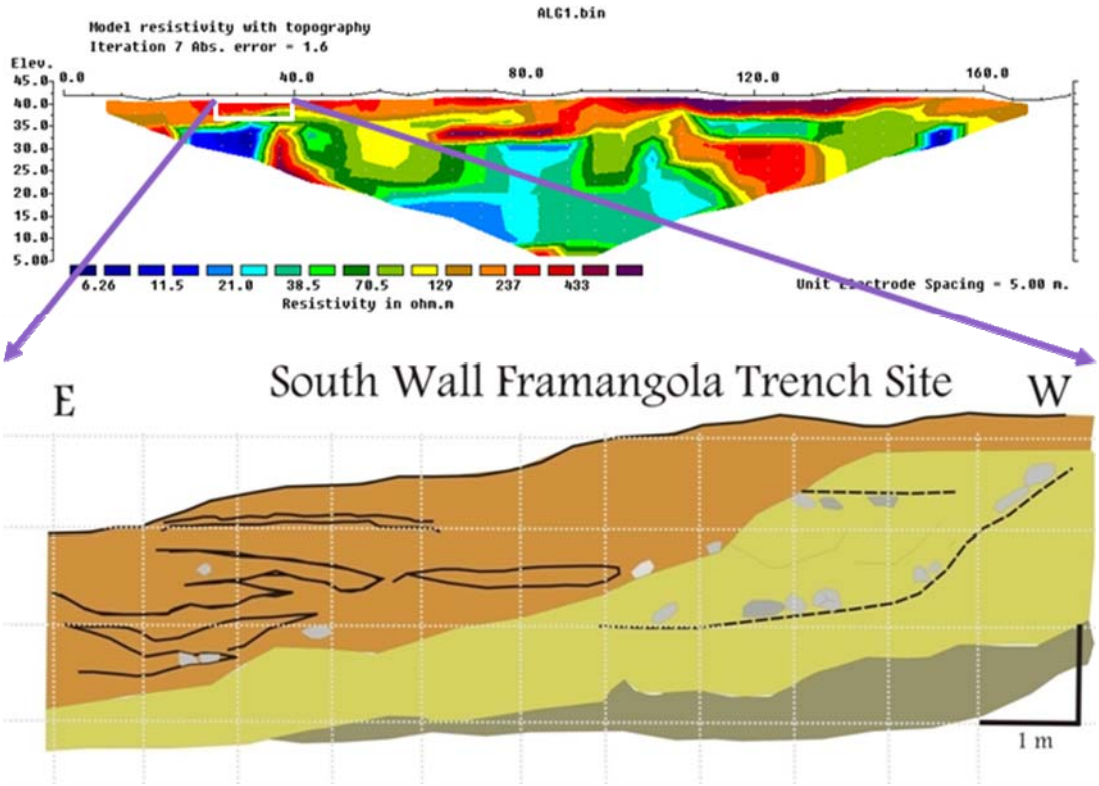

Figure 5.7. Geoelectric tomography profile (using Schlumberger method) *at Framangola site at the alluvial plain, strongest contrast coincides with previously identified fault trace; the trench units identified also correlate with the tomography (1) Clays and fine silts; (2) Very coarse Gravel (3) Silty sandy & fine conglomerate*

If this is the case, then this unit could correspond to the deposit generated by the multiple landslides that were triggered during the 1755 earthquake, that were described in some historical accounts, and that silted the Aljezur basin.

In short, the very coarse sediments and the high water table did not allow us to safely investigate both trench sites at a deeper level, but the studies that were possible to made, allowed to verify a correlation between the geometry of the sediment units found in both trenches and the resistivity measurements.

5.2.3 The Monte Ferreiros site – Aljezur E fault segment

At Aljezur alluvial plain, the Aljezur fault is recognized along the western hillslope of the basin and do active fault has been recognized for the eastern side of the valley. However a well defined morphological lineament is identifiable also along the east side.

Field surveys did not recognize sediments deformed, since at this side of the valley, the paleozoic bedrock is frequently at the surface covered by alluvial plain sediments, probably very modern or by very small alluvial fans. No paleosol is developed and minor references are present to corroborate a displacement. To evaluate or not the presence of a structure along this side of the valley, several geoelectric tomography profiles were done in order to assess the presence of a tectonic structure (Figure 5.8).

Results, evidence the presence of a vertical contrast between medium to high resisitivity values to lower ones, from the depth of circa 10 m downwards. This anomaly also seems to correspond to a separation between a less resistant zone, to the west (miocene carbonate sediments??) from a slighty higher resistant zone to the east (the schists and greywackes from the Paleozoic ??). The anomaly location is consistent with the inferred fault trace by the geomorphology (Figure 5.8). Altough we were not able to ensure the presence of an active strand of the fault at this site, we have reforced the existence of a structure that extends probably to the surface.

The presence of this structure was later confirmed by several field surveys, which allowed the observation of a fault, poorly preserved.

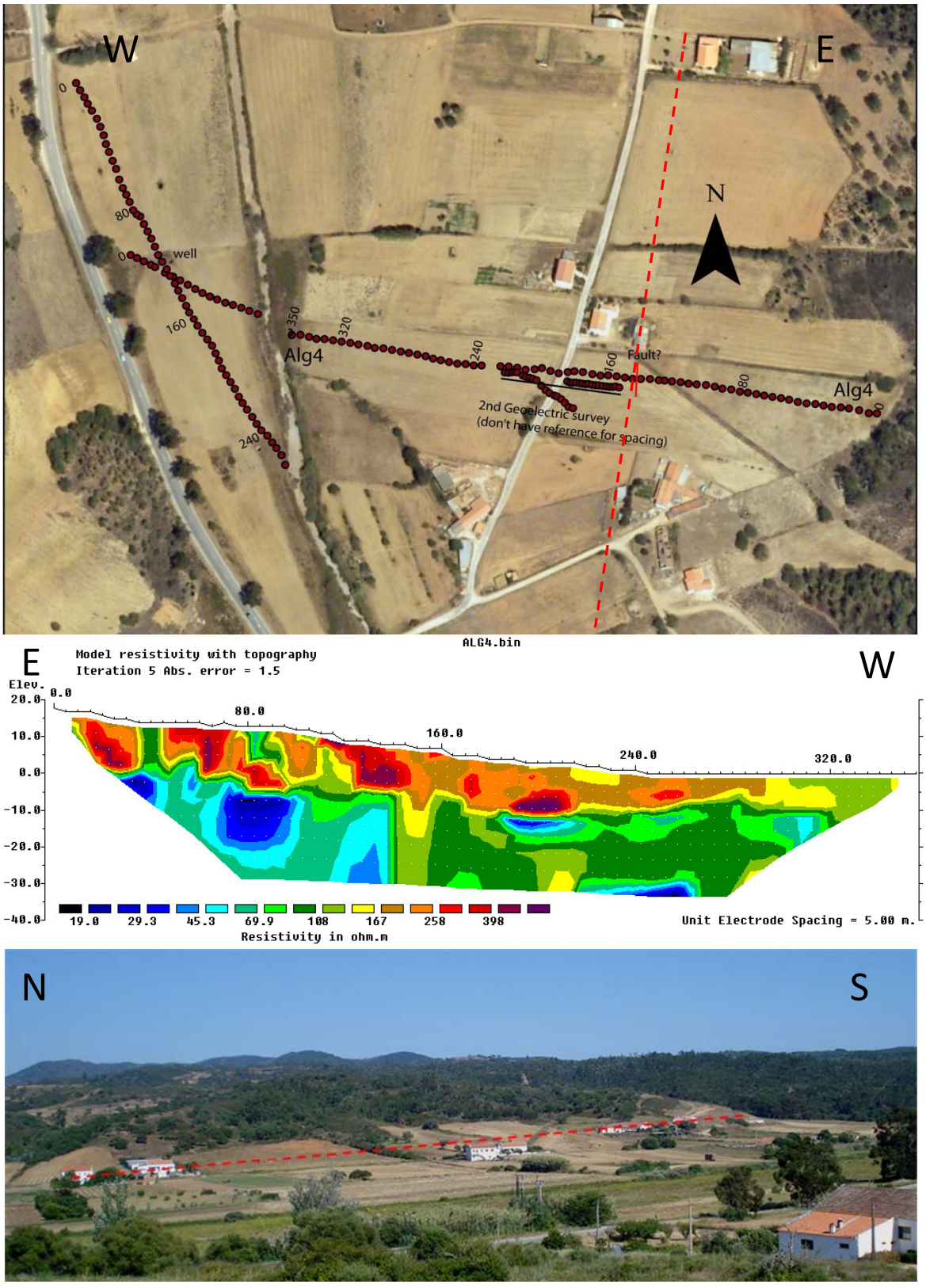

Figure 5.8 – (A) Localization of the geoelectric tomography profiles across the eastern Aljezur Alluvial plain (B). Geoelectric tomography profile (using Schlumberger method) at Monte Ferreiros site, strong contrast coincides with the geomorphologic trace interpreted in the lower image (C).

5.2.4 The ETAR site – Aljezur W fault segment

The Aljezur fault localization is reasonably well constrained at the vicinity of Aljezur village. However, at the end of the Aljezur spur landform (where the Castle is located), when the Aljezur river inflects towards the west, there is no evidence of the fault localization along the alluvial plain.

A northward prolongation of the fault has been assumed, at the northern bank of the alluvial plain, however there is no real knowledge about the exact location of the fault zone at the alluvial plain, which will allow evaluating a suitable location to open a paleoseismologic trench.

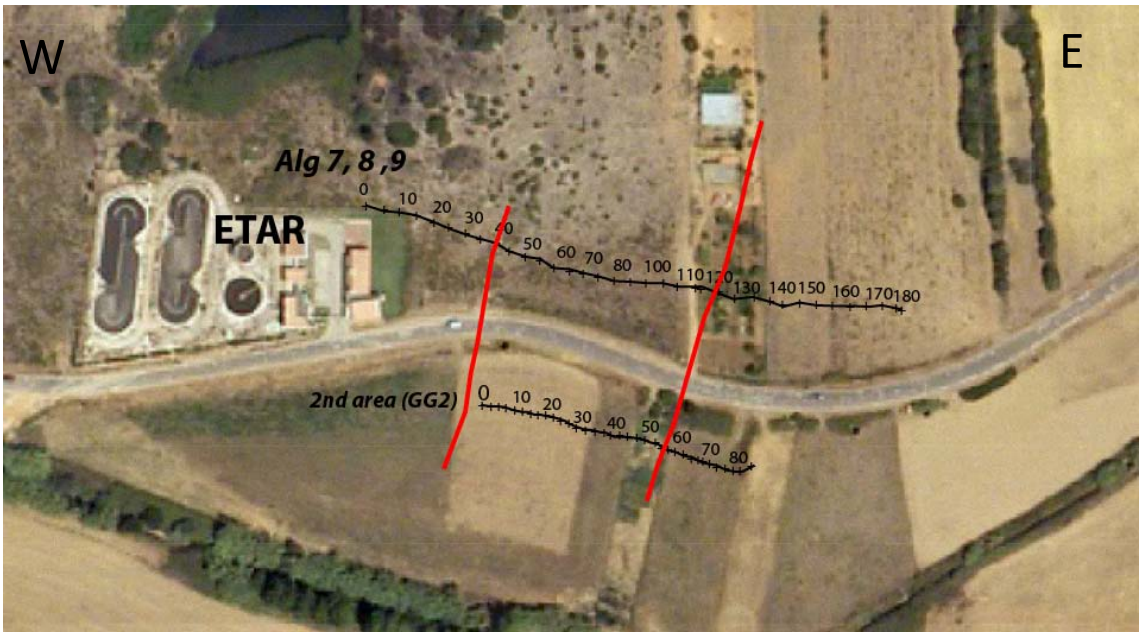

Figure 5.9 - Localization of the Geoelectric tomography profiles at the ETAR site.

With this aim, two geoelectric tomography profiles were done along the inferred fault zone (Figures 5.9 and 5.10): a larger one was initially conducted to identify anomalies and to constrain target zones for a detailed analyses. In this profile, two anomalies were identified, one of them clearly expressed, higher resistivity to the west and lower resistivity to the east, which we have interpreted as being the schists more resistant and the Miocene carbonate sediments as less resistant, similarly to what we have inferred for the Monte Ferreiros site.

The profiles allowed to constrain the fault zone, which is a complex and wide one, with approximately 100 m width. A strong anomaly in the shorter profile (circular shape) is associated with the existence of a well, which is located very close to the fault strand (less than 10 meters), and partially masks the anomaly that might reflect the fault. We choose not to open a trench at this site, because the s superficial sediments were essentially muds, massive fine clays and silts, which would on one hand not favour the preservation of fault planes and

on the other hand, will not favour the presence of stratigraphic markers to conduct an adequate earthquake recognition.

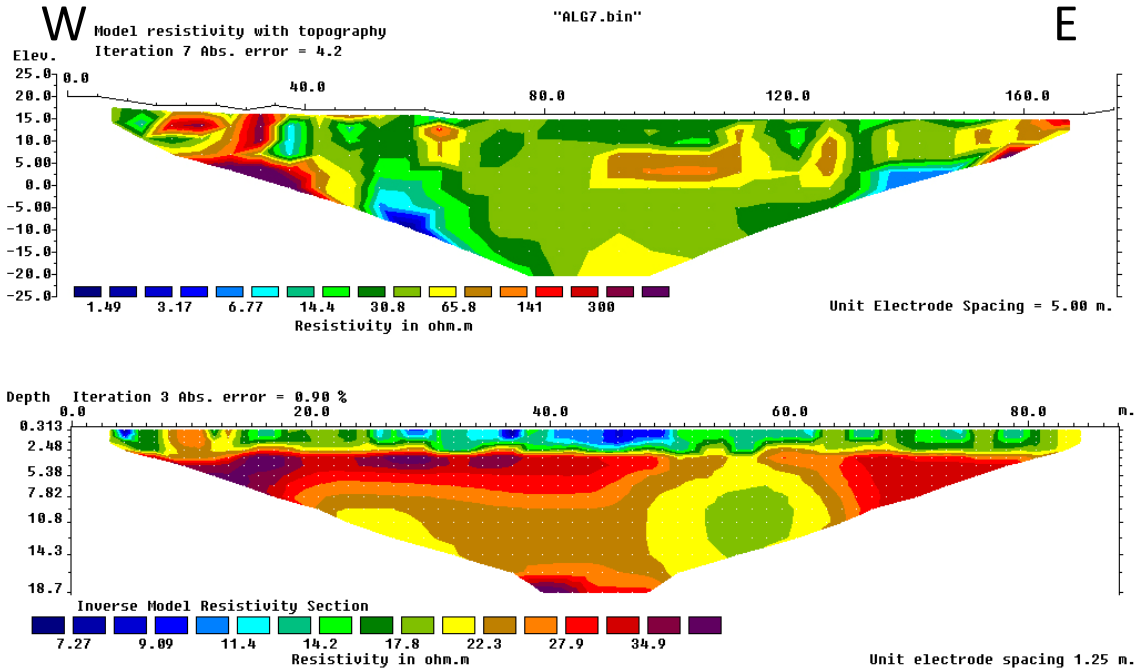

Figure 5.10 – Geoelectric tomography profiles at ETAR site, the longer and the shorter one. In the shorter one, there is a strong anomaly coincident with a well, but also very close of the fault trace.

5.3 Conclusions

Trenches excavated across the São Teotónio–Aljezur–Sinceira fault system (STASFS), exposed faulted sediments that are inset below the regional marine abrasion surface. Sparse age control based on paleosol development, along with the geomorphic position of these deposits relative to the marine deposits, suggests that this faulting occurred in the middle to late Pleistocene timeframe, although we have yet to find evidence of Holocene activity.

A geophysical exploration method, namely the of geoelectric tomography profiles were successfully applied, corroborating the fault presence and allowing to increase the knowledge on the fault localization and fault zone width.

Both, trenching and the geophysical exploration contributed to investigate and verify the presence of several active fault strands along the Aljezur basin.

At its northern end, near São Teotónio, the STASFS joins the Alentejo-Placencia fault (APF). In this area the tectonic deformation becomes distributed, suggesting than APF may have several

splays along this intersection and it is difficult to scrutinize the relationship between both structures. No Holocene or late Pleistocene deposits were recognized in association with the identified fault segments, which increase the uncertainty concerning the recent activity. Presently it is still not clear whether the STASFS extend to the north of the APF.

Towards the south, at the southern sector of the STASFS, south of the Sinceira basin, the local morphology does not evidence any significant Plio-Pleistocene vertical deformation related with this fault system, and it seems that this fault system may splay into several faults. In fact, several parallel faults occur in the Mesozoic bedrock sediments where limestones dominate. Several karst pits are filled with Plio-Pleistocene sands (Faro-Quarteira sands) mainly at the coastal section Martinhal – Zavial where the STASFS should intersect the coastline. The elongated shape those karst sometimes present, suggested a structural control by a previous structural fabric on the karst development (Dias and Cabral, 2002).

Acknowledgements

This work was funded by Fundação da Ciência e Tecnologia, through a PhD scholarship (SFRH/BD/36892/2007) attributed to Paula Marques Figueiredo and Research Project "Paleoseismological study of active faults in Mainland Portugal" (PTDC/CTE-GIN/66283/2006), co-financed by FEDER. The authors also wish to thank the collaboration during field work of Hector Perea and André Tempera.

Chapter 6

Morpho-tectonics of the Aljezur Fault – an active structure in Southwest Iberia

(This chapter is presented in a paper format since it is being prepared to be submitted to a science journal)

Figueiredo, Paula M. (1, 2), Rockwell, Thomas K. (3), Cabral, João (1,2)

Abstract:

The Aljezur fault corresponds to the central section of the São Teotónio – Aljezur - Sinceira fault system, located in southwest Portugal, Iberia. This fault system corresponds to a transpressive structure, mainly left-lateral with a minor reverse component that deforms a large regional abrasion surface. Along the fault system several small tectonic basins are present and filled with sediments from Miocene to Quaternary age. One of these basins is the Aljezur basin, where Plio-Quaternary activity, although poorly constrained, was recognized for the Aljezur fault. To recognize and characterize the Quaternary deformation at this structure, detailed studies were conducted, not only to locate and individualize active fault segments, but also to understand the regional morphology and how is it deformed. With this aim, we applied morpho-tectonic indices to the Aljezur region, such as mountain front sinuosity, valley-floor width/height ratios, stream sinuosity, relief ratio, stream-length, basin elongation ratio and asymmetry, in order to evaluate tectonic activity and incision/erosion rates along distinct sections of Aljezur and Alfambras valleys. Results indicate variations in distinct segments of the fault. Several surfaces are recognized, some interpreted as equivalents of the displaced regional abrasion surface, and others are fluvial surfaces related to Pleistocene eustatic oscillations. A geomorphologic analysis and recognition of displaced features allowed us to infer that this fault has been active and displaces a Plio-Pleistocene surface. A vertical cumulative displacement rate of 0.014 ± 0.001 mm/a, plus an inferred maximum lateral displacement suggest a 0.1 mm/a rate for the São Teotónio- Aljezur- Sinceira fault system.

6. 1 Introduction

Landscape evolution is a consequence of many geomorphic processes, which are controlled by major factors, such as climate, topography, lithology and tectonics. Tectonic activity exerts control in the development and evolution of landscapes in a direct manner, as for example along active faults or tilted and folded surfaces, but also indirectly through tectonic plate motions, where topography and lithology are controlled by geodynamic conditions (Bull, 2007, 2009). In order to understand these effects, the study of landforms related to active tectonics has been successfully conducted through the application of several geomorphic indices (Bull, 1977, 1978, 2007, 2009; Bull and McFadden, 1977; Hare *et al.*, 1985; Rockwell *et al.*, 1985; Merritts *et al.*, 1989, 1994; Ramírez-Herrera, 1998; Wakabayashi *et al.*, 2001; Chen *et al.*, 2003; Silva *et al.*, 2003; Snyder *et al.*, 2003; Troiani *et al.*, 2008; Pedrera *et al.*, 2009; Peréz-Peña *et al.*, 2010; Azañon *et al.*, 2012; Giaconia *et al.*, 2012, among many others) even for areas with low to moderate tectonic rates where the active tectonics trace is less obvious (Silva *et al*., 2003, Pedrera *et al.*, 2009). In such cases, where the active tectonics trace is less obvious and could be disguised by other geomorphic processes, the application of geomorphic indices is relevant and should be wisely applied. Thus, it should be taken into consideration the type of tectonic source and other remaining factors that control local and regional geomorphic processes, in order to select the appropriate indices (Bull, 2007, 2009; Keller and Rockwell, 1984). In this study we will focus on a left lateral strike-slip fault system, the São Teotónio - Aljezur –Sinceira 50 km long NNE-SSW fault system (STASFS), parallel to the Portuguese southwest coastline, aiming to recognize morphologies indicative of the lateral motion but also to investigate a possible vertical component, in order to access the amount of active displacement if any, related with the regional abrasion platform.

A strike-slip fault system is composed of fault segments that are generally organized in an “en-echelon” pattern and connected by oblique bends or jogs. A compressional jog or a restraining bend corresponds to a convergence zone, where local shortening will promote surface uplift, whereas a dilatational jog or a releasing bend corresponds to an extension zone, where local extension will promote vertical downdropping and surface depression. In this manner, although strike-slip displacements are essentially “horizontal” along their direction, a fault system is able to generate topography, according with compressional (push-up) or dilatational (step-over) jogs, which promote the generation of ranges or basins (Sylvester, 1988).

With time, the fault system evolution will generate new fault segments, which will promote the migration and/or the growth of the compressional or dilatational features (Dorsey and Roering, 2006; Wakabayahi, 2007; Walker and Jackson, 2002; Wesnousky, 1988; Westaway, 1995) and geomorphology changes along the fault area. These geomorphic changes, in turn, will cause drainage adjustments (Keller and Pinter, 2002; MacCalpin *et al*., 2009) affecting the drainage network, either through channel deflections, channel captures or changes in the stream gradient. Tectonic uplift or subsidence will also affect drainages directly, if the local base level is affected, or indirectly, if changes in the topography favour erosion or changes in the sedimentation processes (Hoolbrook and Schumm, 1999).

To understand how the STASFS evolved through time and space, a detailed geomorphologic analysis was conducted along the Aljezur fault i.e. spanning the regional abrasion surface that is displaced by the STASFS in the vicinity of Aljezur city and along the tectonic basins located there, Aljezur and Alfambras. For that purpose, several geomorphic indices were applied to the drainages and to the relief of the basin. To analyse streams, Stream Channel Sinuosity (S) was applied to evaluate channel response to the presence of local structures and a Stream Gradient index (SL) was calculated, producing SL maps to detect abrupt stream power modifications that might be controlled by active tectonics. A channel steepness (Ksn) study was also conducted to evaluate changes in the channel steepness that might reflect the presence of structures or responses to variations in base-level. For the basin shape, the applied indices were basin relief ratio (Rh), elongation ratio, and basin asymmetry factor (AF). Valley floor width to height ratio (V_f) and mountain front sinuosity (S_{mf}), which are applied to mountain fronts, are applied in this study to the relief generated by the development of the strike-slip basins.

It should be stated that most of these parameters will provide information concerning vertical deformation, which for this study area is probably of low rate. Nonetheless, there is no certainty about active vertical deformation and for that reason, parameters will be applied.

Analysis of channel deformation such as deflections in order to detect horizontal slip were conducted and several morphological surfaces were also identified, enabling construction of a geomorphological map of the Aljezur basin and the recognition of likely active segments of the STASFS.

6.2 Geological Setting

The São Teotónio Aljezur- Sinceira fault system (STASFS) corresponds to a 50 km long NNE-SSW left lateral strike-slip fault system, with several fault segments arranged in an "*en-echelon*" pattern that are approximately parallel to the southwest Portuguese coastline. Five tectonic basins occur along this fault system, from north to south, the São Miguel, Aljezur, Alfambras, Pedralva, and Sinceira basins (Feio, 1951, Pereira, 1990, Cabral, 1995, Dias, 2001). These are filled with sediments with ages assumed to be from the Miocene and to the Quaternary, although only at the Aljezur basin, the presence of Miocene sediments is undoubtedly corroborated by several isotopic $^{87}Sr/^{86}Sr$ age determinations on marine and estuarine fossils (Pais *et al.*, 2000; 2012), providing ages from the Burdigalian (samples ages from 16.9 to 19.5 Ma) and Tortonian-Serravalian (samples ages from 9.8 to 12.6 Ma).

A large regional surface that corresponds to a 10 km-wide marine abrasion platform that was probably re-trimmed during Pliocene and Pleistocene times, as evidenced by marine terrace remnants, is displaced by the STASFS. A section of the regional surface drops into the tectonic basins depressions, indicating that the STASFS has been active during the Plio-Pleistocene (Figure 6.1). A vertical tectonic slip rate of 0.03-0.06 mm/a, based on vertical post-Pliocene displacements, has been estimated by Dias (2001). This should correspond to a minimum estimate, because the main sense of slip is likely to be strike-slip.

The basins were always recognized as having tectonic control (Feio, 1951), present a narrow and elongated configuration, but with high length/width ratios that are not typical of pull-apart basins (Gurbuz, 2010), and therefore we prefer to characterized them as strike-slip basins. Faults have been recognized mostly at one side of the basins and the basin filling resembles the configuration of a half-graben structures. The main fault is generally recognized near the western boundary of the basins where it puts in contact a strongly sheared and folded Paleozoic sequence of schists and greywackes with much less deformed sediments, generally sands, conglomerates, and limestones of Miocene to Quaternary age.

When the main fault crosses the regional platform stepping out of the tectonic basins, it does not evidence any significant vertical offset and the horizontal slip component is difficult to track in the smoothened regional topography. Thus, apparently the main fault trace does not control significantly the morphology of the regional surface, except for the basins. However, along the basins, several morphological elements are indicative of tectonic control, either directly related with fault strands, such as shutter-ridges and deflected drainages, or related to the rate of incision and erosion, such as terraces, which should be reflecting both local tectonic rates and regional uplift superposed by Quaternary sea-level oscillations which work as the regional base-level.

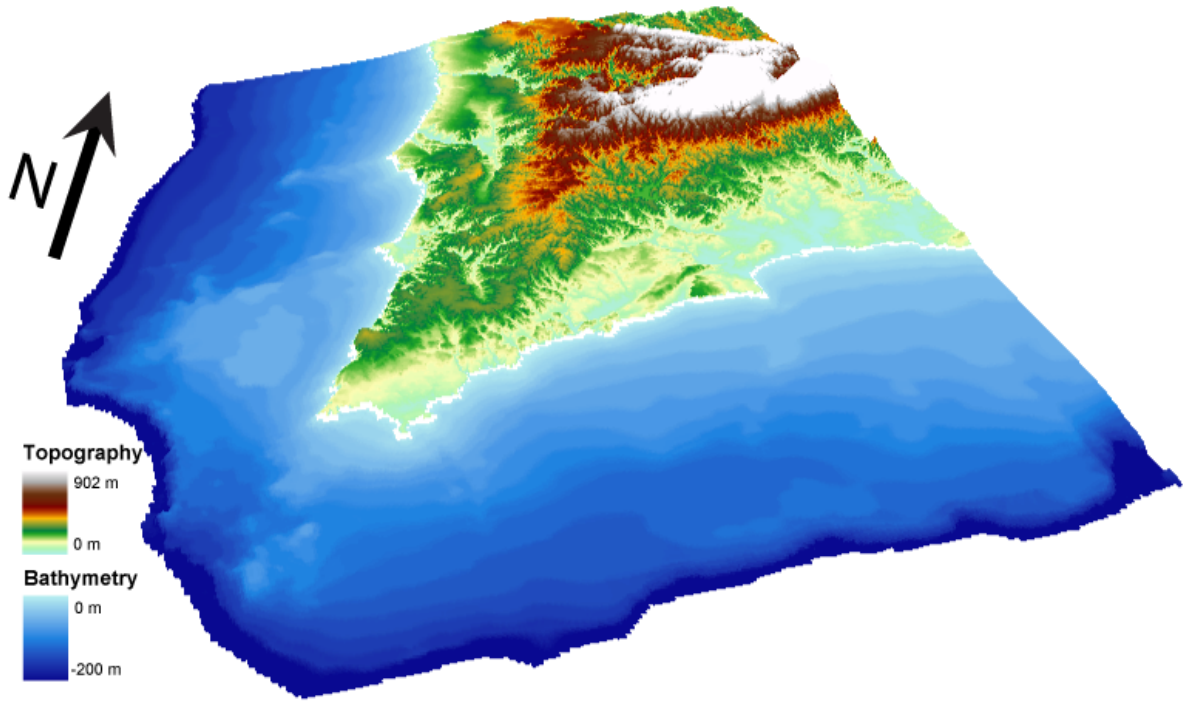

Figure 6.1 – Digital Elevation Model, from the Southwest Portugal and its continental shelf (depth to 200 m). Vertical exaggeration 5x. Along the west coast the regional abrasion platform and the STAS fault system parallel to the coastline, as well as the basins along it, are recognizable.

All tectonic basins along STAS have a main drainage running approximately parallel to the main fault, sometimes crossing it. All the basins have an elongated shape with the main axis striking approximately NNE-SSW to NE-SW, and show an asymmetrical drainage pattern, with longer tributaries to the east and shorter to the west.

For this study purpose, we will focus in the Aljezur and Alfambras basins, which are basins almost in continuity: Aljezur basin is located north of Alfambras and it is wider and longer. Despite Miocene sediments are present at both basins, the ones at Aljezur are probably older and the sedimentary sequence is more complete, and conglomerate units inferred as Miocene (Pimentel and Amaro, 2000) or Pleistocene (Pereira, 1990; Cabral, 1995; Dias, 2001) are also only present at Aljezur basin.

To facilitate the morphological analysis and presentation of data, Aljezur and Alfambras basins will be sub-divided into sections, according with changes of valley directions, distinct sediments or nowadays channel incision modifications.

From the south northwards, Alfambras basin can be divided in two sections: one a southern one, corresponding to a linear valley roughly NE-SW direction, bottom flattened, 3.8 Km long and 300 to 500 m wide, hereafter called the Alfambras section and the second an adjacent valley continuous with Alfambras, circa 3 Km long and 200 to 400 m wide but with a direction NNE-SSW, and where the Aljezur river nowadays channel is more incised and meandering, hereafter called the Alfambras-Framangola section.

Northwards, in continuity with Alfambras-Framangola section, the Aljezur basin will also be divided into two sections: the Aljezur section, which corresponds to Aljezur valley NNE-SSW oriented, characterized by a broad flat-bottomed valley floor (about 800 m in width) and circa 3 Km long, and corresponds to the section where the main drainages (Cerca and Areeiro rivers) converge with Aljezur river before its inflection to the west, towards the Atlantic. North of Aljezur section, a northern section also with a NNE-SSW direction is drained by the Areeiro river that exceptually flows southwards, with similar carbonate Miocene sediments than at Aljezur when close to it but with a thick sand unit towards the north. This section also exhibits a different geomorphology, with a staircase of surfaces that are likely to correspond to terraces, which are not present in the Aljezur section.

6.3 Geomorphology Analysis

6.3.1 The Regional Abrasion Surface

A large regional surface corresponds to an extensive marine abrasion platform (Feio, 1951; Pereira, 1990), corresponds to a sequence of marine terraces forming a relevant geomorphologic element along the southwest coastline.

This regional surface generally exhibits smooth topography with a slope varying from 4 to 7%. It extends inland gently increasing in elevation from the coastline, where it is at an elevation varying from 100 to 120 m, towards the interior at a paleo-shoreline. The shoreline

angle, which was previously described at circa 200 m in elevation (Feio, 1951; Pereira, 1990; Dias, 2001) is difficult to recognize due to the strong drainage incision that has partially erased its expression.

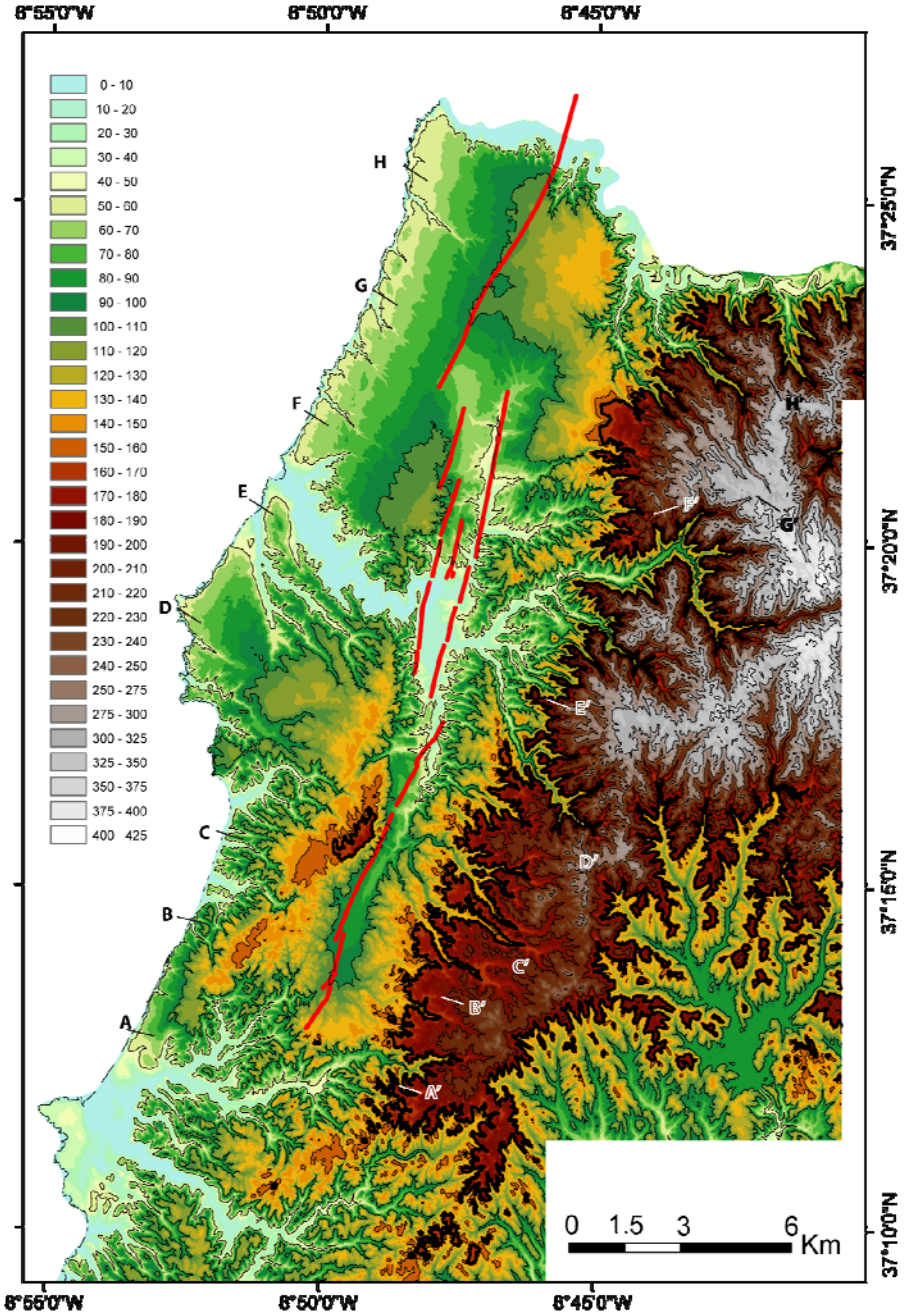

Figure 6.2 - Hypsometric map of the Aljezur county area. Vertical intervals colored each 10 m from 0 to 250 m elevation and 25 m above 250 m; thin contour lines in black, each 25m elevation. Abrasion platform inner edge is marked by the thick black line (circa 160 m elevation). Location of topographic profiles is indicated by letters.

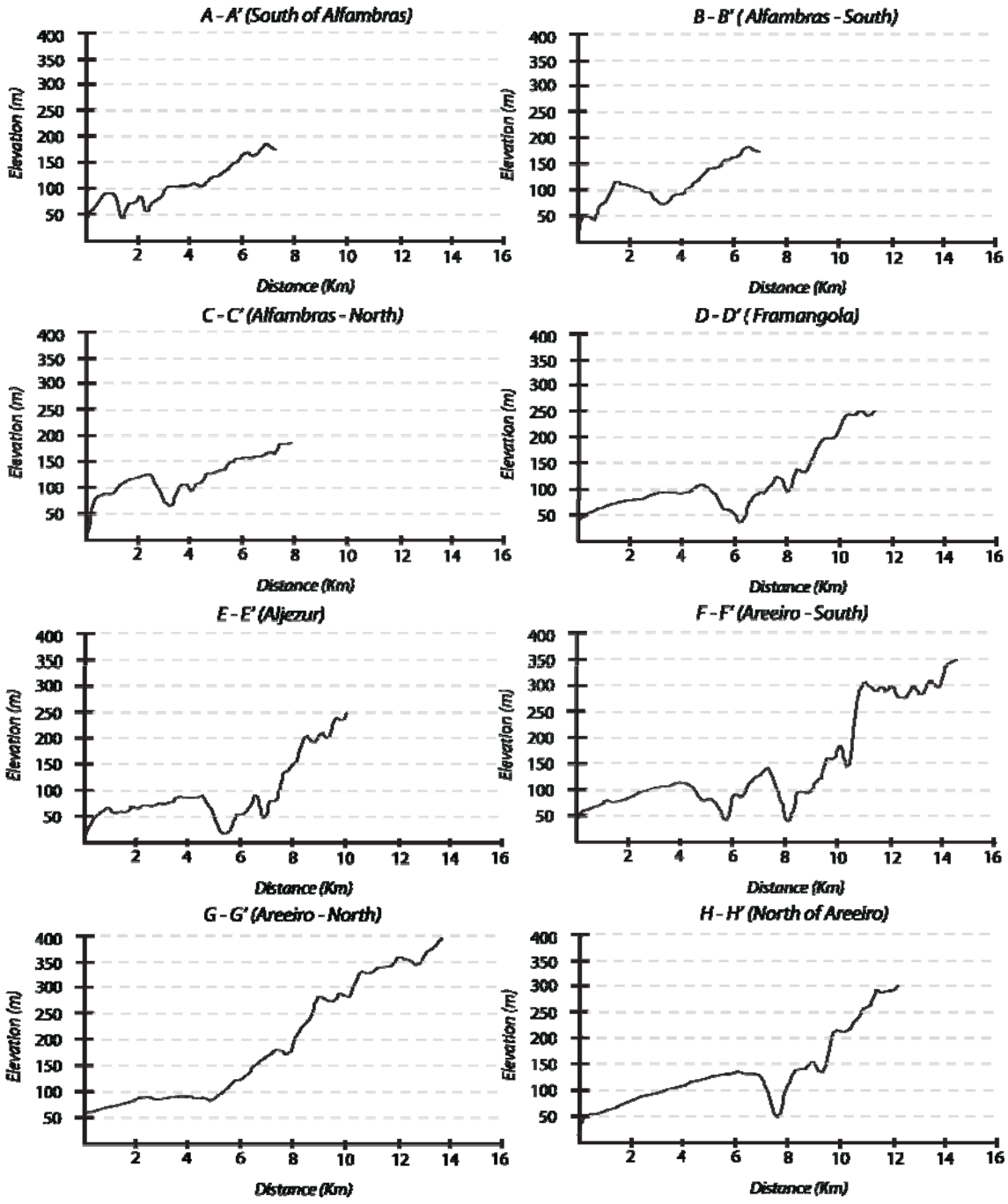

Figure 6.3 – Topographic profiles approximately NW-SE, from the coastline across the regional abrasion surface and the Aljezur valley towards the inland landscape. Vertical exaggeration 20x. The locations are indicated in figure 6.2.

However, recent field and map based geomorphologic analyses show a change of slope from a higher, rough topography to a lower, smoother and flatter topography at circa 160 m elevation. This is consistent with changes in the cover sediments at the same elevation: medium sands with pebbly quartz inferred to be beach or marine sands, although sparse and weathered, can be continuously tracked from 155-160 m elevation towards lower elevations

(~100 m) adjacent to the coastline. From 160 to about 190-200 m elevation, there is an absence of similar deposits, but instead fine sand deposits are locally present (as in Pedra Furada and Corte Sobro), which we interpreted as corresponding to aeolianites that are locally interbedded with colluvium. Both observations suggest that the shoreline angle elevation for this regional abrasion platform is close to 160 m (Figure 5.2 and Figure 5.3). Additional sandy deposits, possibly marine, occur at higher elevations farther inland (to the east) and ranging in altitude from 200 m to 360 m elevation, as for example at Fonte Santa (Figure 5.4), though they correspond to an older marine terrace sequence that is likely to be Pliocene in age according with Feio (1951). Remnants of fossiliferous carbonate marine deposits assumed to be Miocene are present at 170-180 m elevation at Pére Jacques, higher than the regional inner-edge. Carbonate marine deposits overlapping the Paleozoic bedrock are still recognized along the eastern slope of the Alfambras section: here, at elevations lower than 160 m, this carbonate deposit is karstified, frequently covered by sandy deposits.

At the regional abrasion platform, marine sediments are poorly preserved along what are probably marine terraces remnants. Sediments are frequently absent or occur as thin remnants of beach deposits, with quartz pebbles present at most of the terrace exposures associated with the regional surface. All these remnants of marine sediments overly an abrasion surface trimmed on Paleozoic bedrock, which locally contains a thick argillic paleosol (rich in illite with a trace of kaolinite, typical of temperate xeric soils) beneath the marine cover. Nevertheless, the presence of this thick soil indicates that this Paleozoic bedrock was exposed close to the topographic surface during a temperate xeric climate in previous landscape that was later trimmed by a marine transgression.

The genesis and development of the regional abrasion platform has been interpreted as a polygenic morphology resulting from different stages: an oldest stage evidenced by the Miocene marine sediments that are preserved in the tectonic basins as well by some likely remnants present at the abrasion platform. Later, this surface was exposed to superficial weathering expressed by the thick argillic paleosol recognized locally and trimmed by another marine transgression episode, probably during Pliocene, re-trimming and depositing younger sediments. Finally, during the Pleistocene interglacial periods, the Pliocene abrasion platform was partially re-occupied and Pleistocene terraces are built-in in this previous platform.

No absolute geochronology is available for the regional abrasion platform sediments or surfaces, except for some Miocene carbonate deposits displaced, now present in the tectonic basins (Pais *et al*., 2000; 2012). The ages of the marine sediments, frequently azoics and abrasion surfaces have been inferred by correlation with equivalent sediments or surfaces at other regions in Portugal and Iberia. However, these regions might not have been subjected to the same deformation and vertical motion rates, and therefore their marine surfaces might be suitable for a proper correlation. In fact, studies along marine terraces embedded in the regional abrasion platform and morphotectonic analyses suggest that northern areas within this regional feature were subjected to different uplift rate (Figueiredo *et al*., *submitted*). Recent studies conducted to recognize and characterize Pleistocene marine terraces embedded into the regional abrasion platform, recognized at lower elevations along the sea

cliffs, marine terraces inferred as Late Pleistocene (Figueiredo *et al*., 2013) as well as at higher elevations some of which seem to be in the continuity of the regional abrasion platform. A marine terrace with an inferred inner-edge at about 80 m, located near Sagres, was recently dated through the Cosmogenic Nuclide geochronology method providing a preliminary age of 2.0 +0.3/-0.2 Ma, confirming the marine transgression of Pleistocene age (*Figueiredo et al, in preparation*).

The regional surface is therefore interpreted as a sequence of closely spaced marine terraces. The individual inner edge for each of these marine terraces is generally difficult to track, since it has been smoothened and locally eroded through time. The elevation difference between successive terraces seems to be small in most cases, which all together makes it additionally difficult to separate individual terraces. Despite the difficulty to individualize marine terraces along much of the regional surface, distinct flat surfaces are present, that when within a constant elevation and with remain of marine sediments, where interpreted as marine terraces trimmed (or re-trimmed) during the same sea-level position.

Among these flat surfaces, the larger one corresponds to a surface circa 130 m elevation, best expressed north of Sagres, close to Vila do Bispo village and along the west block of STASFS, especially along Aljezur-Alfambras basins. This 130 m high surface seems to be displaced by STASFS Aljezur and Sinceira fault segments.

Figure 6.4 – (A) Uplifted aeolianites strongly cemented with iron enrichment at Fonte Santa site (360 m elevation), assumed to be Pliocene; (B) at the same location, quartz pebbles and sand interpreted as poorly preserved beach deposits, are present above the Paleozoic bedrock and under the aeolianites.

6.3.2 The Valley Surfaces

At the tectonic basins, the valleys are drained through drainage basins where the main channel typically is a subsequent one, *i.e.*, runs parallel to the fault, and its tributaries run roughly perpendicular to it. Each valley has its own drainage basin that flows out towards the

Atlantic Ocean, which is located very close, in most cases less than 5 km away. For this reason, valley terraces that would be interpreted as directly related to the drainage will reflect Quaternary sea-level oscillations, namely they will correspond to eustatic highstands. Along the valleys several surfaces were recognized, and because the valleys are tectonically controlled depressions, it is expected that some of the surfaces may be displaced and consequently their position will not correspond to an original fluvial terrace (or eustatic terrace). For this reason, we have conducted a detailed morphological analysis along four sections of the Aljezur-Alfambras basins in order to identify and interpret correlative surfaces, and quantify observed displacements.

6.3.2.1 Aljezur-Alfambras Basin Sections

6.3.2.1.1 Alfambras Section

As referred, the southern Alfambras section corresponds to a linear valley, about 3800 m in length and about 300 m in width. The elevation of the valley margins varies from 130 m in the west to 150 m in the east, and the elevation of the floodplain decreases northwards from 95 m to 85 m, consistent with the south to north flow direction of the Aljezur River. The floodplain is flat, and the modern channel is incised only a few meters below the plain. Only a few surfaces have been identified at both sides of the valley and the basin filling is also poorly expressed. Sediments covering the Paleozoic bedrock are usually thin; the lower unit corresponds to Miocene sediments outcropping as a thin limestone layer at the southeast border of the valley, directly overlying the Paleozoic. A sequence composed of argillaceous sand interbedded with clayey and silty layers overlying the carbonate Miocene, generally tilted towards the west, occurs at elevations slightly above the floodplain. Colluvial deposits are present along the slope base, in some places interfingered with sandy sediments present at a 115-100 m elevation surface. No deposits, such as debris-flow or coarse fluvial deposits were recognized in this Alfambras sector.

Analysis of the geomorphology of this section indicates the presence of several morphological surfaces at distinct elevations, namely at 140-130 m, 115-100 m and 95-90 m elevation (Figure 6.5).

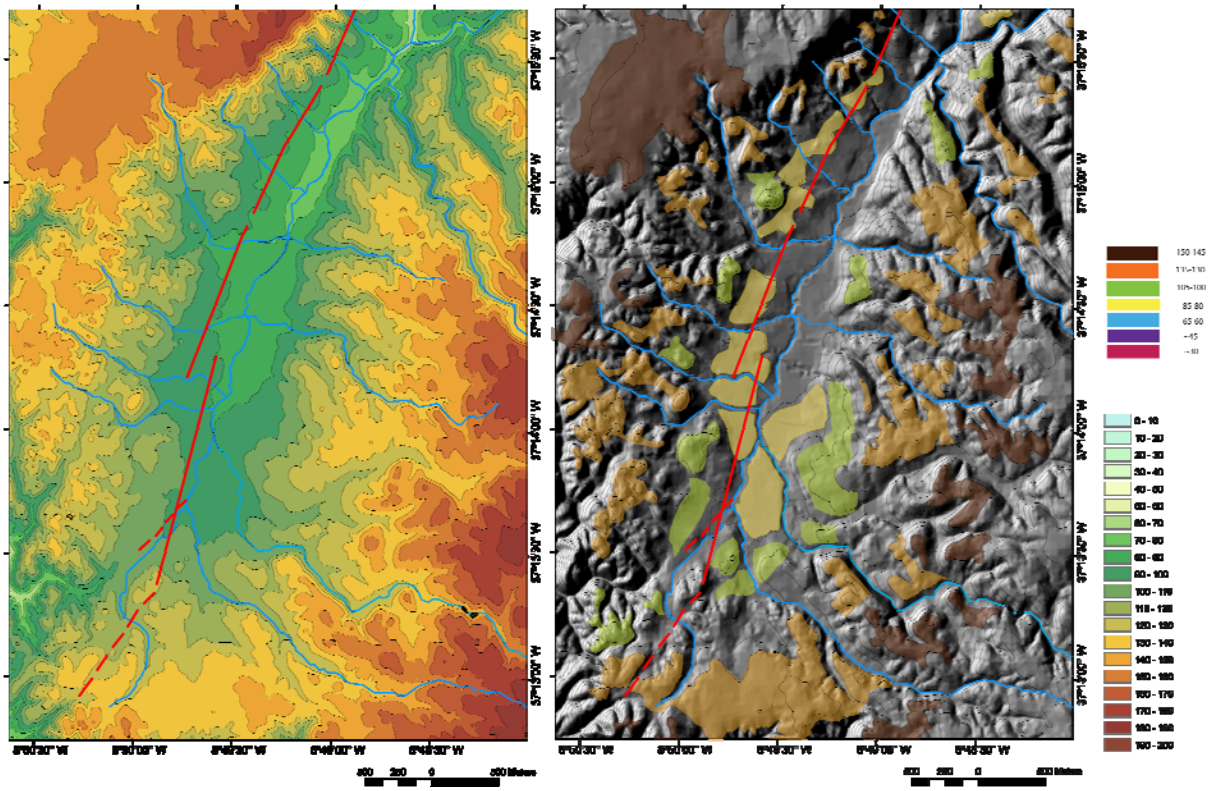

Figure 6.5 - Hypsometric map of the Alfambras section on the left. Geomorphologic interpretation and surface mapping over a shaded relief map for the same area on the right. Scale and hypsometry colour are included.

At the regional abrasion surface west of Alfambras, remnants of a higher surface with elevations higher than 150 m (≥ 154 m) are locally present at residual reliefs,: to the west of the valley, those remnants are covered by remains of a thin cap of sediments, with small rounded quartz pebbles probably of marine origin, up to approximately 160 m elevation, whereas to the east this surface is less preserved and eroded by local stream incision. East of the valley, surfaces at the same elevation hardly preserve sandy sediments, although remnants of Miocene carbonate deposits are present at 170-180 m elevation (Pére Jacques site), sometimes karstified and covered by sands. An erosion surface occurs outside the Alfambras valley at the top of its bordering slopes, at an elevation of approximately 130 m elevation (± 5 m). It is present on both sides of the valley, as well as at the southern tip. It is better preserved on the east side than on the west, and it is very well preserved at the south boundary of this section. We interpret this surface as a part of the regional abrasion surface which seems to correspond to a unique surface that can be correlated through the borders of the valley and that thus pre-dates the development of the valley.

A lower surface, between 100 m and 115 m in elevation, and already inside the valley, is more degraded than the upper (130 m) surface. Along the western and southern valley borders, this surface is cut mainly into the Paleozoic bedrock and is covered with a thin

sequence of yellowish-white, fine to medium sands with rounded to sub-rounded pebbles. The upper section, where a soil has developed, presents angular schist and greywacke clasts, which probably originated from the nearby escarpment. This deposit does not present characteristics of a fluvial deposit, suggesting a marine environment, or re-deposition of marine sediments. The inner-edge of this surface along the western side of the valley coincides with a fault inferred to be present between the Miocene and the Paleozoic rocks and which corresponds to the inferred main fault. At the eastern side, the cover sand deposit is thinner or absent and the same surface is trimmed on the Paleozoic bedrock and carbonate Miocene sediments, which at the southeast border correspond to a thin carbonate layer.

A surface between 90 to 95 m occurs inside the valley commonly cut into a detrital sequence composed by sand and clayey/silty sand that overlies the carbonate Miocene sediments and is better expressed along the western valley side. Locally this sequence is gently tilted towards the west, which can be attributed to the active fault segments that is recognized affecting the surface at the top. The valley floor, which is also the floodplain, has an elevation of 85-80 m, and the active channel is incised only a few meters into the floodplain surface.

6.3.2.1.2 Alfambras-Framangola section

The next section to the north, the Alfambras-Framangola section, is about 4000 m long and is characterized by a very narrow valley that is generally no more than 200 m wide. The elevation of the valley's borders is similar to that along the Alfambras section but the floodplain is lower, at 83-65 m, and the modern channel is deeply incised, generally about 10-12 m below the floodplain. At certain locations, approximately 20 m of recent incision can be seen. The main channel of the Aljezur River is much more incised after crossing from the Alfambras to the Alfambras – Framangola section of the basin, which is also evidenced by the drainage profile. At this section, some morphological surfaces were recognized and some were confirmed as fluvial terraces by field surveys, and the terrace sediments along this sector are thicker than along the Alfambras section. A lower sequence present at this section is characterized by coarse sediments and some carbonates are inferred to be Miocene in age. An upper sequence, with clayey sand, silt, and sand is tilted towards the west and is locally dragged into the fault zone, as described in Figueiredo *et al*. (2011). Similarly, with the Alfambras section, colluvial deposits are present along the slope base, as well as covering some terrace surfaces. At Framangola, the valley widens, the floodplain is better expressed, the modern channel is less incised, and along the valley slopes several terraces are present (Figure 6.6). A significant change when compared with Alfambras, is the greater incision of the modern channel along the Alfambras-Framangola section, which transforms the valley floor from a broad, flat floodplain surface to a narrow V-shaped valley carved during a stronger phase of incision of at least 20 m.

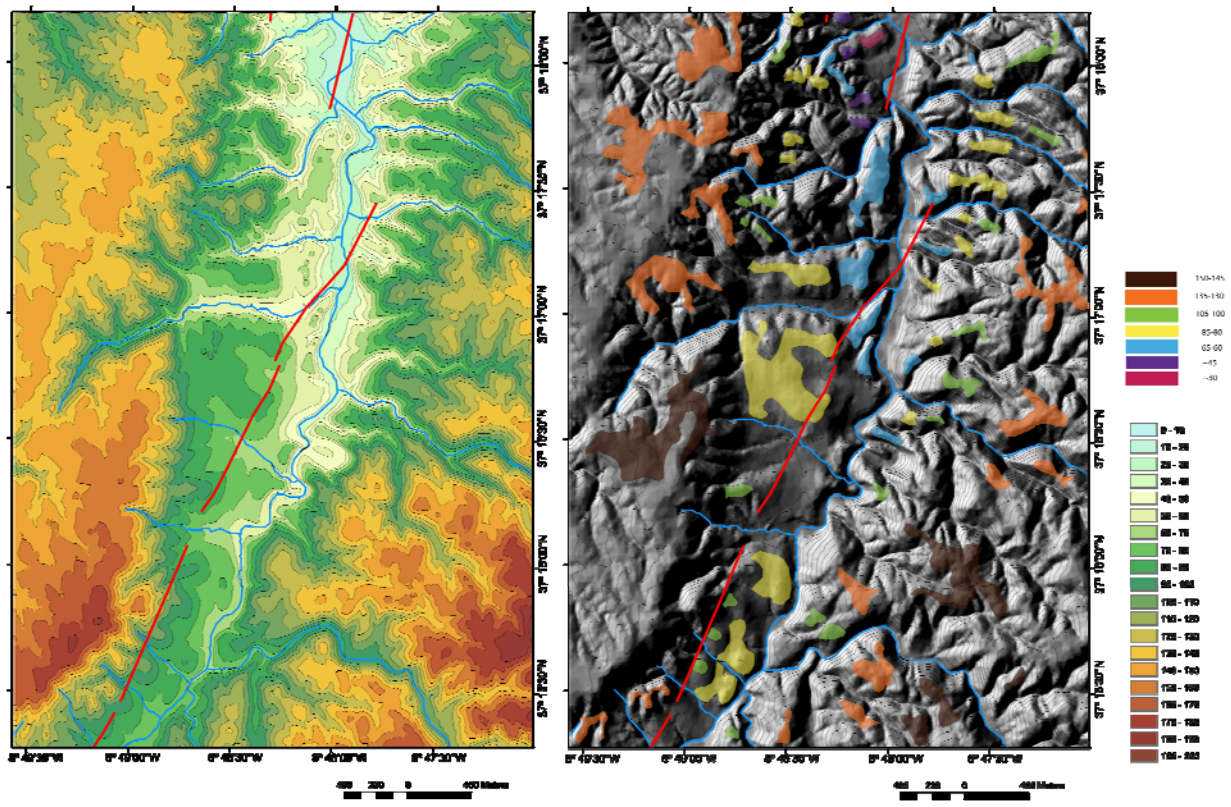

Figure 6.6 - Hypsometric map of the Alfambras-Framangola section on the left. Geomorphologic interpretation and surface mapping over a shaded relief map for the same area on the right. Scale and hypsometry color are included.

The higher surface at circa 150 m (± 5 m) is still present as the regional abrasion surface in the vicinity of this valley section, and is expressed as a flattened surface at 152- 154 m in the west (Cadaveiro) and in the east (Charneca das Lebres and Vale dos Corvos). This surface descends in a smooth ramp to a lower surface at about 135 to 130 m (± 5 m) elevation, which is recognizable at several locations at the regional abrasion surface in the vicinity of the valley. When close to the valley border, is less preserved.

The next surface, the highest one inside the valley is present at 100-110 m elevation, which locally reaches to 115 m (as in Saltadouro). It is generally preserved only as small linear terraces, where locally an inner edge is recognized at about 108 m elevation. Higher elevations are present on the eastern side, and in this manner a vertical difference of probably less than 5 m might be present between opposite valley walls. This surface is generally erosional, but at Barranco da Vaca, a thick conglomerate unit is present, and the gravel was interpreted as a terrace deposit that was later deformed by an active fault segment (Figueiredo *et al*., 2010, 2011). It was previously proposed that these terraces topography is tilted towards the hill slope (Pereira, 1990), but field surveys were not able to confirm an exclusive tectonic control, since large mass movement scars indicate a rooted paleo-landslide at this area.

The 95 m surface along the Alfambras section is lower along the Alfambras-Framangola section, ranging from 80 to 90 m. This surface which is erosive is well preserved on both sides of the valley. Along the western side of the valley, the terrace remnants are large and predominantly cut on a sequence of Miocene carbonate sediments, of which the best example is at Alcaria. The terrace morphology at Alcaria is partially controlled by faulting, as terrace inner edges coincide with inferred fault segments between the Paleozoic and the Miocene rocks. North of the Alcaria area, 80 to 90 m surface is still present, but instead terraces remnants are present with linear and narrow shapes and also present in the top of some spurs due to the strong drainage incision

A new surface, ranging from 60 to 65 m elevation, which was not recognized in Alfambras, is recognizable northwards from Alcaria and corresponds to a flat surface, trimmed on the Paleozoic and without cover sediments. It is better expressed along the western side of the valley, especially as the top surface of linear ridge features. One of these ridges seems to block the drainage that flows from Alcaria (Barranco da Alcaria) at Santa Susana as its channel appears to be displaced with a left-lateral sense of motion suggesting that the ridge is a tectonic shutter-ridge. Detailed field surveys conducted on the bedrock and lower unit filling sediments near Barranco da Alcaria at Santa Susana corroborate the presence of a fault with left lateral motion along the margins of the ridge. Furthermore, a change in the Miocene bedding attitudes and sediment characteristics suggests that the Santa Susana–Alcaria zone may correspond to a push-up structure. The modern channel is strongly incised by about 20 m below this surface, although evidence of recent meandering on this surface is suggested by the presence of an oxbow lake and paleo-channel with higher sinuosity, east of this push-up structure and immediately upstream.

Two other surfaces can be recognized near Framangola at about 45 m and 30 m elevation. Both are represented by very small terraces, embedded on a strongly dissected morphology, sometimes with remnants of fluvial or colluvial sediments covering a surface carved in the Paleozoic bedrock. At Framangola a flat valley floor at approximately 28-25 m elevation is the lowest surface for this section, and the modern channel is incised less than 5 meters into it.

6.3.2.1.3 Aljezur Section

The central area of the Aljezur-Alfambras basins corresponds to the southern section of Aljezur basin, and corresponds to the section where the Aljezur fault was first recognized and where Miocene limestone was clearly identified and dated. It is a wide valley varying from as much as 800 m in the central reaches to about 200 m at the ends. It has a length of about 4000 m, similar with the previous Alfambras and Alfambras-Framangola *sections*.

A significant difference is that along this section, the floodplain is very well developed at about 13-12 m elevation, and it corresponds to a primary geomorphologic feature. The elevation of the valley border to the west is about 120 m, whereas to the east, the relief is downgraded and eroded, mostly by the Cerca River. To the east, some higher elevations are locally

preserved at some interfluve positions with elevations ranging from 150 to 180 m. Distinct types of sediments are present along Aljezur section: carbonate deposits with fossils indicative of marine shallow waters are interbedded with sand and conglomerate. The fossils were dated from the Burdigalian and Tortonian Miocene stages (Pais *et al*., 2000). This Miocene sequence is strongly deformed by a set of NW-SE faults, as well as by the STASFS itself, generating several tilted blocks. An upper mostly conglomeratic clastic unit is present, interpreted as Miocene (Pimentel and Amaro, 2000) or as late Pliocene to Pleistocene (Pereira, 1990; Cabral, 1995; Dias, 2001). Small alluvial fans appear to be present in shape, but field surveys reveal an absence of sediments. Terraces are also present, especially along the east hill slope (Figure 6.7).

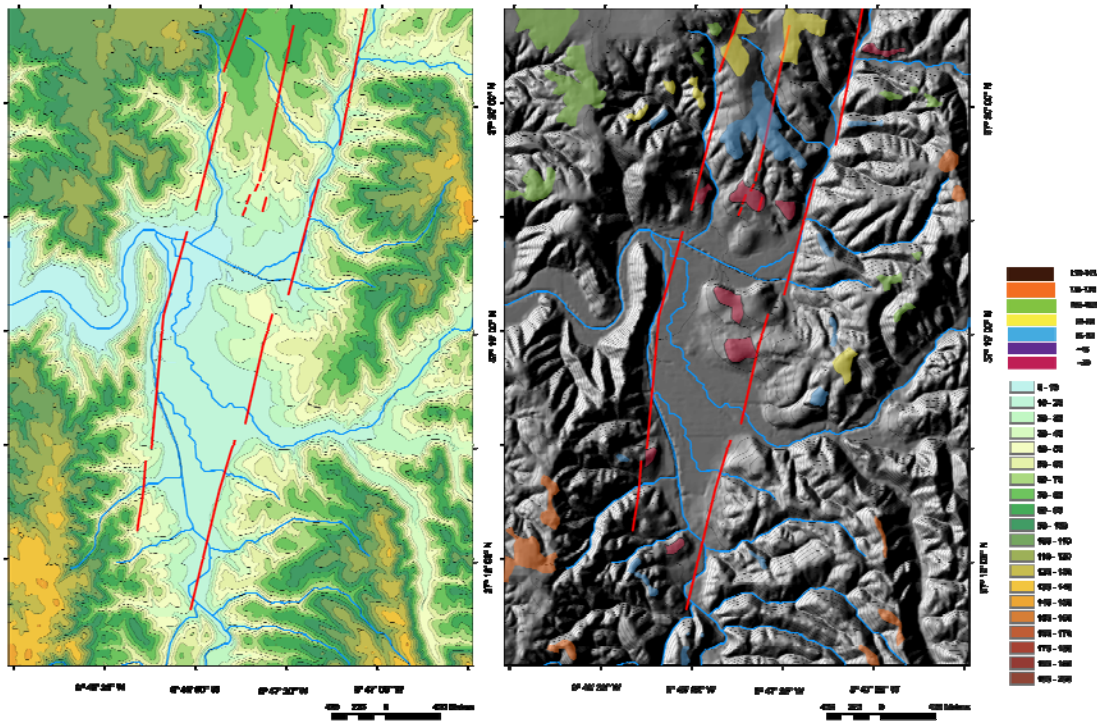

Figure 6.7 - Hypsometric map of the Aljezur section on the left. Geomorphologic interpretation and surface mapping over a shaded relief map for the same area on the right. Scale and hypsometry colour are included.

In general, the marine terraces present in the regional abrasion platform are more degraded in the vicinity of the Aljezur section. Some of them, such as the 150 m one, are absent due primarily to the incision and erosion caused by the larger drainages, like the Cerca River, which converges with the Aljezur River in this section. Towards the east side, the valley border is difficult to interpret, because the hill slopes are gentler and smoother, dissected by drainages and the surfaces are all poorly preserved.

The highest surface near the valley margins, east of the tectonic basin corresponds to the circa 130 m surface, which is poorly preserved and recognizable only at the top of a few interfluves (like at geodesic mark Pais, 131 m). However, towards the west at the regional

abrasion platform, it is better preserved (such at Portela Alta) but not widely expressed. It should be stated that there are no ages for these surfaces or equivalent sediments to corroborate that these surfaces are equivalents. The next lower surface present in the regional abrasion platform is the 100-115 m elevation terrace, very well expressed west of the basin, namely to the west of Portela Alta and at the northwest of Aljezur, where is covered by a thin cap of sand, most of which is interpreted as beach sand. Along the eastern valley border, at equivalent elevations, remnants poorly preserved and without sediments, of a flat surface are recognized at the top of some interfluves.

At the basin, the highest surface is at an elevation of 80-85 m, recognizable mostly along the western side of the valley, north of the Aljezur River. This surface generally does not exhibit cover sediments, and the inner edge sometimes coincides with faults which affect sediments attributed to the Miocene. At the southeast area of Aljezur section, a lower surface at about 75 m elevation is present and might correspond to a degraded part of that surface.

A surface at 60-65 m elevation is also locally present at the Aljezur section, and although it is generally poorly preserved, it is well exposed to the north of the Aljezur River. A lower surface, at about 30 m elevation, is well and widely present, mostly in the vicinity of Aljezur city, in an area where the large tributaries converge to Aljezur River. This surface most likely corresponds to remnants of a plain related with a Late Pleistocene interglacial. Most of this surface is cut on the calcareous Miocene sediments, as in Mesa de Niz (30-32 m), Palazim (31-28 m) or at Igreja Nova (34 m). The wide valley floor is the lowest of all the sections at Aljezur-Alfambras basins, decreasing from 12 m in the south to 8 m in the north where the Aljezur River inflects to the west, towards the Atlantic Ocean.

6.3.2.1.4 Areeiro Section

The northernmost section, the Areeiro section (named after the river that drains this valley), is slightly longer at approximately 5000 m, and has a total width of about 1000 m, although this width does not reflect the width of the lower section of the valley (Figure 5.8). At this section, the drainage runs parallel to the fault, but now towards the south, as the Areeiro River is a tributary of the Aljezur River. The Areeiro sector is characterized by a staircase of surfaces, some of them likely to be tectonically controlled by an *en-echelon* array of fault segments along the western valley margin (Novas Castelãs and Rogil Faults). The valley margins in the west range in elevation from 120 m to 100 m, whereas in the east, they range from 120 m to 140 m in elevation. The valley floor does not exhibit a well-developed floodplain, but rather is expressed as a narrow valley that indicates a minimum of 10 m of recent incision. The sediments present along this sector are distinct from the other sectors. Although carbonate Miocene sediments are present and generally overlie the Paleozoic or an argillaceous lower Miocene unit, there is a thicker clastic sequence present in the northern end that is composed predominantly of sand interbedded with fine sand and silty and clay-enriched layers. This unit is assumed to be Pliocene in age, despite the absence of any absolute dating (Feio, 1951).

In the vicinity of the Areeiro section, the 130 m surface is included in the regional abrasion surface, but only to the north of the valley and to the east of the STAS fault system in the Cabeço da Eira (132 m) – Boavista (135 m) area. It is covered by a thin cap of sediments, which locally are a few meters thick, composed predominantly of white to light yellow quartz sand, which have been considered to be Pliocene in age. The area north of Areeiro is incipiently drained as a consequence of headward erosion of the Areeiro River. Towards the west, at the regional abrasion platform, the highest preserved surface corresponds to the 100-115 m terrace that, as also present at the Aljezur section. Locally, what it resembles to an inner edge exists at about 108 m in elevation, what it may suggest that this surface could in fact correspond to more than one marine terrace. Along the southwest margin of this valley section, this surface is bounded by two fault segments: the north prolongation of the Aljezur fault segment and the Nova Castelãs fault segment, but no significant vertical deformation was recognized at this location. A lower surface at 90-95 m elevation is recognizable at several sites in the northern area.

In the valley, at the northern, east of the Rogil fault an 80-90 m surface (locally 85-90 m) with fine sediments such as clayey and fine sand interbedded with fine white sand is dissected by tributary drainages. The inner edge of the same surface about 5 Km southward coincides with the northern prolongation of the Aljezur fault.

A surface ranging in height from 70 m to 75 m, but presenting flat surfaces at 72-73 m is present in both sides of the valley, along most of its length. Frequently, this surface is covered with fine sands with paleosols and occasional rounded quartz pebbles. It is difficult to state whether these sediments are related with the terrace formation, or if they correspond to an older clastic unit latter trimmed, resulting in an erosive terrace. It can be stated that no evidence of fluvial sediments was recognized, and that the sediments evidence a marine genesis. A surface ranging from 65-73 m elevation is also recognized. This surface corresponds to the more extensive terrace and it is mostly present in the central region of the section at several locations. The inner edges of this surface are parallel to the orientation of the fault, and most of them are located along extensions of known fault segments, suggesting a tectonic control.

Along the Alfambras-Framangola section, a 45 m elevation terrace was recognized although with only minor expression. Here, along the Areeiro section, it was also recognized as having a minor expression when compared with other surfaces, but it is better preserved than at the Alfambras – Framangola section. Several small terraces at about 45 m elevation were recognized. Finally, a 30 m elevation terrace, identified in all sections except Alfambras is also recognized better expressed where the valley floor is flat and wider, circa 200 m width.

In general the modern channel has just some meters incision, but at certain locations, a circa 10 m incision is identified. Overall, the valley presents a height of approximately 80 m, but where Areeiro River incision can be as high as 40 m and is present along most of this

section.

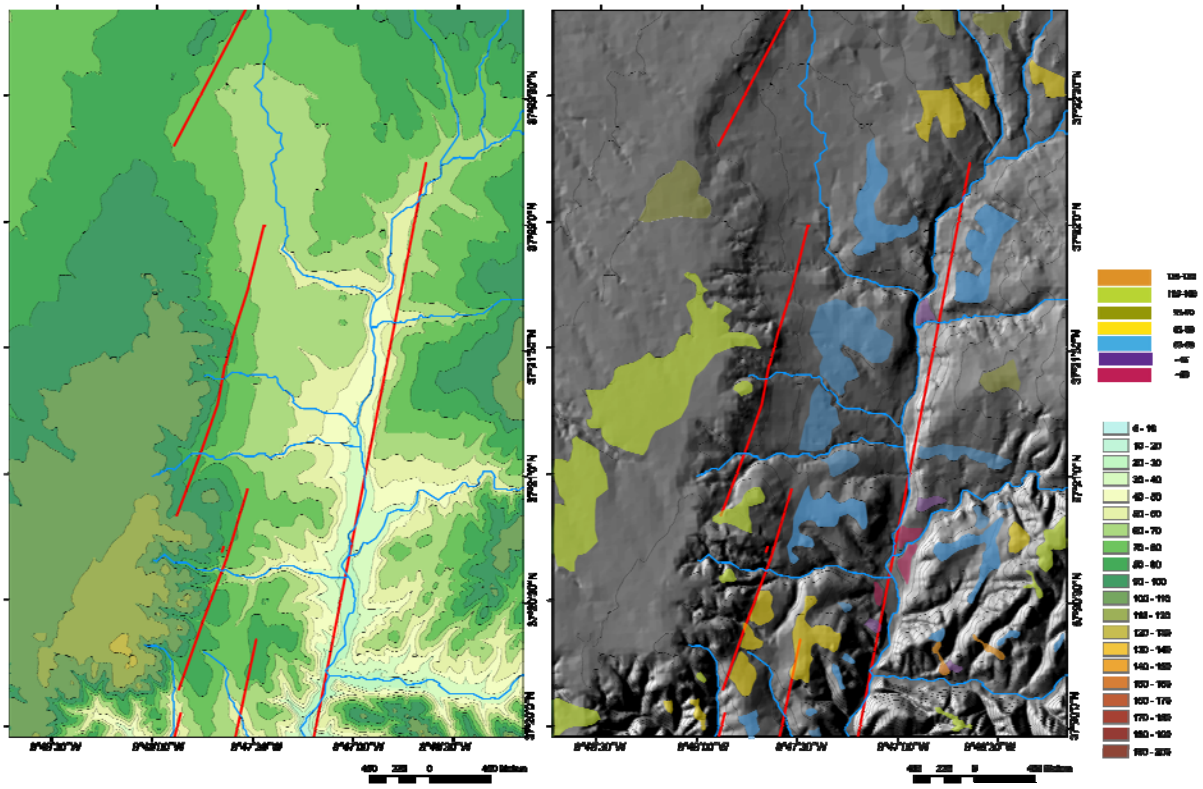

Figure 6.8 - *Hypsometric map of the Areeiro section on the left. Geomorphologic interpretation and surface mapping over a shaded relief map for the same area on the right. Scale and hypsometry colour are included.*

6.4 Morpho-tectonic Analysis

6.4.1 Methodology

A detailed morpho-tectonic analysis was conducted along the Aljezur valley by the application of a set of geomorphic indices with the purpose of recognizing the active fault segments of the STASFS, and to quantify the amount of Quaternary deformation. Our topographic database is a 1/10,000 digital topography (provided by Aljezur County), which allowed us to generate a 10 m Digital Elevation Model using the ArcGIS software (©ESRI). Geological maps and orthophotomaps from the Portuguese surveys were also integrated into the database to provide lithological and structural information to aid the morphotectonic interpretation. For the hypsometric studies of basins, we used CalHypso, a free-ware ArcGIS extension (Pérez-Peña *et al*., 2009a), for the channel steepness analysis we used Stream Profiler (Whipple *et al.,* 2007), and for the stream channel sinuosity Hawth's Analysis tools for ArcGIS (Beyer, 2004).

The geomorphic indices that we applied were Mountain-Front Sinuosity (Smf) and Valley Floor Width to Height ratio (Vf) (Bull and McFadden, 1977; Bull, 2007), Stream Channel Sinuosity (S) (Schumm, 1963), Basin Relief Ratio (Rh) and Basin Elongation (R_e) (Schumm, 1956), and Asymmetry Factor (AF) (Hare and Gardner, 1985). Additionally, several analysis were conducted, namely drainage profiles interpretation, production of Stream Gradient Index (SL) maps (Hack, 1973) and channel steepness analysis.

These geomorphic indices were successfully applied at a regional scale for southwest Portugal, although with a different digital resolution database. Consequently, we followed the same methodology but now applied to a higher resolution digital topography; detailed descriptions were previously described at Figueiredo et al. (XXXX). For the computation of the indices, we applied the following formulas:

The Mountain-Front Sinuosity (Smf),

$$S_{mf}=\frac{L_{mf}}{L_s} \quad (1)$$

the sinuosity of the mountain-piedmont junction (S_{mf}) is defined as the ratio between the length of the mountain front along the foot of the mountain, measured along the change of slope (L_{mf}), and the length of the mountain front, measured as a straight line (L_s).

The Valley Floor Width to Height Ratio (V_f) is calculated as

$$V_f = \frac{V_{fw}}{[(E_{ld} - E_{sc})] + (E_{rd} - E_{sc})] / 2} \quad (2)$$

with V_{fw} being the valley floor width, E_{ld} and E_{rd} being the left and right elevations of the valley divides, respectively, and E_{sc} being the stream channel elevation, all measured at a certain basin or channel location relative to the drainage divide. In this study, we will measure the V_f along valleys from tributaries of the main drainage (Aljezur River) and access changes that might reflect perturbation of their base level controlled by the main drainage which in turn is controlled by the sea-level. At both sides of the bedrock is Paleozoic schist and greywacke, although there is a change in lithology when crossing to the valley itself, which ultimately corresponds to crossing the main tectonic structure. For this reason, we have measured V_f ratios for all the tributary drainage basins at about 300 m upstream from the tributary confluence with the main drainage channel. For most of the cases, this measurement was made in a location between an active trace of the structure and the main drainage channel.

The stream Channel Sinuosity (*S*) is calculated as the ratio between the channel length (Ch_l) and the length of the straight line defined by the channel endpoints (Ch_{sl}) (Schumm, 1963),

$$S = \frac{Ch_l}{Ch_{sl}} \quad (3)$$

which is generally assumed as equivalent to the valley length, or the average of the sinuosity of several reaches along the channel, which is the more correct way to measure the sinuosity of a channel, as

$$S = \sum_{i=1}^{n} \frac{Ch_L}{Ch_{SL}} / n \quad (4)$$

Basin Relief Ratio (Rh) (Schumm, 1956) is defined as the ratio between the amplitude of the elevation of a basin ΔE (elevation difference of the lowest and the highest point of a basin) and the longest length of the basin parallel to the principal drainage channel, L. This ratio is dimensionless and measures the average gradient of a basin.

$$Rh = \frac{\Delta E}{L} \quad (5)$$

Basin Elongation (R_e) is defined as:

$$R_e = \frac{\emptyset \ Area\ Basin\ circle}{L} \quad (6)$$

where Ø corresponds to the diameter of a circle with the same area as that of the basin, and L is the distance between the drainage mouth and the most distant point in the basin.

The Basin Shape index (B_s) is a similar parameter, defined as:

$$B_s = \frac{B_l}{B_w} \quad (7)$$

where B_l is the basin length from the mouth to the most distant point along the drainage divide and B_w is the largest basin width measured perpendicularly to B_l.

The Asymmetry Factor (AF) is calculated as a ratio between the area to the right (Ar) of the main channel and the total basin area (At),

$$AF = \frac{A_r}{A_t} \times 100 \quad (8)$$

allowing for the detection of tectonic tilting transverse to the average flow direction of the basin (Hare and Gardner, 1985).

The Stream Gradient index (SL) (Hack, 1973) relates to stream power relationships (Bull, 1979) and changes in channel slope. SL is defined as,

$$SL = \frac{\Delta E}{\Delta L} \times L \quad (9)$$

where ΔE is the change in elevation of the end points and ΔL the length for a given channel reach, and L is the horizontal distance from the midpoint of the reach to the drainage divide.

Hack suggested that it is possible to compare different drainages at a regional scale by "...plotting regularly spaced index values on the map..." (1973, p.427). According to that assumption, SL maps were produced that initially had channel information extracted directly from printed topographic maps (Keller and Pinter, 1996 and references therein), and more recently with data extracted from digital topography (Chen *et al.*, 2003; Troiani *et al.*, 2008;

Pérez-Peña *et al.*, 2009b). In this manner, we calculated the SL index with a regularly 150 m spaced interval and generated a SL map following these steps: we extract the channel profiles from a DEM, processed them to smooth out DEM irregularities, then SL values were calculated for each channel reach and plotted in ArcGIS. Finally SL values were interpolated with the Spatial Analyst tool.

6.4.2 Data Analysis

The basin drainages for Aljezur area were organized according to their position relative to the main drainage channel. In this way tributary basins were numbered from the south northwards and organized into western or eastern basins, according to their code termination, as e.g. 1w, 2w, 3w for the three southern tributary basins for the west valley side. In general, the basins have small areas, smaller than 2 km^2, although larger basins also exist. Head elevations are higher in the east side and eastern basin channels are also longer, leading to less steep drainage profiles along them. The main exceptions correspond to the larger tributaries, namely Cerca River (13e) which corresponds, in fact, to a larger drainage whose basin was captured by the Aljezur River. All the calculated basin index results were compiled (Tables 6.1, 6.2 and 6.3) and interpreted according to their position regarding the four sections defined for the Aljezur basin.

	Alfambras		**Alf. -Framangola**		**Aljezur**		**Areeiro**	
	E side	*W side*	*E side*	*W side*	*E side*	*W side*	*E side*	*W side*
Smf	1.25	1.35	1.14	1.22	1.18	1.35	1.04	1.09

Table 6.11 – *Results calculated for the mountain front sinuosity index for the 4 sections defined along Aljezur basin.*

The Mountain-Front Sinuosity index measured along the Aljezur basin between the slope of the valley and the piedmont should reflect the vertical rate of activity, but also the rate of incision of the main drainage that runs parallel to the main fault trace. Mountain Front Sinuosity (S_{mf}) values were calculated for all the sections, and for all of them values are lower than 1.5, which is assumed as an indicator of active tectonics, with tectonic rates higher than erosion and sedimentation rates (Table 6.1). From all the sections, the one that presents lower sinuosity is the Areeiro section and the one that presents higher sinuosity is the Alfambras section. In general, sinuosity is higher along the west valley side. Generally the modern channels of the Aljezur and Areeiro Rivers run mostly along the east side of the valley, which might explain the lower sinuosity along the east side of the valley and not necessarily the presence of more active or more recently active structures along it. Nevertheless, when we analysed all the basins without considering the sections, a value of 1.02 is obtained for the west side while a value of 1.09 is calculated for the east side, indicating that, overall, the west side has a lower sinuosity.

Stream Sinuosity for the main channel of the tributary basins was also measured and, for the majority of them, sinuosity is lower than 1.5, which indicates that these channels can be

classified as straight. For all the sections, an average was obtained for each side of the valley, and, as expected, east basin side channels which are longer and slopes are lower have higher sinuosity values than the western ones. Lower sinuosity is present when crossing from the Alfambras to the Alfambras-Framangola section, especially along the western side. A higher sinuosity of 1.64 was measured for channel 13e (Cerca River).

Sector	Code	Basin area (Km^2)	Main Channel Lenght (Km)	Head Elev. (m)	Morpho Indexes						
					Stream Sinuosity	Relief ratio	Elongation ratio	Valley-floor width	Asymmetry	ksn	HI
Alfambras sector	1e	2.24	24.59	197	1.55	0.01	0.07	1.74	47.35	16.40	0.39
	2e	6.38	5.78	229	1.29	0.04	0.49	2.00	79.74	19.20	0.66
	3e	1.37	2.49	169	1.24	0.07	0.53	2.44	83.91	26.60	0.59
	4e	0.44	1.31	145	1.08	0.11	0.57	1.20	52.87	17.10	0.62
	average east side				*1.29*	*0.06*	*0.42*	*1.85*	*65.97*	*19.83*	*0.56*
	1w	0.95	22.67	143	1.51	0.01	0.05	1.60	44.47	10.60	0.36
	2w	0.50	1.52	135	1.22	0.09	0.53	3.33	63.24	10.10	0.53
	3w	0.51	1.69	139	1.15	0.08	0.47	2.73	45.62	12.80	0.57
	4w	0.44	1.38	135	1.22	0.10	0.54	4.29	50.23	11.40	0.51
	5w	1.39	2.02	150	1.29	0.07	0.66	1.00	71.79	19.60	0.55
	6w	0.49	1.11	145	1.21	0.13	0.71	2.35	69.59	16.60	0.43
	06&7	0.19	0.73	135	1.06	0.27	0.68	0.44	58.80	18.50	0.35
	7w	0.21	0.62	137	1.06	0.22	0.83	1.21	58.72	22.40	0.47
	average west side				*1.22*	*0.12*	*0.56*	*2.12*	*57.81*	*15.25*	*0.47*
average					*1.24*	*0.10*	*0.50*	*2.01*	*60.95*	*17.01*	*0.50*
Alfambras-Framangola	5e	5.69	7.03	216	1.22	0.03	0.38	1.04	78.00	23.40	0.60
	6e	13.87	7.38	249	1.43	0.03	0.57	1.09	52.31	29.00	0.56
	7e	4.66	3.78	203	1.13	0.05	0.65	0.70	70.08	33.50	0.59
	8e	0.91	2.31	154	1.18	0.07	0.47	0.47	49.95	32.10	0.57
	average east side				*1.24*	*0.05*	*0.52*	*0.82*	*62.59*	*29.50*	*0.58*
	8w	0.20	0.56	133	1.03	0.24	0.91	0.86	65.24	25.00	0.40
	9w	0.57	0.94	152	1.09	0.16	0.90	2.38	69.57	32.20	0.50
	10w	0.78	1105.45	131	1.10	0.00	0.00	1.38	63.50	19.30	0.47
	11w	2.12	2.61	138	1.17	0.05	0.63	0.60	40.09	28.20	0.62
	12w	0.54	1.31	98	1.19	0.07	0.63	0.40	48.79	19.20	0.48
	average west side				*1.12*	*0.11*	*0.61*	*1.12*	*57.44*	*24.78*	*0.49*
average					*1.18*	*0.08*	*0.57*	*0.97*	*60.01*	*27.14*	*0.53*

Table 6.2. Compilation of results obtained for the morpho-tectonic indices applied to the Aljezur basin for the Alfambras and Alfambras-Framangola sections. Average values for each section, as well as for average values for the east and west sides of the valley, are also presented.

Relief Ratio is generally higher for the west side, especially along the transition from the Alfambras to the Alfambras-Framangola section, where ratio values are double of the neighbouring basins. Since the amplitudes of elevation are similar, this implies shorter average

drainage lengths. Relief Ratio average for both valley sides of the Areeiro section are similar and do not reflect a significant change.

Concerning the basin shape indices, Elongation Ratio is in generally lower than 0.7, which means that the majority of the basins are elongated. The eastern ones have lower elongation ratios, which can be explained by their greater lengths. Less elongated basins can be identified along the Alfambras to Alfambras-Framangola transition and to the north of the Aljezur section in the vicinity of the confluence of the Cerca and Aljezur Rivers.

Sector	Code	Basin area (Km^2)	Main Channel Lenght (Km)	Head Elev. (m)	Morpho Indexes						
					Stream Sinuosity	Relief ratio	Elongation ratio	Valley-floor width	Asymmetry	ksn	HI
Aljezur sector	9e	0.35	1.62	128	1.10	0.08	0.41	0.41	56.17	21.80	0.56
	10e	0.74	2.14	137	1.27	0.06	0.45	0.63	55.91	23.10	0.59
	11e	0.61	1.58	102	1.22	0.06	0.56	1.28	33.33	21.30	0.48
	12e	0.53	1.55	52	1.18	0.03	0.53	5.33	64.44	7.73	0.00
	13e	54.26	18.49	366	1.64	0.02	0.45	4.00	31.36	33.20	0.46
	14e	0.60	1.03	71	1.07	0.07	0.84	2.11	20.52	22.90	0.42
	15e	0.68	1.63	118	1.34	0.07	0.57	0.61	49.59	26.90	0.55
	average east side				*1.26*	*0.06*	*0.54*	*2.05*	*44.47*	*22.42*	*0.44*
	13w	1.09	1.78	123	1.30	0.07	0.66	0.46	28.98	22.40	0.52
	14w	0.26	0.73	81	1.06	0.11	0.79	0.80	33.82	21.10	0.42
	15w	0.64	1.30	125	1.11	0.10	0.70	1.11	21.99	27.50	0.55
	16w	2.01	2.05	109	1.18	0.05	0.78	1.26	55.55	26.90	0.50
	average west side				*1.17*	*0.08*	*0.73*	*0.91*	*35.08*	*24.48*	*0.50*
average					*1.23*	*0.07*	*0.61*	*1.67*	*41.34*	*23.10*	*0.50*
Areeiro sector	16e	8.59	7.05	282	1.24	0.04	0.47	0.81	36.53	40.00	0.34
	17e	5.37	7.15	292	1.26	0.04	0.37	0.62	55.45	39.90	0.41
	18e	1.25	2.32	129	1.13	0.06	0.54	1.06	35.20	33.70	0.60
	19e	2.05	2.97	179	1.10	0.06	0.54	1.11	48.63	30.70	0.52
	average east side				*1.18*	*0.05*	*0.48*	*0.90*	*43.95*	*36.08*	*0.47*
	17w	0.45	1.29	98	1.11	0.08	0.59	0.49	53.05	16.50	0.53
	18w	0.01	1.57	107	1.09	0.07	0.05	1.35	55.77	22.10	0.62
	19w	0.84	1.73	105	1.12	0.06	0.60	2.67	49.82	22.90	0.62
	20w	0.48	1.37	97	1.16	0.07	0.57	2.29	51.79	16.50	0.54
	21w	4.52	4.01	100	1.32	0.02	0.60	1.05	52.12	9.60	0.55
	22w	1.44	2.86	110	1.28	0.04	0.47	2.46	46.50	31.70	0.58
	23w	0.96	1.88	114	1.10	0.06	0.59	1.18	62.69	20.00	0.57
	24w	2.91	3.00	126	1.21	0.04	0.64	1.79	19.27	27.70	0.44
	average west side				*1.17*	*0.06*	*0.51*	*1.66*	*48.87*	*20.88*	*0.56*
average					*1.18*	*0.05*	*0.50*	*1.37*	*46.98*	*26.72*	*0.53*

Table 6.3. Compilation of results obtained for the morpho-tectonic indices applied to Aljezur basin for the Aljezur and Areeiro sections. Average values for each section, as well as average values for the east and west sides of the valley, are also presented.

Valley-Floor Width for all sections shows that the average V_{fw} for the western valleys is generally higher than for the eastern ones. An exception is the Aljezur section, where eastern valleys have higher V_{fw} than the western ones. This can be justified by the Cerca River and neighbouring basins, that correspond to basins where degradation of the interfluves and enlargement of the valley have been more significant than channel incision. Lower V_{fw} values for all the basins were recognized for the segment corresponding to the transition from Alfambras-Framangola to Aljezur, in both east and west sides

We define four classes of Basin Asymmetry Factor values (AF) in order to distinguish the degree of basin asymmetry. Class 1 represents symmetrical basins where 45≤AF≤55, whereas class 2 basins are slightly asymmetrical with AF values between 40 and 45 or between 55 and 60.

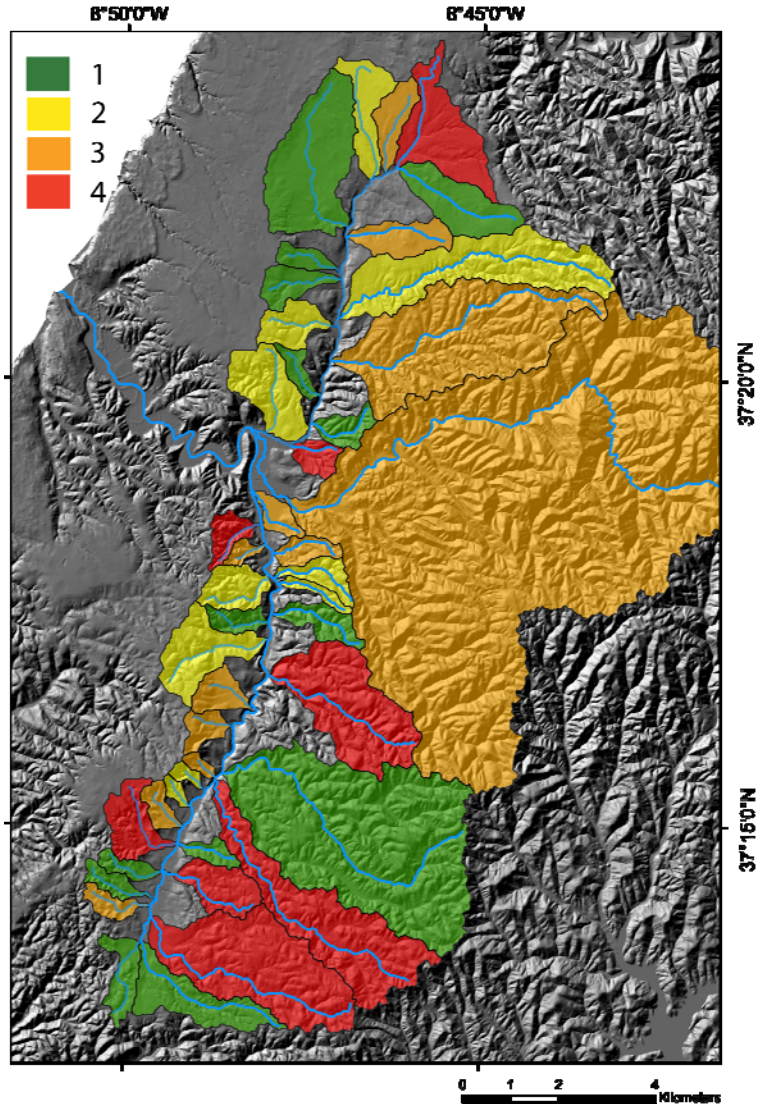

Figure 6.9 - Asymmetry Factor classes defined for the Aljezur River tributary basins. A coloured scale was attributed to each class.

Basins with values between 30 and 40 or 60 and 70 are "moderately asymmetrical", whereas class 4 basins are asymmetric with values less than 30 or greater than 70 (Figure 6.9). Asymmetry Factor average values for all sections are a way to evaluate how asymmetry may vary, and based upon average values, there is a difference between the southern and the northern sections. The Alfambras and Alfambras-Framangola sections have basins that are moderately asymmetrical, while at the northern sections basins are slightly asymmetrical to symmetrical. However, when looking at the individual AF values, it is clear that some basins present a higher degree of asymmetry than others, on both sides of the Alfambras, Alfambras-Framangola and Aljezur sections.

For the Alfambras and Alfambras-Framangola sections, basins along the east side of the valley have higher asymmetries, suggesting a tilting from the NNE towards the SSW. The same situation can be observed along the west side of the valley, but in this case the tilting will be from the SW towards the NE. Since the lithologies and their bedding disposition and structural framework on the bedrock are equivalent on both sides of the valley, and no distinct erosion process was recognized for both sides of the valley, this difference on the basin asymmetries and consequent tilting might be interpreted as an indicator of the fault movement that could behave at these sections as a "scissors fault".

Values of the Hipsometric Integral (HI) are very similar but reflect a change from the south sections towards the north ones: for the Alfambras and Alfambras – Framangola sections HI is higher on the east side basins, which is not the case along the Aljezur and Areeiro section, where higher HI values are along the western side basins.

We have conducted a preliminary analysis for the channel steepness variations across the area but results were not thoroughly detailed: we consider that the tributary basins have small areas which would condition the adequate analysis of the channel steepness index and for that reason, we have not detailed it in this study. However we have included the graphics elaborated for this analysis in the Annex 2.

Drainage profiles conducted along all basins exhibit evidence for some slope changes, the majority of them not directly related with the active segments of STAS fault system. Longitudinal profiles for all tributary basins were included in Annex 3.

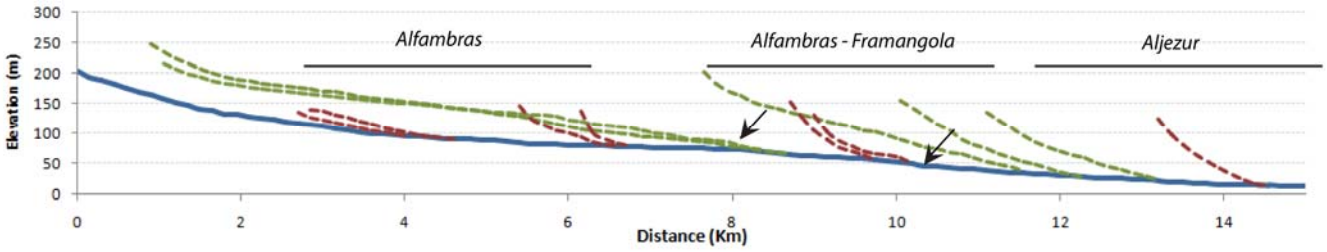

Figure 6.10 – Drainage profiles for the Aljezur River across the Alfambras, Alfambras-Framangola and Aljezur sections: Blue colour corresponds to the Aljezur River, green colour dashed line corresponds to east side tributary channels, and red colour dashed line corresponds to west side tributary channels. Vertical exaggeration circa 10 x. Direction of the profile approximately S – N.

The Aljezur River channel profile exhibits two major knick points (Fig. 6.10): one on the transition from the Alfambras to Alfambras-Framnagola section and another immediately south of the Framangola site, close to the confluence of tributary 11w (Alcaria Creek).

Along the Areeiro River a major knick point is recognized upstream of the 23w and 19e confluence, at the north end of the Areeiro section (Fig.6.11).

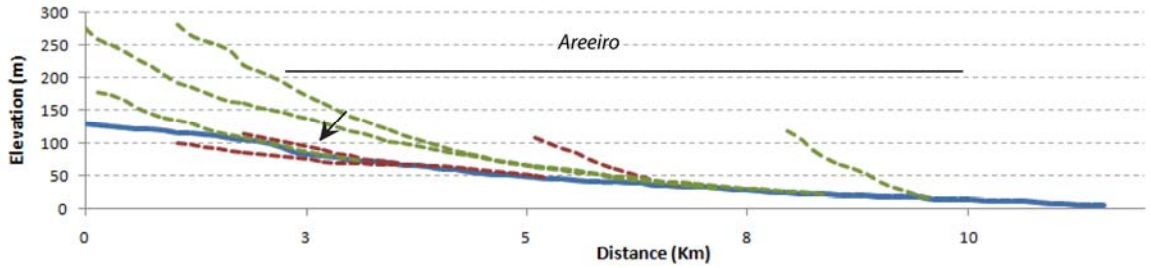

Figure 6.11 – Drainage profiles for the Areeiro River across the Areeiro section: Blue colour corresponds to Areeiro River, green colour dashed line corresponds to east side tributary channels, and red colour dashed line corresponds to west side tributary channels.

A Stream Gradient Index map was produced, based upon the measurement of the SL index for each 150 m along the main channel of the Aljezur River and its tributary channels (Figure 6.12). These measurements allow evaluating changes between 150 m reaches, which in turn will allow detecting anomalous changes of the channel slope. These changes could be due to rock resistance, but can also be due to a tectonic control if the active structure affects the basin. For this reason, a Stream Gradient Index map was produced along the STAS fault segments to evaluate for a tectonic control along the Aljezur main channel and its tributary channels.

The SL map shows that higher SL values are present for the downstream half of the eastern channels, suggesting that there is a general response that increases the channel steepness for the east side. Along the west side of the valley, SL values are lower than in the east, and no significant changes are present, except for the Alfambras–Framangola section where two SL anomalies were identified. One of the anomalies is localized near a fault segment, and elongated parallel to the fault, along the site Barranco da Vaca–Framangola and extends for approximately 2 km. Simultaneously the end of this anomaly corresponds to one of the knick points identified in the Aljezur river (Fig.6.10).

The second anomaly at this section is more localised between two fault segments; the transition between the Framangola alluvial plain and the Aljezur plain, in the Aljezur section. This transition corresponds to an increase in the slope of the channel: the channel elevation drops from 22 to 17 m along a distance of circa 700 m. A slight increase in the SL of the east tributaries that outflow near this anomaly is also visible. A very small and localized anomaly is present in the Aljezur alluvial plain in the Aljezur section near Monte dos Ferreiros, and most

likely should be related to the modern alluvial plain incision. Along the Areeiro section, no relevant SL anomalies are identified, although a reference to higher SL towards the east is also present.

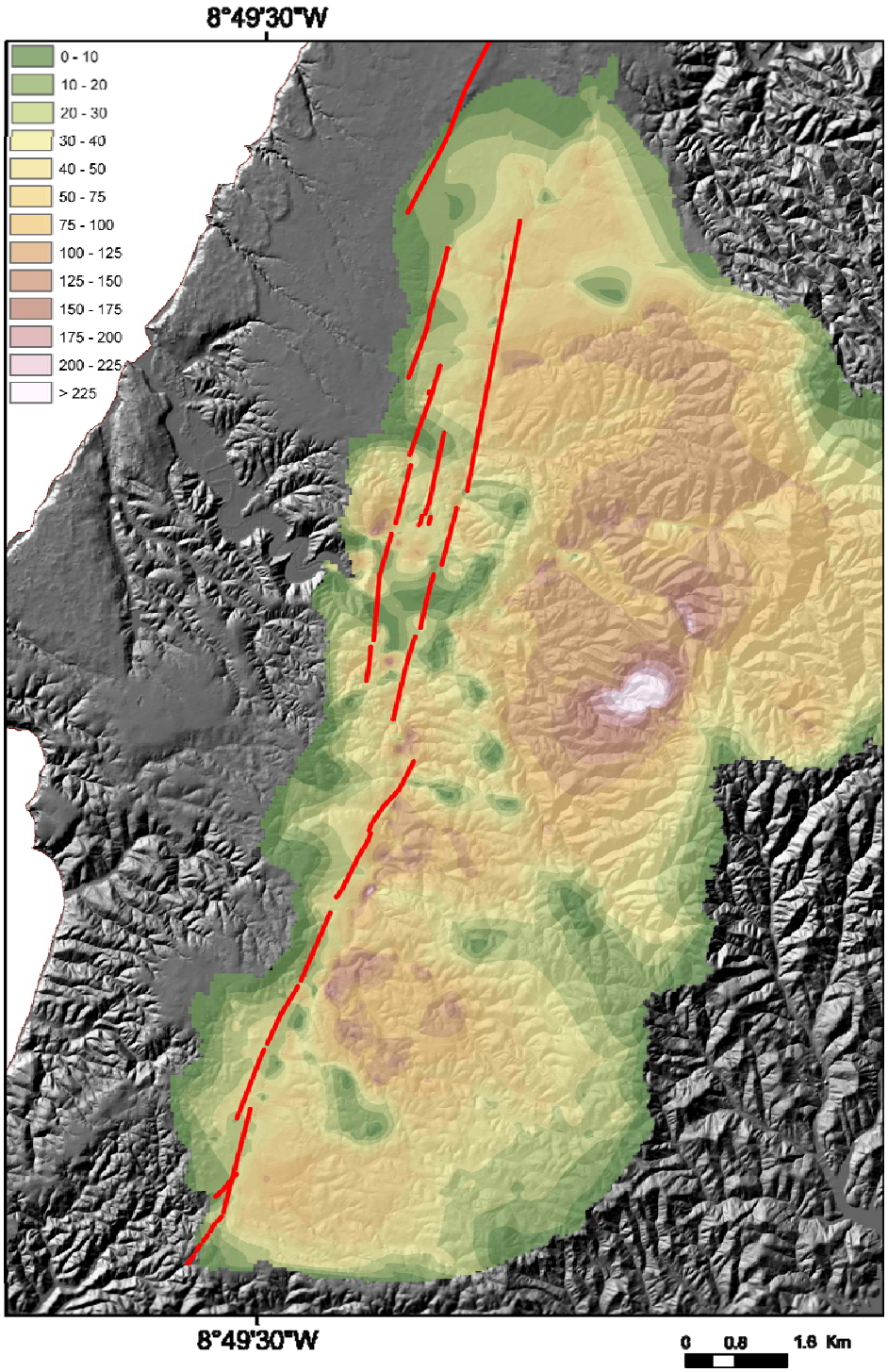

Figure 6.12 – Stream Gradient Index interpolation map, with a 150 m measurement data spacing produced for the Aljezur river and its tributary channels. Scale and colour legend are included in the figure.

We infer that this generally presents higher SL values along the downstream eastern channels, which likely corresponds to a response of a fall of the local base level, which is not recognizable along the western channels. We assume that the fact than SL values are lower along the western channels and that do not reflect as much of a base-level fall compared with the eastern ones, could be due to the continuous fault activity that has been uplifting the western side relative to the eastern one, where the more recent incision has occurred.

In order to detect morphologic features related with active faulting, a detailed analysis of the landforms was conducted, namely along terrace surfaces, ridges, and at channels along the fault segments. These maps are presented at Annex 1. Channel bends were recognized, but a consistent lateral displacement could not be identified along parallel channels, and some of those bends are not located along active fault strands. For some channels, deflections by fault segments were recognized in the range of some tens of meters. Although channel bends are abundant, we cannot assert that those bends are deflections due exclusively to tectonic activity and consequently quantify a lateral displacement.

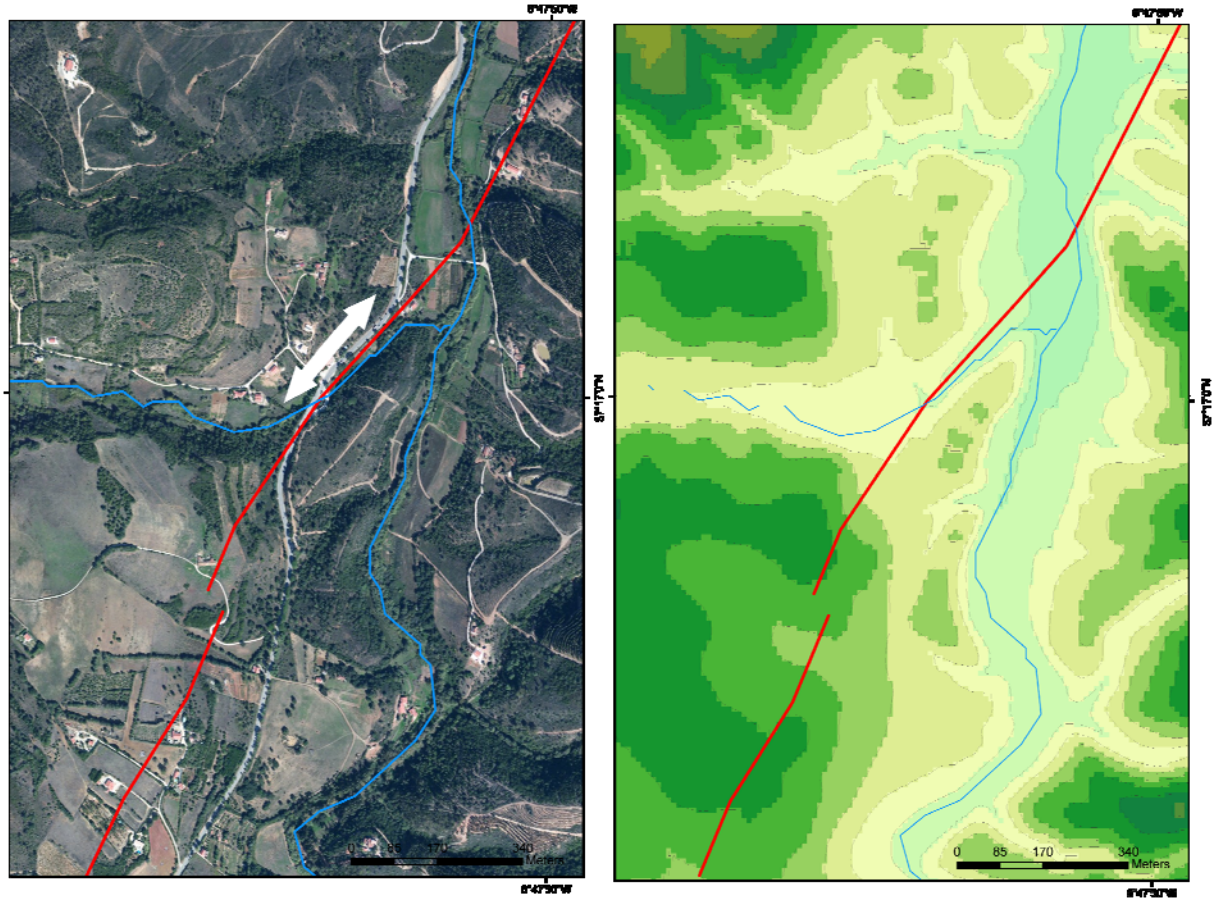

Figure 6.13 – Ortophotomap, on the left, and Hypsometric map, on the right, for the area of confluence of the Alcaria Creek with the Aljezur River, where a landform interpreted as a shutter ridge was recognized. The inferred displacement is marked in the orthophotomap with a white arrow.

However, at the confluence of the Alcaria Creek with the Aljezur River (Santa Susana) we recognized a landform that we interpreted as a shutter ridge (Figure 6.13). This landform blocks the outflow of the Alcaria Creek into the Aljezur River alluvial plain at the Framangola site. This shutter ridge is associated with the fault-strand previously recognized during trenching conducted for paleoseismology studies, also detected by geoelectric tomography surveys conducted at Framangola (Figueiredo *et al.*, 2011). The fault at this site is inferred to displace Miocene detrital and carbonate sediments located on the east block from the Palaeozoic schist bedrock on the west block. At this site the Miocene beds dip 10º to the south, which is different from the 10º westwards tilting recognized in Barranco da Vaca and other locations, suggesting that this ridge could also correspond to a structural compressional zone, a "*push-up"*, that differentiates Alfambras from Aljezur basin.

At the top of the Santa Susana ridge, a surface was previously recognized and correlated with the surface at the same elevation (60-65 m, as exposed in 5.3.2.1.2) along the left bank of the Alcaria Creek: in fact, both of these surfaces should correspond to a fluvial terrace from Aljezur River, well preserved in this area. If this is the case, and if Alcaria Creek valley is incised into this terrace, then the terrace age pre-dates the creek incision and its displacement.

We were not able to establish well-defined piercing points to correctly measure the displacement along this feature. We opted to estimate an order of magnitude of the displacement, evaluating a maximum and a minimum displacement as we were not able to quantify erosion or deposition that might mask the real length of the displacement. One estimative is the distance corresponding to the deflection of the Alcaria Creek central valley line relatively to the channel confluence into the alluvial plain at Framangola, where it crosses the front of the ridge: we measured about 240 m for this inferred displacement, and assumed that this value likely corresponds to a maximum displacement. Another hypothesis is considering that the ridge could have controlled the Alcaria Creek incision, favouring an angular disposition in the confluence. If this is the case, then we should measure the shutter-ridge length between the Alcaria Creek channel and the confluence, which corresponds to circa 140 m length, assuming that this measurement is likely to correspond to a minimum displacement. So we assume a likely cumulative displacement between 240 to 140 m for a period of time younger than the age of the 60-65 m surface.

6.5 Discussion

We have analysed the geomorphology of the region close to and along the Aljezur-Alfambras basins and applied several geomorphic indexes in order to evaluate the activity of the STASFS along the Aljezur fault, through the drainage basins analysis and the morphometry of the Aljezur-Alfambras valley itself. Due to the type of structure being a major strike-slip fault system, the shape of the valley, trending linear and running parallel to the fault, and the pattern of the subsidiary drainages, several geomorphic indexes were applied in conditions that were not the ideal ones. However, due to the lack of knowledge regarding the morphotectonics and tectonic activity of this fault system, this exercise was conducted being all the results cross correlated to better support the analysis.

Distinct ranges of elevations were analysed (at heights of 130-140 m, 100-115m, 95-85 m, 75-85 m, 60-65 m, ~45 m and ~30 m), and evidences for morphologic surfaces were recognized either inside the Aljezur-Alfambras basins or at its vicinity along the regional abrasion platform that is deformed by the STASFS.

At the 130 m interval we found a higher surface surrounding the studied basins, which corresponds to a terrace included into the regional abrasion platform that characterizes the broad coastal plateau, despite occasional remains of a higher terrace, namely at 150 m height. With this assumption two hypotheses arise, one is that the valley precedes the surface which then was simultaneously developed through it and second that the surface precedes the valley development and evolution:

- In case the valley precedes the 130 m terrace, then the valley should have been filled by marine sediments, most likely nearshore sediments. There is no evidence of a fully filled basin along the Alfambras section, where the Miocene carbonate sediments are still preserved, and the only remains of sediments other than the carbonates one are a thin cap of sediments, which we interpreted as a mix of paleosoils with coluvium deposits. On the other hand, at Areeiro section, on the northern extreme the tectonic basin, sediments younger than the Miocene are present at the valley which is partially filled, and those sediments can be understood as being in continuity with sediments present at the valley edges;

- The second hypothesis, it is if the terrace precedes the valley development, this would imply then that there wouldn't be a marine sedimentary filling contemporaneous of the terrace, and that this terrace is downgraded into the valley either by erosion processes, either by tectonic deformation.

The 100-115 m is the following elevation interval surface that is best preserved at Alfambras although present in the remaining sectors. At Alfambras, it is located inside the basin and its back-edge coincides with the fault trace that displaces Miocene and the Paleozoic, suggesting that this surface may correspond to the regional abrasion platform (the higher surface described above) displaced. If so, then this is evidence for circa 15-20 m of vertical displacement. On Aljezur and Areeiro sections (the Aljezur basin), we also recognize surface ranging from 100-115 m elevation, but here interpreted as a terrace located at the regional abrasion platform although close to the valley edges. Here at Areeiro as well as at Alfambras-Framangola a slight break of slope at an elevation of ~108 m can be recognized, suggesting that it could evidence either elements of marine terrace morphology or a topography break due maybe to tectonic deformation.

The interval of 95-85 m is not well expressed in general, but it is present along all sections. Along northern Alfambras and the southern part of Alfambras-Framangola it can be described a poorly preserved surface ranging mostly from 90-95 m, expressed by very small areas at the top of some interfluves. A surface better expressed within the same elevation is recognized along Areeiro section, near to the valley edges. For Aljezur section instead, this 95-85 m interval is expressed as a poorly preserved surface in the top of the Aljezur spur.

In the range 75-85 m of elevation, at all sections except for Alfambras it is possible to recognize surfaces, although for Aljezur, we recognize surfaces at circa 75-80 m in elevation. However at Alfambras-Framangola it is very well expressed by a wide terrace ranging 80-85 m, trimmed on Miocene carbonate rocks and Paleozoic schists and with the back-edge partially coincident with the mapped fault trace, which is the boundary between the Paleozoic and the Miocene. At Areeiro, within 80-85 m elevation, there are some surfaces whose inner edges in the west side of the valley are located along fault segments, which suggest that this surface has been displaced both at Alfambras-Framangola and at Areeiro sections.

In fact, at circa 85 m elevation the Nova Castelãs fault outcrop shows Paleozoic schists thrusting sands with quartz and some feldspar interpreted as marine sands, of probable Plio-Pleistocene age. However, we only recognized a flat surface with remnants of sediments at circa 72-73 m surface. Altogether, we consider that it is a strong evidence to assume that this surface could correspond to the regional abrasion surface displaced, at least for the Areeiro section, which would then imply circa 20 m displacement.

Within the 60-65 m elevation interval, there are evidences better exxpressed along Alfambras-Framangola and Aljezur sections. At Alfambras-Framangola, it corresponds to a clear surface 400 m long and 200 m wide, present only at the western side of the valley and corresponds to the surface at the top of an elongated interfluve interpreted as a shutter ridge, blocking the Barranco Alcaria creek. At Aljezur it is present at both sides of the valley and possibly limited internally by inferred faults, but no outcrops were identified with field surveying.

At Areeiro, we recognize a surface present mostly at the western side of the valley, which is covered by a thin cap of fine sands, generally white in colour, essentially with quartz grains well sorted and fine to medium size, overlaying carbonate Miocene bedrock. This sand is similar to the sand that covers the regional abrasion platform at this region and it is assumed as marine although could also have been reworked as aeolianites sand, during Plio-Pleistocene. Although it was not possible to verify deformation along these sediments, the back-edge of this surface along the western side of the valley, is parallel to the trend of STAS faults.

At circa 45 m elevation, we recognize a surface usually with a very small area and present at the top of interfluves, while at circa ~30 m elevation, we recognize small terraces is better expressed at Aljezur above the floodplain. These terraces are mostly erosional, without sediments, and are probably fluvial terraces. Nonetheless at the Aljezur west valley side, we don't recognize these terraces, but we recognize the presence of coarse sediments, with sub-angular to sub-rounded clasts interpreted as sheetflood deposits. These sediments were interpreted as the "Lower Alluvial fan" unit of Late Pliocene – Early Pleistocene (Vilafranquian) age overlapping the sands of the "Formação Vermelha", of Pliocene age (probably Zanclean) (Pereira, 1990; Cabral, 1995; Dias, 2001). The sheetflood deposit is faulted and provides evidence of left-lateral slip; there is no morphological expression of this fault trace in the vicinity of this outcrop.

We interpret these surfaces present at these elevation intervals surfaces as possibly being of two types:

- one, as corresponding to the abrasion platform displaced, although could have been reworked as fluvio marine, during the Pleistocene highstands such as the 100-115m, 95-85 m and the 75-85 m;

- a second type, related to the valley drainage, primarily as a consequence of the Pleistocene eustatic oscillations, some tectonically deformed, such as the 60-65 m, ~45 m and ~30 m.

Cross correlation of several geomorphic indexes highlighted some zones with anomalous values, or values changes for different indexes at the same locations, providing consistency to the observations: these zones are the transition from Alfambras to Alfambras – Framangola sections, the Framangola alluvial plain and Alcaria Creek. These anomalies or changes could be related with tectonic forcing or with erosion: in case erosion is the driving factor this could be due to differential erosion or by propagating the erosion headwards. This seems to be the case in the transition from Alfambras to Alfambras-Framangola sections, where the main factor to differentiate these two sections was the change in the slope of the Aljezur river channel caused by a readjustment to the modern base-level and generating incision that is propagating headwards. The fault trace at this location does not coincide with the knickpoint and no evidence of deformation was recognized in the field.

As for the Framangola alluvial plain and Alcaria, the situation is different, since a fault segment crosses the valley and the anomalies' location is coincident with the fault trace. This strongly supports the evidence of a continued fault activity, although incision and erosion are both also taking place. Close to Alcaria, at the Framangola plain, electric resistivity tomography profiles conducted across the plain and crossing the fault trace corroborated the presence of a discontinuity. All these observations lead to the opening of a trench to conduct paleoseismic studies, but the field conditions especially due to the superficial sediments characteristics and water content did not allow the observation in detail of this structure in Late Pleistocene to Holocene sediments (Figueiredo *et al*., 2011). Along the length of the same fault segment that crosses Framangola plain, changes in the stream sinuosity, relief ratio, elongation ratio, lower valley-floor width ratios, lower mountain-front sinuosity and increased SL values were observed, making up a strong basis to reasoning that this fault segment is active. Paleoseismic studies were conducted through a trench localised at Barranco da Vaca, 2 km south of Framangola plain, where the fault was recognized strongly deforming sediments younger than the Miocene limestones which are stratigraphically lower and outcroping near the trench site (Figueiredo *et al*., 2010, 2011). Although is was not possible to individualise paleoseimic events and established a chronology of seismic events, a alluvium deposit interpreted as Pleistocene terrace deposit (~ 100-90 m elevation) was deformed and a total of circa 1.5 m of vertical displacement was recognised for a paleosol: considering that the fault is essentially left lateral strike-slip, this cumulative vertical displacement refers to multiple events, which is further evidence for a continued fault activity.

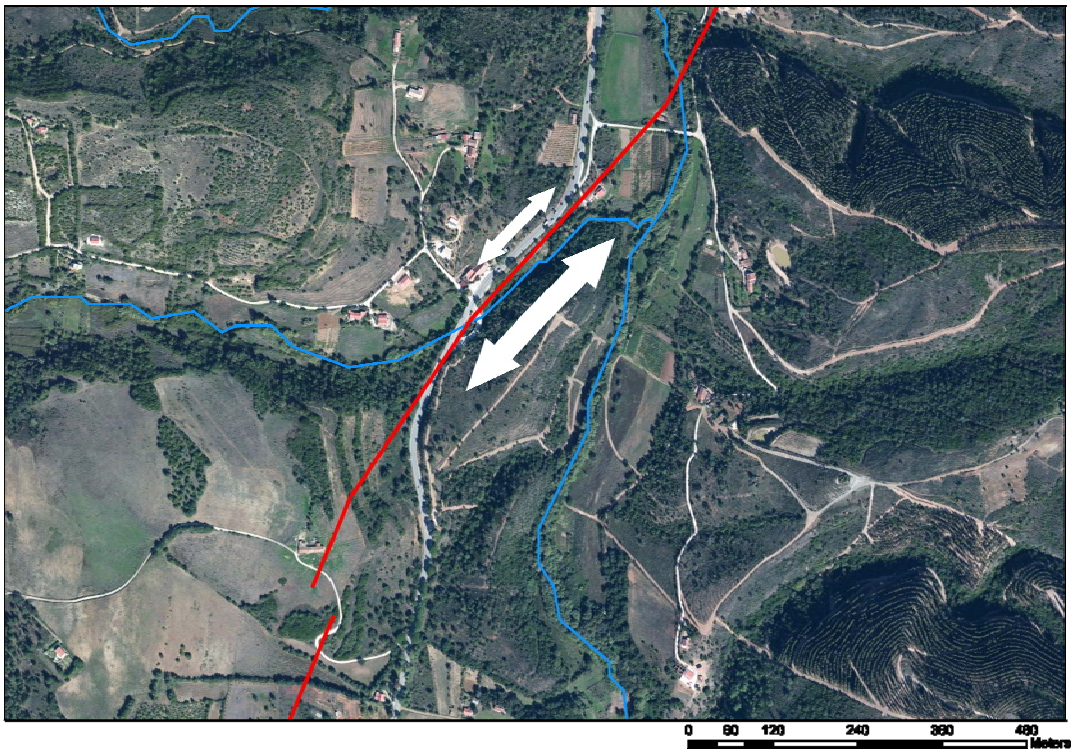

Figure 6.14 - Measurements along the shutter-ridge located at Santa Susana – Alcaria, near Framangola. The large arrow indicates the measurement between the Alcaria creek middle valley line and the tip of the ridge, corresponding to approximately 240 m. The small arrow corresponds to the length of shutter ridge along the deflection, corresponding to approximately 140 m.

At other sections of the Aljezur valley, like in Aljezur and Areeiro there were no significant recognized changes of the geomorphic indexes, although some subtle knickpoints were identified for drainages crossing the Aljezur fault at the Areeiro section. Here, the morphology is disposed in a sort of stair case, controlled by fault segments, Aljezur, Nova Castelãs and Rogil, but we were not able to establish a relationship between these fault segments and the geomorphic indexes analysis. This section is also partially filled with sediments, of which the top sequence, at the area between Rogil and Priorada are very similar with the ones that are present in the regional abrasion platform for the same locations. A thicker filling at Areeiro section could also be related with a sedimentary sequence of fine sands located east of Rogil, from Carrascalinho to Corte de Sobro and Pedra Furada (profile G-G', fig. 6.3): this wedge is characterized by fine sands, which we interpret as aeolianite units. Some of these aeolianite units have iron oxide cementation some of them were explored at Corte do Sobro at circa 150 m elevation. The fine sands can be recognized until circa 180 m elevation, where they are interbedded with coarser colluvium deposits. We inferred that this sequence is only present at this location and not along other locations, because it was closer to sources with sedimentary sources, probably related with the abrasion platform cover sediments.

At Areeiro section, there is no evidence of a significant erosion, or incision, despite the higher mountain-front sinuosity ratio, higher surfaces are still preserved, with sediments that

can be described as marine or beach sediments, with rounded quartz pebbles sometimes covered with a thin cap of angular to semi-angular clasts from the hillslopes.

The analysis of the terraces distribution as well as the Aljezur-Alfambras valley morphology suggest that the fluvial incision propagated from the Aljezur section that has a direct connection with the Atlantic Ocean through a large valley. This fluvial incision and erosion propagated from this section northwards through the Areeiro River and southward by the Aljezur River, first to Alfambras-Framangola section and later to Alfambras section. At Alfambras, the modern channel is just slightly incised on the alluvial plain, the marginal hillslopes are well preserved and the landscape seems to be less degraded. In fact this section seems the best preserved from the erosion that is recognized along the other sections.

In order to access the timing of the deformation there is a need to estimate the ages of the surfaces that have been recognized, since there is not any absolute dating for any of these surfaces or sediments. We have presented our reasoning to assume that the high regional abrasion platform is polygenic, having been trimmed more than once since the Miocene.

The last marine transgression probably occurred during the Pleistocene, which extension inland is poorly constrain, partially overrunning and re-trimming a Pliocene platform, which is still preserved at higher areas along the regional abrasion surface and whose inner-edge is probably circa 160 m elevation.

It is reasonable to assume that the inner edge for the regional abrasion platform at circa 160 m elevation should correspond to the high stand for the mid-Pliocene (Piacenzian) warm period (MPWP) that lasted from 3.3 to 2.9 Ma, with an eustatic peak 22 ± 5 m higher than the modern sea level, and with a 95% probability of having been 22 ± 10 m (Miller *et al*., 2012). If so then we can calculate an uplift rate of 0.042 ±0.003 mm/a for this geomorphic feature, meaning that the regional abrasion platform should has been re-occupied during the middle Pliocene –Pleistocene.

This reasoning and inferred uplift rate is corroborated by a recent dating of a marine terrace: a preliminary absolute age for a marine terrace with an inneredge of circa 80 m elevation at Telheiro, in the vicinity of Sagres, was obtained through the cosmogenic nuclides geochronology method, providing an age of 2.0 +0.3/-0.2 Ma, which according the sea level eustatic curve of Miller *et al.*, (2011) for the Pleistocene, we obtain an uplift rate in the range of 0.03 to 0.04 mm/a, which is consistent with the uplift rate inferred for the regional abrasion platform inneredge assuming a mid-Pliocene age.

Assuming that a value of 0.03 to 0.04 mm/a as a regional uplift rate and according with Miller *et al*. (2011) eustatic sea level curve, we can estimate that:

- the extension of the Pleistocene transgression may have reached as high as the nowadays 110-115 m elevation;
- the marine terrace at circa 130 m elevation, should be approximately 2.8 to 3 Ma of age;

- the marine terrace at circa 150 m elevation, should be approximately 3 Ma of age.

If in fact the Pleistocene transgression extended as far as reaching nowadays 110-115 m elevation, then the sediments covering the platform at the northern section of STAS fault system, namely the white sands are probably of Pleistocene age. This is consistent with the similarity between those sediments and sediments at the abrasion platform. As a consequence, it is likely that the abrasion platform was displaced at the Areeiro section during the Pleistocene as well as the Pleistocene transgression has occupied the tectonic basin.

As for the 130-140m surface it seems reasonable to assume a late Pliocene age for it, which probably predates the development of the valley associated with the Alfambras section.

The analysis of Areeiro section topographic profiles (Fig. 6.3) suggests that this valley is primarily controlled by tectonics and has not been significantly carved by erosion or incision. Taking into account the valley depth for this section as approximately 40 m, and that the valley edges have ranging 100-120 m elevation, we consider this measure as an indicator of vertical displacement since at least the base of Pleistocene, *i.e*. 2.6 Ma, and consequently we estimate a vertical rate of about 0.015 mm/a rate for that section. The same observation is valid for the Alfambras section, were we also considered 40 m of displacement since approximately 3.0 Ma which equals a rate of circa 0.014 mm/a. At Alfambras-Framangola and Aljezur, the valley depth increases reaching 80 m along Aljezur and 60 m along Alfambras-Framangola, which we interpret as the tectonic vertical displacement plus the drainage incision. Efforts were made to differentiate tectonic forcing from erosion processes especially at the Aljezur section: here the valley depth could be from 80 to 100 m, and considering that we estimate circa 40 m of vertical displacement since late Pliocene/early Pleistocene, this could imply approximately 40 to 60 m of incision, likely to be majority of Pleistocene age plus probable an older tectonic displacement, related with previous tectonic stages that have initiated the tectonic basin. However, Aljezur section has a complex evolution and was probably the mouth of an older drainage that outflowed towards the regional abrasion platform, even before the evolution of the Aljezur basin to its present state. In order to understand this evolution a detailed sedimentologic and morphological study calibrated with absolute geochronology methodologies should be conducted, in order to access rates of incision and erosion quantification and consequently determine the tectonic input.

Field surveys conducted by several authors (Cabral, 1995; Dias, 2001) and corroborated in this study indicated that the fault is mainly strike slip, with a minor vertical component. The striae identified in outcropping fault planes present generally a low angle, with variable rake between 10^{o} and 7^{o}. We calculated how much horizontal displacement (lateral) should have occurred for a total of 40 m of vertical displacement: for a rake of 7^{o} we obtained 325 m of left-lateral displacement and for a rake of 10^{o} we obtained 227 m. Although this is a rough approach and estimate, in the absence of further information this estimation provides an order of magnitude of the deformation. Thus, and for the same time interval considered for the 40 m of vertical displacement, an horizontal displacement rate of 0.12 ±0.003 mm/a (for a striae rake of 7^{o}) or 0.08 ± 0.01 mm/a (for a striae of 10^{o}) are obtained.

To estimate the lateral displacement recognized at Santa Susana, and to delimit the timing of the deformation, there is a need to understand the likely age of the 60-65 m surface present at the top of the interpreted shutter ridge. We consider that this surface corresponds to a fluvial terrace, in close association with the eustatic sea level position, due to the proximity with the Atlantic Ocean. We also assume that vertical deformation for this terrace is not significant, since we have not found evidences for it. Based upon that and assuming a regional uplift rate of 0.03- 0.04 mm/a, we estimate that this terrace should have an age ranging from 2 to 1.5 Ma. Since we considered that the landform interpreted as a shutter-ridge has evolved mainly after the incision of Alcaria creek into the 60-65 m terrace, we choose to considered 1.5 Ma as the reasonable age.

We have considered two measurements for the displaced channel at Alcaria: 240 m maximum and 140m minimum displacements, thus interpreted as having occurred since 1,5 Ma. In this way we can estimate a maximum horizontal displacement rate of 0.16 mm/a and a minimum horizontal displacement rate of 0.09 mm/a since the last 1.5 Ma. This order of magnitude of horizontal displacement is the same that the order of magnitude of the horizontal displacement previously inferred.

Finally, we summarize the development of the tectonic basins and valley and the STAS fault system evolution into several stages, according with the geomorphology and morphotectonic analyses:

- during the Miocene, small tectonic depressions were generated as pull-apart basins on the strike-slip STASFS, favouring the preservation of marine carbonate sediments originally deposited in a broad abrasion platform. The fault, dipping strongly (70-80^{o}) to the west, promoted an asymmetric geometry, similar to a half-graben and the development of a small fluvio-estuarine system, as evidenced by the sediments underlying the carbonate sediments. More than one episode of deformation occurred during the Miocene;

- Later, during the Pliocene, the regional abrasion platform was re-occupied by the marine transgression, which re-trimmed the previous landform, reaching an elevation of 160 m or slightly higher. There are no absolute ages for the sediments overlying the Miocene carbonates, and consequently those sediments could be Miocene or Pliocene. The Pliocene transgression could have then invaded the tectonic depressions, that could had been already partially formed, depositing coarse deposits and sands over the Miocene expressed by unconformities. These depressions favoured the development of a drainage system, flowing from the west (Cerca River). No direct evidence of deformation is recognized for this stage, at least a significant vertical sign;

- Since late Pliocene, the faults seem to have been reactivated, displacing the Plio-Pliestocene abrasion platform, and evolving as an active fault system. The fault system has evolved intra-basin and younger fault strands are now active at the tectonic basins, mostly with a strike-slip component rather than with a vertical component, whereas the old fault strands do not evidence relevant deformation. The previous tectonic basins that may have not

been connected (Alfambras and Aljezur) are now connected through the same drainage, whose position is controlled by the active faults strands.

6.6 Conclusions

Several geomorphic indexes were applied to conduct a morpho-tectonic interpretation of the Aljezur-Alfambras basin and evaluate rates of activity for the fault segments identified along the Aljezur fault, the central fault along the São Teotónio – Aljezur – Sinceira fault system. Although not all of the geomorphic indexes were adequate to apply, and the deformation rates for STASFS are very low, a cross correlation of analysis conducted trough different approaches lead to the identification of fault activity.

Distinct morphological surfaces were recognized in the vicinity of the Aljezur-Alfambras basin, as well as inside the basin. Ages for these surfaces were estimated, since no absolute ages are available for them. Field surveys and detailed geomorphologic analysis lead to the identification of landforms characteristics of strike-slip structures, allowing estimating for the first time a horizontal displacement for STAS fault system. Through morpho-tectonic interpretation, a continued fault activity for the Alfambras fault segment, Aljezur fault segment and the Nova Castelãs fault segment was identified. Based upon age estimations, geomorphic analysis and fault characterization, we estimate a vertical displacement rate of approximately 0.015 mm/a for the STAS along the Aljezur-Alfambras basin, since late Pliocene/early Pleistocene and a horizontal displacement rate in the range of 0.09-0.16 mm/a since the last 1.5 Ma.

Acknowledgements

This work was funded by Fundação da Ciência e Tecnologia, through a PhD scholarship (SFRH/BD/36892/2007) attributed to Paula Marques Figueiredo and Research Project "Fault Activity and Seismicity Triggered by Ocean Loading in West Iberia" (PTDC/GEO-GEO/2860/2012)

Chapter 7

Seismotectonics of Southwest Portugal active structures

7.1 Introduction

In order to evaluate the seismic hazard associated to the seismogenic structures located along Southwest Portugal, there is a need to describe the characteristics associated to earthquakes generated along them, the seismic cycle associated to each structure and finally how seismicity can occur.

A major goal is to estimate the amount of energy released during an earthquake generated by the regional active structures. The amount of seismic energy that is released during an earthquake is proportional to the magnitude[1] , which can also be calculated through the seismic moment. The seismic moment[2] can be measured either through seismograms or can be estimated from geological observations such as the size of the fault rupture and the displacement that occurred.

The seismic moment[3] can also be related with the moment magnitude (Hanks and Kanamori, 1979) and it is possible to access the potential of the seismic moment and the moment magnitude for a certain structure through geological observations. For that, several fault parameters need to be estimated, namely the length of the fault, its width based upon the inferred average seismogenic thickness of the crust, the fault dip and kinematics as well as the average displacement per seismic rupture, whose input greatly benefits from paleoseismological observations.

Estimations to access the magnitude of a possible earthquake and likely fault rupture parameters are conducted using empirical relationships that were established based upon large earthquake databases of distinct orders of magnitude covering several types of faulting and a broad distribution covering distinct tectonic environments. The empirical relationships most frequently used are the ones from Wells and Coppersmith (1994), which allow us to estimate for a specific fault, based upon geological assumptions, the maximum magnitude that can occur and the correspondent coseismic fault rupture parameters.

---

[1] log E(s) = 11.8 + 1.5 M_S (E(s) in erg)

[2] Mo = □ A D, where □ is the shear modulus (generally taken as 3 x 10^{10} Pa), A the area of fault rupture (in m^2) and D the average displacement (in m)

[3] Mw= 2/3 log Mo - 6.0 (Mo in Nm)

However, calculations of moment magnitude and displacement inferred through these specific empirical relationships for specific faults have not always been confirmed by the moment magnitudes and displacements measured after the occurrence of earthquakes. This discrepancy has been interpreted as due to several limitations of the empirical approach, mostly related with the quality, size and tectonic setting of the database from where the empirical relationships were obtained. Since the first empirical relationships were established, the availability and quality of relevant information improved greatly, either by improvements on the seismic instrumental data, further occurrence of relevant earthquakes or even the inclusion of detailed paleoseismological information that has substantially improved the knowledge about earthquake geology and earthquake characteristics.

This led to the development of more databases that enabled the formulation of further empirical earthquake magnitude. Those, built-on specific tectonic environments, specific type of faulting, or even for distinct slip rates or different size of fault rupture areas can be then more specific than the Wells and Coppersmith relationships and consequently provide a better approximation between empirical calculations and real observations, as it is exposed in a compilation of earthquake scaling relationships for seismic hazard purposes (Stirling *et al*., 2013). Nonetheless, depending on regional characteristics, calculations based on specific empirical relationships may provide similar values to those obtained from more general empirical relationships such as the Wells and Coppersmith (1994) regressions.

For this study we selected a set of empirical relationships from Wells and Coppersmith (1994) but also some more specific ones according with the tectonic setting (Stirling *et al.,* 2008), kinematics of the fault (Wesnousky, 2008) and size of the rupture area (Hanks and Bakun, 2008). We applied these empirical relationships to estimate moment magnitude and displacement for the São Teotónio-Aljezur-Sinceira fault system (STASFS), as well as for some other regional faults evidencing Plio-Pleistocene activity, in order to obtain moment magnitude values for the maximum expectable earthquake, as well as maximum and average expectable displacement for each structure. The average recurrence period for the maximum expectable earthquake was also estimated through the relationship between the seismic moment rate and the expectable seismic moment (Wesnousky, 1986).

7.2 Earthquake Scaling Relationships and Time Recurrence

7.2.1 Wells and Coppersmith (1994)

Calculations to estimate the moment magnitude for the maximum expectable earthquake, as well as the maximum and the average displacement per event were based on Wells and Coppersmith (1994) empirical relationships, considering the coseismic rupture length of the fault. The length of the fault was chosen as the main input, since it corresponds to the best know input for the faults studied. The following relationships were considered:

- Regression of surface rupture length (SRL) on moment magnitude (Mw),

$$Mw = 5.08 + 1.16 * \log (SRL) \quad (1)$$

- Regression of surface rupture length (SRL) on maximum displacement (MD),

$$\text{Log } MD = -1.38 + 1.02 * \log (SRL) \quad (2)$$

- Regression of maximum surface displacement (MD) on moment magnitude (Mw),

$$\text{Log } MD = (M_w - 6.69)/0.74 \quad (3)$$

- Regression of average surface displacement (AD) on moment magnitude (Mw),

$$\text{Log } AD = (M_w - 6.93)/0.82 \quad (4)$$

- Regression of surface rupture length (SRL) on average displacement (AD),

$$\text{Log } AD = -1.43 + 0.88 * \log SRL \quad (5)$$

7.2.2 Stirling *et al.* (2008)

The empirical relationship proposed by Stirling *et al*. (2008) has been developed for transpressive environments, with oblique slip, namely for the New Zealand strike-slip to reverse-slip faults, where relationships from provided lower magnitudes than the observed ones. It is recommended that the regression should be applied for strike-slip to convergent dip-slip faults, were it has proven to provide a good estimation, but not along primarily plate boundaries faults, where its application is not as robust. If applied in low strain rate regions, such as Southwest Portugal, it can provide larger magnitudes than the empirical relationship of Wells and Coppersmith (1994) based on fault length. The empirical relationship applied was:

- Regression of width of the rupture area (W) and subsurface surface length (L) on moment magnitude for oblique slip, strike-slip to reverse-slip faults,

$$M_w = 4.18 + (2/3) \log W + (4/3) \log L \quad (6)$$

7.2.3 Wesnousky (2008)

The database used to build the relationship proposed by Wesnousky (2008) refers to earthquakes with surface rupture lengths larger than 15 km, and therefore should be applied to faults with surface lengths larger than that value. There is a distinct relationship for each type of faulting and one generic, although the author points out that the strike-slip relationship seems to be the most relevant. The following relationships were thus applied, despite the length of the studied faults:

- Regression of the surface rupture length (L) on moment magnitude for all types of faulting,

$$M_w = 5.30 + 1.02 \log L \quad (7)$$

- Regression of the surface rupture length (L) on moment magnitude for strike-slip faults,

$$M_w = 5.56 + 0.87 \log L \quad (8)$$

- Regression of the surface rupture length (L) on moment magnitude for reverse faults,

$$M_w = 4.11 + 1.88 \log L \quad (9)$$

7.2.4 Hanks and Bakun (2008)

The relationships that Hanks and Bakun (2008) established were developed from a small number of large strike-slip earthquakes, and consequently their application is best for great strike-slip faults along plate boundaries. The regressions are differentiated according to the fault area. They seem to be unsuitable for faults with slip rates lesser than 1 mm/a, however they have been widely applied successfully. The empirical relationships applied according with these authors were:

- Regression of the fault area (A) on moment magnitude for A < 537 km^2,

$$M_w = \log A + (3.98 \pm 0.03) \quad (10)$$

- Regression of the fault area (A) on moment magnitude for A > 537 km^2,

$$M_w = (4/3) \log A + (3.07 \pm 0.04) \quad (11)$$

7.2.5 Maximum Expectable Earthquake and Recurrence Time

To estimate the recurrence time for a maximum expectable earthquake, Wesnousky (1986) established a relationship between the seismic moment of the maximum expectable earthquake and a foreseen seismic moment rate, based upon the slip rate of the fault. This relationship assumes that all the displacement occurred at a given fault is the result of a sum of displacements generated along multiple maximum expectable earthquakes for a given period of time, provided by geological markers.

The seismic moment of a fault can be expressed by

$$M_o = \mu A D \quad (12)$$

where μ is the shear modulus (generally taken as 3 x 10^{10} Pa), A the area of fault rupture and D the average coseismic displacement. Assuming that the total displacement D_t, was generated by a fault with a area A during a period of time T, then it is possible to consider that the seismic moment rate of a given fault is

$$M_o^g = (\mu A D_t) / T \qquad (13)$$

which equals to,

$$M_o^g = \mu A v \qquad (14)$$

and v corresponds to the slip rate of the fault.

If the total displacement corresponds to a cumulative displacement generated during multiple maximum expectable earthquakes, considering those as characteristic earthquakes, then the time T corresponds also to a cumulative period of time, during which all the slip occurred. Considering (12) for the seismic moment for the maximum expectable earthquake then,

$$\frac{Mo^e}{Mo^g} = \frac{\mu A D}{\mu A Dt/T} \Leftrightarrow \frac{Mo^e}{Mo^g} = T$$

Consequently the average recurrence period corresponds to the ratio between the seismic moment for the maximum expectable earthquake and the seismic moment rate for the same fault assuming a constant slip rate. The relationship between the moment magnitude (M_w) and the seismic moment (M_o^e) is given by

$$M_o^e = \log^{-1} [(M_w+6)/0.67] \qquad (15)$$

enabling to estimate average recurrence periods from inferred magnitudes and known slip rates.

Another way to estimate the average recurrence period is to calculate the period of time needed to achieve a given displacement occurred during multiple maximum expectable earthquakes, according with a known slip-rate (the velocity),

$$T = D / v$$

with D is average displacement and v is the slip rate .

Average recurrence periods, were estimated for the faults selected in this study.

7.3 Maximum Expectable Earthquake and Average Recurrence Time for the Studied Structures

Calculation of the maximum expectable earthquake according with several earthquake scaling relationships, as well as average displacements, where performed for the following faults:

- São Teotónio-Aljezur Sinceira fault system,
- Quarteira fault
- Portimão fault
- Albufeira fault
- a proposed fault located at the near offshore

The selection of these faults to apply calculations was made according with their Plio-Pleistocene tectonic activity, which stood out through the research conducted in this thesis.

The depth of the structures is poorly constrained, having been inferred by the depth of the hypocenters as being in the order of at least 20 km. We have chosen to consider the value of maximum depth equal to the value that is available in the "Quaternary Active Faults Database of Iberia" [4] (QAFI) which is 20.5 km for the onshore faults, while the large faults located in the offshore present deeper seismicity, with depths ranging from 40 to 60 km.

We have measured the map-length of the faults and compared it with the QAFI database; when significantly different, as in the case of Quarteira fault, we have considered both lengths. The dip of the faults was also assumed from outcrop measurements and when needed completed through the QAFI database.

We have considered 3 distinct seismic sources

- one considering individual fault segments of the STASFS;
- a second one considering all segments present along the tectonic basins, such as Aljezur-Alfambras tectonic basins and different rupture scenarios - rupture of the faults present in Aljezur-Alfambras simultaneously with the faults present in the São Miguel tectonic basin or with the faults present in the Pedralva-Sinceira tectonic basins, or rupture of all the STASFS extension;
- and finally a third group of sources that includes other relevant faults where Plio-Pleistocene activity is recognized in the scope of this thesis, such as the Quarteira, Portimão, Albufeira and an unknown but probable fault localized in the near offshore, along the Portuguese southwest continental shelf.

To estimate the average recurrence period for the maximum expectable earthquake, we have only considered the STASFS, since the slip rate for the remaining faults is poorly constrain.

The results for the moment magnitude and displacement per event are presented in Table 7.1 and the average recurrence period results are presented in Table 7.2.

[4] Version 2, available in http://info.igme.es/qafi/ (access date April 2015)

	Fault	Lenght (km)	Dip ± error	Depth (km)	Width (km)	Area (km²)	(a) Mw (L)	(a) Max D (SRL) (m)	(a) Max D (Mw) (m)	(a) AD (Mw) (m)	(a) AD (m)	(b) Mw (L)	(c) Mw (L) (all)	(c) Mw (L) (s.s.)	(c) Mw (L) (rev.)	(d) Mw (A) <537 km²	(d) Mw (A) >537 km²
STASFS segments	Alfambras W- Framangola	7	78±12	20.5	20.4	142.8	6.06	0.30	0.14	0.09	0.21	6.18	6.16	6.30	5.70	6.13	-
	Alfambras E*	**5.5**	**78±12**	**20.5**	**20.4**	**112.2**	**5.94**	**0.24**	**0.10**	**0.06**	**0.17**	**6.04**	**6.06**	**6.20**	**5.50**	**6.03**	**-**
	Aljezur E	9	78±12	20.5	20.4	183.6	6.19	0.39	0.21	0.12	0.26	6.33	6.27	6.39	5.90	6.24	-
	Aljezur	**6**	**78±12**	**20.5**	**20.4**	**122.4**	**5.98**	**0.26**	**0.11**	**0.07**	**0.18**	**6.09**	**6.09**	**6.24**	**5.57**	**6.07**	**-**
	Nova Castelãs	4	78±12	20.5	20.4	81.6	5.78	0.17	0.06	0.04	0.13	5.86	5.91	6.08	5.24	5.89	-
	Rogil	**7**	**78±12**	**20.5**	**20.4**	**142.8**	**6.06**	**0.30**	**0.14**	**0.09**	**0.21**	**6.18**	**6.16**	**6.30**	**5.70**	**6.13**	**-**
	Rogil (south)	9	78±12	20.5	20.4	183.6	6.19	0.39	0.21	0.12	0.26	6.33	6.27	6.39	5.90	6.24	-
	Baiona	**8**	**78±12**	**20.5**	**20.4**	**163.2**	**6.13**	**0.35**	**0.17**	**0.11**	**0.23**	**6.26**	**6.22**	**6.35**	**5.81**	**6.19**	**-**
	Sinceira (Basin)*	7	78±12	20.5	20.4	142.8	6.06	0.30	0.14	0.09	0.21	6.18	6.16	6.30	5.70	6.13	-
	Sinceira (towards coast)*	**13**	**78±12**	**20.5**	**20.4**	**265.2**	**6.37**	**0.57**	**0.37**	**0.21**	**0.36**	**6.54**	**6.44**	**6.53**	**6.20**	**6.40**	**-**
STASFS	All segments Aljezur	25	78±12	20.5	20.4	510	6.70	1.11	1.04	0.53	0.63	6.92	6.73	6.78	6.74	6.69	-
	Aljezur & Sinceira	**37**	**78±12**	**20.5**	**20.4**	**754.8**	**6.90**	**1.66**	**1.92**	**0.92**	**0.89**	**7.14**	**6.90**	**6.92**	**7.06**	**-**	**6.91**
	Aljezur& Baiona	33	78±12	20.5	20.4	673.2	6.84	1.48	1.60	0.78	0.81	7.08	6.85	6.88	6.96	-	6.84
	Baiona-Aljezur-Sinceira	**44**	**78±12**	**20.5**	**20.4**	**897.6**	**6.99**	**1.98**	**2.52**	**1.17**	**1.04**	**7.24**	**6.98**	**6.99**	**7.20**	**-**	**7.01**
	STASFS	52	78±12	20.5	20.4	1060.8	7.07	2.35	3.27	1.48	1.20	7.34	7.05	7.05	7.34	-	7.10
	Quarteira	30	73±18	20.5	20.3	609	6.79	1.34	1.38	0.68	0.74	7.02	6.81	6.85	6.89	-	6.78
	Quarteira (QAFI)	**55**	**73±18**	**20.5**	**20.3**	**1116.5**	**7.10**	**2.48**	**3.57**	**1.61**	**1.26**	**7.37**	**7.08**	**7.07**	**7.38**	**-**	**7.13**
	Quarteira (ocean)	74	73±18	20.5	20.3	1502.2	7.25	3.36	5.68	2.44	1.64	7.54	7.21	7.19	7.62	-	7.31
	Portimão	**15**	**82±8**	**20.5**	**20.45**	**306.75**	**6.44**	**0.66**	**0.47**	**0.26**	**0.40**	**6.62**	**6.50**	**6.58**	**6.32**	**6.47**	**-**
	Albufeira	15	83±8	20.5	20.5	307.5	6.44	0.66	0.47	0.26	0.40	6.62	6.50	6.58	6.32	6.47	-
	Off-shore	**70**	**30±10**	**40**	**70**	**4900**	**7.22**	**3.18**	**5.21**	**2.26**	**1.56**	**7.87**	**7.18**	**7.17**	**7.58**	**-**	**7.99**

Table 7.1 – Moment magnitude (Mw) and average displacements (AD) values calculated according to several earthquake-scaling relationships. (a) calculations based in Wells and Coppersmith (1994) according with: [Mw (L)] *Mw= 5.08 +1.16 * log (SRL);* [Max D (SRL)] *Log MD= -1.38 +1.02 *log (SRL);* [Max D (Mw)] *Log MD = (M_w-6.69)/0.74;* [AD (Mw)] *Log AD= (M_w-6.93)/0.82;* [AD] *Log AD = -1.43+0.88 *log SRL.* (b) according to Stirling *et al.* (2008) [Mw (L)] M_w *=4.18 + (2/3) log W + (4/3) log L.* (c) based on Wesnousky (2008), [Mw (L) (all)] M_w *=5.30 + 1.02 log L;* [Mw (L) (s.s.)] M_w *=5.56 + 0.87 log L;* [Mw (L) (rev.)] M_w *=4.11 + 1.88 log L.* (d) based on Hanks and Bakun (2008), according with [Mw (A)<537 km²] M_w *=log A+ (3.98 ±0.03);* [Mw (A)>537 km²] M_w *=(4/3) log A+ (3.07 ±0.04).*

	Fault	Area (km^2)	Mw (1)	AD (Mw) (m)	AD (m)	Mw (2)	rate (mm/a)	Mo		Mo rate	Time (a)		AD/ rate (a)	
								Mw (1)	Mw(2)		Mw (1)	Mw (2)	AD (Mw)	AD
STASFS segments	Alfambras W-Framangola	142.8	6.06	0.09	0.21	6.18	0.1	1E+18	1.51E+18	4.28E+14	2337	3524	870	2059
	Alfambras E*	**112.2**	**5.94**	**0.06**	**0.17**	**6.04**	**0.1**	**6.59E+17**	**9.34E+17**	**3.37E+14**	**1959**	**2776**	**618**	**1665**
	Aljezur E	183.6	6.19	0.12	0.26	6.33	0.1	1.55E+18	2.49E+18	5.51E+14	2808	4520	1241	2569
	Aljezur	**122.4**	**5.98**	**0.07**	**0.18**	**6.09**	**0.1**	**7.67E+17**	**1.11E+18**	**3.67E+14**	**2088**	**3026**	**699**	**1798**
	Nova Castelãs	81.6	5.78	0.04	0.13	5.86	0.1	3.8E+17	4.96E+17	2.45E+14	1552	2025	394	1258
	Rogil	**142.8**	**6.06**	**0.09**	**0.21**	**6.18**	**0.1**	**1E+18**	**1.51E+18**	**4.28E+14**	**2337**	**3524**	**870**	**2059**
	Rogil (south)	183.6	6.19	0.12	0.26	6.33	0.1	1.55E+18	2.49E+18	5.51E+14	2808	4520	1241	2569
	Baiona	**163.2**	**6.13**	**0.11**	**0.23**	**6.26**	**0.1**	**1.26E+18**	**1.97E+18**	**4.9E+14**	**2577**	**4023**	**1051**	**2316**
							0.05			**2.45E+14**	**5153**	**8045**	**2101**	**4632**
	Sinceira (Basin)*	142.8	6.06	0.09	0.21	6.18	0.1	1E+18	1.51E+18	4.28E+14	2337	3524	870	2059
							0.05			2.14E+14	4674	7049	1740	4118
	Sinceira (towards coast)*	**265.2**	**6.37**	**0.21**	**0.36**	**6.54**	**0.1**	**2.92E+18**	**5.18E+18**	**7.96E+14**	**3675**	**6505**	**2088**	**3550**
							0.05			**3.98E+14**	**7350**	**13010**	**4176**	**7101**
STASFS	All segments Aljezur	510	6.70	0.53	0.63	6.92	0.1	9.07E+18	1.9E+19	1.53E+15	5928	12429	5266	6312
	Aljezur & Sinceira	**754.8**	**6.90**	**0.92**	**0.89**	**7.14**	**0.1**	**1.79E+19**	**4.15E+19**	**2.26E+15**	**7897**	**18323**	**9169**	**8913**
	Aljezur& Baiona	673.2	6.84	0.78	0.81	7.08	0.1	1.47E+19	3.3E+19	2.02E+15	7263	16361	7799	8059
	Baiona-Aljezur-Sinceira	**897.6**	**6.99**	**1.17**	**1.04**	**7.24**	**0.1**	**2.41E+19**	**5.86E+19**	**2.69E+15**	**8964**	**21752**	**11716**	**10381**
	STASFS	1060.8	7.07	1.48	1.20	7.34	0.1	3.22E+19	8.17E+19	3.18E+15	10129	25664	14840	12025

Table 7.2 – Calculations of the average recurrence period according to Wesnousky (1986) or by displacement and fault slip rate. Moment magnitudes from Table 7.1 are applied in this calculation. Mw (1) corresponds to moment magnitude calculated from Wells and Coppersmith (1994) whereas Mw 2 from Stirling *et al.* (2008). [Mo] indicates the seismic moment for both Mw according to $M_o^e = log^{-1}[(M_w+6)/0.67$ and Mo rate is calculated as $M_o^g = \mu A v$. Average recurrence time is then Time for both Mw assuming that $Mo^e / Mo^g = T$ according to Wesnousky (1986) or AD/rate if it based upon a ratio between the average displacement and the slip rate, as $T = D / v$

A comparison between the different empirical relationships that were chosen evidences that the estimated moment magnitudes are within the same range of values. As expected, according to the comments made about each set of relationships, the moment magnitudes estimated with the regression of Stirling et al., (2008) proved to be slightly larger than the ones estimated with the regressions by Wells and Coppersmith (1994), but that was not always the case for the values estimated with the Wesnousky (2008) and Hanks and Bakun (2008) relationships. The results obtained using the Wesnousky (2008) relationship vary with the type of faulting, but tend to be very similar to the ones obtained by the Wells and Coppersmith expressions, if the length of faults is larger than 15 km and if it is a strike-slip fault. The calculation made with Hanks and Bakun (2008) relationships presents slight changes from the previous results when the fault area is very small or very large, despite the fact that slip rates for all the faults considered are lower than 1 mm/a. Based upon this comparison, the reference values that we have chosen to consider are the ones obtained through the Wells and Coppersmith (1994) regressions and the Stirling *et al*. (2008) as maximum expectable moment magnitude.

The analysis of the values suggests that:

- individual segments of the STASFS are capable to generate a maximum expectable earthquake in the range of a Mw 6 to 6.5;
- a simultaneous rupture of all segments along the Aljezur- Alfambras tectonic basin is capable to generate an earthquake with a moment magnitude in the range of Mw 6.7 to 6.9;
- a simultaneous rupture of all segments along the Aljezur- Alfambras tectonic basin plus other tectonic basins, northward and southward, is capable to generate an earthquake with a moment magnitude in the range of Mw 6.9 to 7.2;
- a rupture of all the inland extension of the STASFS, including the fault segments that have not evidenced significant activity in the Pleistocene, is capable to generate a moment magnitude in the range of Mw 7.1 to 7.3.

Other structures in the region are also capable to generate moment magnitudes in the range Mw 6.5 to 7.4, the Quarteira fault being the structure with capabilty to generate the larger magnitude, based upon its size. We must stress though that the Plio-Pleistocene tectonic activity along this structure is not clearly expressed constraining the evaluation of slip rate, which probably is low.

A proposed fault which was inferred located close to the western coastline, may have the capability to generate large earthquakes, with moment magnitude ranging from Mw 7.2 to 7.9. If this is the case, then this offshore structure poses an additional seismic hazard for the study region.

Calculations of the recurrence periods for the maximum expectable earthquake for the STASFS faults, assuming a slip rate of 0.1 mm/a, and 0.05 mm/a for the segments that evidence a lower tectonic activity, indicate that:

- the average recurrence periods for individual fault segments along the Aljezur-Alfambras basin, assuming a 0.1 mm/a slip rate are in the order of 1552 to 4520 years;
- the average recurrence periods for individual fault segments along the Aljezur-Alfambras basin, assuming a 0.05 mm/a slip rate are in the order of 4674 to 13010 years;
- the average recurrence period for a simultaneous rupture of fault segments along the Aljezur-Alfambras basin, assuming a 0.1 mm/a slip rate is in the range of 5928 to 12429 years;
- the average recurrence period for a simultaneous rupture of fault segments along the Aljezur-Alfambras basin and other tectonic basins, assuming a 0.1 mm/a slip rate is in the range of 7263 t to 21752 years;
- the average recurrence period for a simultaneous rupture of fault segments along the Aljezur-Alfambras basin and other tectonic basins, assuming a 0.1 mm/a slip rate is in the range of 7263 t to 21752 years;
- and finally the average recurrence period for a simultaneous rupture of all STASFS assuming a 0.1 mm/a slip rate, corresponds to a period ranging from 10129 to 25664 years

7.4 Conclusions

Based upon the calculations of the moment magnitude for a maximum expectable earthquake, coseismic average displacements and recurrence periods, we conclude that:

- The STASFS is capable of generating medium to large magnitude earthquakes, with magnitudes ranging from Mw 7.0 to 7.3, with an average displacement per event in the order of 1.20 to 1.48 m and a recurrence period from 10 to 25 ka years, meaning that rupture along the entire length of the STASFS may have not occurred during the Holocene;
- A rupture of the STASFS along the entire length of the Aljezur-Alfambras tectonic basin, which seems to correspond to the more active section of STASFS, is capable to generate a medium to large earthquake with a moment magnitude for a maximum expectable earthquake close to Mw 7, ranging from 6.7 to 6.9, with an average displacement per event of circa 0.5 m, ranging from 0.53 to 0.63, and with a recurrence period of 6 to 12.4 ka, meaning that it is possible that the last maximum expectable earthquake has occurred during the Holocene.
- In the case that a simultaneous rupture occurs in Aljezur-Alfambras and other tectonic basins, then the moment magnitude and the average displacement per event increase, but are still in the order of a Mw 6.0 to 7.1, with average displacements lower than 1 m. In this case, the recurrence period also varies from circa 8 to 18 ka.

Chapter 8

Synthesis and future work

8.1 Synthesis

Southwest Portugal is located close to the plate boundary Eurasia- Nubia and corresponds to the region of Portugal with higher occurrence of instrumental seismicity as well as large historical seismicity, namely the Mw>8 1st November 1755 which was generated offshore Southwest Portugal. Despite previous studies conducted partially in the southwest of Portugal provided improvements to the characterization of the tectonic activity for the Plio-Pleistocene period, open questions remained for this region, particularly concerning the Pleistocene tectonic activity. An open question was also the quantification and characterization of vertical crustal motion and its relationship with the Pleistocene sea level oscillations: only some few marine terraces had been recognized along the coastal zone and their ages poorly constrained. Another open question was the identification of coastal geological or geomorphic markers that might indicate Holocene or late Pleistocene vertical motion, which could be related with the large historical seismicity.

The present thesis is an attempt to address these questions, presenting and discussing relevant information some of which is unpublished data, in the several chapters of this work. A significant contribution to the knowledge on the regional marine terraces and their spatial distribution, especially concerning the Late Pleistocene marine terraces, is presented in Chapter 2. Chapter 2 also addresses the investigation of Holocene vertical motion, which can be related with historical seismicity. Recognition of older Pleistocene marine terraces and unpublished ages are presented in Chapter 3, which also discusses the regional uplift rate, and Chapter 4 presents a model upon geomorphic analyses for a Pleistocene regional uplift, for an area limited to the north by the Alentejo-Placencia fault and to the east by the São Marcos-Quarteira fault. The recognition of marine terraces present along the region and understanding of their ages was crucial, namely to interpret the age of the regional abrasion platform which is displaced by the São Teotónio – Aljezur – Sinceira fault system.

As for the São Teotónio – Aljezur – Sinceira fault system, which corresponds to the more significant fault within the area of study with Plio-Pleistocene tectonic activity, a detailed recognition of the active fault segments was conducted as it is presented in Chapter 5 and 6. Chapter 5 presents results from paleoseismological studies, however without the recognition

of a Holocene event or the recognition of the timing of occurrence of the surface rupture. Characterization of the quaternary deformation was accomplished through a detailed morpho tectonic analysis, which also enabled the recognition of lateral displacement for the first time for this fault system. Chapter 6 also presents a discussion about the slip rate inferred for this fault system. Finally, as a contribution for the regional seismic hazard assessment, moment magnitude for the maximum expectable earthquakes, average displacements per event and average recurrence periods for the more relevant faults are presented in Chapter 7.

8.1.1 Vertical Crustal Motion

8.1.1.1 The Plio-Pleistocene Marine Terraces

Several marine terraces were recognized along the southwest Portuguese coast, along the western and the southern coastline. A sequence of two marine terraces present at lower elevations (T1 and T2) were recognized in the study area and assumed to correspond to the late Pleistocene, probably correlating to abrasion terraces cut during the last interglacial period (MIS 5). The last interglacial had 3 sea level high-stands (MIS 5e, MIS 5c and MIS 5a), one of which, the MIS 5e, approximately at 130 ±2 ka to 119±2ka during the beginning of the last interglacial period is interpreted to have been higher than current mean sea level and a long lasting one, which should have generated a broad wave-cut platform and marine terrace.

With these assumptions, we have assumed that the higher and better preserved of the lower terraces, T2, should correspond to the MIS 5e. T1 seems to have been cut into the T2 terrace, and therefore we conclude that if T2 is likely to correspond to MIS 5e then T1 would correspond to MIS 5c or MIS 5a. Inner edges for T1 and T2 were recognized at consistent elevations of 8 m and 21 m, respectively at distinct sites, which enable the interpretation of a regional sequence of marine terraces.

At Castelejo site, at circa 1.5 m elevation, a section of T1 has a layer of beach sand that is overlying an abrasion platform trimmed on the Paleozoic bedrock: absolute ages for this sediment were obtained through Optical Stimulated Luminescence technique applied to feldspar grains (pIRIR), providing an age of 112 ± 7 ka and 110 ± 5 ka. Overlaying this layer of T1 beach sand and boulders, a sequence of consolidated aeolianites is present and its lower level was also dated, providing an age of 84 ± 6 ka through OSL using quartz and 98 ± 6 ka through OSL-pIRIR applied to feldspar grains. Both results indicate that T1 at Castelejo site corresponds to the MIS 5c. We have initially assumed that T1 should correspond to MIS 5a (Figueiredo et al., 2013), since MIS 5c corresponds to a very short peak at 103-105 ka, which may have been re-occupied by the longer MIS 5a highstand at 80 ka, as it is frequently the case for regions oflow uplift rate.

The eustatic sea level for the MIS 5c is less constrained than for the MIS 5e or even the MIS 5a, and for that reason we estimated the uplift rate using T2 references. The eustatic sea level for the MIS 5e has been estimated as to be in the range of +2 to +9 m (Hearty *et al*., 2007;

Sidall *et al*., 2006; Pedoja *et al*., 2011) with a high probability to have reach +6.6 m (Kopp *et al*., 2009). Assuming that the MIS 5e may have reached +9m elevation, then T2 has been uplifted approximately 10 m since the last interglacial (21 m minus the modern inner edge elevation (+2m) and minus the assumed +9 m at the time of formation). If we assume that the eustatic sea level was +6.6 m, then we may infer a maximum of 12.4 m of uplift (21 m minus the modern inner edge elevation (+2m) and minus the assumed +6.6 m at the time of formation).

There are no references for the timing of the MIS 5e along the Portuguese coast; Hearty *et al.* (2007 and references within) suggest that the last interglacial had an average duration from 130 ±2 ka to 119±2ka; Muhs *et al*. (2011) identify a peak that started at 127 and lasted until 114 ka through a fossil reef complex at Florida, and Muhs *et al.* (2002b) based upon high precision dating of solitary corals from the MIS 5e terrace along the west coast of North America, suggest that the last interglacial peak lasted from ~128 ka to 116 ka.

Considering a total of 9 m of uplift (or 12.4 m if we consider the initial MIS 5e position at +6.6m) during the last 119-116 ka, we calculate an uplift rate of 0.08 mm/a (or a maximum of 0.1 mm/a), corresponding to a mean uplift rate of 0.09 ± 0.001 mm/a.

Marine terraces at higher elevations than T1 and T2 corresponding to Pleistocene highstands older than MIS 5e, probably related with MIS 7, MIS 9 and MIS 11, were also recognized with inner-edges at elevations of 26 m, 32 m and circa 40 m, but their characterization was not possible in the scope of this thesis. A sequence of higher marine terraces is also present, although poorly preserved, at elevations ranging from circa 75 m to 100 m, recognized mostly along the western coast, from Aljezur to Sagres. These higher terraces are embedded in a regional abrasion platform that reaches circa 120 – 130 m elevation in the southwestern coastline, but with lower elevations, circa 100-110 m north of Aljezur. This regional abrasion platform, likely to be late Pliocene to early Pleistocene in age and interpreted as a sequence of marine terraces closely spaced in elevation, has a regional inner-edge at circa 160 m in Southwest Portugal.

At circa 75 m elevation, a section of a marine terrace with an inner-edge poorly constrain at circa 80 m elevation was recognized close to Castelejo site, at Telheiro, just north of Sagres. This terrace comprises a sequence a few meters thick of marine sands followed by aeolianites. This sedimentary sequence is overlying a basal coarser layer of boulders that lay directly on the abrasion surface trimmed on the Paleozoic bedrock. This terrace was previously described in several studies (Feio, 1951; Pereira, 1990; Dias, 2001), though its absolute age was only now obtained in the scope of this thesis. We dated the basal coarser layer of his terrace using Cosmogenig Nuclide Dating (26 Al and 10 Be), which provided a preliminary age of 2.0 + 0.3/ - 0.2 Ma. Assuming an inner-edge of circa 80 m elevation, and considering a paleo sea level position equivalent to the nowadays one, then we will have an uplift rate of circa 0.04 ± 0.005 mm/a, for the last 2 Ma.

Assuming that the regional abrasion platform has been uplifted at the same rate as the terrace at Telheiro, then this implies that the Pleistocene transgression could have reached as high as circa 100 to 115 m, and that the regional inner-edge at circa 160 m could have an age ranging from 4.6 to 3.6 Ma, which might correspond to a late Zanclean sea level highstand.

Vertical motion rates are not the same when considering late Pleistocene and early Pleistocene references. It seems reasonable to assume that the uplift rate calculated for the 2.0 Ma terrace at Telheiro was the same during early Pleistocene and part of Pliocene, but we can only be certain after having more absolute ages in order to obtain more references. However, despite uplift rates calculated for Telheiro terrace (0.04 ±0.005) or for Castelejo T1 terrace (0.09 ± 0.001 mm/a) are in the same order of magnitude, i.e. both are inferior to 0.1 mm/a, younger references provide information for a faster uplift rate than older ones. Based upon this comparison, we interpret this as evidence for a Pleistocene acceleration of uplift rates, which started between approximately 120 ka and circa 2.0 Ma.

8.1.1.2 Holocene Coastal Markers Correlation With Historical Seismicity

Considering that this area should be uplifting at a rate of 0.09 ± 0.001 mm/a, it would be expectable an uplift of circa 1 m for the entire Holocene. This uplift can be representative of an almost instantaneous motion related to a single seismogenic faulting event, be the cumulative of multiple events meaning that individual uplift events could be in the range of centimetres to decimetres, or even as resulting from a continuous uplift due to buckling. Either case, it would be very difficult to differentiate those scenarios in a high energy mesotidal environment coast such as Southwest Portugal.

However, as the last large earthquake occurred 260 years ago (the 1755 Mw>8 event), and vertical deformation along the nowadays abrasion platform was never investigated, a thorough survey along the entire coastline was conducted in order to identify geomorphic coseismic evidence of the 1755 rupture or other large earthquakes that may have uplifted the coastal area during the Holocene. Subtle evidence of a possible embedded section of the nowadays abrasion platform as well as for ichnofossils slightly above the nowadays high tide, suggest a small difference in elevation in the order of circa 20 to 50cm. However, since the nowadays abrasion platform is re-trimming a late Pleistocene terrace, we cannot assure that this difference in elevation corresponds to a Holocene uplift event.

Previous studies on sedimentary fills of two fluvial valleys near the coastline, in the Sagres vicinity (Hidson *et al*., 1999), Koortekas and Dawson, 2007), have interpreted abrupt sedimentary changes which may have happened twice, once following the 382 AD earthquake and again following the 1755 earthquake. Nevertheless, it is also possible that these environmental changes were partially due to the local perturbations caused by the tsunami flooding, local landsliding, or for other reasons.

These interpretations as well as the geomorphic field survey conducted during this thesis were not able to undoubtedly recognize the occurrence of Holocene uplift, but the exclusion of this hypothesis was also not possible to confirm.

8.1.1.3 Coastal Basin Geomorphic Analysis

Several geomorphic indexes were applied to basins that outflow to the Atlantic Ocean, from south of Lisbon towards the eastern south Portuguese coastline. The aim of this study

was to indirectly evaluate changes in the vertical rate of motion between the study area and neighbouring regions. Results suggest that the study area at the southwest Portugal may be uplifting at higher rates than the north section of the western coastline as well as the eastern section of the southern coastline.

Along the western coastline, uplift rates seem to decrease northward from approximately south of Mira River, which corresponds approximately to the location of the Alentejo-Plasensia fault and eventually a northern prolongation of the São Marcos-Quarteira fault (if any). The Alentejo-Plasensia fault does not exhibit a clear evidence for a significant morphotectonic control, although it presents rather subtle evidence of some tectonic control. The eastern Algarve region appears to have a very low uplift rate, and the eastern Algarve region close to Faro may be tilted towards the west, which would be consistent with a tectonic control by the São Marcos Quarteira fault.

It is also inferred that the study area seems to be uplifting as a block because we do not see evidence of regional tilting. All observations suggest that this block seems to be limited inland by the São Marcos Quarteira fault, despite its apparently low level or rate of tectonic activity during the Quaternary. Nonetheless, channel pattern changes were recognized close to the fault, as well as local tilting towards the fault zone as indicated by several drainage basins in eastern Algarve, are supporting evidence of Quaternary activity.

8.1.1.4 Conclusions

The study area corresponds to a section of the southwest Portugal, which seems to be uplifted at higher rates than neighbouring regions in south Portugal, with rates that have not been recognized for other regions. We have found uplift rates of 0.04 ±0.005 mm/a probably since Pliocene to early Pleistocene and a higher rate of 0.09 ± 0.001 mm/a for late Pleistocene that should have initiated during the Pleistocene. This supports evidence for an acceleration of vertical rates for recent times. We were not capable to undoubtedly recognize evidences for Holocene co-seismic deformation; nevertheless we assume that two events might have generated a small amount of uplift.

This regional uplift could be due to several factors, such as faulting or very large wavelength topographic folding due to lithospheric folding. However, since the change on uplift rates seems to be localized we favour that this uplift should be controlled by faulting.

There are no structures inland that are capable to produce the regional uplift signal, nor are there known structures in the offshore that have adequate size or proximity to the coast to be associated with this differential uplift. The closest large active structure known in this region is the Marquês de Pombal thrust, a 70 km long structure located circa 100 km west-southwest of Sagres, and motion on this fault is not likely to have produced vertical motions at the coastline. We therefore speculate on the presence of a roughly N-S trending fault system located parallel to the coastline in the near offshore, whose existence and characteristics are yet to be confirmed. Furthermore, if there was any vertical motion associated with the two historical events, as inferred by the changes in the valley infilling close to Sagres, it is likely to have been generated by a more local, currently unknown source.

We conclude that Southwest Portugal has been uplifting faster than surrounding areas and that an unknown local tectonic source, located along the nearshore may be responsible for the long-term uplift of this region. Based on bathymetric evidence we have estimated the length of this proposed fault as circa 70 km long, meaning that it has the capability to generate earthquakes with moment magnitude greater than Mw 7, ranging from Mw 7.2 to 7.9 and therefore posing an additional seismic hazard for the region.

8.1.2 Plio-Pleistocene Faulting

Several faults with Plio-Pleistocene tectonic activity are present in the study area, but initial field surveys and geomorphologic analyses led to conclude that the structure that exhibits the evidences for a higher tectonic rate as well as a stronger morphotectonic control is the São Teotónio-Aljezur-Sinceira fault system (STASFS). Based upon that interpretation, we have focused on a detailed study of this fault, namely at its central section, the Aljezur-Alfambras tectonic basins, which are the basins that provide not only a longer sedimentary sequence, but also where deformation is most exposed.

The STASFS corresponds to a NNE-SSW 50 km long, strike-slip left lateral fault system parallel to the southwest Portuguese coast and located just some kilometres inland from it. It displaces the wide regional abrasion platform, of Pliocene age which has been partially re-trimmed during the early Pleistocene, into several tectonic basins. These basins are, from the north to the south, the São Miguel basin, which is tectonically controlled by the Baiona fault, the Aljezur basin which is tectonically controlled by the Rogil, Nova Castelãs and Aljezur faults, the Alfambras basin which is in the continuation of Aljezur and is tectonically controlled by the Alfambras fault, and the small Pedralva and Sinceira tectonic basins, both in continuity and controlled by the Sinceira fault.

The fault system was recognized at the S.Miguel basin, along its western border, as the Baiona fault segment where it displaces sands inferred as marine sediments, probably of early Pleistocene age as well as coarse conglomeratic deposits, inferred as alluvium deposits from the “Lower Alluvial fan” unit from the late Pliocene – early Pleistocene (Vilafranquian) (Pereira, 1990; Dias, 2001). Another strand of the fault, with a subtle morphological expression was recognized in the S. Miguel basin, at Portela-Quarteirães trending parallel to the main one and displacing sediments of probable Pliocene to Pleistocene age, which probably corresponds to an active segment of the STASFS, though it was not possible to confirm its prolongation northwards or southwards.

At its northern end, near São Teotónio, the STASFS joins the Alentejo-Placencia fault (APF). In this area the tectonic deformation becomes distributed, suggesting that the APF may have several splays, and it is not clear if APF propagates southward as an active structure. We have recognized a large deformation zone, with igneous lithologies intruded, along a coastal sector south of Zambujeira do Mar, which we have assumed to correspond to the intersection of APF with the coastline. However, no evidence for a significant Plio-Pleistocene deformation was recognized. If any activity exists then it should be mainly as strike-slip, since there is no vertical expression and of low rate. The intersection between the STASFS and the APF, and

their geometrical relationship is thus difficult to scrutinize. Furthermore, no Holocene or late Pleistocene deposits were recognized in association with the identified fault segments, at this area, which increases the uncertainty concerning the recent activity and their relationship during the Plio-Pleistocene. Presently we consider that the STASFS does not extend to the north of the APF, in fact it seems that the APF corresponds to a deformation "barrier", which is also recognized through the instrumental seismicity distribution pattern.

Towards the south, the fault is poorly exposed along the Sinceira and Pedralva tectonic basins. Its presence is locally evidenced by faulted contacts between the Paleozoic bedrock and marine sands, as at the southern end of the Sinceira basin, though the fault outcrop as described by previous studies is not preserved (Cabral, 1995; Dias, 2001). Along Pedralva basin, anomalous contacts and deformed alluvial sediments were also recognized along the fault trace, but it was not clear whether these contacts are due to faulting or to slope failure. At the southern sector of the STASFS, south of the Sinceira basin, the local flat morphology does not evidence any Plio-Pleistocene deformation related to this fault system, suggesting that this segment may be less active. Another hypothesis is that this region could correspond to an area with distributed deformation, since it seems that this fault system may have splayed into several faults that outcrop along the Martinhal – Zavial coastal section, though still lacking evidence of Plio-Pleistocene deformation.

As stated, the fault segments where deformation is most exposed correspond to the fault segments along the Aljezur-Alfambras tectonic basin. For this reason, efforts were made to recognize active fault strands and to estimate Plio-Pleistocene deformation. In a first stage, field surveys and detailed geomorphologic analyses led to the recognition of probable fault segments which were further investigated through geophysical exploration methods, namely geoelectric tomography profiles and trenche excavation for paleoseismology studies. In a second stage it was conducted a morpho-tectonic study through the application of geomorphic indexes complemented with further field surveys. At the same time, a detailed study on marine terraces present along the regional abrasion platform was conducted, in order to provide age control on the abrasion platform that was assumed to be displaced.

Previous studies had already mentioned fault segments evidencing Plio-Pleistocene tectonic activity, such as the Nova Castelãs and Aljezur faults (Pereira, 1990; Cabral, 1995; Dias, 2001). In the scope of this thesis, further fault strands were recognized as having Plio-Pleistocene activity such as the Alfambras-Framangola fault, the northen prolongation of the Aljezur fault, the Rogil fault and other fault strands that are also probably active, but with lower rates such as the fault in the eastern side of the Aljezur basin, which was inferred and later confirmed through geoeletric tomography profiles.

Trenches were excavated for paleoseismology studies at two sites across the Alfambras-Framangola fault, at Barranco da Vaca and Framangola alluvial plain. At Barranco da Vaca, two trenches exposed sediments inset below the regional marine abrasion surface and overlying the Miocene carbonate layers. Samples were collected for OSL dating, which was not possible to accomplish due to the fact that quartz grains had exceeded the capacity to accumulate radiation dose, i.e. the quartz grains were saturated, indicating that the sediments are

probably older than 300 ka. Those sediments were deformed, folded and faulted. The fault zone at this site was characterized by a narrow deformation zone, with several fault splays, where sediments were dragged, difficulting the individualization of seismic events.

We were able to identify vertical deformation through a paleosol displaced about 1.5 m; although we are not certain of the age of this soil, we consider that it is a Pleistocene paleosol, and therefore this displacement provides evidence for Pleistocene activity of the Alfambras-Framangola fault. At the Framangola alluvial plain, the existence of the fault was confirmed by the geoelectric tomography profiles, and later trenches were excavated in order to identify Holocene sediments that might be displaced. We were not able to excavat deep enough due to the high water table, but we found a thick deposit with large blocks and boulders with archaeological pieces from the Arabic occupation (up to XIII century), that was interpreted as possible evidence for an aggradation phase related with strong mass movements likely to be related with the 1755 event and after-shocks.

Further detailed geomorphologic analysis along the Alfambras-Framangola fault led to the identification of a landform characteristic of strike-slip structures, interpreted as a shutter ridge blocking the Alcaria creek. This enabled the first estimation of a horizontal displacement for STASFS.

Assuming the uplift rate estimated for the region for the early Pleistocene, ages for marine terraces at distinct elevations present in the regional abrasion platform in the vicinity of the Aljezur-Alfambras basin were estimated, as well as for the morphological benches within the basin, assuming a close relationship with the eustatic sea-level, due to the close proximity to the Atlantic Ocean. In this way ages were estimated for the marine terraces embedded on the abrasion platform that seem to be displaced as well as for the fluvial terrace located at the top of the shutter-ridge structure blocking the Alcaria creek. Based upon this evidence, we have estimated a horizontal displacement rate of 0.09 mm/a to 0.16 mm/a since the last 1.5 Ma.

Although not all of the geomorphic indexes were adequate to apply along a strike-slip fault, we decided to proceed with the study to evaluate if there was a clear sign of vertical displacement, since the vertical displacement of the abrasion platform corresponds to the more significant morphological expression of the STASFS. Results from the application of the geomorphic indexes are not obvious, since deformation rates for the STASFS are indeed very low and its morphotectonic expression can be masked or even erased by the significant incision that has been taking place during Quaternary, most likely triggered by the ongoing uplift. Nonetheless the cross correlation of the analyses conducted by different approaches supported the identification of fault activity and corroborates that the STASFS has been active during the Plio-Pleistocene.

Vertical displacement for the STASFS was estimated taking in consideration that part of the valleys depth reflects fluvial erosion and therefore it is not exclusively tectonic. Based upon age estimations, geomorphic analysis and fault characterization, we estimate a vertical displacement rate of approximately 0.015 mm/a for the STASFS along the Aljezur-Alfambras

basin since late Pliocene/early Pleistocene and a horizontal displacement rate in the range of 0.09-0.16 mm/a since the last 1.5 Ma.

Calculations of the seismic capability of the STASFS, indicate that:

- A complete rupture of all STASFS length is capable to generate medium to large magnitude earthquakes, with magnitudes ranging from Mw 7.0 to 7.3, with an average displacement per event in the order of 1.20 to 1.48 m and a recurrence period from 10 to 25 thousand years. This also points out that a complete rupture of the STASFS may have not occurred during the Holocene, and since we are not aware of the timing of the last occurred earthquake, we cannot formulate any reasoning about the status of the STASFS seismic cycle;

- A complete rupture of the STASFS along the Aljezur-Alfambras tectonic basin is capable to generate a medium to large earthquake with a moment magnitude for a maximum expectable earthquake close to Mw 7, ranging from 6.7 to 6.9, and an average displacement per event of circa 0.5 m, ranging from 0.53 to 0.63 m. The estimated recurrence period is in the range of 6 to 12.4 ka, meaning that it is possible that the last maximum expectable earthquake has occurred during the Holocene. However we have not found sure evidences for that;
- In case a simultaneous rupture occurs in the Aljezur-Alfambras basin and other tectonic basins along the STASFS, then the moment magnitude and the average displacements increase, but still in the order of Mw 6.0 to 7.1, with average displacements per event lower than 1 m. In this case, the average recurrence ranges from 8 to 18 ka.

In conclusion, the STASFS corresponds to the more significant Plio-Pleistocene active structure in the study area, has a low slip-rate in the order of 0.1 mm/a, with a weak geomorphic expression along the fault trace. In spite of the low slip rate and weak surface expression, it evidences activity during the Pleistocene at the Aljezur-Alfambras basin sector, and likely to be as well for the Baiona fault (São Miguel basin), and it is capable to generate medium to large earthquakes in the range Mw >6 to 7. These moment magnitudes are also consistent with the weak surface expression that has been described for this fault system.

8.2 Future Work

The research conducted in this thesis opened several questions, which should be addressed in the future.

- A major line of research is related with additional detailed characterization of marine terraces, some of which have been already identified in this thesis. It has been recognized an acceleration of the uplift rate during the Pleistocene, but the timing for

this change is not known, neither the mechanism that has triggered this change. It is also not clear whether this change of uplift rate has occurred simultaneously for the whole study region or if it has nucleated in one area and propagated aside. This is a question that only a detailed mapping of marine terraces could access. In this sense further work is needed, especially to constrain the age of the sediments and the age of the erosional surfaces when sediments are not present, to properly assess the time and space variation of short and long-term rates of vertical motion;

- We have inferred the existence of an active fault located in the nearshore, which should be investigated and considered for seismic hazard analysis;

- The difficulty on finding evidences for paleoseismic events reflects the long quiescence period of low rate active faults, and not that these slow faults are inactive. Thus, in order to characterize the detailed behavior of the STASFS, more paleoseismology studies should be conducted, in order to estimate the timing of the last event, the seismic cycle and foresee the likelihood of an occurrence in the near future;

A recent study conducted in the scope of FASTLOAD research project, has investigated static stress variations due to the lithosphere bending in response to the increase of the water column along the continental shelf, and whether they may contribute to facilitate or to condition the rupture of regional active faults and the triggering of earthquakes (Lutrell and Sandwell, 2010; Neves *et al*., 2014; Neves *et al*., submitted).The extent of the ocean loading effect is conditioned not only by the total change of the water column, but also by the velocity of the sea level rising and by the position of the active fault system relatively to coast line. Modelling of static stress variations on the STASFS for the sea rise since the Last Maximum Glacial, is presented in Figure 8.1, where it is clear that east of -8.85^0, there is a positive variation on the Coulomb stress which promotes failure.

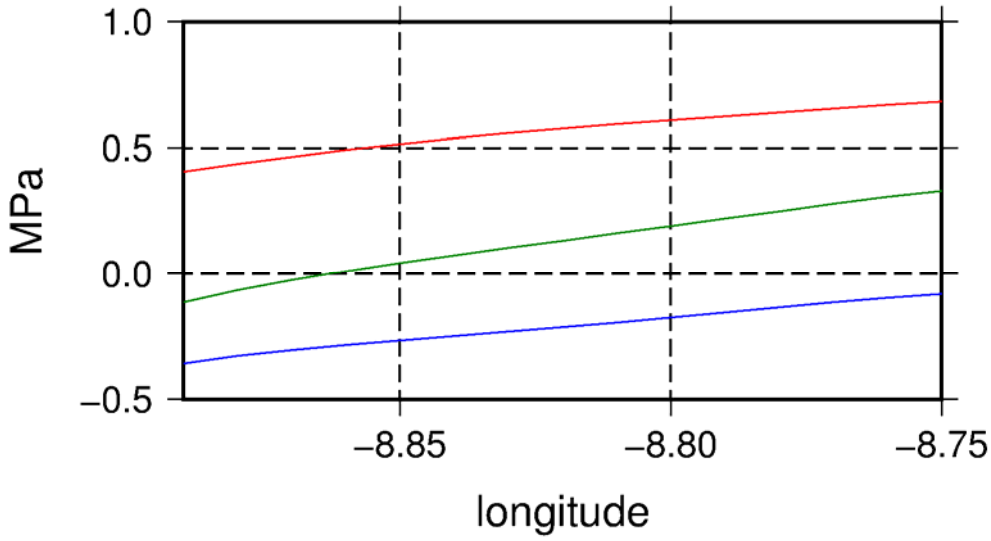

Figure. 8.1 - Normal (red, $\Delta\tau_n$) and Coulomb (green, $\Delta\sigma_c$) stress changes resolved for STASFS (adapted from Neves et al., submitted).

The fault segments of the STASFS that may have been subjected to an increase on the Coulomb stress during periods of sea level rise correspond exactly to the more active segments (Alfambras, Aljezur and possibly Baiona sectors) while the less active correspond to the segments that are located west of meridian -8.85^0 (Sinceira fault and extension south of Sinceira). Since the Pleistocene sea level fluctuations were very large and cyclic, especially since the Middle Pleistocene until the present, this possible stress variation conditioned by the oceanic loading effect, may have played a significant role on the STASFS seismic cycle and even promote a higher slip rate for the Pleistocene. This is a research line that should be pursued in the future, since it has impact in the understanding of the seismic cycle for low slip-rate active faults located along coastlines all around the world.

We emphasize major aspects that should be addressed in the future:

- A fundamental need is a control in absolute ages for the geological and geomorphic markers, which can only be obtained through the application of Geochronology methods. Since the time frame considered is in the range of Ma to ka, distinct dating techniques should be applied, such as the Cosmogenic Radionuclide dating, Optically Stimulated Luminescence, Electron Spin Resonance, Amino Acid Racemization dating and others. One that has proven to be successfully applied in Southwest Portugal, where sediments easily exceed the time range adequate for other methods, is the Cosmogenic Radionuclide dating. Any research line providing a better age control should be pursued.

- Along with the age characterization of sediments and erosional surfaces, there is a fundamental need to conduct a thorough geological mapping for the Pliocene and Pleistocene in Portugal. The lack of a detailed geological cartography conditions the progress of detailed structural geology and geomorphology studies.

- There is a lack of detailed mapping for active faults for the characterization of the regional active or potentially active faults. No sufficient paleoseismic studies have been conducted. This should be pursue through field reconnaissance, as well as through detailed morphotectonic studies based on remote sensing imagery, such as LiDAR, or derived from satellite imagery like SPOT, Pleiades and other satellites.

Ultimately, addressing these aspects would significantly improve the understanding of the Active Tectonics and Neotectonics in Portugal, and provide bases for an adequate seismic hazard knowledge.

References

Abad, M., Rodríguez-Vidal, J., Aboumaria, K., Zaghloul, M.N., Cáceres, L.M., Ruiz, F., Martínez-Aguirre, A., Izquierdo, T. and Chamorro-Moreno, S., 2013. Evidence of MIS 5 sea-level highstands in Gebel Mousa coast (Strait of Gibraltar, North of Africa), Geomorphology, 182, 133-146.

Abe, K., 1979. Size of Great Earthquakes of 1837-1974 inferred from Tsunami Data, Journal of Geophysical Research, 84 (B4), 1561 – 1568.

Andrade, C.F., 1990. O ambiente de barreira da Ria Formosa (Algarve-Portugal), Doctoral Thesis, Lisbon University, 654 p..

Andrade, C., Marques, F., Freitas, M.C., Cardoso, R. and Madureira, P., 2002. Shore platform downwearing and cliff retreat in the Portuguese West Coast, in: Gomes, F.V. et al Littoral 2002 6th International Symposium Proceedings: a multi-disciplinary Symposium on Coastal Zone Research, Management and Planning, 2, 423 – 431.

Azañon, J.M., Pérez-Peña, J.V., Giaconia, F., Booth-Rea, G., Martínez-Martínez, J.M. and Rodríguez-Peces, M.J., 2012. Active tectonics in the central and eastern Betic Cordillera through morphotectonic analysis: the case of Sierra Nevada and Sierra Alhamilla, Journal of Iberian Geology, 38 (1), 225-238.

Baptista, M.A., Miranda, P.M.A., Miranda, J.M. and Mendes Victor, L., 1998. Constraints on the source of the 1755 Lisbon tsunami inferred from numerical modelling of historical data on the source of the 1755 Lisbon tsunami, J. Geodynamics, 25, 159-174.

Baptista, M.A., Miranda, J.M., Lopes, F.C. and Luis, J.F., 2007. The source of the 1722 Algarve Earthquake: evidence from MCS and tsunami data, Journal of Seismology, 11 (4), 371-380.

Baptista, M.A. and Miranda, J.M., 2009. Revision of the Portuguese catalog of tsunamis. Natural Hazards and Earth Systems Sciences, 1, 25- 42.

Barata, M.R.S.T., Braga, L., Noronha Wagner, M., Guerra, B., Félix Alves, J. and Neto, J., 1989. Sismicidade de Portugal. Estudo da documentação dos séculos XVII e XVIII. II - Apêndice documental. GPSN, Lisboa.

Bartolome, R., Gràcia, E., Stich, D., Martínez-Loriente, S., Klaeschen, D., Mancilla, F.L., Iacono, C.I., Dañobeitia, J.J. and Zitellini, N., 2012. Evidence for active strike–slip faulting along the Eurasia–Africa convergence zone: implications for seismic hazards on the SW Iberian Margin. Geology, G33107.1, http://dx.doi.org/10.1130/G33107.1.

Beyer, H.L., 2004. Hawth's Analysis Tools for ArcGIS. Available at http://www.spatialecology.com/htools.

Bezzeghoud, M. and Borges, J.F., 2003. Mecanismos focais dos sismos em Portugal Continental e margem adjacent. Física de la Tierra, Sismicidade de la Península Ibérica, Eds. E. Buforn y U.Dias, 15, 229-245.

Bezzeghoud, M., Adam, C., Buforn, E., Borges, J.F. and Caldeira, B., 2014. Seismicity along the Azores-Gibraltar region and global plate kinematics. J.Seismology, 18(2), 205-220.

Bloom, A.L., Broecker, W.S., Chappel, J.M.A., Mattews, R.K. and Mesolella, K.J., 1974. Quaternary sea-level fluctuations on a tectonic coast: New Th/U dates from the Huon Peninsula, new Guinea, Quaternary Reseacrh, 4, 185-205.

Borges, J.F., Fitas, A.J., Bezzeghoud, M. and Teves-Costa, P., 2001. Seismotectonics of Portugal and its adjacent Atlantic area, Tectonophysics, 337, 373-387.

Bradley, W. C. and Griggs, G.B., 1976. Form, genesis, and deformation of central California wave-cut platforms: Geol. Soc. of Am. Bull., 87, 433-449.

Brandão, F., 1672. Sexta Parte da Monarquia Lusitana contém a história dos ultimos 23 anos de el rei D. Dinis, Livros XVIII e XIX, edição João da Costa.

Brito, B., 1597. Monarchia Lusytana, Parte primeira que contém as historias de Portugal, desde a criação do mundo até o nascimento de nosso senhor Jesu Christo. Re-edition Craesbeeckiana Press (1690).

Bull, W.B., 1977. Tectonic geomorphology of the Mojave Desert: US. Geological Survey Contract Report 14-08-001-G-394, Office of Earthquakes, Volcanoes, and Engineering, Menlo Park, California, 188 p..

Bull, W.B., 1978. Geomorphic tectonic activity classes of the south front of the San Gabriel Mountains, California: U. S. geological Survey Contract Report 14 -08-001-G-394, Office of Earthquakes, Volcanoes, and Engineering, Menlo Park, California, 59 p..

Bull, W.B., 2007. Tectonic Geomorphology of Mountains: A New Approach to Paleoseismology. Wiley-Blackwell, Oxford, 316 p..

Bull, W.B., 2009.Tectonically Active Landscapes, Wiley-Blackwell, 326 p..

Bull, W.B. and McFadden, L., 1977. Tectonic geomorphology north and south of the Garlock fault, California. In: Dohering, D.O. (Ed.), Geomorphology in Arid Regions. Publ. In Geomorphology. State University of New York, Binghamton, 115–138.

Burbank, D.W. and Anderson, R.S., 2001. Tectonic Geomorphology. Blackwell Science, Oxford.

Cabral, J., 1995. Neotectónica em Portugal Continental, Mem. Nº31, Inst.Geol.Min., 265 p..

Carrilho, F., Teves-Costa, P., Morais, I., Pagarete, J. and Dias, R., 2004. GEOALGAR Project: first results on seismicity and fault-plane solutions, Pure appl. Geophys., 161, 589–606.

Cardoso, M.T., 1997. Estudo do Manuscrito Anónimo do Séc. XVIII: Descrição da Cidade de Lagos. Amadora: Livro Aberto, Editores Livreiros Lda, 72 p..

Carrilho, F., 2005. Estudo da Sismicidade do Sudoeste de Portugal Continental, Master Dissertation, Physics Department, Lisbon University, 172 p..

Chen, Y.C., Sung, Q.C. and Cheng, K.Y., 2003. Along-strike variations of morphotectonic features in the Western Foothills of Taiwan: tectonic implications based on stream-gradient and hypsometric analysis, Geomorphology, 56, 109-137.

Clarka, P.U., Archerb, D., Pollardc, D., Blumd, J.D., Riale, J.A., Brovkinf, V., Mixg, A.C., Pisiasg, N.G. and Royh, M., 2006. The middle Pleistocene transition: characteristics, mechanisms, and implications for long-term changes in atmospheric pCO2 Quaternary Science Reviews 25, 3150–3184.

Costa, M., Silva, R. and Vitorino, J., 2001. Contribuição para o Estudo do Clima de Agitação Marítima na Costa Portuguesa. Instituto Hidrográfico, Lisboa.

Cox, R.T., 1994. Analysis of drainage-basins symmetry as rapid technique to identify areas of possible Quaternary tilt-block tectonics: an example from Mississippi Embayment. Geological Society of America Bulletin, 106, 571–581.

Cunha, T.M., Matias,L.M., Terrinha, P., Negredo, A.M., Rosas, F., Fernandes, R.M.S. and Pinheiro, L.M., 2012. Neotectonics of the SW Iberia margin, Gulf of Cadiz and Alboran Sea: a reassessment including recent structural, seismic and geodetic data, Geoph. J. Int.l, 188 (3), 850-872, doi: 10.1111/j.1365-246X.2011.05328.x.

Custódio, S., Cesca S. and Heimann, S., 2012. Fast Kinematic Waveform Inversion and Robustness Analysis: Application to the 2007 Mw 5.9 Horseshoe Abyssal Plain Earthquake Offshore Southwest Iberia, Bull. of the Seism. Soc. of Am., 102(1), 361–376, doi: 10.1785/0120110125.

Dabrio, C.J., Zazo, C., Cabero, A., Goy, J.L., Bardají, T., Hillaire-Marcel, C., González- Delgado, J.A., Lario, J., Silva,P.G., Borja, F. and García-Blázquez, A.M., 2011. Millennial/ submillennial-scale sea-level fluctuations in western Mediterranean during the second highstand of MIS 5e. Quaternary Science Reviews, 30, 335-346.

Davis, W.M., 1899. The Geographical Cycle. The Geographical Journal, 14(5), 481-504.

DeMets, C., Gordon, R.G., Argus, D.F. and Stein, S., 1994. Effect of recent revisions to the geomagnetic reversal time scale on estimates of current plate motions Geoph. Res. Lett., 21 (20), 2191, doi:10.1029/94GL02118.

DeMets, C., Gordon, R. and Argus, D., 2010. Geologically current plate motions, Geophys. J. Int., 181, 1-80, doi: 10.1111/j.1365-246X.2009.04491.x.

Desprat, S., Sánchez Goñi, M.F., Naughton, F., Turon, J.-L., Duprat, J., Malaizé, B., Cortijo, E., and Peypouquet, J.-P., 2007. Climate variability of the last five isotopic interglacials: Direct

land-sea-ice correlation from the multiproxy analysis of north-western Iberian Margin deep-sea cores, in The Climate of Past Interglacials, edited by F. Sirocko et al., 375–386, Elsevier, Amsterdam.

Dias, R., 2001. Neotectónica da Região do Algarve, Doctoral Dissertation, Lisbon University, 369 p..

Dias, R.P. and Cabral, J., 2002. Interpretation of recent structures in an area of cryptokarst evolution - neotectonic versus subsidence genesis. Geodinamica Acta, 15 (4), 233-248.

Dias, R.P. and Cabral, J., 2002. Neotectonic activity of the Algarve region (S of Portugal), Comun. Inst. Geol. e Mineiro, t.89, 193-208.

Duarte, J.C., Rosas, F.M., Terrinha, P., Gutscher, M.-A., Malavieille, J., Silva, S. and Matias, L., 2011. Thrust–wrench interference tectonics in the Gulf of Cadiz (Africa–Iberia plate boundary in the north-east Atlantic): insights from analog models. Marine Geology, 289, 135–149. doi:10.1016/j.margeo.2011.09.014.

Duarte, J., Rosas, F., Terrinha, P., Schellart, W., Boutelier, D., Gutscher, M.-A. and Ribeiro, A., 2013. Are subduction zones invading the Atlantic? Evidence from the southwest Iberia margin. Geology, 41, 839-842. doi:10.1130/G34100.1.

Dutton, A. and Lambeck, K., 2012. Ice Volume and sea level during the last interglacial, Science, 337, 216-219, doi: 10.1126/science.1205749.

Feio, M., 1949. O litoral ao largo do cabo São Vicente, Notas geomorfológicas, IV.Separatado Bolhetim da Sociedade Geológica de Portugal, VIII, 22 p..

Feio, M., 1951. A evolução do relevo do Baixo Alentejo e Algarve. Com. Serv. Geol. Portugal, t. XXXII, 2nd section, 303 – 447.

Fernandes, R.M.S., Miranda, J.M., Meijninger, B.M.L., Bos, M.S., Bastos, L., Ambrosius, B.A.C. and Riva, R.E.M., 2007. Surface velocity field of the Ibero-Maghrebian segment of the Eurasia–Nubia plate boundary. Geoph. J. Int., 169 (1), 315–324.

Figueiredo, P.M., Cabral, J. and Rockwell, T.K., 2010 - Neotectonics and paleoseismic studies at SW Portugal mainland: The S. Teotónio – Aljezur – Sinceira Fault System, VIII Portuguese Geology Congress, Geosciences On-line Journal, 11 (8), ISSN 1645-0388.

Figueiredo, P.M., Cabral, J. and Rockwell, T., 2010. Southwest Portugal Plio-Pleistocene tectonic activity studies: the S.Teotónio-Aljezur-Sinceira fault system and coastal tectonic uplift evidences. In: J. M. Insua and F. Martín González (eds.), Contribución de la Geología al Análisis de la Peligrosidad Sísmica, Livro de Resumos da 1ª Reunião Ibérica sobre Falhas Activas e Paleossismologia, Sigüenza, 49-52.

Figueiredo, P.M., Cabral, J. and Rockwell, T. K., 2011. Plio- PLeistocene Tectonic Activity in the Southwest of Portugal. In: C. Grützner, R. Pérez-López, T. Fernández-Steeger, I. Papanikolaou, K. Reicherter, P.G. Silva and A. Vött (eds.), 2nd INQUA-IGCP 567

International Workshop Proccedings, Earthquake Geology and Archaeology: Science, Society and Critical facilities, 2, 30-33.

Figueiredo, P.M., Cabral, J. and Rockwell, T.K., 2013. Recognition of Pleistocene marine terraces in the Southwest of Portugal (Iberian Peninsula): Evidences of regional Quaternary uplift. Annals of Geophysics, 56 (6), Special Issue Earthquake Geology, S0672, doi:10.4401/ag-6276.

Figueiredo, P.M., Rockwell, T. K., Cabral, J., Cunha, P. and Rood, D., in prep. The Plio-pleistocene regional abrasion platform in the Southwest of Portugal (Iberian peninsula as evidence for regional uplift).

Freitas, M.C. and Andrade, C., 2005. Global vs Local Forcing Factors and Paleoenvironmental Changes of Estuaries and Lagoons of SW Portugal Since the Late Glacial. In: Freitas, M.C. & Drago, T. (eds), Proceedings, Iberian Coastal Holocene Paleoenvironmental evolution, Coastal Hope 2005, Lisbon, 64-70.

Fukao, Y., 1973. Thrust faulting at a lithospheric plate boundary: the Portugal earthquake of 1969, Earth Planet. Sci. Lett., 18, 205-216.

GEBCO Digital Atlas, 2003. Centenary Edition of the GEBCO Digital Atlas, published on CD-ROM on behalf of the Intergovernmental Oceanographic Commission and the International Hydrographic Organization as part of the General Bathymetric Chart of the Oceans, British Oceanographic Data Centre, Liverpool, U.K.

Geissler, W.H., Matias, L., Stich, F., Carrilho, F., Jokat, W., Monna, S., IbenBrahim, A., Mancilla, F., Gutscher, M.-A., Sallarès, V. and Zitellini, N., 2010. Focal mechanisms for sub-crustal earthquakes in the Gulf of Cadiz from a dense OBS deployment. Geoph. Res. Lett., 37, L18309.

Giaconia, F., Booth-Rea, G., Martínez-Martínez, J.M., Azañón, J.M., Pérez-Peña, J.V., Pérez-Romero, J. and Villegas, I., 2012. Geomorphic evidence of active tectonics in the Sierra Alhamilla (eastern Betics, SE Spain), Geomorphology, 145-146, 90-106, doi:10.10 16/j.geomorph.2011.12.043.

Gràcia, E., Dañobeitia, J., Vergés, J. and Bartolomé, R., 2003a. Crustal architecture and tectonic evolution of the Gulf of Cadiz (SW Iberian margin) at the convergence of the Eurasian and African plates. Tectonics, 22 (4), 1033–1052.

Gràcia, E., Dañobeitia, J., Vergés, J. and Team, P., 2003b. Mapping active faults offshore Portugal (36 degrees N–38 degrees N): implications for seismic hazard assessment along the southwest Iberian margin. Geology, 31 (1), 83–86.

Gràcia, E., Vizcaino, A., Escutia, C., Asioli, A., Rodés, A. Pallàs, R., Garcia-Orellana, J., Lebreiro, S. and Goldfinger, C., 2010. Holocene earthquake record offshore Portugal (SW Iberia): testing turbidite paleoseismology in a slow-convergence margin. Quat. Sc. Rev. 29, 1156–1172.

Gürbüz, A., 2010. Geometric characteristics of pull-apart basins, Lithosphere, 2, 199-206.

Gutscher, M.A., Dominguez, S., Westbrook, G.K., Le Roy, P., Rosas, F., Duarte, J.C., Terrinha, P., Miranda, J.M., Graindorge, D., Gailler, A., Sallares, V. and Bartolomé, R., 2012. The Gibraltar subduction: A decade of new geophysical data. Tectonophysics, 574-575, 72-91. doi.org/10.1016/j.tecto.2012.08.038.

Hack, J.T., 1973. Stream-profile analysis and stream-gradient index. U.S. Geological Survey Journal of Research, 1, 421–429.

Hack, J.T., 1982. Physiographic divisions and differential uplift in the piedmont and Blue Ridge: U.S. Geological Survey Professional Paper 1265, 49 p..

Hanks, T. C. and Kanamori, H., 1979. A Moment Scale Magnitude, J. of Geophysical Research, Solid Earth, 84(B5), 2348-2350.

Hanks, T.C. and Bakun, W.H., 2008. M-log A observations of recent large earthquakes, Bull. Seimol. Soc. Am, 94 (3), 490-494.

Hanson, K. L., Wesling, W. R., Lettis, W. R., Kelson, K. I. and Mezger, L., 1994. Correlation, ages, and uplift rates of Quaternary marine terraces, south-central California, in Alterman, I.B., McMullen, R.B., Cluff, L.S., and Slemmons, D.B. (eds.), Seismotectonics of the Central California Coast Ranges: Geol. Soc. of Am. Sp. Paper, 292, 45-72.

Hare, P.W. and Gardner, T.W., 1985. Geomorphic indicators of vertical neotectonism along converging plate margins, Nicoya Peninsula, Costa Rica. In: Morisawa, M., Hack, J.T. (Eds.), Tectonic Geomorphology. Proceedings of the 15th Annual Binghamton Geomorphology Symposium. Allen and Unwin, Boston, MA, 123–134.

Harlin, J., 1978. Statistical moments of the hypsometric curve and its density function. Mathematical Geology, 10(1), 59-72.

Hearty, P., Hollin, J., Neumann, A.C., O'Leary, M. and McCulloch, M., 2007. Global sea-level fluctuations during the Last Interglaciation (MIS 5e), Quat. Sc. Rev., 26 (17-18), 2090 – 2112.

Hindson, R., Andrade, C. and Parish R., 1999. A microfaunal and sedimentary record of environmental change within the late Holocene sediments of Boca do Rio (Algarve, Portugal). Geologie en Mijnbouw, 77, 311-321.

Iberian Climate Atlas, 2011. Compiled and produced by State Meteorological Agency of Spain and by the Institute of Meteorology, Portugal. ISBN: 978-84-7837-079-5, 80 p..

I.G.E.O.E. - Instituto Geográfico do Exército, Carta Militar de Portugal, série M888, .1 : 25 000 scale.

I.H. - Instituto Hidrográfico, Divisão de Oceanografia, Portugal Batimetry.

Johnston, A., 1996. Seismic moment assessment of earthquakes in stable continental regions – III. New Madrid 1811-1812, Charleston 1886 and Lisbon 1755," Geophys. J. Int., 126, 314 - 344.

Keller, E. A. and Rockwell, T.K., 1984. Tectonic geomorphology, Quaternary chronology, and paleoseismicity. In Costa, J. E. and Fleisher, P. J. (eds.) Developments and Applications of Geomorphology. Springer-Verlag, New York, 203-239.

Keller, E. A. and Pinter, N., 1996. Active tectonics: earthquake, uplift, and landscape. Prentice Hall, New Jersey, 338 p..

Kern, J.P. and Rockwell, T.K., 1992. Chronology and deformation of Quaternary marine shorelines, San Diego County, California: in Quaternary Coasts of the United States: Marine and Lacustrine Systems: Society of Economic Paleotologists and Mineralogists Special Publication, 48, 377-382.

Kopp, R.E., Simons, F.J., Mitrovica, J.X., Maloof, A.C., and Oppenheimer, M., 2009. Probabilistic assessment of sea level during the last interglacial stage. Nature, 462, 863-868.

Kortekaas, S. and Dawson, A.G., 2007.Distinguish tsunami and storm deposits: An example from Martinhal, SW Portugal, Sedimentary Geology, 200, 208-221.

Laughton, A.S., Whitmarsh, R.B., Rusby, J.S.M., Somers, M.L., Revie, J., McCartney, B.S. and Nafe, J.E., 1972. A continuous East-West fault on the Azores-Gibraltar ridge. Nature, 237, 217–220.

Lopes, F., 2002. Análise tectono-sedimentar do Cenozoico da margem Algarvia. Doctoral Dissertation, Coimbra University.

Lopes, F.C., Cunha, P.P. and Le Gall, B., 2006. Cenozoic seismic stratigraphy and tectonic evolution of the Algarve margin (offshore Portugal, southwestern Iberian Peninsula), Marine Geology, 231, 1-36.

Lopes, J.B.S., 1842. Corografia ou Memória Económica, Estatística e Topográfica do Reino do Algarve, 528 p..

Luo, W., 2000. Quantifying groundwater sapping landforms with a hypsometric technique. J. Geophys. Res., 105(E1), 1685-1694.

Manuppella, G. (Coordination), 1992. Carta Geológica da Região do Algarve, 1/100 000 scale., Serviços Geológicos de Portugal.

Marques, F.M.S.F., 1997. As arribas do Litoral do Algarve Dinâmica - processos e mecanismos. Doctoral Dissertation, Lisbon University, 560 p..

Martínez-Loriente, S., Gràcia, E., Bartolomé, R., Sallarés, V., Connors, C., Perea, H., Iacono, C., Klaeschen, D., Terrinha, P., Dañobeitia, J. and Zitellini, N., 2013. Active deformation in old oceanic lithosphere and significance for earthquake hazard: Seismic imaging of the Coral

Patch Ridge area and neighboring abyssal plains (SW Iberian Margin). Geochem. Geophys. Geosyst., 14, doi:10.1002/ggge.20173.

Martinez Solares, J. and Lopez Arroyo A., 2004. The great historical 1755 earthquake, effects and damage in Spain, J. Seism., 8, 275-294.

Martins, J., 2014. A Plataforma Continental Algarvia como arquivo de Paleoambientes e Paleoclimas Holocénicos. O papel do ^{14}C no seu estudo. Doctoral Thesis, Algarve University, 278 p..

McCalpin, J., Rockwell, T.K. and Weldon II, R.J., 2009. Paleoseismology of strike-slip environments, 421-496 in Paleoseismology, 2nd edition, International Geophysics Series, Volume 95, Elsevier Publishing, 647 p..

Merritts, D.J. and Vincent, K.R., 1989. Geomorphic response of coastal streams to low, intermediate, and high rates of uplift, Mendocino triple junction region, northern California. Geological Society of America Bulletin, 101, 1373–1388.

Merritts, D.J., Vincent, K.R. and Wohl, E.E., 1994. Long river profiles, tectonism, and eustasy: a guide to interpreting fluvial terraces. Journal of Geophysical Research, 99, 14,031–14,050.

Miller, K.G., Mountain, G.S., Wright, J.D., and Browning, J.V., 2011. A 180-million-year record of sea level and ice volume variations from continental margin and deep-sea isotopic records.Oceanography, 24(2), 40–53, doi:10.5670/oceanog.2011.26.

Miller, K.G., Wright, J.M., Browning, J.V., Kulpecz, A., Michelle, M., Naish, T.R., Cramer, B.S., Rosenthal, Y., Peltier, W.R. and Sosdian, S., 2012. High tide of the warm Pliocene: Implications of global sea level for Antarctic deglaciation, Geology, 40 (5), 407–410, doi:10.1130/G32869.1.

Moniz, C., 1992. Análise de Fracturação. Exemplos de Aplicação nas Dunas Consolidadas de Oitavos e Praia da Aguda. Master thesis, Lisbon University, 172 p..

Moreira de Mendonça, J.M., 1758. História Universal dos Terremotos, Lisboa.

Morisawa, M., 1957. Accuracy of determination of stream lengths from topography maps American Geophysical Union Transactions, 38, 86-88.

Moura, D., 1998. Estratigrafia do Quaternário da Orla Costeira do Médio Algarve, Dissertation thesis, Algarve University.

Muhs, D.R., Kennedy, G.L. and Rockwell, T.K., 1994. Uranium-series Ages of Marine terrace Corals from the Pacific of North America and Implications for Last- Interglacial Sea Level History, Quaternary Research, 42, 72-87.

Muhs, D.R., Simmons, K.R. and Steinke, B., 2002a. Timing and warmth of the last interglacial period: New U-series evidence from Hawaii and Bermuda and a new fossil compilation for North America. Quat. Sc. Rev. (21), 1355-1383.

Muhs, D.R., Simmons, K.R., Kennedy, G.L. and Rockwell, T.K., 2002b. The last interglacial period on the Pacific Coast of North America: Timing and paleoclimate: Geol. Soc. of Am. Bull., 114, 569-592.

Muhs, D.R., Simmons, K.R., Schumann, R.R. and Halley, R.B., 2011. Sea-level history of the past two interglacial periods: new evidence from U-series dating of reef corals from south Florida, Quaternary Science Reviews, 30, 570-590.

Neves, M.C., Cabral, J., Figueiredo, P.M., Neves, R., Sandwell., D., Rockwell, T. and Lutrell , K., 2014. Stress changes in Iberia induced by eustatic sea-level rise, 2nd Iberfault Abstract book, 209-212.

Neves, M.C., Cabral, J., Lutrell, K., Figueiredo, P.M., Rockwell, T. Sandwell., D., (submitted). The effect of sea level changes on fault reactivation potential in Portugal. (submitted to Tectonophysics).

Nocquet, J. M. and Calais, E., 2004. Geodetic measurements of crustal deformation in the Western Mediterranean and Europe, Pure Appl. Geophys., 161, 661–681.

Oliveira, C.S., Monteiro, F. and Pereira, J., 1986. A sismicidade Histórica e a revisão do catálogo Sísmico, Proc. 36/11/7368 I & D Estruturas, Relatório 99/86, Núcelo de Dinâmica Aplicada, Laboratório Nacional de Engenharia Civil, 192 p..

Ouchi S., 1985. Response of alluvial rivers to slow active tectonic movement. *Geological* Society of America Bulletin, 96, 504–515.

Pais, J., Legoinha, P., Elderfield, H., Sousa, L. and Estevens, M., 2000. The Neogene of Algarve (Portugal). Ciências da Terra, 14, 277-288.

Pais, J., Cunha, P.P., Pereira, D., Legoinha, P., Dias, R., Moura, D., Silveira, A.B., Kullberg, J.C. and González-Delgado, J.A., 2012. The Paleogene and Neogene of Western Iberia (Portugal).in A Cenozoic record in the European Atlantic domain, Springer-Verlag Berlin Heidelberg Edition, 158 p..

Pedoja, K., Husson, L., Regard, V., Cobbold, P.R., Ostanciaux, E., Johnson, M.E., Kershaw, S., Saillard, M., Martinod, J., Furgerot, L., Weill, P. and Delcaillau, B, 2011. Relative sea-level fall since the last interglacial stage: Are coasts uplifting worldwide?, Earth Sc.Rev., 108 (1-2), 1-15.

Pedrera, A., Pérez-Peña, J.V., Galindo-Zaldívar, J., Azañón, J.M. and Azor, A., 2009. Testing the sensitivity of geomorphic indices in areas of low-rate active folding (eastern Betic Cordillera, Spain). Geomorphology, 105, 218–231.

Pereira, A.R., 1990. A plataforma Litoral do Alentejo e Algarve Ocidental. Estudo de geomorfologia. Doctoral Dissertation, Lisbon University 450 p..

Pereira, A.R. and Angelucci, D., 2004. Formações dunares no litoral português, do final do Plistocénico e inícios do Holocénico, como indicadores paleoclimáticos e

paleogeográficos, in Evolução geohistórica do litoral português e fenómenos correlativos. Geologia, História, Arqueologia e Climatologia, Universidade Aberta, 221-256.

Pereira, R. and Alves, T., 2011. Post-rift compression on the SW Iberian Margin (eastern North Atlantic): a case for prolonged inversion in the ocean-continent transition zone. Journal of the Geological Society, 168, 1249-1263.

Pereira, R. and Alves, T., 2013. Crustal deformation and submarine canyon incision in a Meso-Cenozoic first-order transfer zone (SW Iberia, North Atlantic Ocean). Tectonophysics, 601, 148-162.

Pérez-Peña, J.V., Azañón, J.M. and Azor, A., 2009a. CalHypso: an ArcGIS extension to calculate hypsometric curves and their statistical moments. Applications to drainage basin analysis in SE Spain. Computers & Geosiences, 35, 1214–1223.

Pérez-Peña, J.V., Azanon, J.M., Azor, A., Delgado, J. and Gonzalez-Lodeiro, F., 2009b. Spatial analysis of stream power using GIS: SLk anomaly maps. Earth Surface Processes and Landforms, 34(1), 16-25.

Perez-Peña, J.V., Azor, A., Azañon, J.M. and Keller, E.A., 2010. Active tectonics in the Sierra Nevada (Betic Cordillera, SE Spain): insights from geomorphic indexes and drainage pattern analysis. Geomorphology, 119, 74–87.

Pike, R.J. and Wilson, S.E., 1971. Elevation-Relief ratio, Hypsometric Integral, and Geomorphic Area-Altitude analysis, Geological Society of America Bulletin, 82, 1079–1084.

Pimentel, N., 1997. O Terciário da Bacia do Sado, sedimentologia e análise tectono-sedimentar. Doctoral thesis, doutoramento, Univ. Lisboa, 383 p..

Pimentel, N. and Amaro, H., 2000. Contribuição para a análise tectono-sedimentar do Fosso de Aljezur (SW de Portugal), Ciências da Terra, 14, 233-242.

Pro, C., Buforn, E., Bezzeghoud, M. and Udias, A., 2013. The earthquakes of 29 July 2003, 12 February 2007 and 17 December 2009 in the region of Cape Saint Vicent (SW Iberia) and their relation with the 1755 Lisbon earthquake, Tectonophysics, 583, 16-27.

Prudêncio, M.I., Marques, R., Rebelo, L., Cook, G.T., Cardoso, G.O., Naysmith, P., Freeman, S.P.H.T., Franco, D., Brito, P. and Dias M.I., 2007. Radiocarbon and Blue Optically Stimulated Luminescence chronologies of the Oitavos Consolidated Dune (Western Portugal), Radiocarbon, 49 (2), 1145-1151.

Ramírez-Herrera, M.T., 1998. Geomorphic assessment of active tectonics in the Acambay Graben": Earth Surface Processes and Landforms. 23, 317–332.

Regnauld, H., Fournier J. and Pereira A.R., 1995. Approche quantitative de la discontinuité de l'évolution de formes littorales à différentes échelles de temps. Exemple du recul de la côte de l'Arrábida (Portugal)/Quantitative approach of a non linear and scale dependand

landform evolution : rate of a retreat coastline in Portugal, Arrábida. In: Géomorphologie : relief, processus, environnement., 1 (1), 7-27.

Ribeiro, A., 2002. Soft Plate and Impact Tectonics , Springer, 324 p. ISBN-3540679634.

Ribeiro, A., Cabral, J., Baptista, R. and Matias, L., 1996. Stress pattern in Portugal mainland and the adjacent Atlantic region, West Iberia. Tectonics, 15 (2), 641–659.

Ribeiro, A., Mendes-Victor, L., Cabral, J., Matias, L. and Terrinha, P., 2006. The 1755 Lisbon earthquake and the beginning of closure of the Atlantic. European Review, 14 (2), 193-205. doi: 1O.1017/SI062798706000196, Cambridge University Press.

Rockwell, T.K., Keller, E.A. and Johnson, D.L., 1985. Tectonic geomorphology of alluvial fans and mountain fronts near Ventura, California. In: Morisawa, M., Hack, J.T. (Eds.), Binghampton Symposia in Geomorphology International Series, NY: Tectonic geomorphology, 183–207.

Rockwell, T.K., Muhs, D.R., Kennedy, G.L., Wilson, S., Hatch, M.E. and Klinger, R., 1989. Uranium-series ages, faunal correlations and tectonic deformation of marine terraces within the Agua Blanca fault zone at Punta Banda, northern Baja California, Mexico: in P.L. Abbott (ed.), Geologic Studies in Baja California, Soc. Econ. Paleon. and Min. Book, 63, 1-16.

Rockwell, T., Vaughan, P., Bickner, F. and Hanson, K.L., 1994. Correlation and age estimates of soils developed in marine terraces across the San Simeon fault zone, central California: in Alterman, I.B., McMullen, R.B., Cluff, L.S., and Slemmons, D.B., eds., Seismotectonics of the central California Coast Ranges, Boulder, CO, Geological Society of America Special Paper, 292, 151-166.

Rodriguez, G.J., 1932. Catalogo sísmico de la zona compreendida entre los meridianos 5^{o}E y 20^{o}W, de Greenwhich y los paralelos 45 y 25^{o}N. Tomo I, Direcion General del Instituto Geográfico, Catastral y de Estatistica, Madrid.

Rodriguez, G.J., 1940. Catalogo sísmico de la zona compreendida entre los meridianos 5^{o}E y 20^{o}W, de Greenwhich y los paralelos 45 y 25^{o}N. Tomo II, Instituto Geográfico y Catastral, Madrid.

Roque, C., 2007. Tectonostratigrafia do Cenozóico das margens continentais Sul e Sudoeste portuguesas: um modelo de correlação sismostratigráfica, Doctoral Dissertation, Lisbon University.

Rosas, F.M., Duarte, J.C., Neves, M.C., Terrinha, P., Silva, S., Matias, L., Grácia, E. and Bartolomé, R., 2012. Thrust–wrench interference between major active faults in the Gulf of Cadiz (Africa–Eurasia plate boundary, offshore SW Iberia): Tectonic implications from coupled analog and numerical modeling, Tectonophysics, doi:10.1016/j.tecto.2012.04.013.

Sartori, R., Torelli, L., Zittelini, N., Peis, D. and Lodolo, E., 1994. Eastern segment of the Azores-Gibraltar line (Central- Eastern Atlantic): an oceanic plate boundary with diffuse compressional deformation, Geology, 22, 555-558.

Schumm, S.A., 1963. Sinuosity of Alluvial Rivers on the Great Plains, Geol. Soc. Am. Bull., 74 (9), pp. 1089-1100.

Schumm, S.A., Dumont, J.F. and Holbrook, J.M., 2000. Active Tectonics and Alluvial Rivers, Cambridge University Press, 276 p..

Senos, M.L. and Carrilho, F., 2003. Sismicidade de Portugal Continental, Física de la Tierra, 15, 93-110.

Serpelloni, E., Vannucci, G., Pondrelli, S., Argnani, A., Casula, G., Anzidei, M., Baldi, P. and Gasperini, P., 2007. Kinematics of the Western Africa-Eurasia plate boundary from focal mechanisms and GPS data. Geoph. J. Int., 169(3), 1180-1200.

Shackleton, N. and Opdyke, N., 1973. Oxygen isotope and palaeomagnetic stratigraphy of equatorial Pacific core V28-238: oxygen isotope temperatures and ice volumes on a 10^5 and 10^6 year scale. Quaternary Research, 3, 39 – 55.

Siddall, M., Chappell, J. and Potter, E.-K., 2006. Eustatic Sea Level During Past Interglacials, in "the climate of past interglacials", Sirocko F., Litt M., Claussen, M., Sanchez-Goni, F. (eds) Elsevier, Amsterdam.

Silva, P.G., Goy, J.L., Zazo, C. and Bardajm, T., 2003. Fault generated mountain fronts in Southeast Spain: geomorphologic assessment of tectonic and earthquake activity. Gemorphology 250, 203-226.

Silva, L.F., 2007. Balsa, Cidade Perdida: a capital do Algarve Oriental na Época Romana. Tavira: Campo Arqueológico de Tavira, Câmara Municipal de Tavira, ISBN: 978-972-97648-9-9.

Silva, S., Romsdorf, M., Matias, L., Geissler, W. H., Terrinha, P., Carrilho, F. and Nearest Working Group, 2010. Characterization of the seismicity in the Gulf of Cadiz based on eleven month monitoring by the NEAREST OBS network., Geoph. Res. Abstr.12, EGU2010-11554.

Snyder, N.P., Whipple, K.X., Tucker, G.E. and Merritts, D.J., 2003. Channel response to tectonic forcing: field analysis of stream morphology and hydrology in the Mendocino triple junction region, northern California. Geomorphology, 53, 97–127.

Soares, A.M.M., Moniz, C. and Cabral, J., 2006. The consolidated Dune of Oitavos (West of Cascais–Lisbon Region) – its dating by the Radiocarbon Method, Comunicações Geológicas, 13, 105-118.

Speed, R.C. and Cheng, H., 2004. Evolution of marine terraces and sea level in the last interglacial, Cave Hill, Barbados, Geological Society of America Bulletin, 116 (1-2), 219-232.

Stich, D., Serpelloni, E., Mancilla, F.L. and Morales, J., 2006. Kinematics of the Iberia–Maghreb plate contact from seismic moment tensors and GPS observations, Tectonophysics, 426, 295–317.

Stich, D., Martin, R. and. Morales J., 2010. Moment tensor inversion for Iberia-Maghreb earthquakes 2005–2008, Tectonophysics, 483, 390–398, doi:10.1016/j.tecto.2009.11.006.

Stirling, M.W., Gerstenberger, M.C., Litchfield, L., McVerry, G.H., Smith, W.D., Petting, J. and Barnes, P., 2008. Seismic hazard of the Canterbury region, New Zealand: New earthquake source model and methodology, Bull.New Zeal.Soc. Earthq. Eng., 41, 51-67.

Stirling, M., Goded, T., Berryman, K. and Litchfield, N., 2013. Selection of Earthquake Scaling Relationship for Seismic-Hazard Analysis, Bull. Seism. Soc. Am., 103 (6), 2993-3011.

Strahler, A.N., 1952. Hypsometric (area-altitude) analysis of erosional topography. Geological Society of America Bulletin, 63, 1117–1142.

Strahler A.N., 1964. Quantitative geomorphology of drainage basin and channel network, pp.39-76, In: VT Chow (ed), Handbook of applied hydrology, McGraw Hill, New York.

Strahler, A.N., 1958. Dimensional analysis applied to fluvially eroded landforms, Geological Society of America Bulletin, 69, 279-299.

Sylvester, A.G., 1988. Strike-slip faults. Geological Society of America Bulletin, 100, 1666–1703.

Terrinha, P., 1998. Structural Geology and Tectonic Evolution of the Algarve Basin, South Portugal. Department of Geology, University of London, London.

Terrinha, P., Pinheiro, L.M., Henriet, J.-P., Matias, L., Ivanov, M.K., Monteiro, J.H., Akhmetzhanov, A., Volkonskaya, A., Cunha, T., Shaskin, P. and Rovere, M., 2003. Tsunamigenic-seismogenic structures, neotectonics, sedimentary processes and slope instability on the southwest Portuguese Margin, Marine Geology, 195, 55-73.

Terrinha, P., Matias, L., Vicente, J., Duarte, J., Luis, J., Pinheiro, L., Lourenço, N., Diez, S., Rosas, F., Magalhães, V., Valadares, V., Zitellini, N., Roque, C., Victor, L.M. and Team, M.A.T.E.S.P.R.O., 2009. Morphotectonics and strain partitioning at the Iberia–Africa plate boundary from multibeam and seismic reflection data. Marine Geology, 267 (3–4), 156–174.

Terrinha, P., Rocha, R., Rey, J., Cachão, M., Moura, D., Roque, C., Martins, L., Valadares, V., Cabral, J., Azevedo, M.R., Barbero, L., Clavijo, E., Dias, R.P., Gafeira, J., Matias, H., Matias, L., Madeira, J., Marques da Silva, C., Munhá, J., Rebelo, L., Ribeiro, C., Vicente, J., Youbi, N. and Bensalah, K., 2013. A Bacia do Algarve: Estratigrafia, Paleogeografia e Tectónica. In Geologia de Portugal no contexto da Ibéria,in, Geologia de Portugal, Vol. II Geologia Moso-Cenozóica de Portugal (R. Dias, A. Araújo, P. Terrinha & J.C. Kullberg, Eds.).

Troiani, F. and Della Seta, M., 2008. The use of the Stream Length–Gradient index in morphotectonic analysis of small catchments: A case study from Central Italy. Geomorphology, 102, 159–168.

USGS, 2004. Shuttle Radar Topography Mission (SRTM), 1 Arc Second scene SRTM_u03_n008e004, Unfilled, Unfinished 2.0, Global Land Cover Facility, University of Maryland, College Park, Maryland.

Villamor, P., Capote, R., Stirling, M.W., Tsige, M., Berryman, K.R., Martínez-Dias, J.J. and Martín-González, F., 2012. Contribution of active faults in the intraplate area of Iberia to seismic hazard: The Alentejo- Plasencia Fault, Journal of Iberian Geology, 38(1), 85-111.

Vizcaino, A., Gràcia, E., Pallàs, R., Garcia-Orellana, J., Escutia, C., Casas, D., Willmott, V., Diez, S. and Dañobeitia, J.J., 2006. Sedimentology, physical properties and ages of mass-transport deposits associated to the Marquês de Pombal Fault, Southwest Portuguese Margin. Norw. J. Geol., 86, 173-182.

Wakabayashi, J. and Sawyer, T.L., 2001. Stream incision, tectonics, uplift and evolution of topography of the Sierra Nevada, California. Journal of Geology, 109, 539–562.

Wells, D. and Coppersmith, K., 1994. New empirical relationships among magnitude, rupture length, rupture width, rupture area and surface displacement. Bulletin of the Seismological Society of America, 84 (4), 974-1002.

Wesnousky, S.G., 1986. Earthquakes, Quaternary faults, and seismic hazard in California. Journal of Geophysical Research, 91(B12), 12587-12631.

Wesnousky, S. G., 1988. Seismological and structural evolution of strike-slip faults. Letters to Nature, 335, 340–343.

Wesnousky, S. G., 2008. Displacement and geometrical characteristics of earthquake surface ruptures: Issues and implications for seismic hazard analysis and the process of earthquake rupture, Bull. Seismol. Soc. Am., 98, (4), 1609–1632.

Westaway, R., 1995, Deformation around stepovers in strike-slip fault zones. Journal of Structural Geology, 17, 831–846.

Whipple, K., Wobus, C., Crosby, B., Kirby, E. and Sheehan, D., 2007. Stream Profiler freeware software. Available at www.geomorphtools.org.

Wright, L.W., 1970. Variation in the level of the Cliff/Shore platform junction along the south coast of great Britain, Marine Geology, 9, 347-353.

Wziatek, W., Vousdoukas, M., and Terefenko, P., 2011. Wave-cut notches along the Algarve coast, S. Portugal: Characteristics and formation mechanisms, J. of Coast. Res., Sp. Iss., 64, 855 – 859.

Zazo, C., Goy, J.L., Dabrio, C.J., Bradaji, T., Somoza, L. and Silva, P.G., 1993. The last interglacial in the Mediterranean as a model for the present interglacial. Global and Planetary Change, 7 (1), 109-117.

Zazo, C., Mercier, N., Lario, J., Roquero, E., Goy, J.L., Silva, P.G., Cabero, A., Borja, F., Dabrio, C.J., Bardají, T., Soler, V., Garcia-Blázquez, A. and Luque, L., 2008. Palaeoenvironmental evolution of the Barbate–Trafalgar coast (Cadiz) during the last ~140 ka: Climate, sea-level interactions and tectonics, Geomorphology, 100, 212-222.

Zitellini, N., Mendes, L.A., Cordoba, D., Danobeitia, J., Nicolich, R., Pellis, G., Ribeiro, A., Sartori, R., Torelli, L., Bartolomé, R., Bortoluzzi, G., Calafato, A., Carrilho, F., Casoni, L., Chierici, F., Corela, C., Correggiari, A., Della Vedova, B., Gràcia, E., Jornet, P., Landuzzi, M., Ligi, M., Magagnoli, A., Marozzi, G., Matias, L., Penitenti, D., Rodriguez, P., Rovere, M., Terrinha, P., Vigliotti, L. and Zahinos Ruiz, A., 2001. Source of 1755 Lisbon earthquake and tsunami investigated. Eos Transactions, Am. Geoph. Un., 82 (26), 290–291.

Zitellini, N., Rovere, M., Terrinha, P., Chierici, F., Matias, L. and Bigsets Team, 2004. Neogene through Quaternary tectonic reactivation of SW Iberian passive margin. Pure and Applied Geophysics, 161 (3), 565–587.

Zitellini, N., Gracia, E., Matias, L., Terrinha, P., Abreu, M.A., DeAlteriis, G., Henriet, J.P., Danobeitia, J.J., Masson, D.G., Mulder, T., Ramella, R., Somoza, L. and Diez, S., 2009. The quest for the Africa–Eurasia plate boundary west of the Strait of Gibraltar, Earth and Pl. Sc. Lett., 280 (1-4), 13-50.

Annex I

Morpho tectonic

Maps

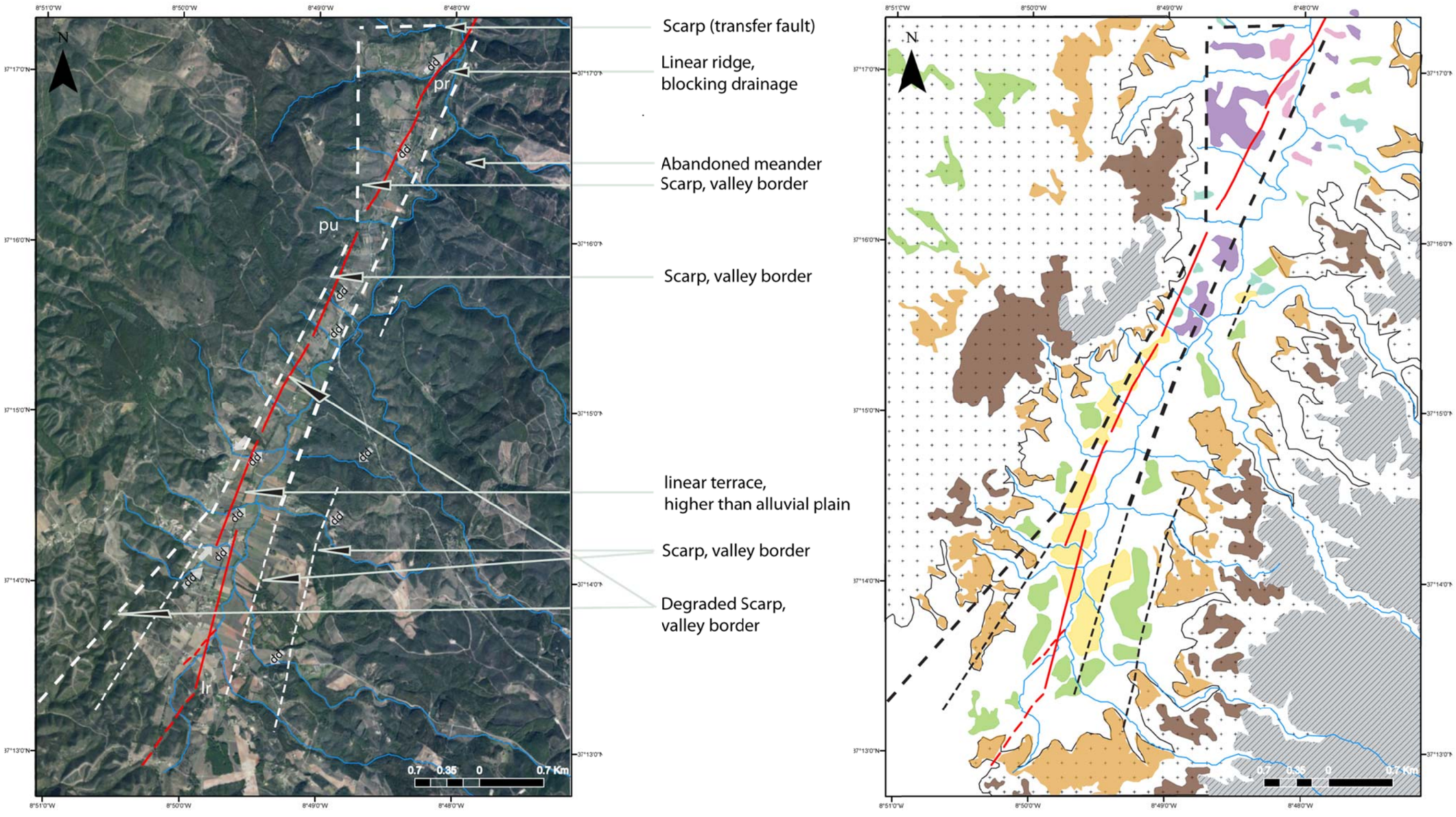

I.I Morphotectonic map for Aljezur- Alfambras basin, south sector

Morphotectonic maps

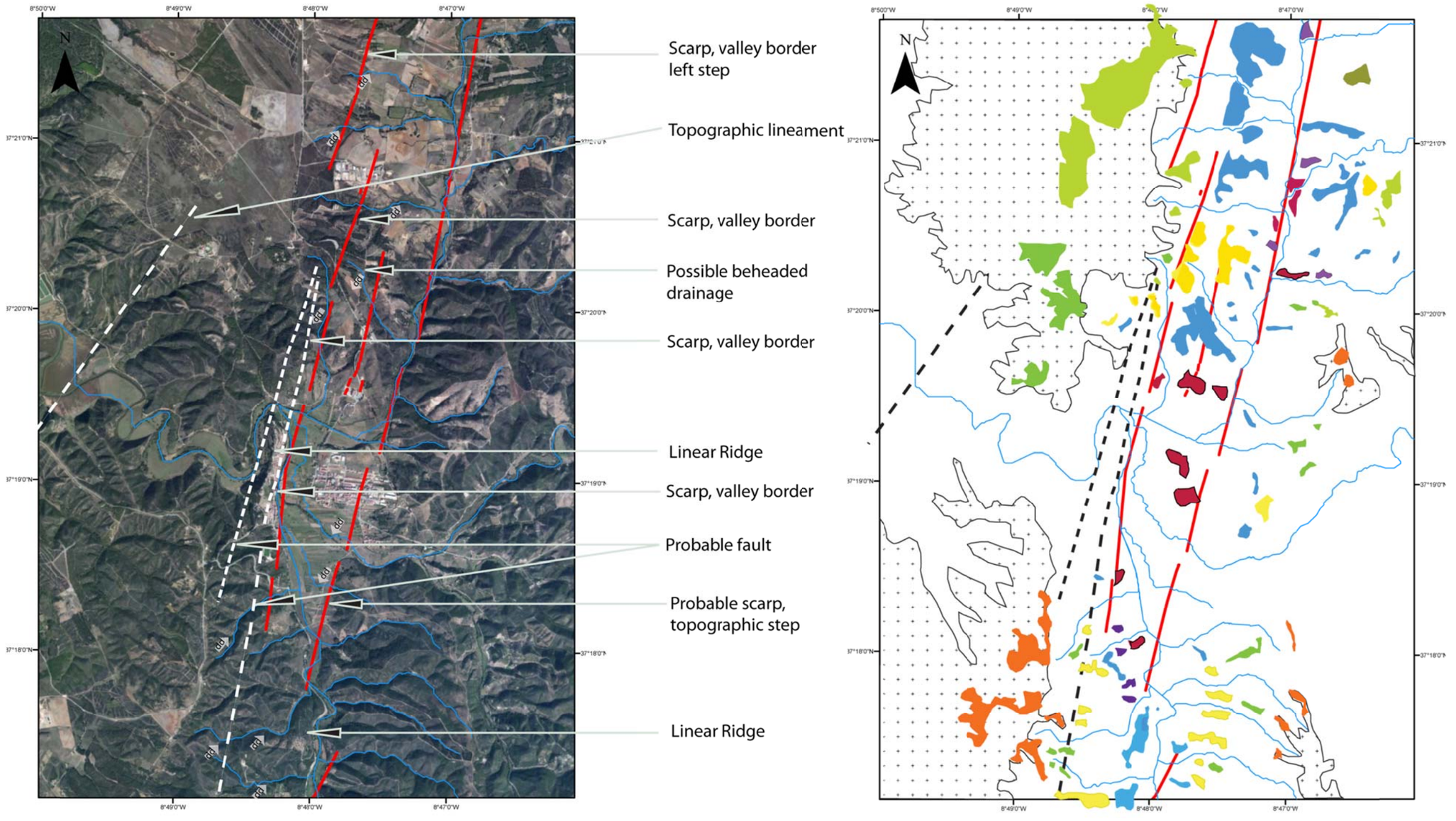

I.II Morpho tectonic map for Aljezur- Alfambras basin, central sector

Morphotectonic maps

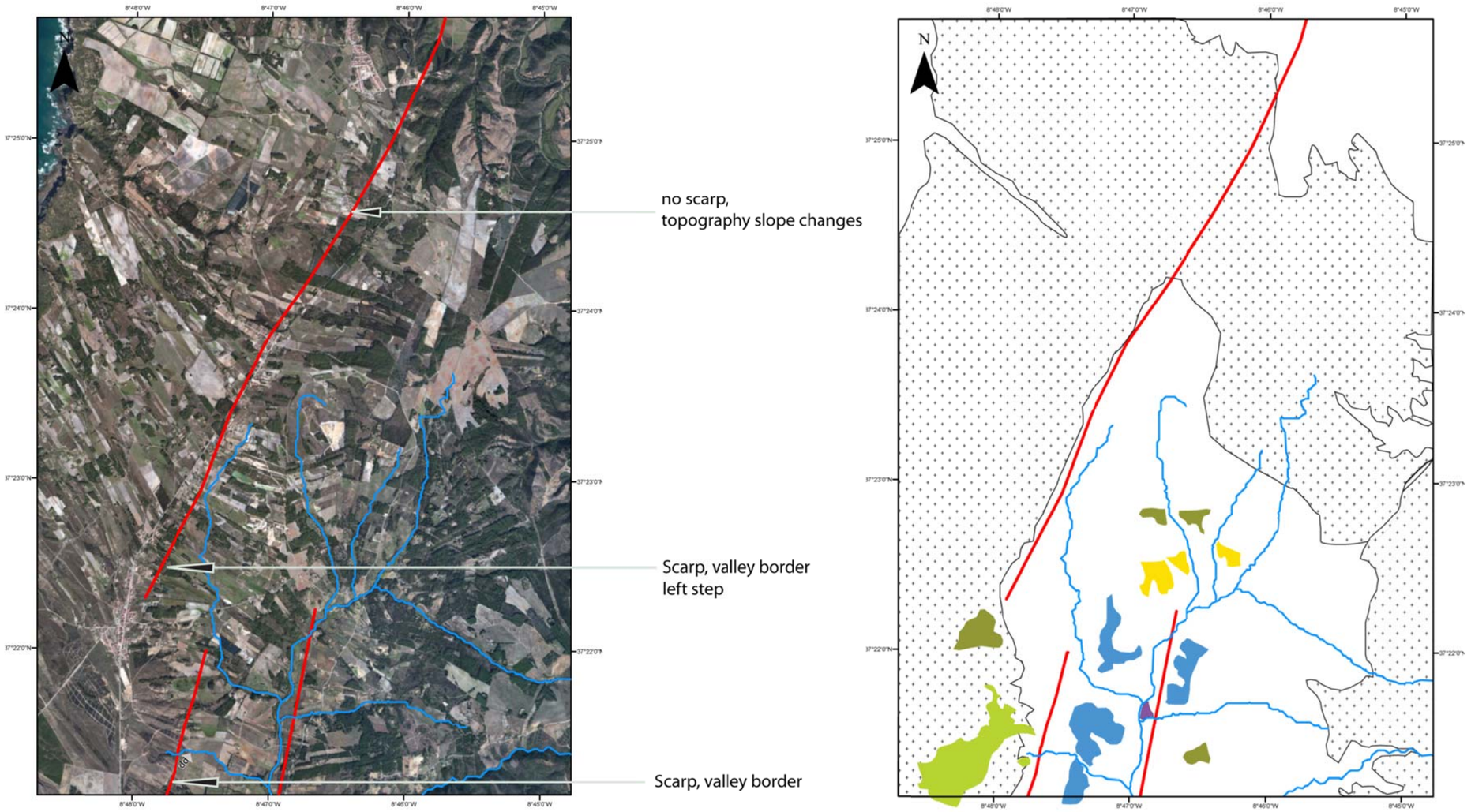

I.III Morpho tectonic map for Aljezur- Alfambras basin, north sector

I.V Morphotectonic map of Aljezur-Alfambras basin

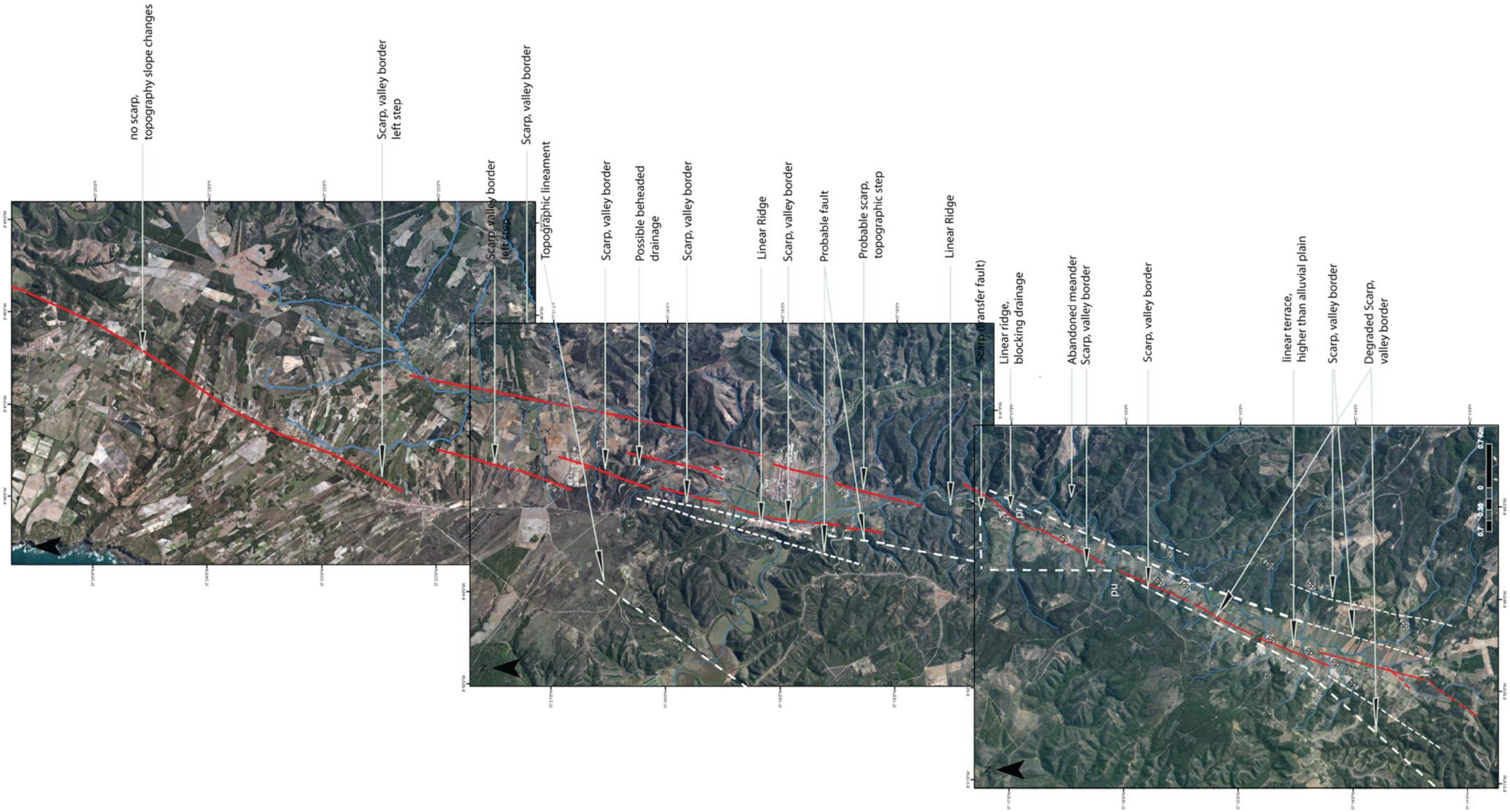

Annex II

Channel Steepness index analysis (Ksn)

Annex II

Channel Steepness index analysis (Ksn)

Eastern basins:

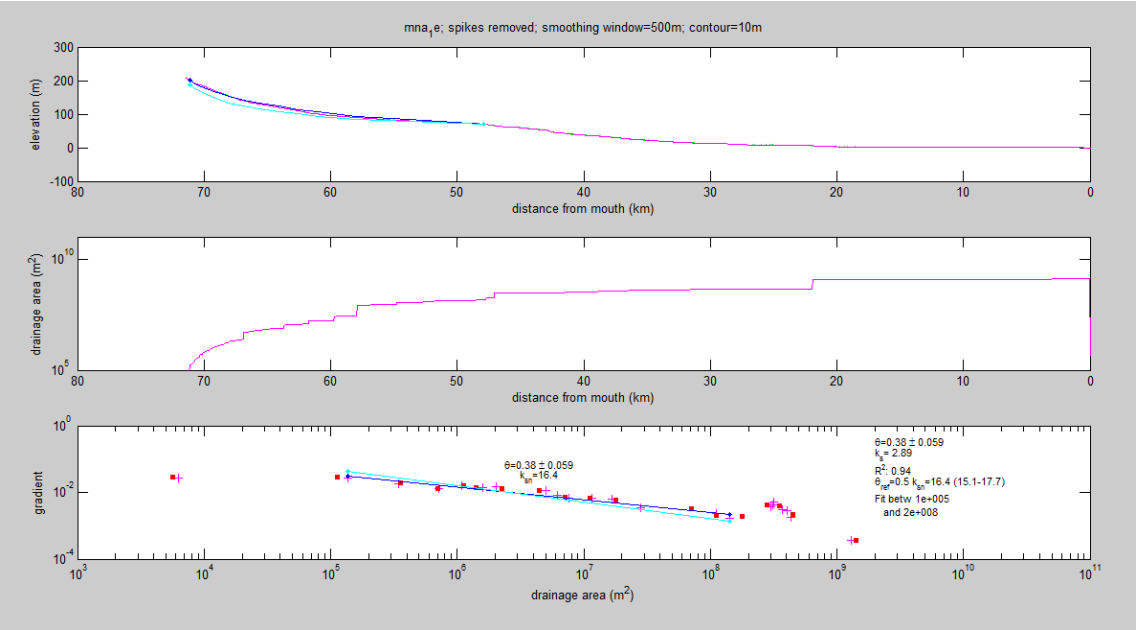

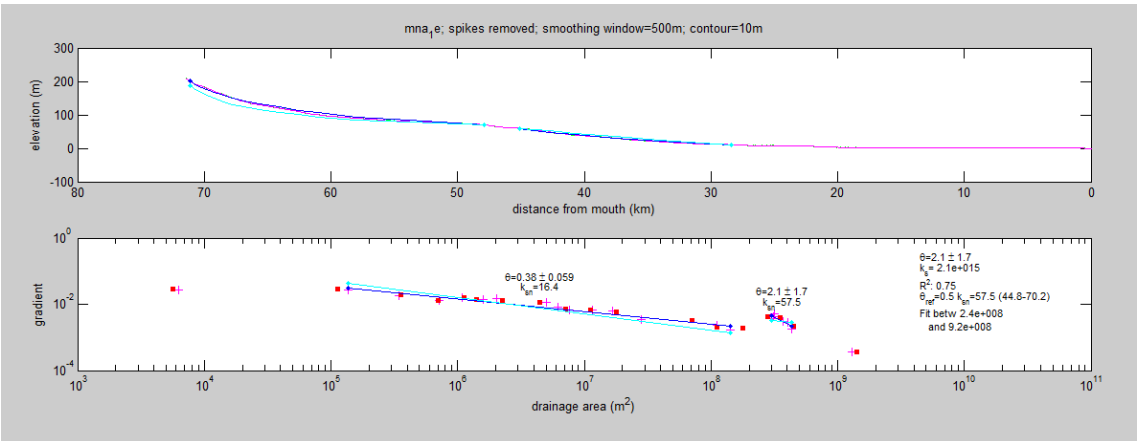

Longitudinal profile, area- length relationship, gradient-area relationship and values of concavity and Ksn obtained for channel 1e.

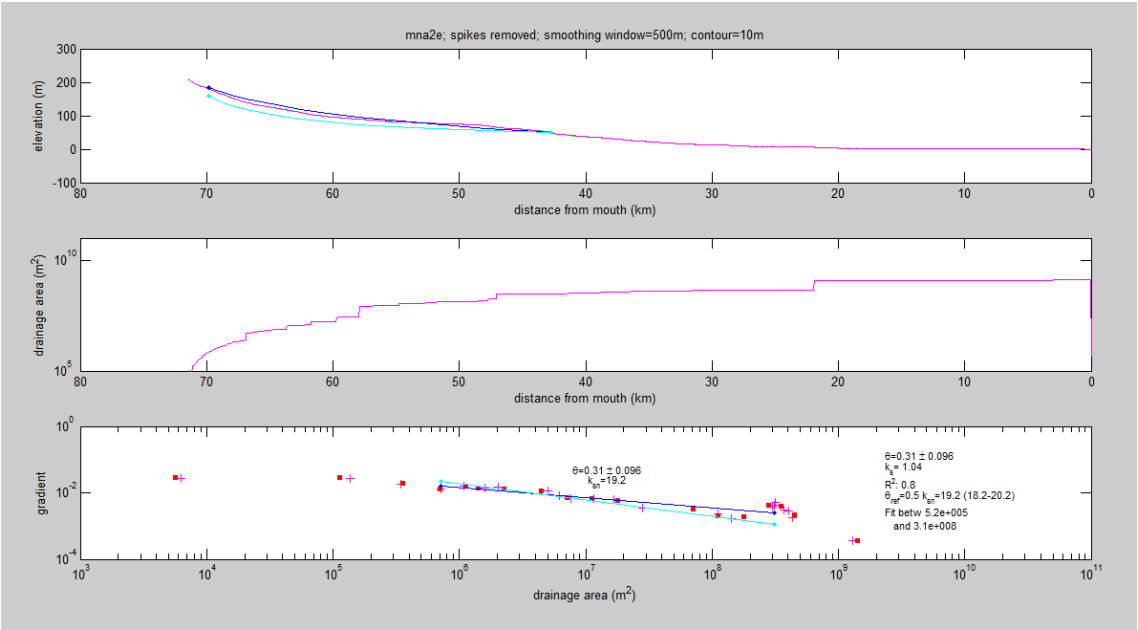

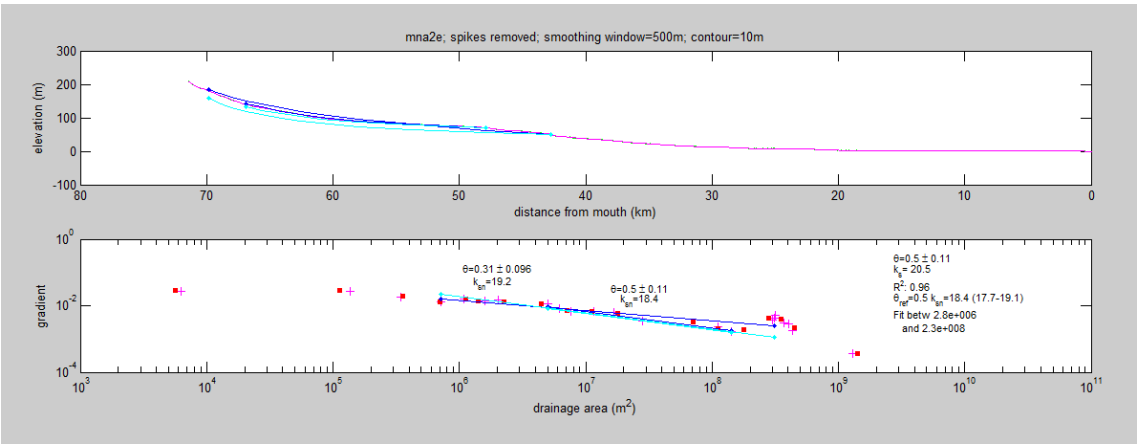

Longitudinal profile, area- length relationship, gradient-area relationship and values of concavity and Ksn obtained for channel 2e.

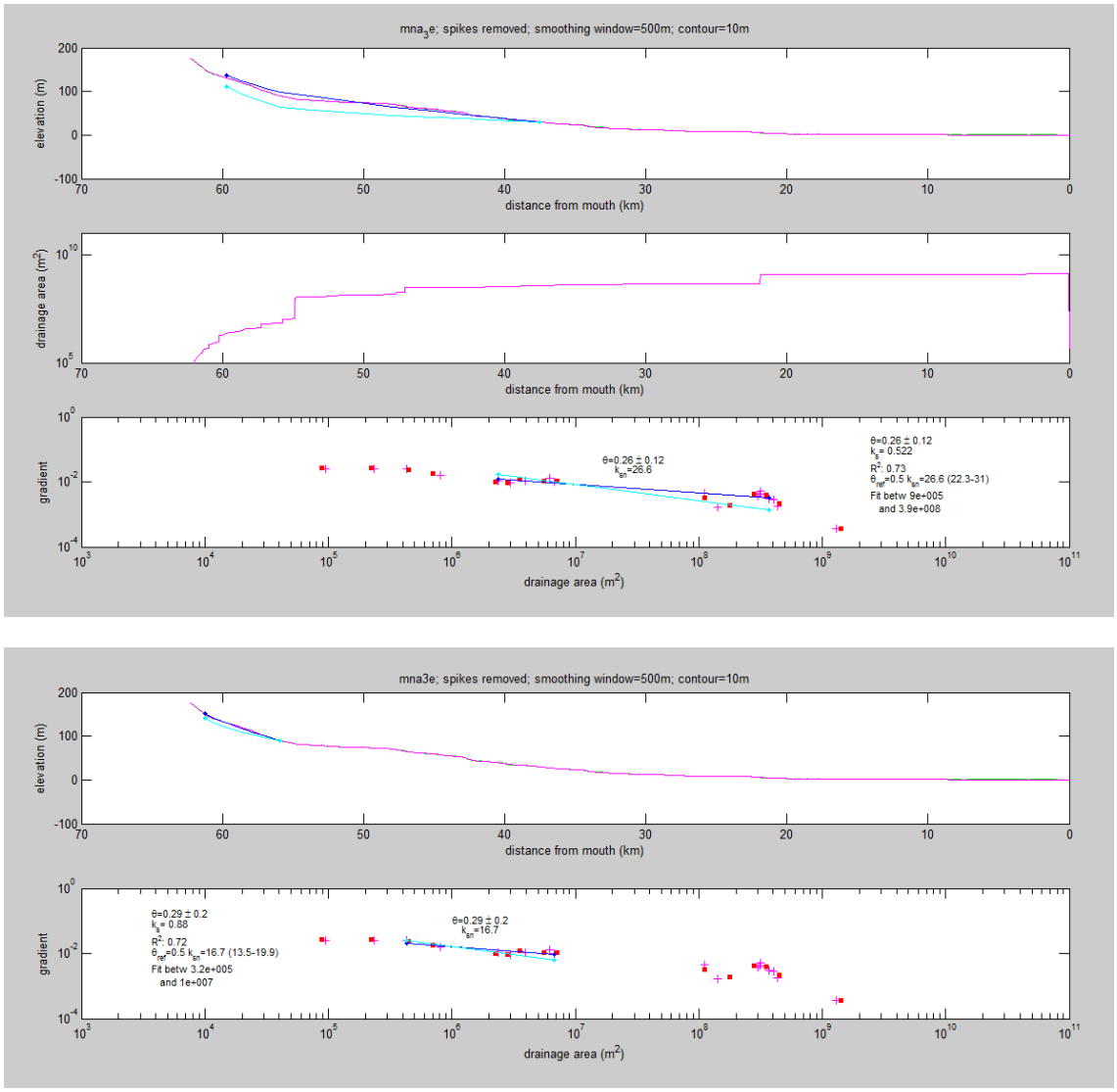

Longitudinal profile, area- length relationship, gradient-area relationship and values of concavity and Ksn obtained for channel 3e.

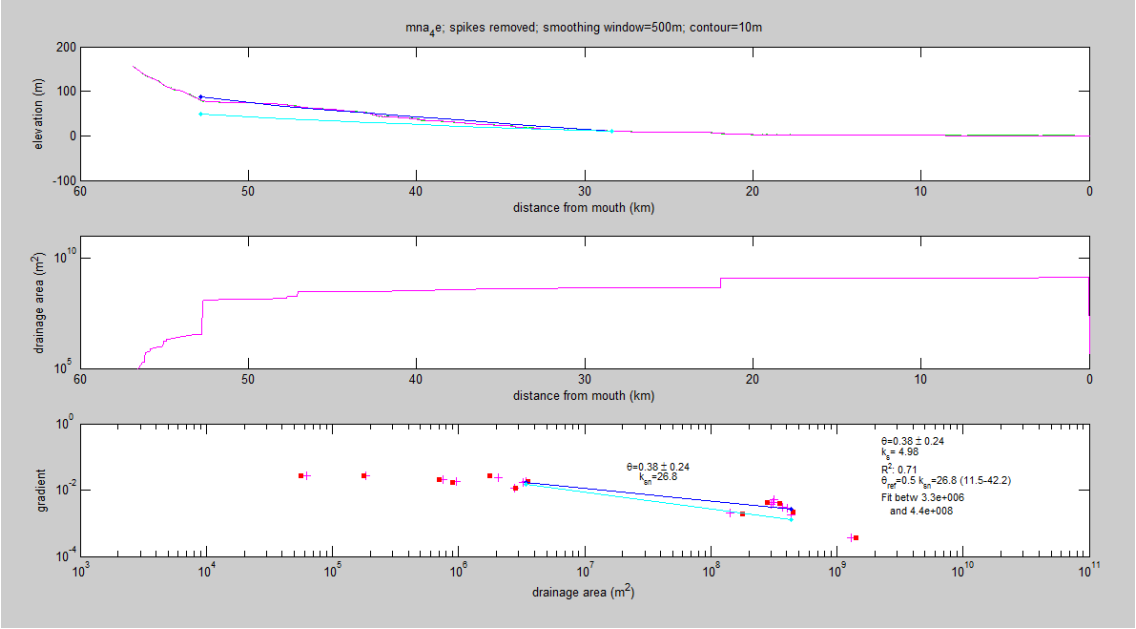

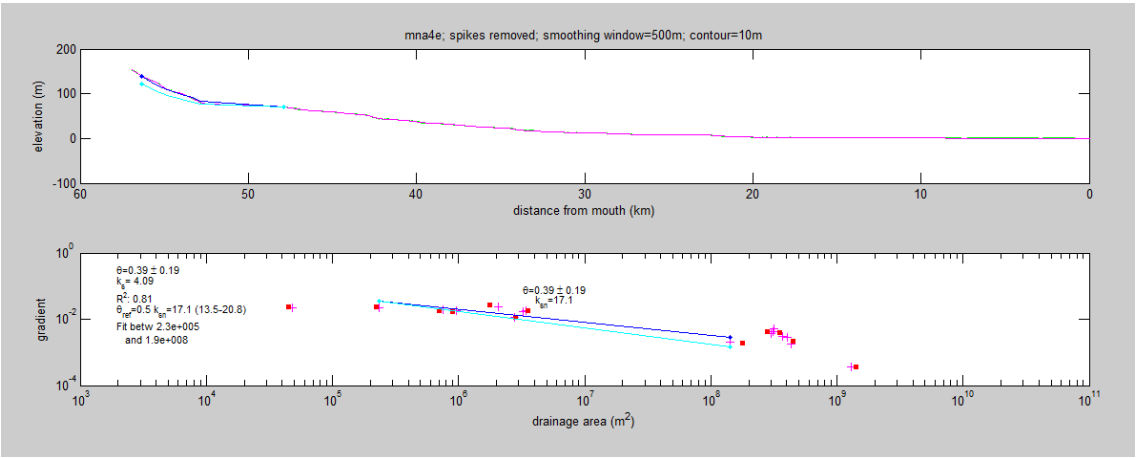

Longitudinal profile, area- length relationship, gradient-area relationship and values of concavity and Ksn obtained for channel 4e.

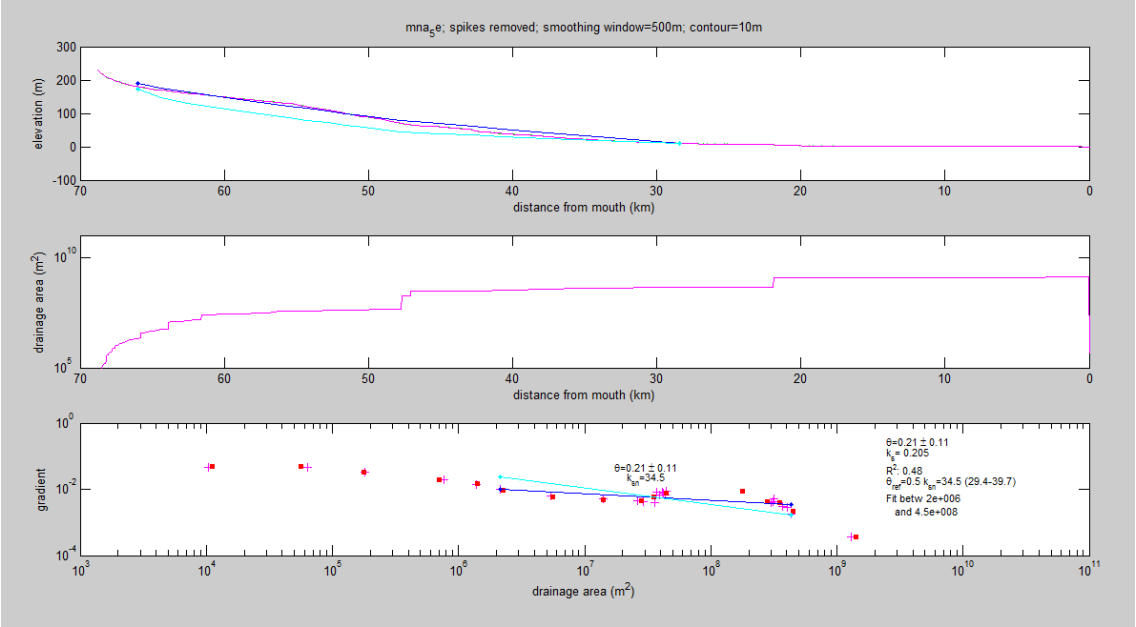

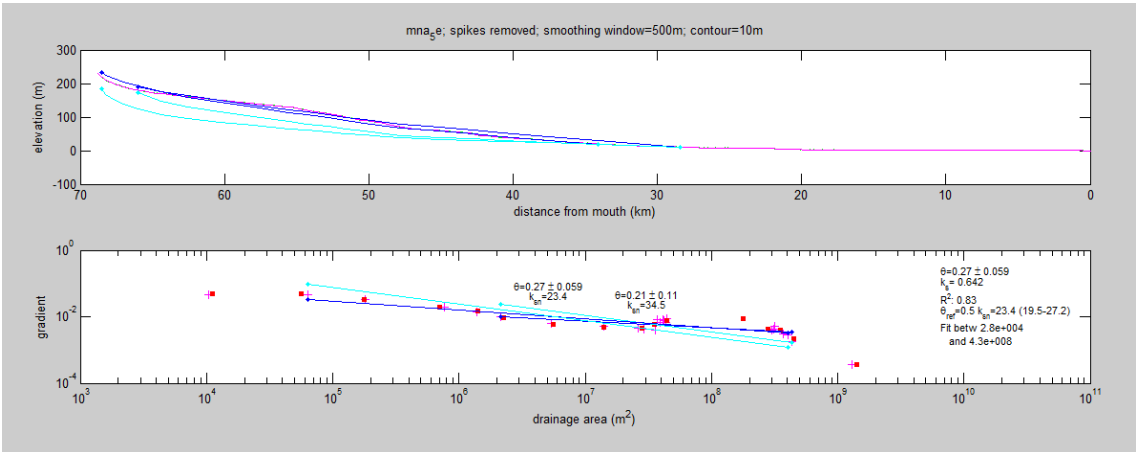

Longitudinal profile, area- length relationship, gradient-area relationship and values of concavity and Ksn obtained for channel 5e.

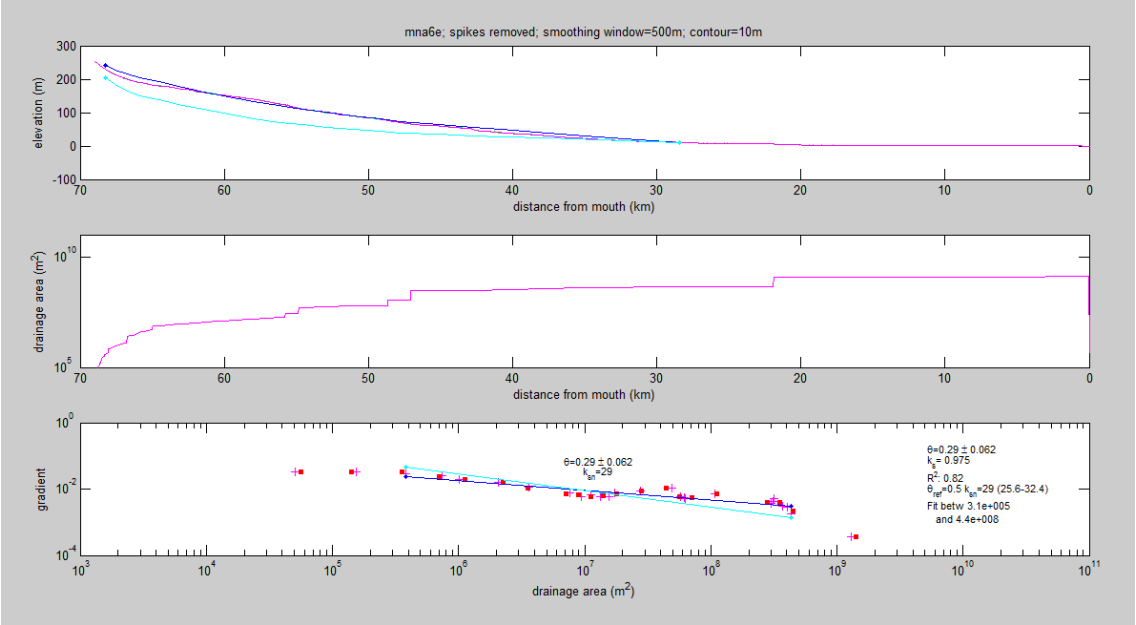

Longitudinal profile, area- length relationship, gradient-area relationship and values of concavity and Ksn obtained for channel 6e.

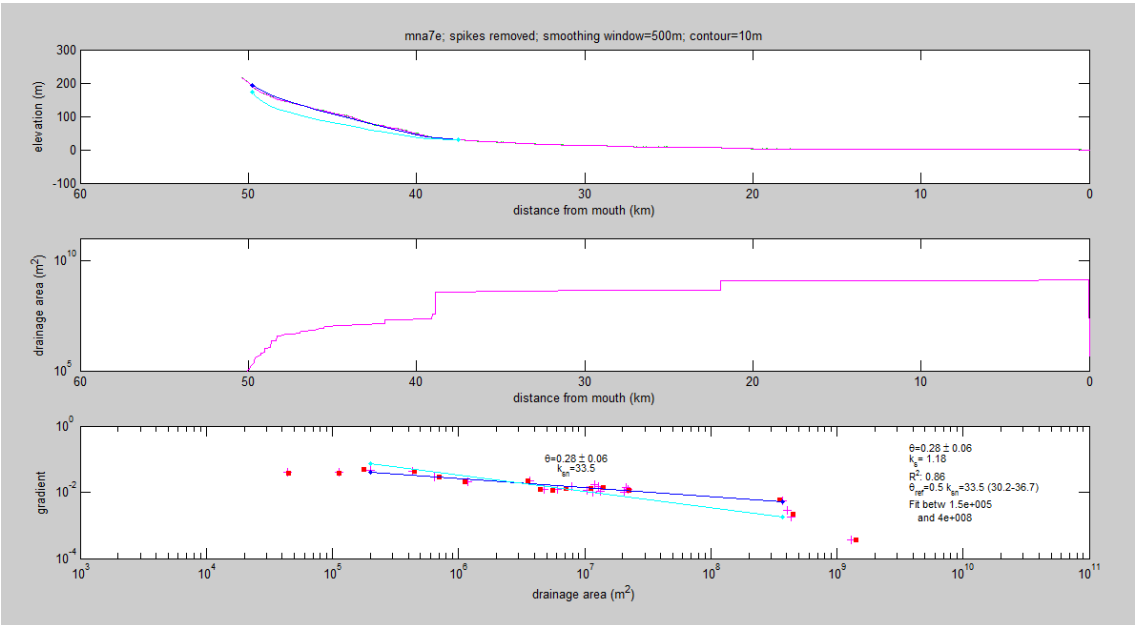

Longitudinal profile, area- length relationship, gradient-area relationship and values of concavity and Ksn obtained for channel 7e.

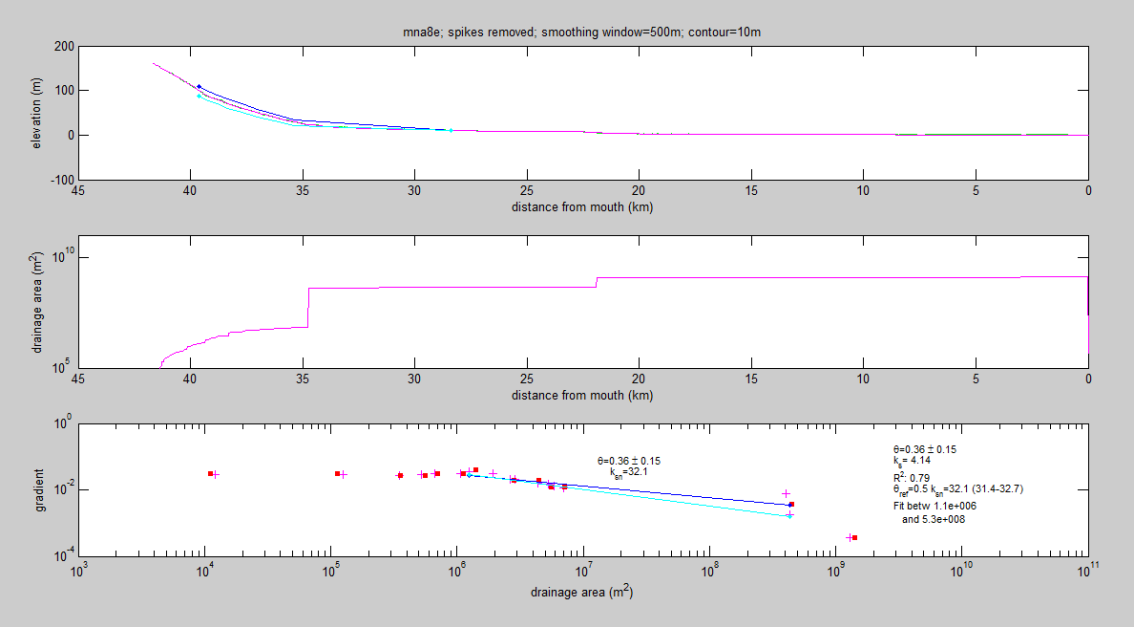

Longitudinal profile, area- length relationship, gradient-area relationship and values of concavity and Ksn obtained for channel 8e.

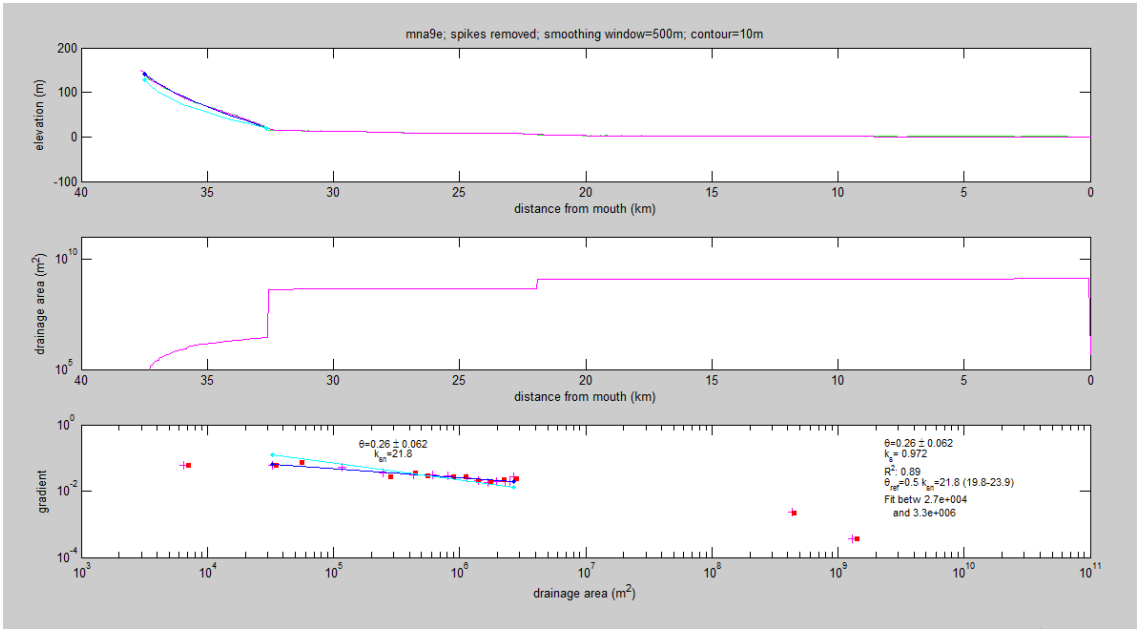

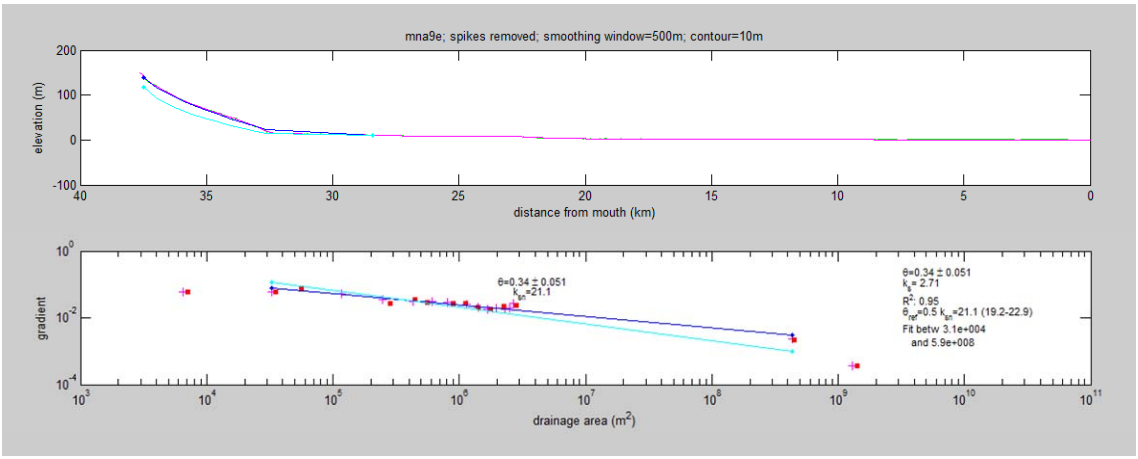

Longitudinal profile, area- length relationship, gradient-area relationship and values of concavity and Ksn obtained for channel 9e.

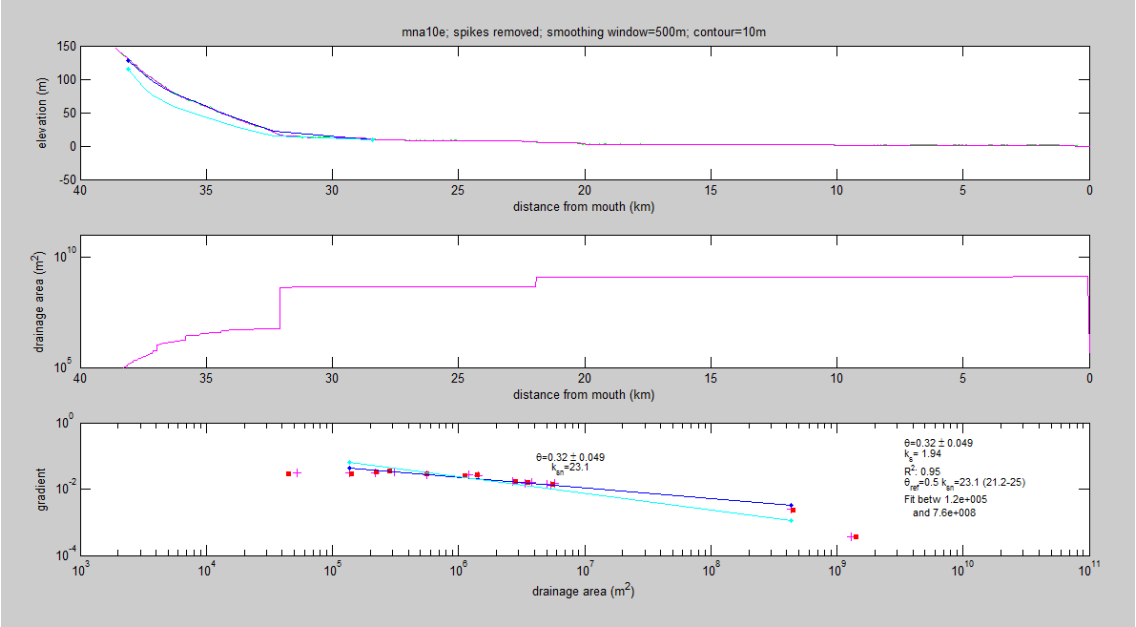

Longitudinal profile, area- length relationship, gradient-area relationship and values of concavity and Ksn obtained for channel 10e.

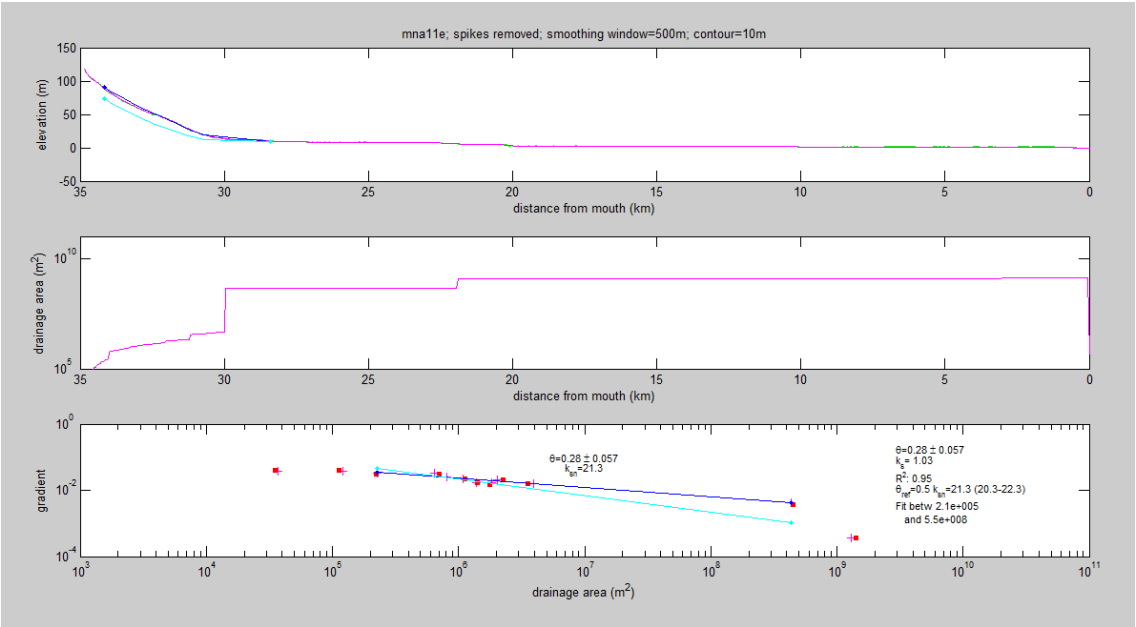

Longitudinal profile, area- length relationship, gradient-area relationship and values of concavity and Ksn obtained for channel 11e.

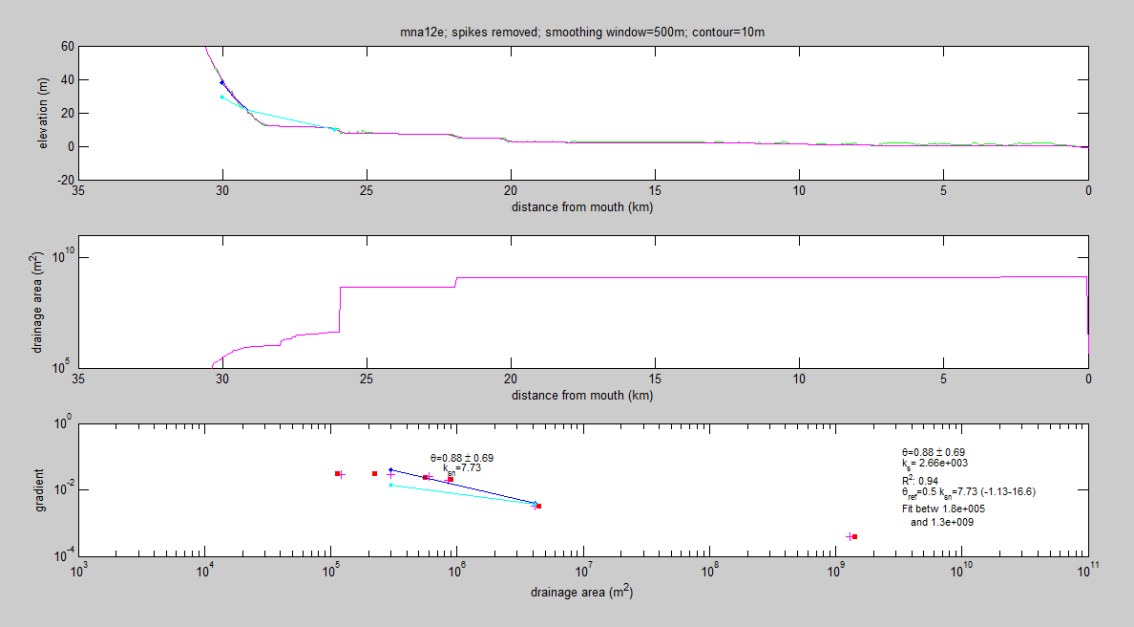

Longitudinal profile, area- length relationship, gradient-area relationship and values of concavity and Ksn obtained for channel 12e.

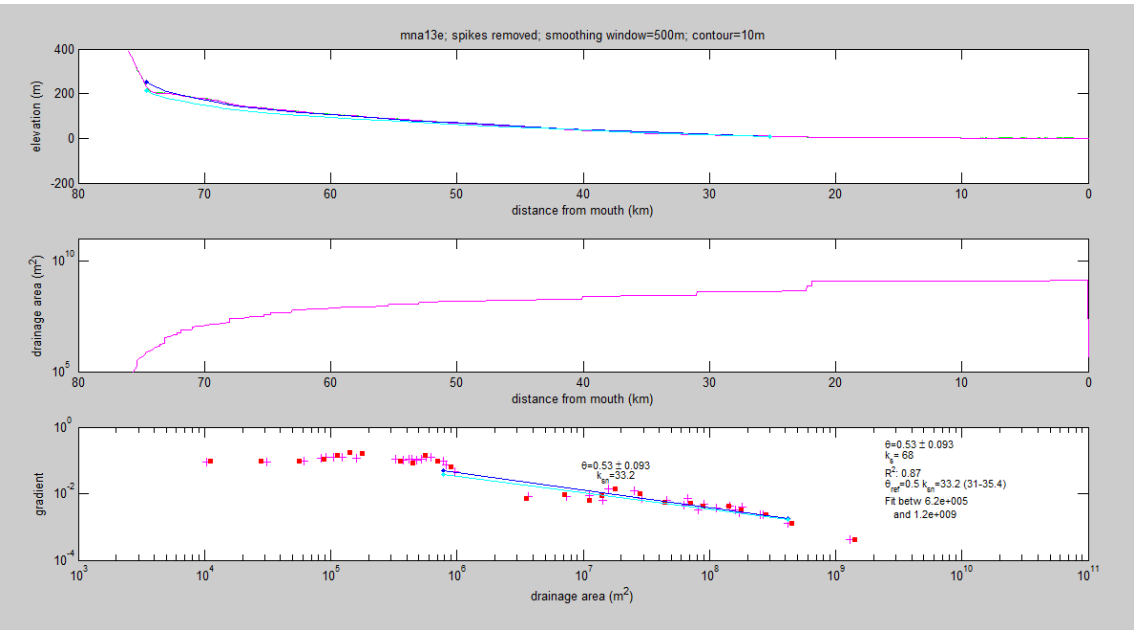

Longitudinal profile, area- length relationship, gradient-area relationship and values of concavity and Ksn obtained for channel 13e.

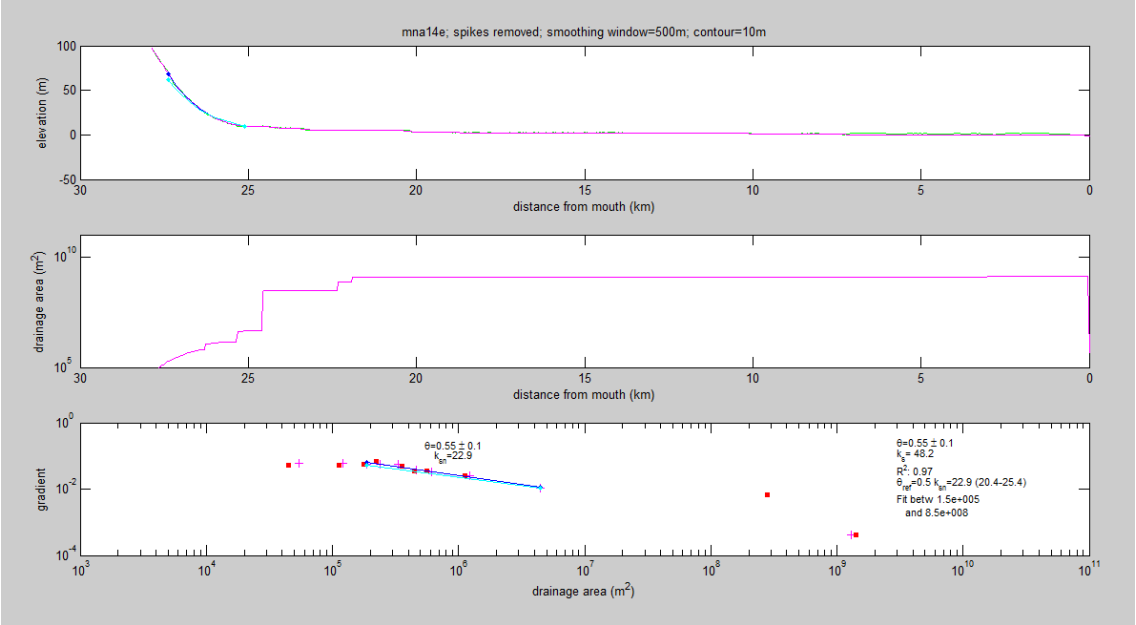

Longitudinal profile, area- length relationship, gradient-area relationship and values of concavity and Ksn obtained for channel 14e.

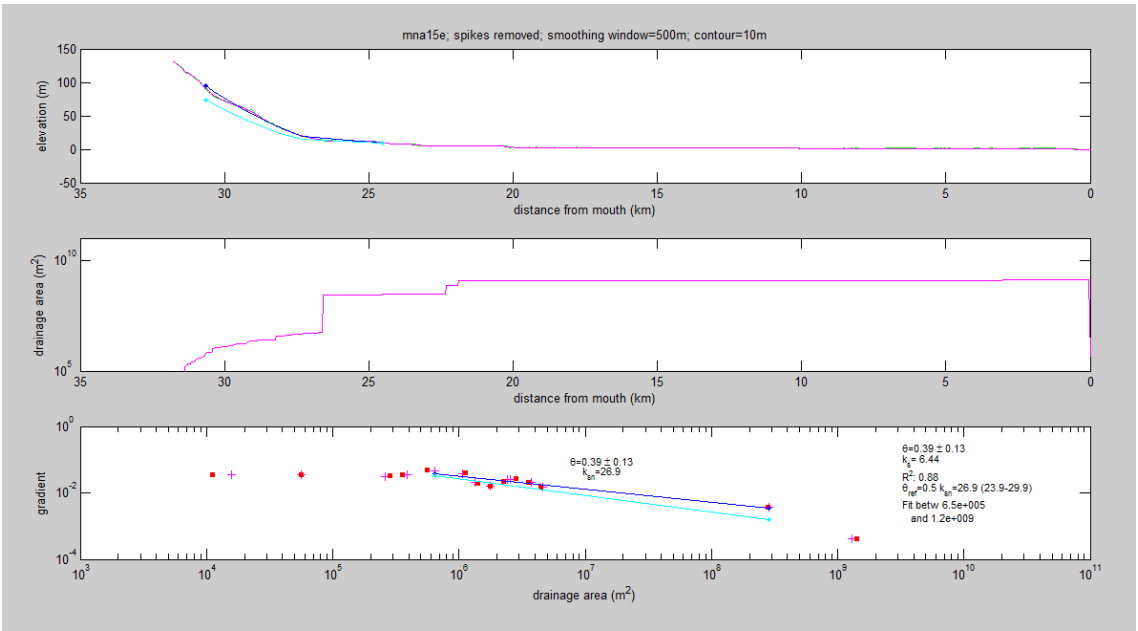

Longitudinal profile, area- length relationship, gradient-area relationship and values of concavity and Ksn obtained for channel 15e.

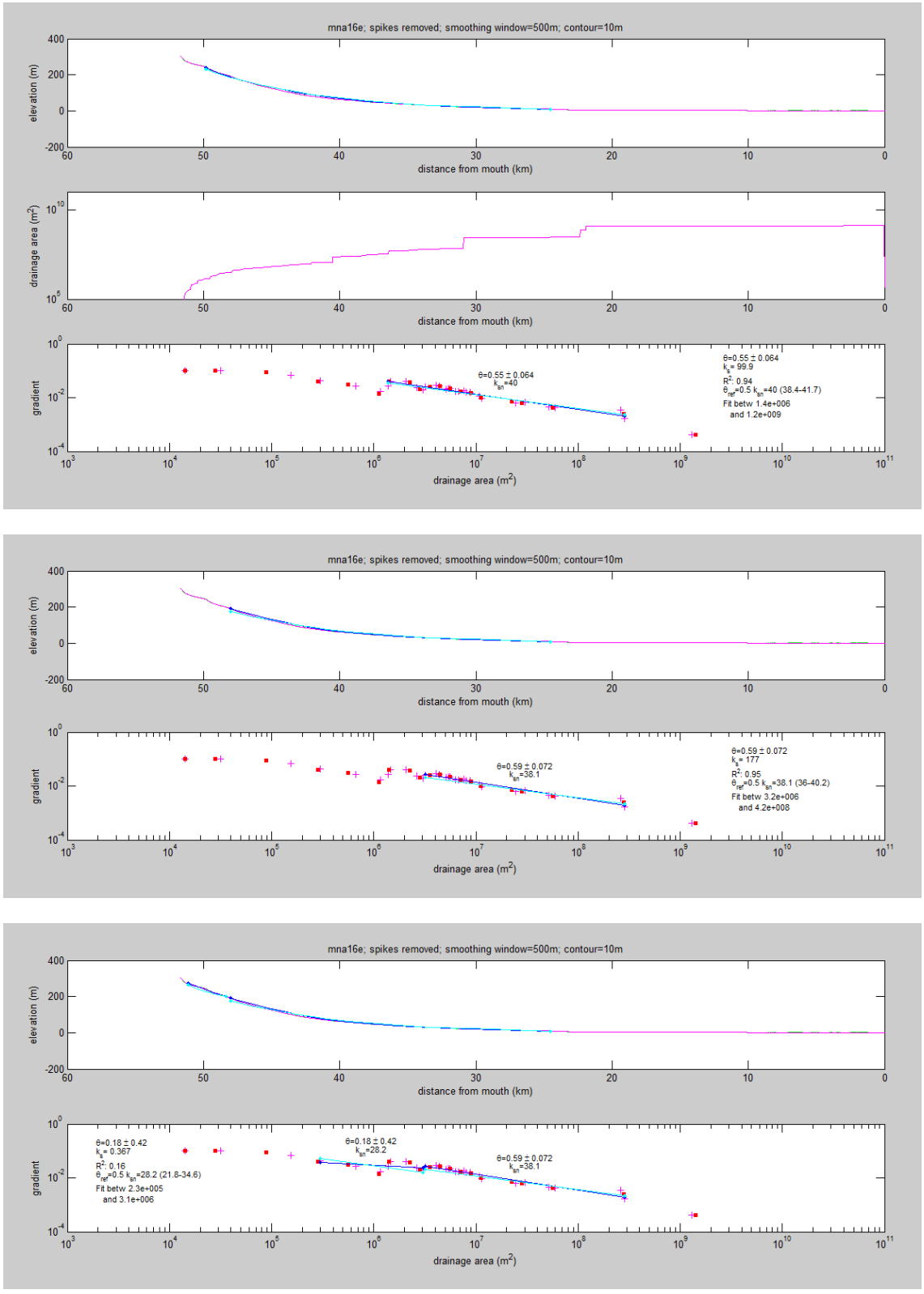

Longitudinal profile, area- length relationship, gradient-area relationship and values of concavity and Ksn obtained for channel 16e.

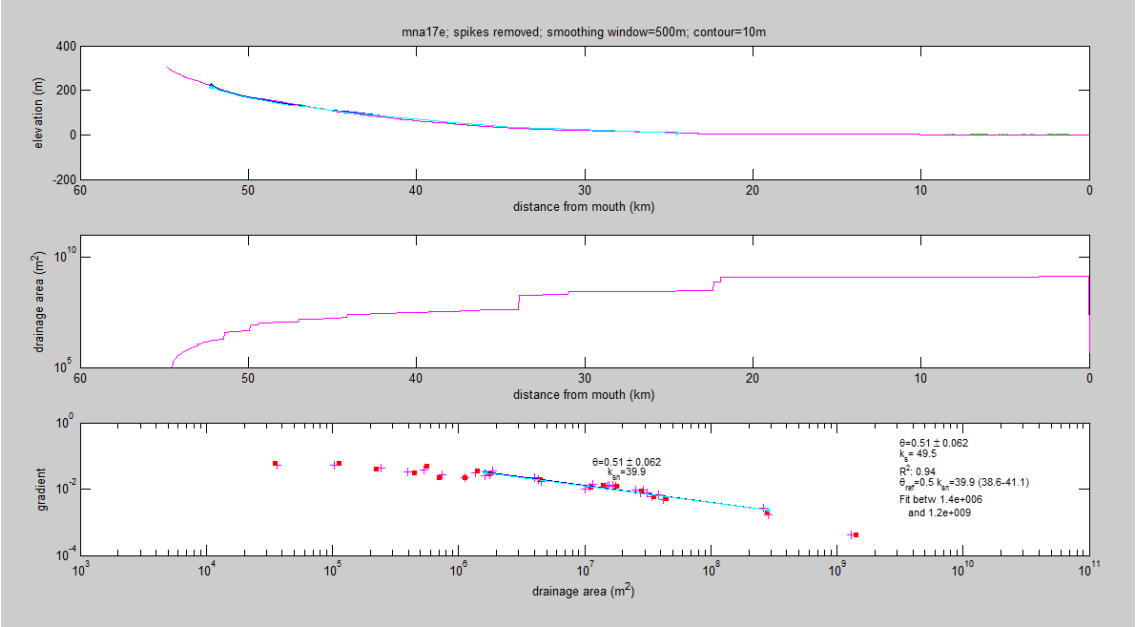

Longitudinal profile, area- length relationship, gradient-area relationship and values of concavity and Ksn obtained for channel 17e.

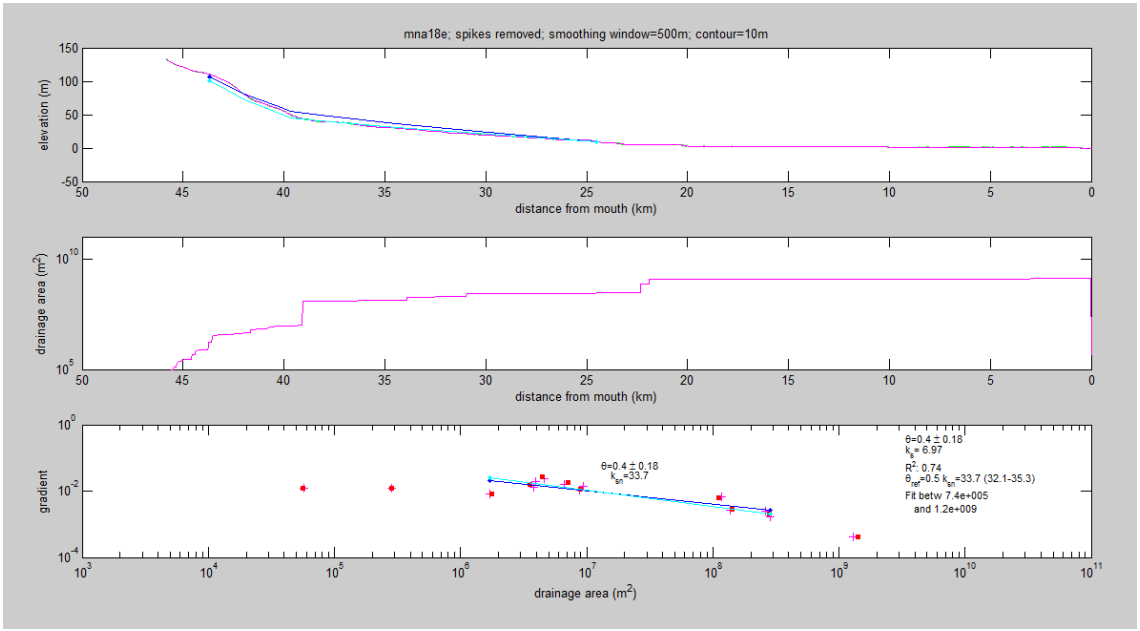

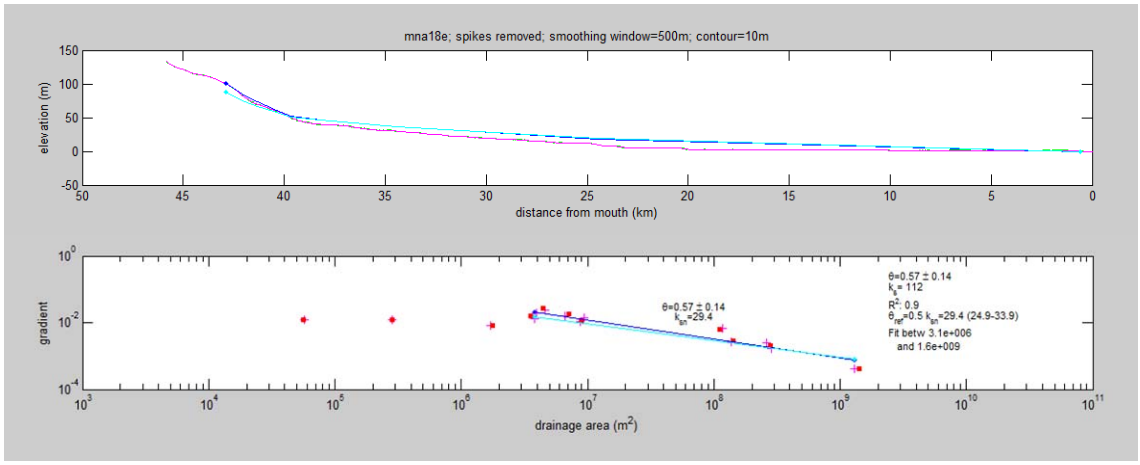

Longitudinal profile, area- length relationship, gradient-area relationship and values of concavity and Ksn obtained for channel 18e.

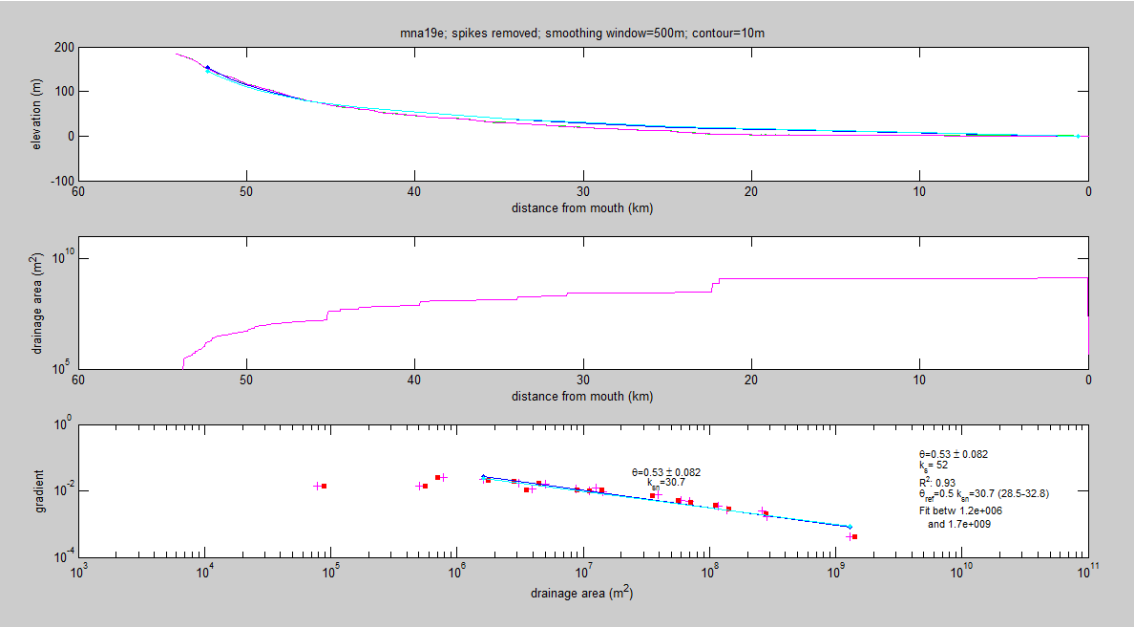

Longitudinal profile, area- length relationship, gradient-area relationship and values of concavity and Ksn obtained for channel 19e.

Western basins:

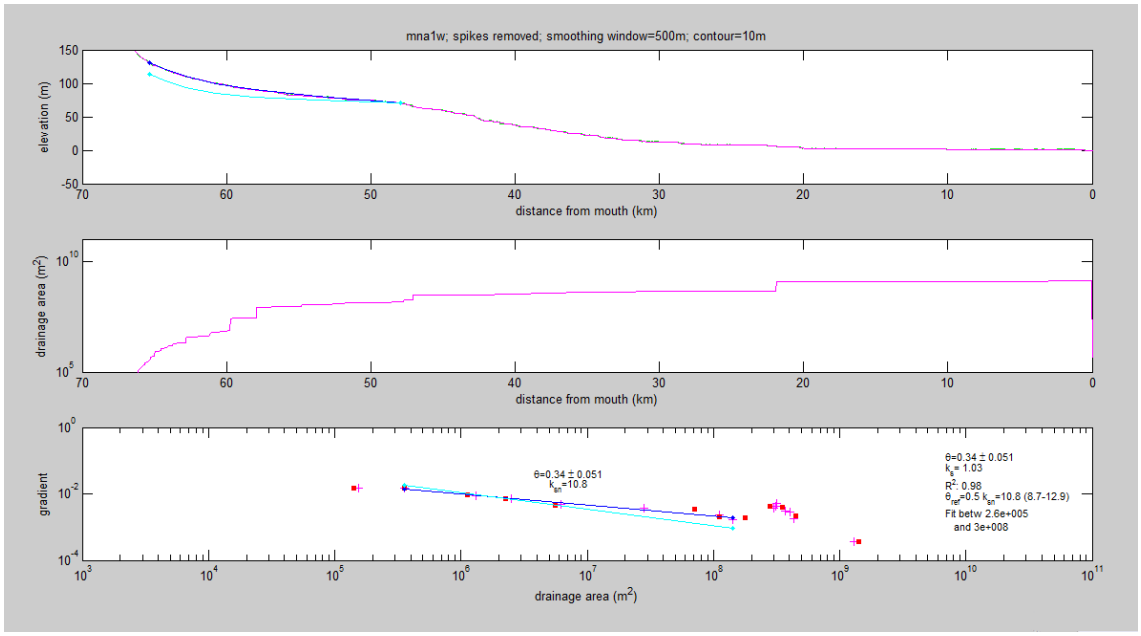

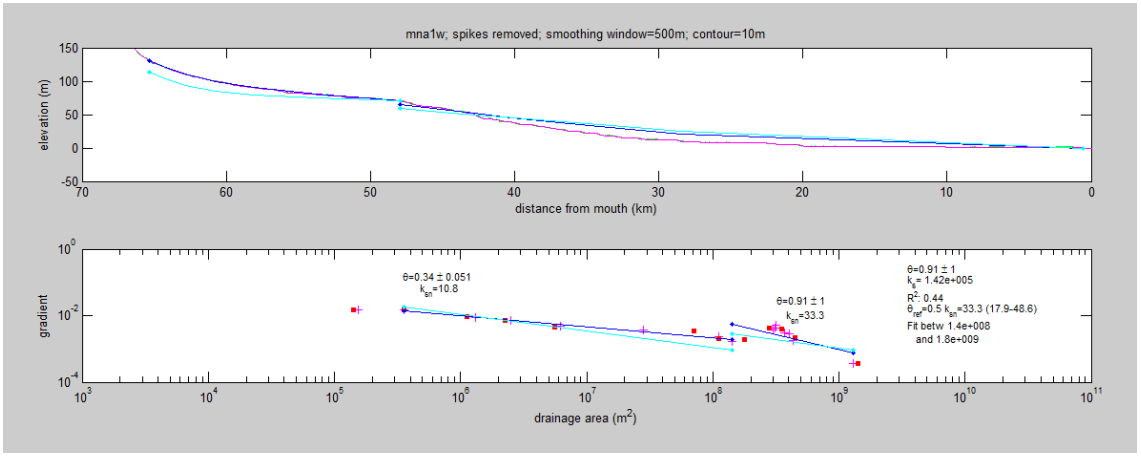

Longitudinal profile, area- length relationship, gradient-area relationship and values of concavity and Ksn obtained for channel 1w.

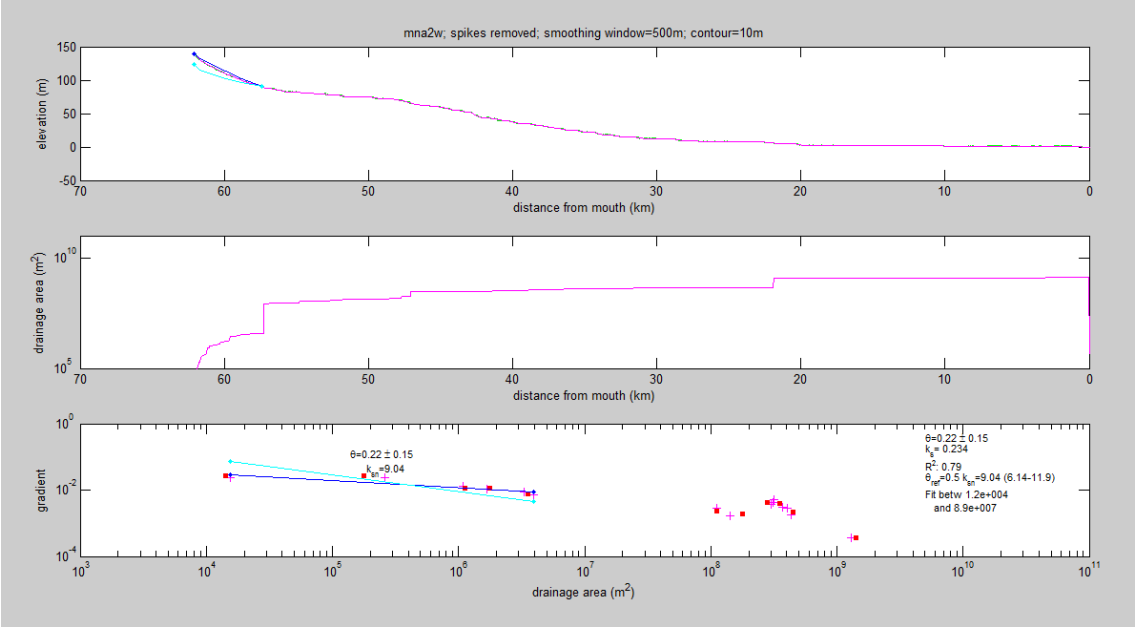

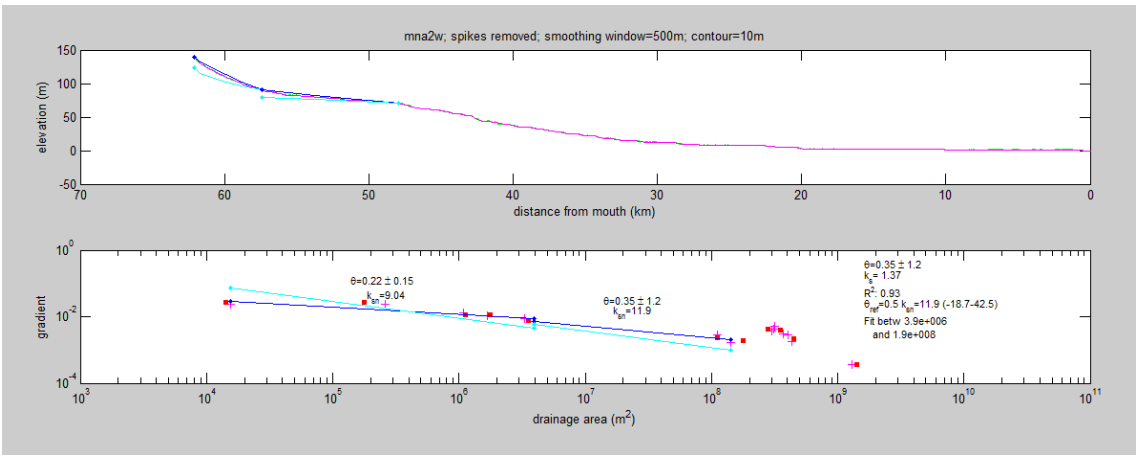

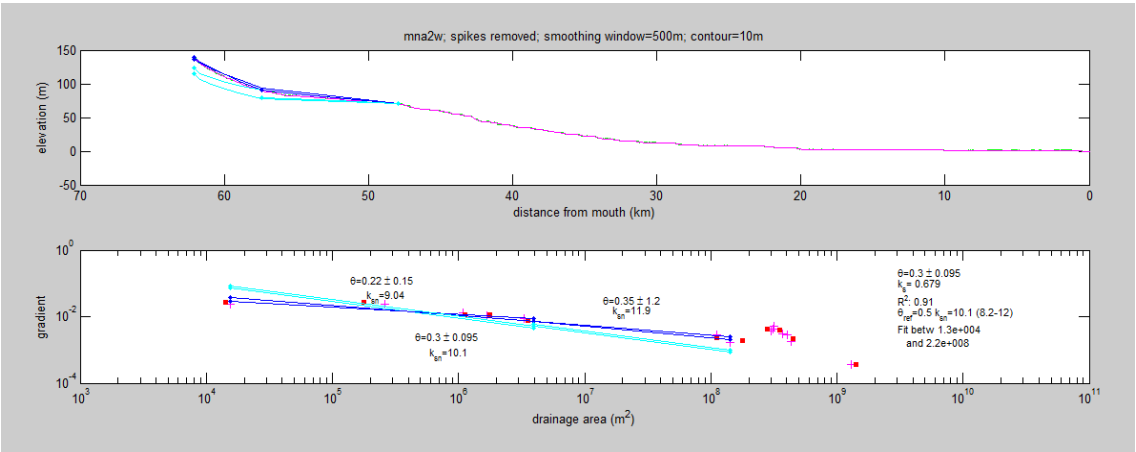

Longitudinal profile, area- length relationship, gradient-area relationship and values of concavity and Ksn obtained for channel 2w.

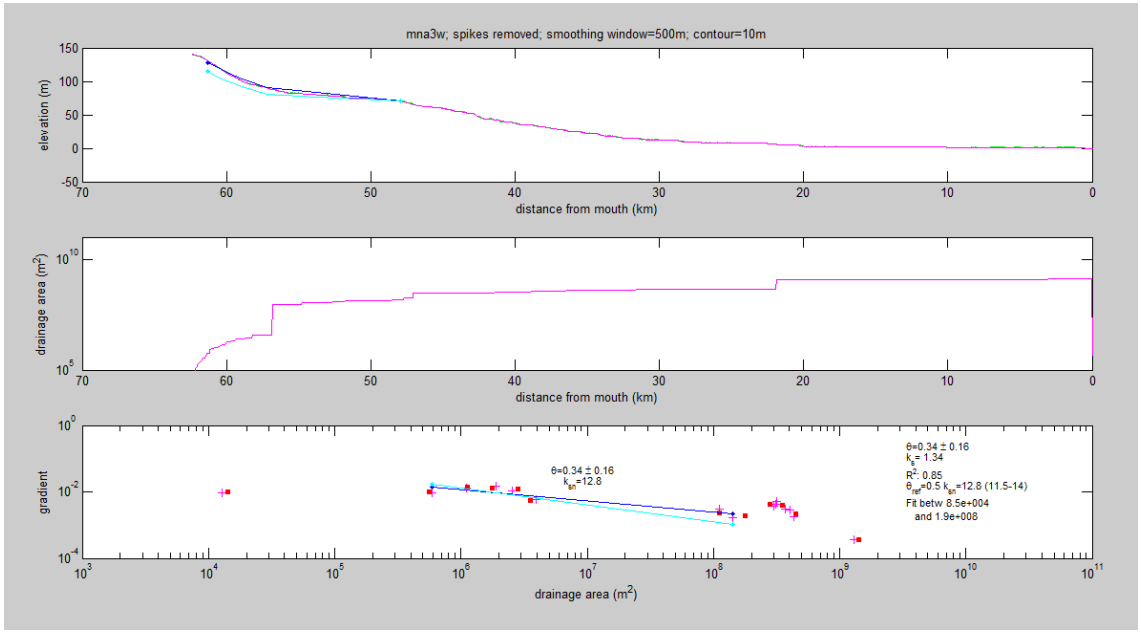

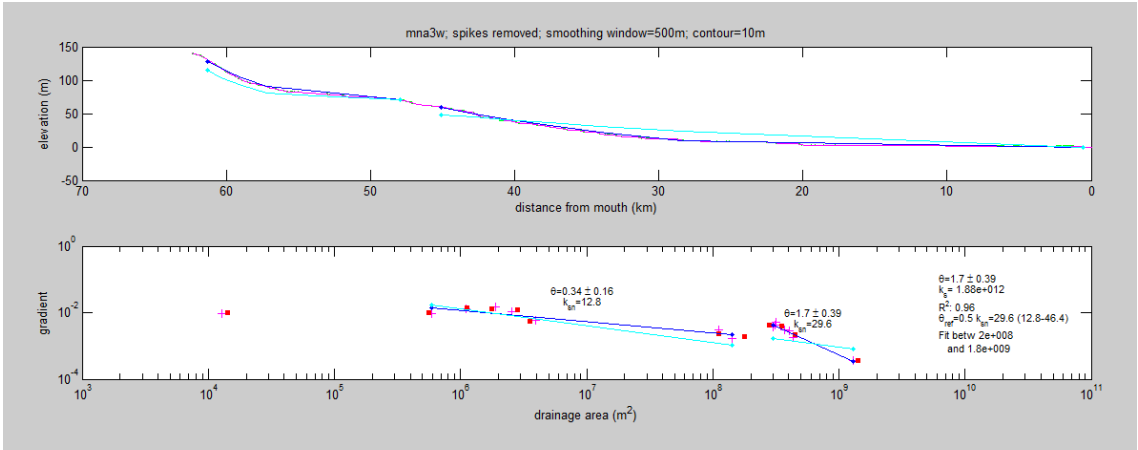

Longitudinal profile, area- length relationship, gradient-area relationship and values of concavity and Ksn obtained for channel 3w.

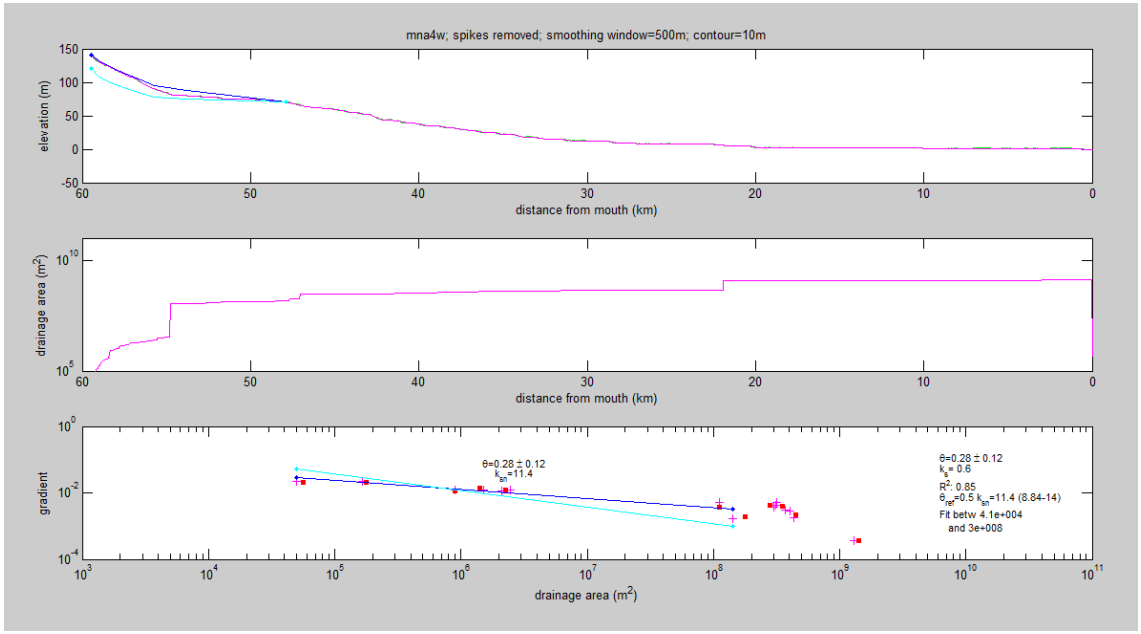
mna4w; spikes removed; smoothing window=500m; contour=10m
elevation (m)
distance from mouth (km)
drainage area (m²)
distance from mouth (km)
gradient
θ=0.28 ± 0.12
k_sn=11.4
θ=0.28 ± 0.12
k_s= 0.6
R²: 0.85
θ_ref=0.5 k_sn=11.4 (8.84-14)
Fit betw 4.1e+004
and 3e+008
drainage area (m²)

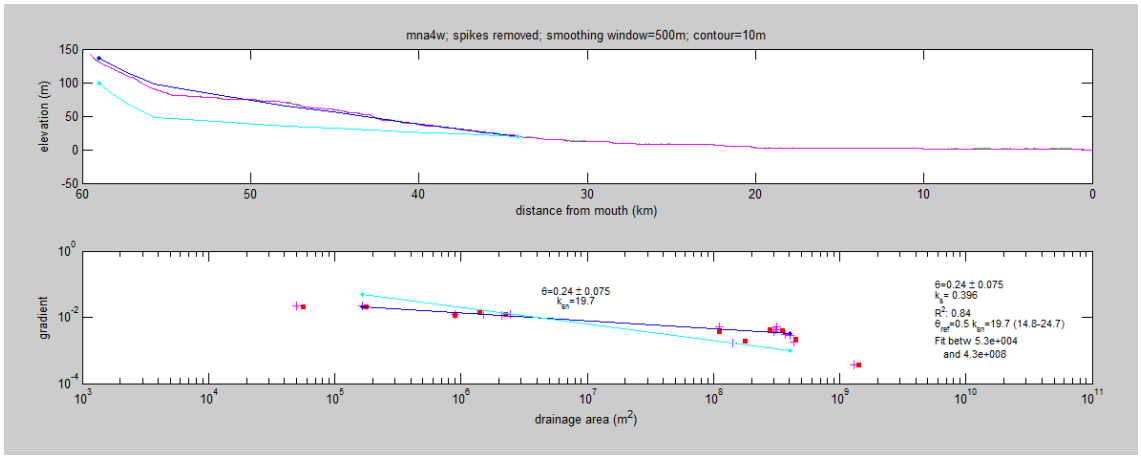
mna4w; spikes removed; smoothing window=500m; contour=10m
elevation (m)
distance from mouth (km)
gradient
θ=0.24 ± 0.075
k_sn=19.7
θ=0.24 ± 0.075
k_s= 0.396
R²: 0.84
θ_ref=0.5 k_sn=19.7 (14.8-24.7)
Fit betw 5.3e+004
and 4.3e+008
drainage area (m²)

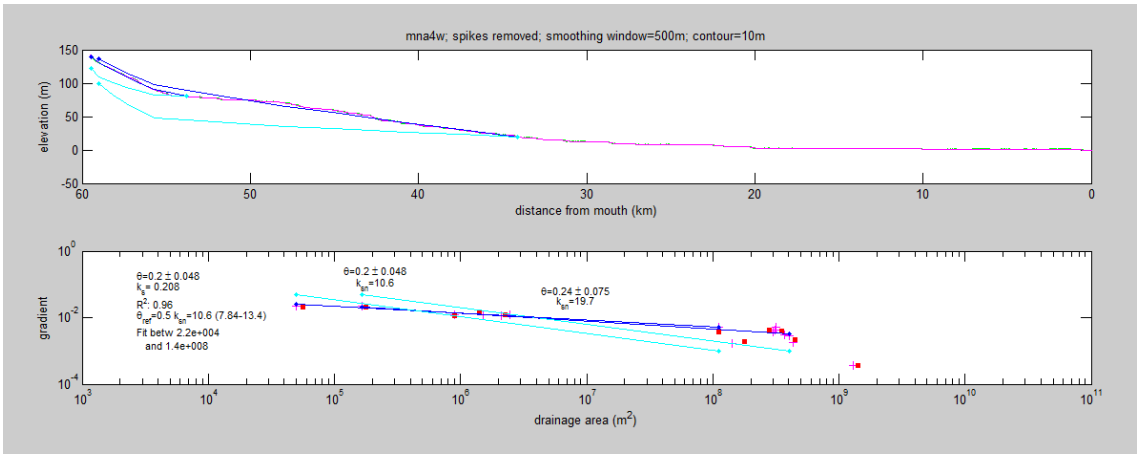
mna4w; spikes removed; smoothing window=500m; contour=10m
elevation (m)
distance from mouth (km)
gradient
θ=0.2 ± 0.048
k_s= 0.208
R²: 0.96
θ_ref=0.5 k_sn=10.6 (7.84-13.4)
Fit betw 2.2e+004
and 1.4e+008
θ=0.2 ± 0.048
k_sn=10.6
θ=0.24 ± 0.075
k_sn=19.7
drainage area (m²)

Longitudinal profile, area- length relationship, gradient-area relationship and values of concavity and Ksn obtained for channel 4w.

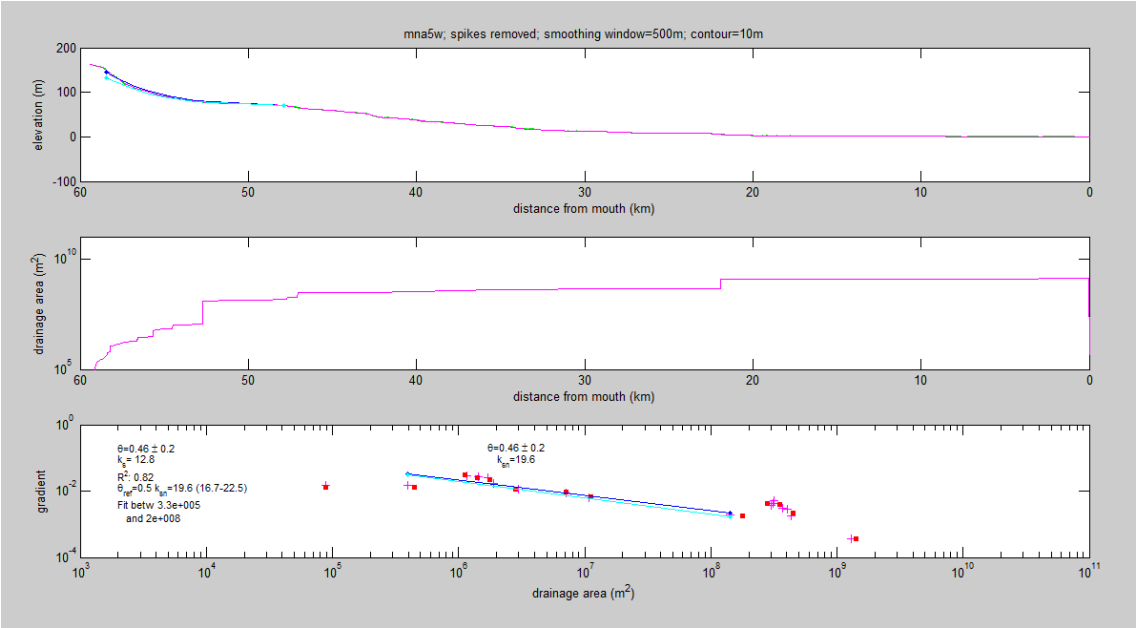

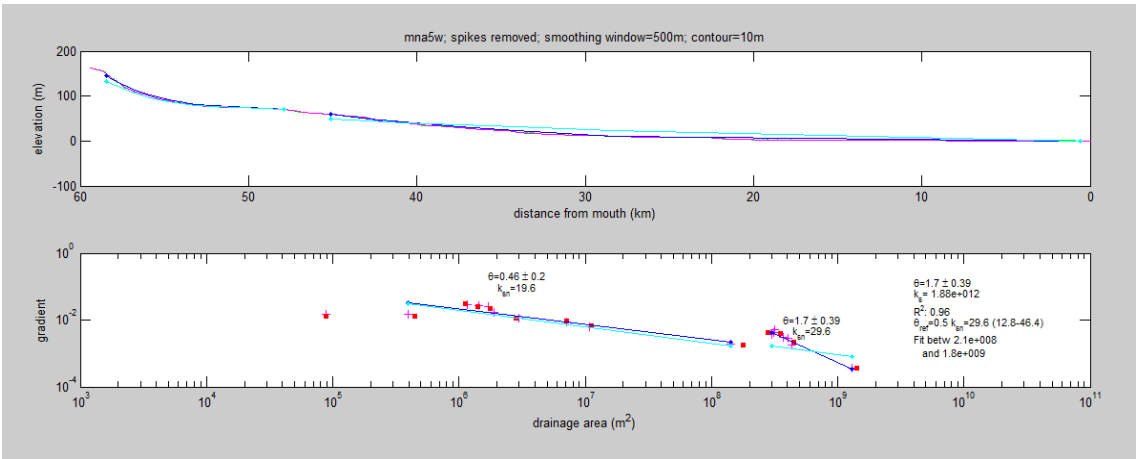

Longitudinal profile, area- length relationship, gradient-area relationship and values of concavity and Ksn obtained for channel 5w.

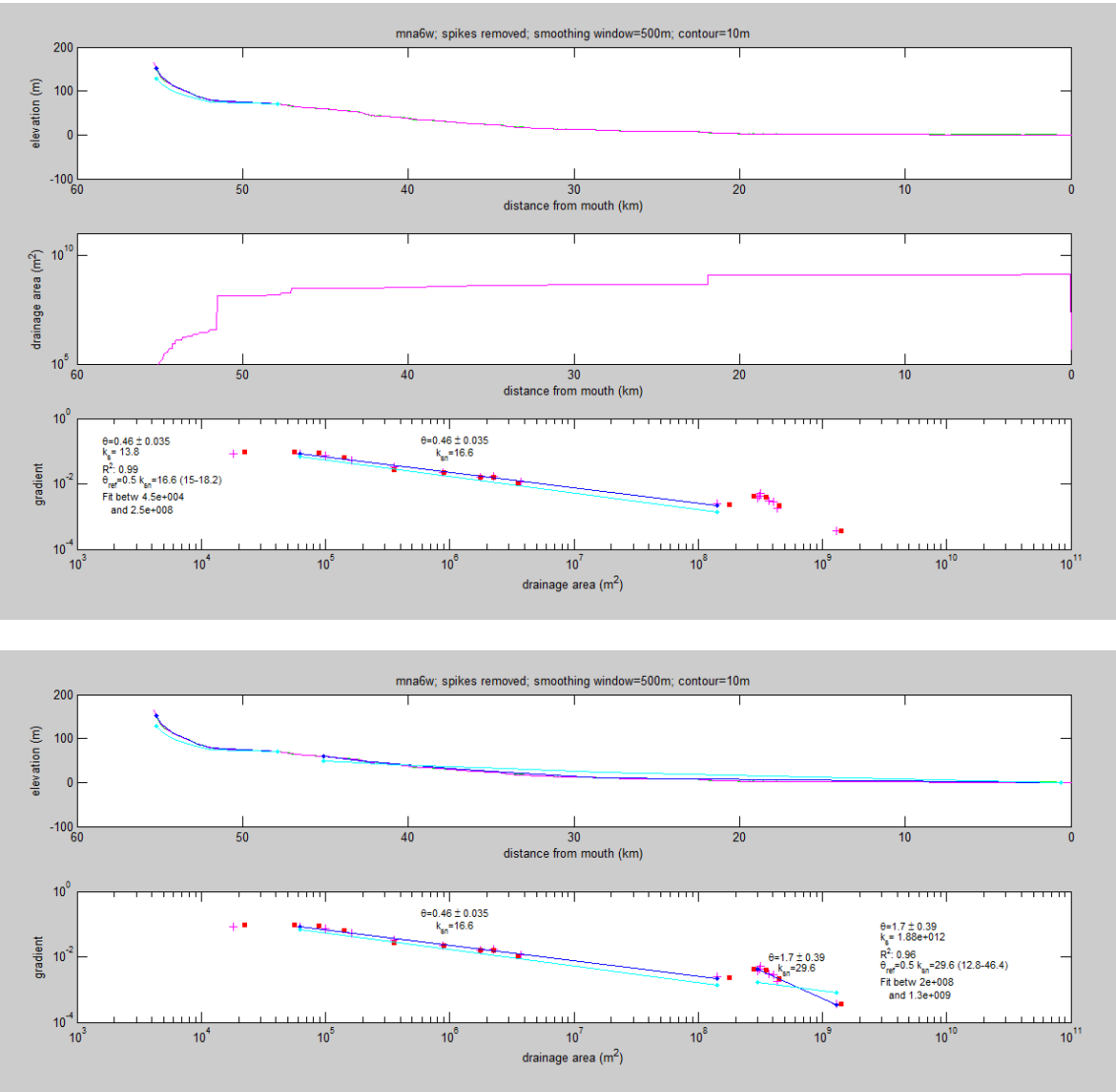

Longitudinal profile, area- length relationship, gradient-area relationship and values of concavity and Ksn obtained for channel 6w.

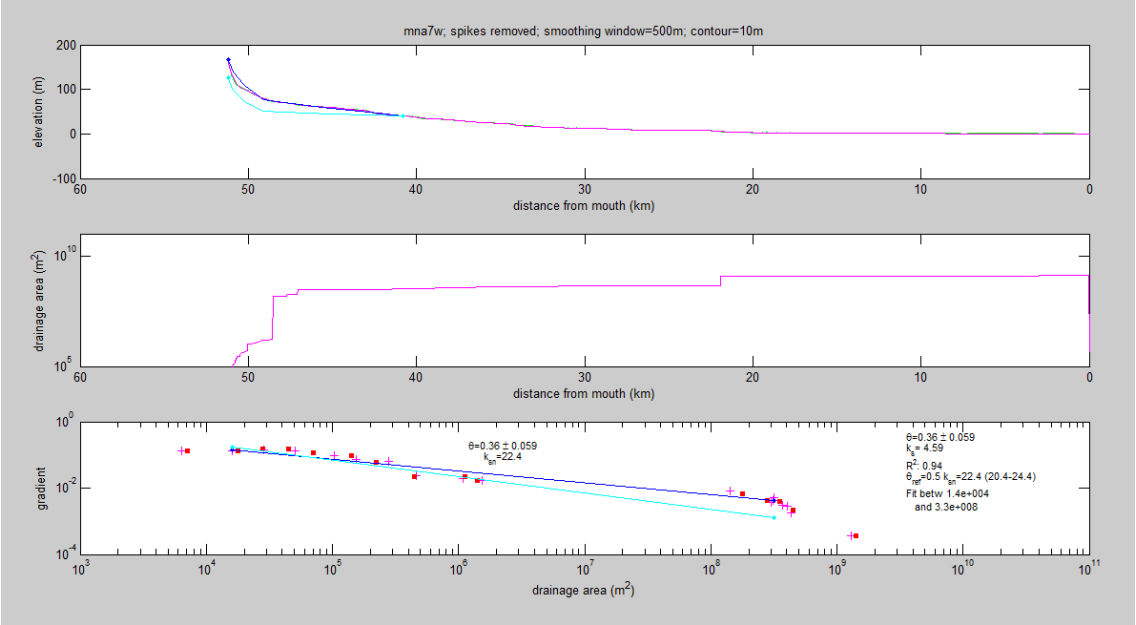
mna7w; spikes removed; smoothing window=500m; contour=10m
elevation (m)
distance from mouth (km)
drainage area (m²)
distance from mouth (km)
gradient
θ=0.36 ± 0.059
k_sn=22.4
θ=0.36 ± 0.059
k_s= 4.59
R²: 0.94
θ_ref=0.5 k_sn=22.4 (20.4-24.4)
Fit betw 1.4e+004
and 3.3e+008
drainage area (m²)

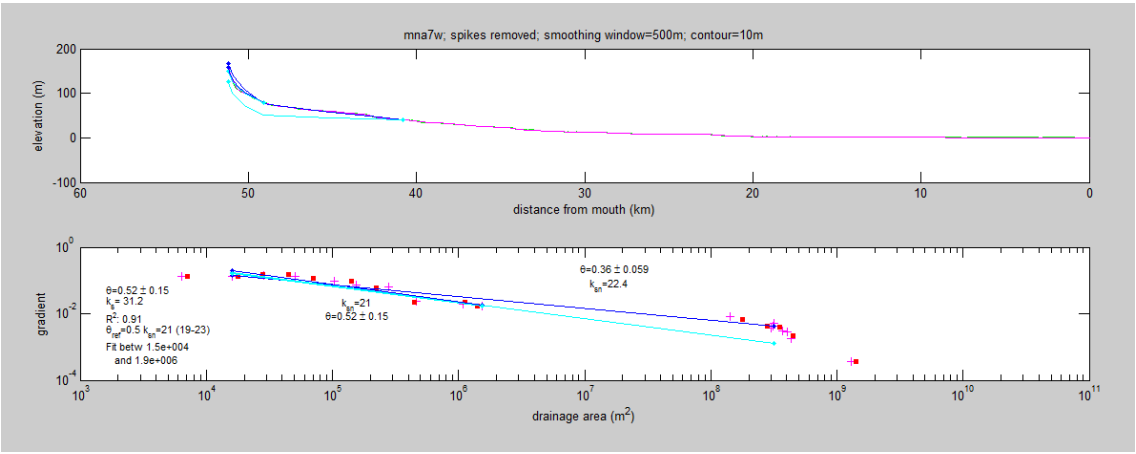
mna7w; spikes removed; smoothing window=500m; contour=10m
elevation (m)
distance from mouth (km)
gradient
θ=0.52 ± 0.15
k_s= 31.2
R²: 0.91
θ_ref=0.5 k_sn=21 (19-23)
Fit betw 1.5e+004
and 1.9e+006
k_sn=21
θ=0.52 ± 0.15
θ=0.36 ± 0.059
k_sn=22.4
drainage area (m²)

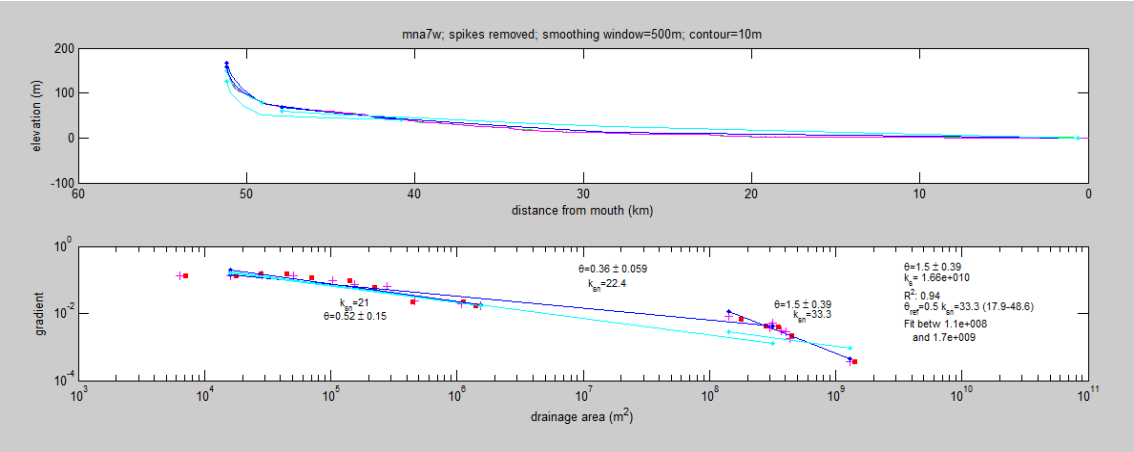

Longitudinal profile, area- length relationship, gradient-area relationship and values of concavity and Ksn obtained for channel 7w.

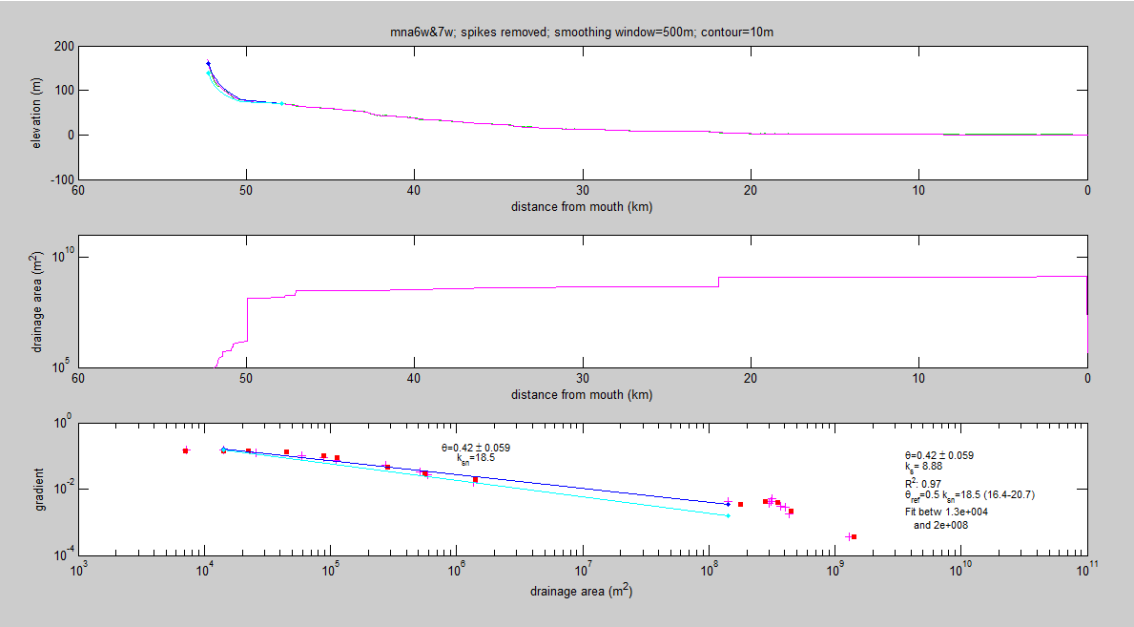

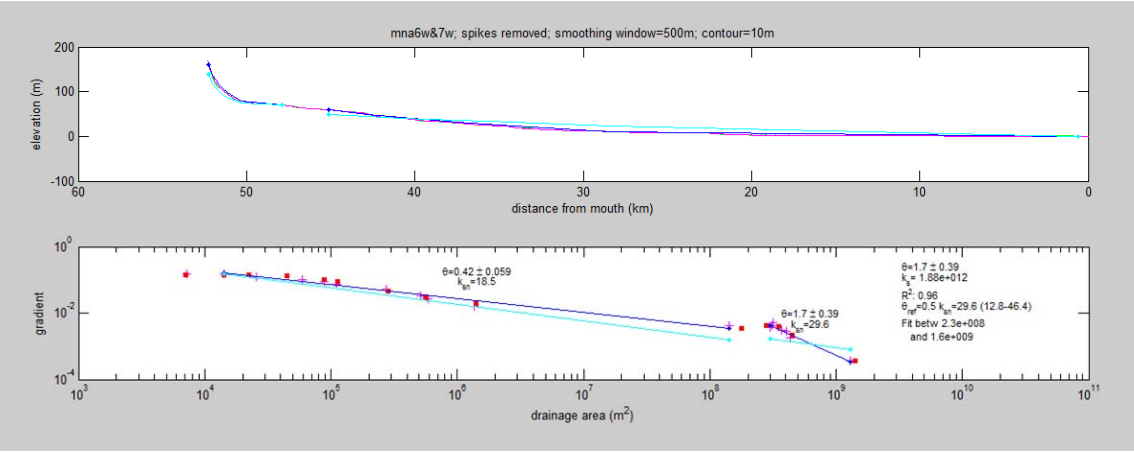

Longitudinal profile, area- length relationship, gradient-area relationship and values of concavity and Ksn obtained for channel 6w & 7w.

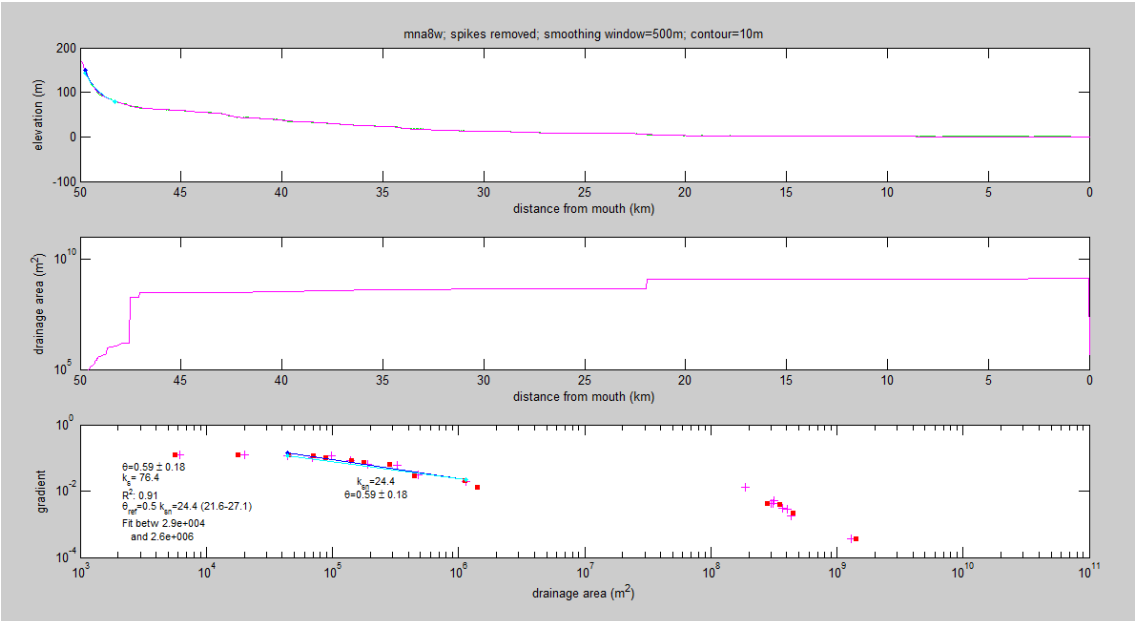

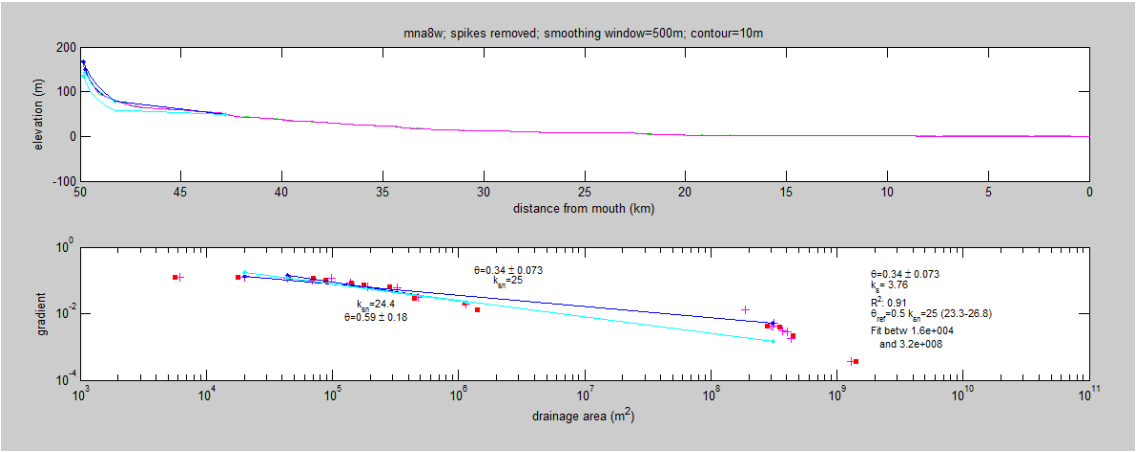

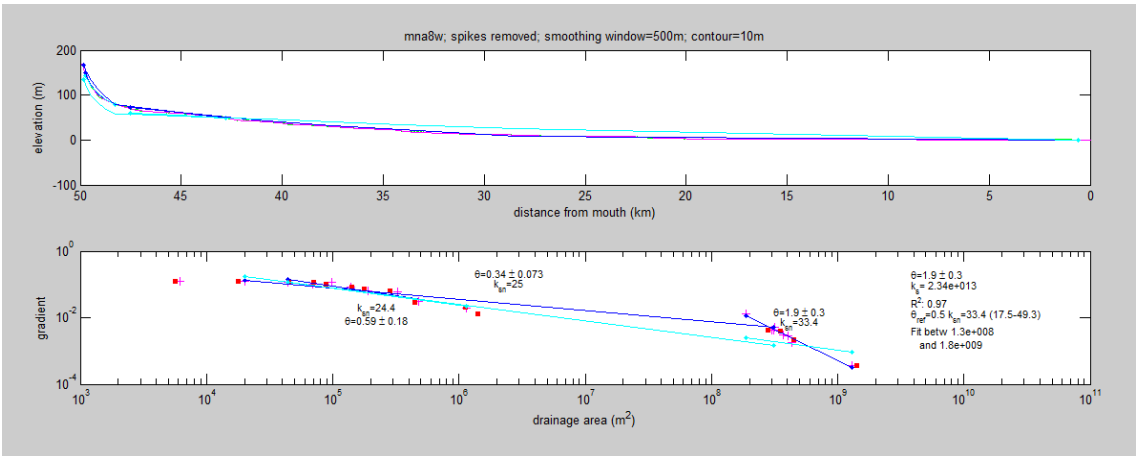

Longitudinal profile, area- length relationship, gradient-area relationship and values of concavity and Ksn obtained for channel 8w.

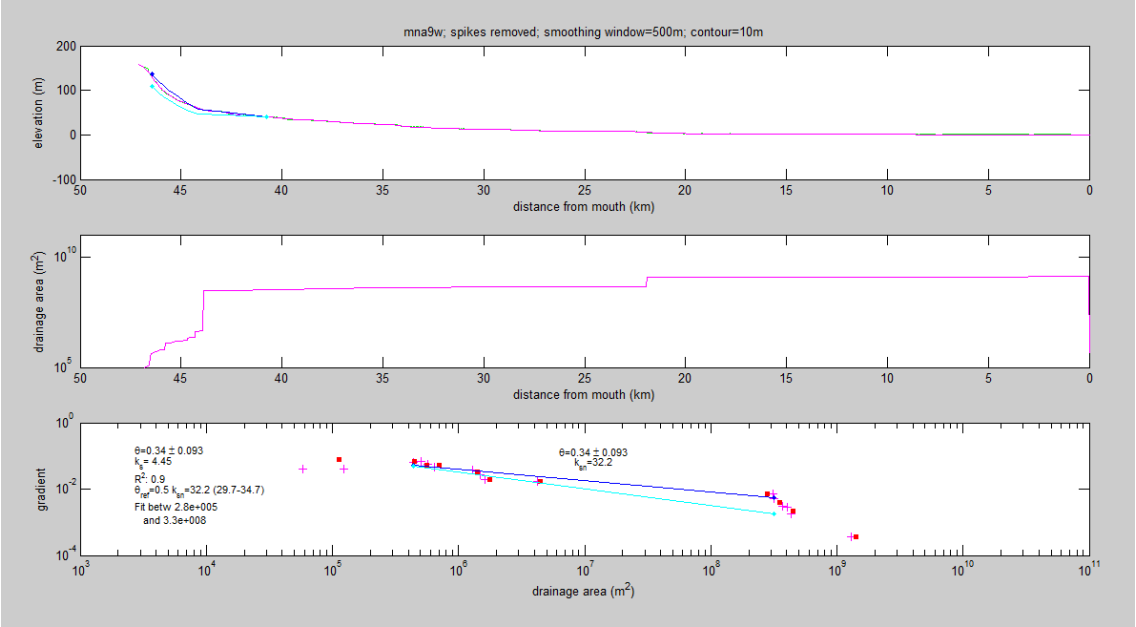

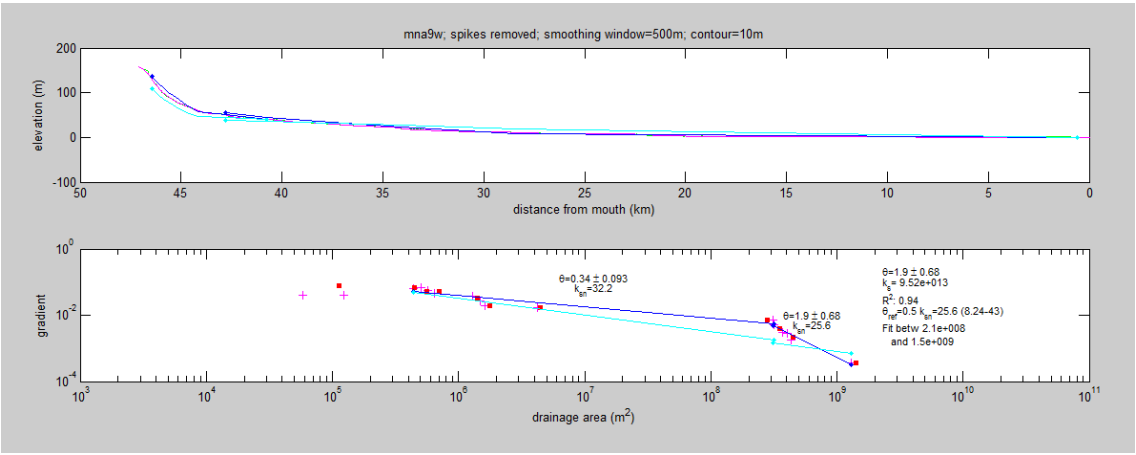

Longitudinal profile, area- length relationship, gradient-area relationship and values of concavity and Ksn obtained for channel 9w.

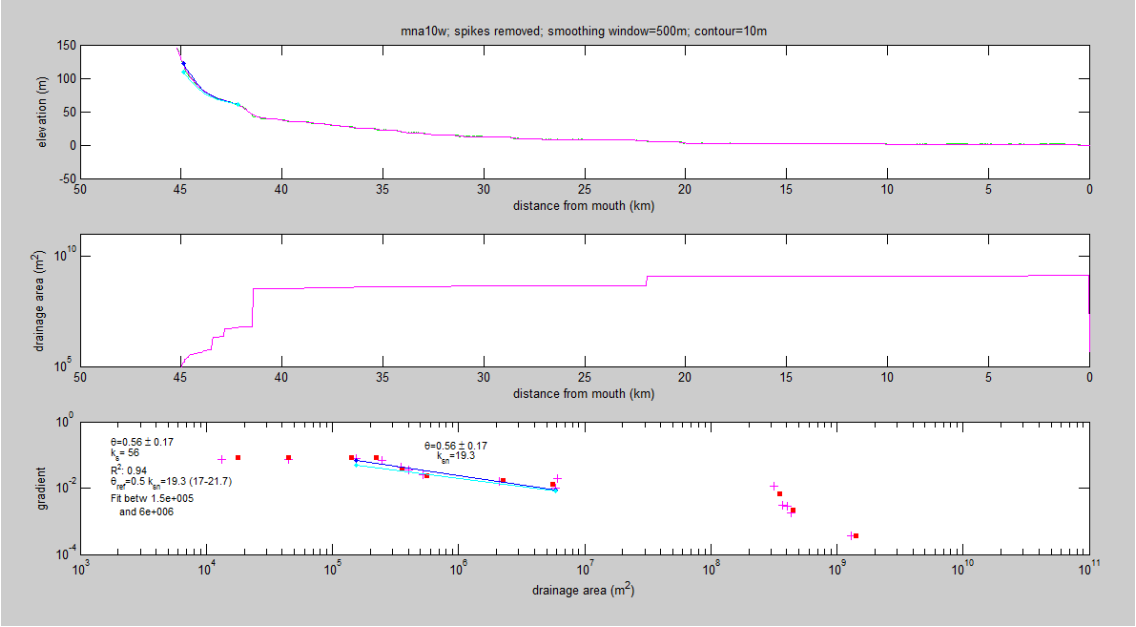

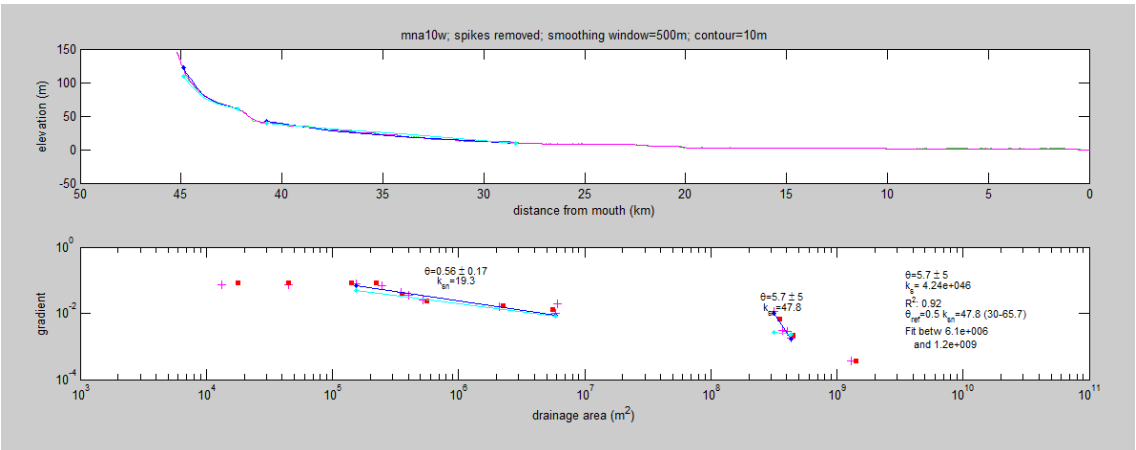

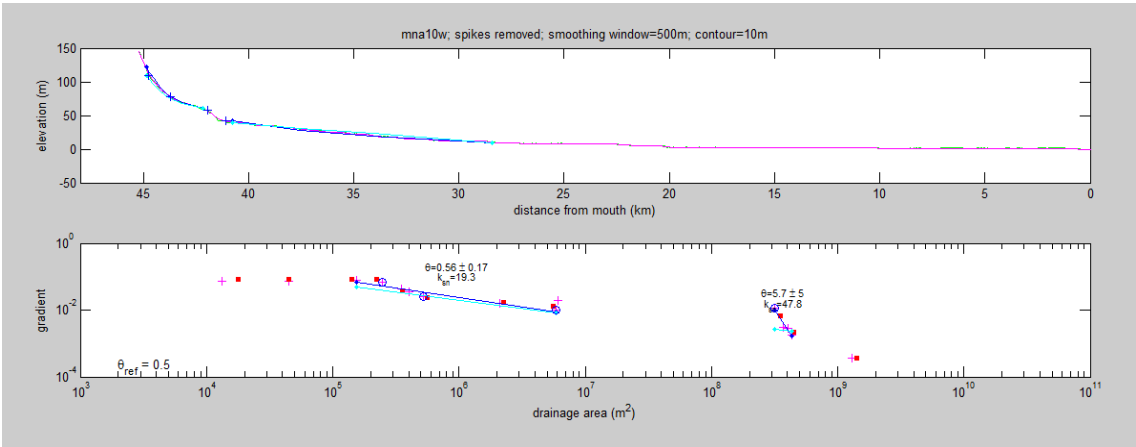

Longitudinal profile, area- length relationship, gradient-area relationship and values of concavity and Ksn obtained for channel 10w.

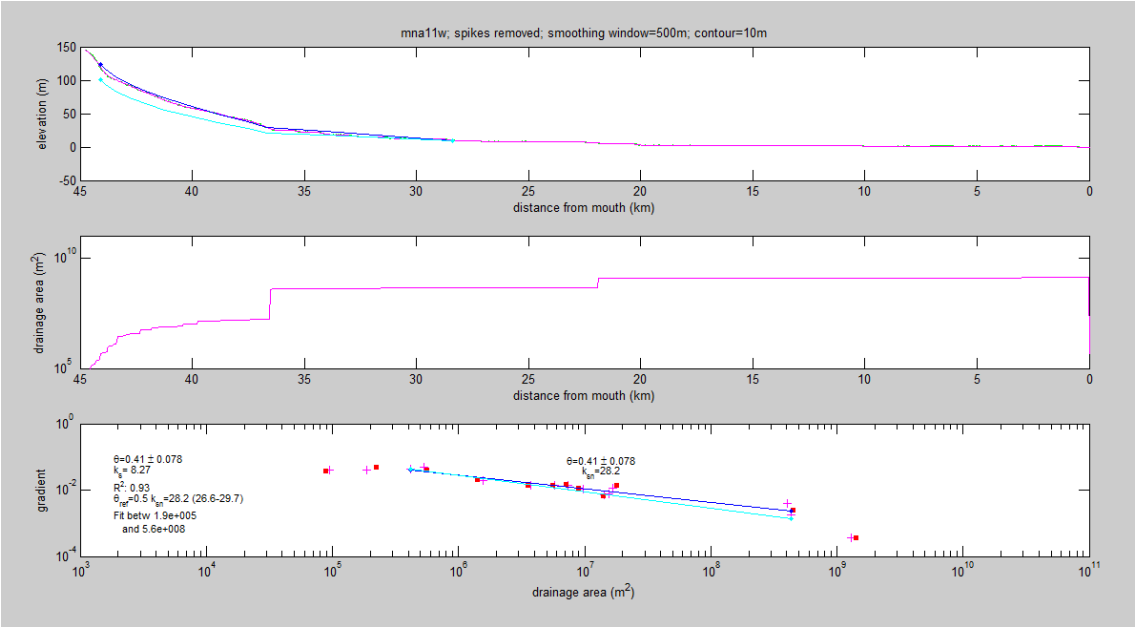

Longitudinal profile, area- length relationship, gradient-area relationship and values of concavity and Ksn obtained for channel 11w.

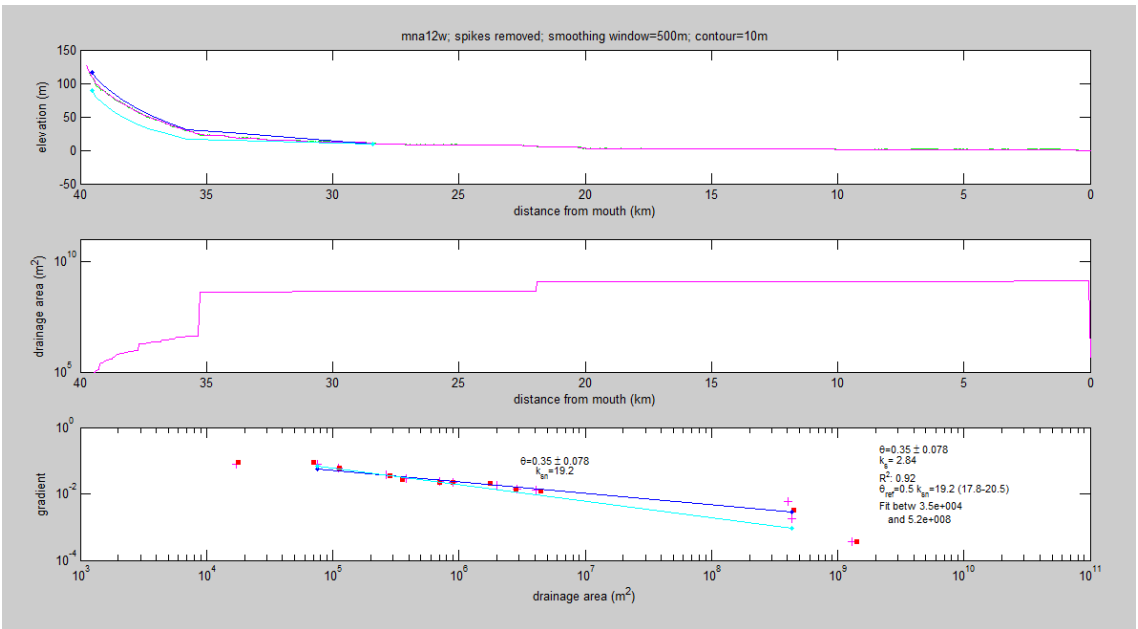

Longitudinal profile, area- length relationship, gradient-area relationship and values of concavity and Ksn obtained for channel 12w.

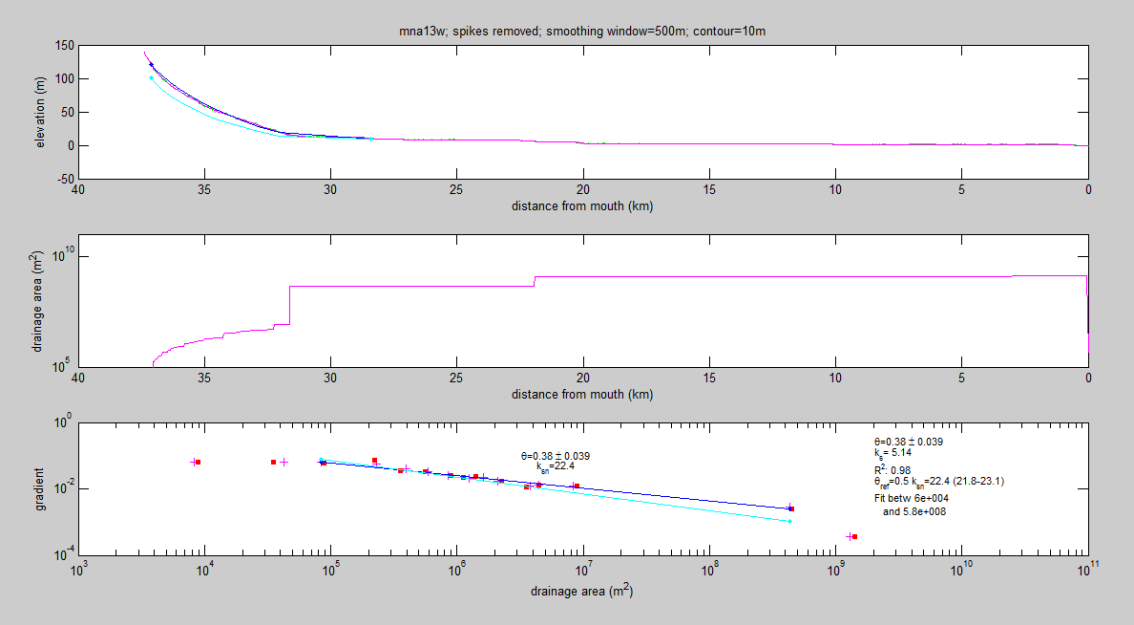

Longitudinal profile, area- length relationship, gradient-area relationship and values of concavity and Ksn obtained for channel 13w.

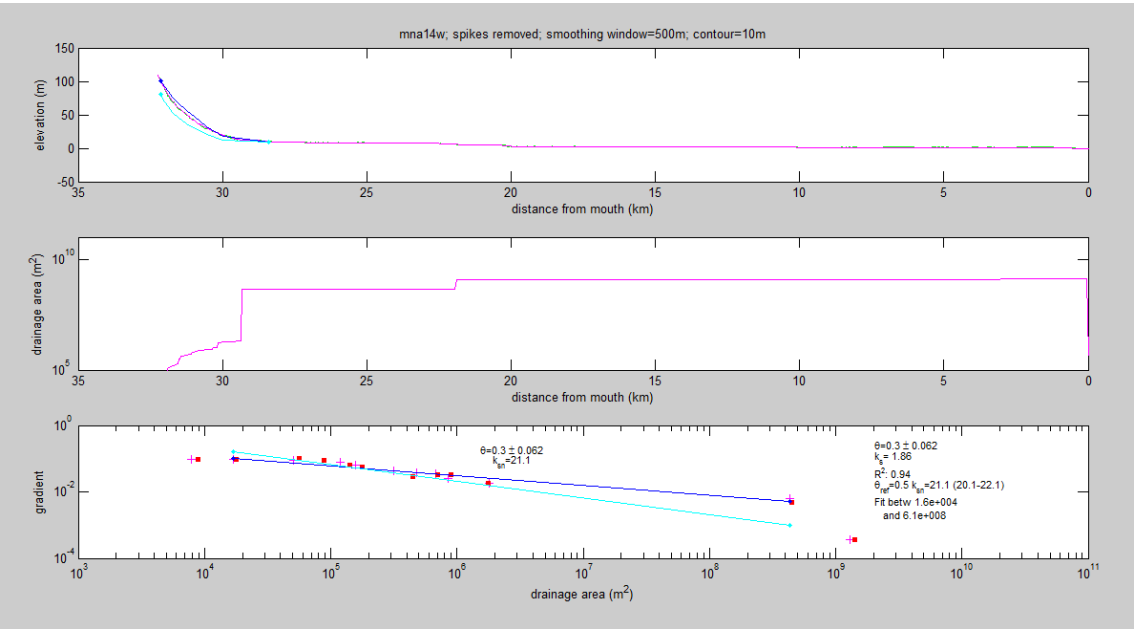

Longitudinal profile, area- length relationship, gradient-area relationship and values of concavity and Ksn obtained for channel 14w.

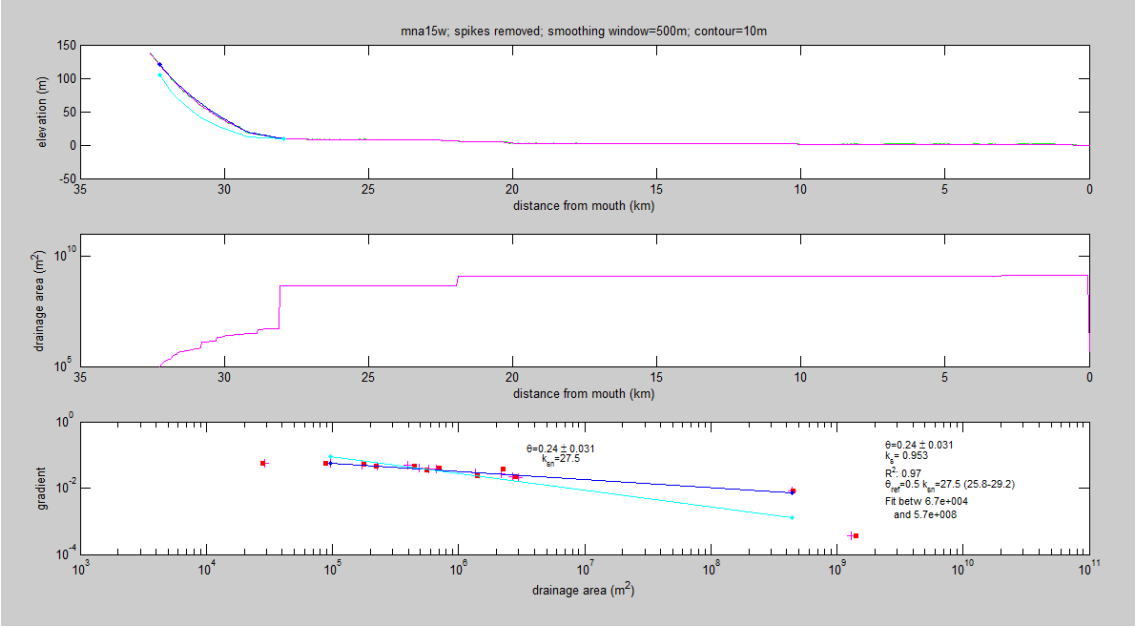

Longitudinal profile, area- length relationship, gradient-area relationship and values of concavity and Ksn obtained for channel 15w.

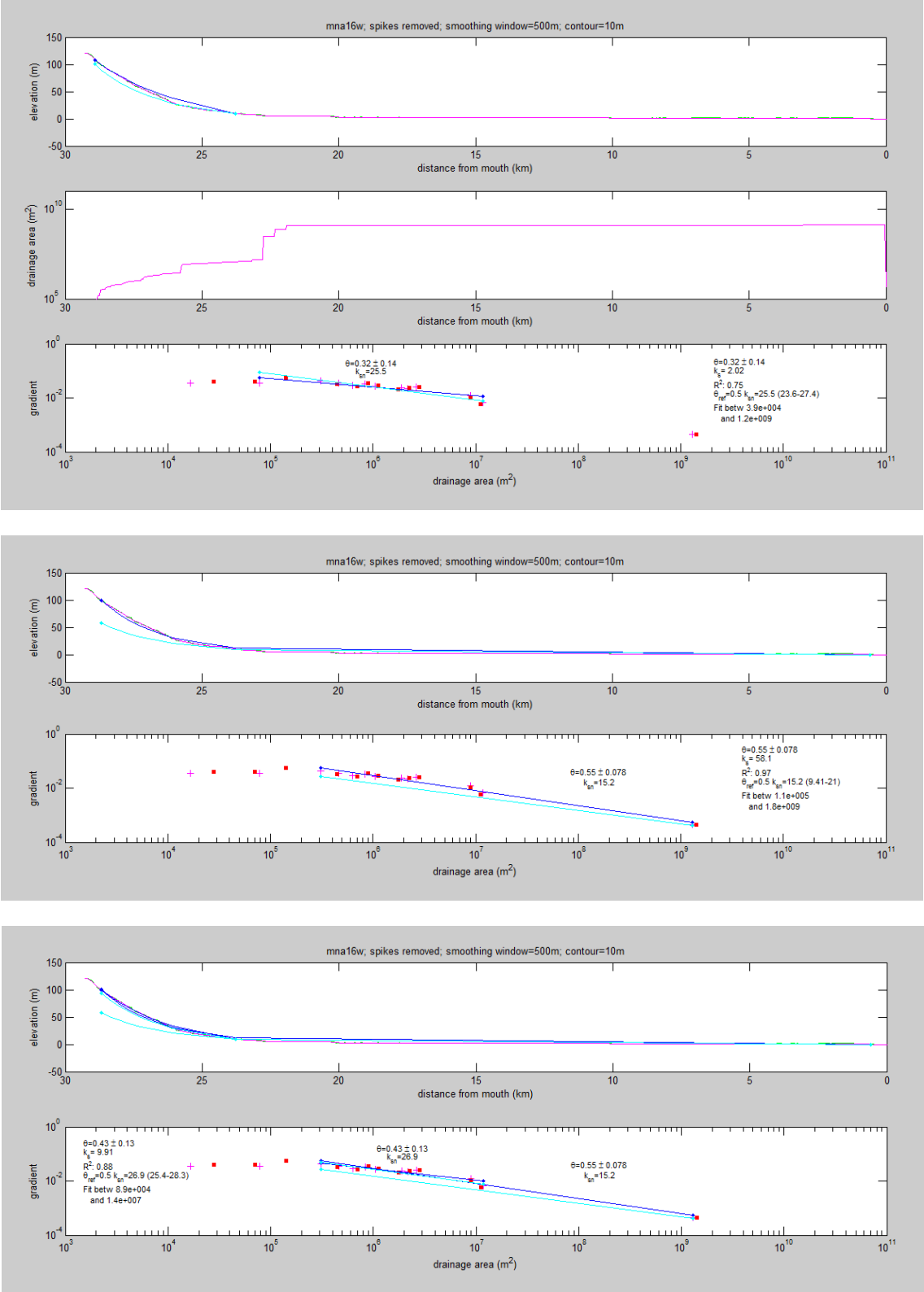

Longitudinal profile, area- length relationship, gradient-area relationship and values of concavity and Ksn obtained for channel 16w.

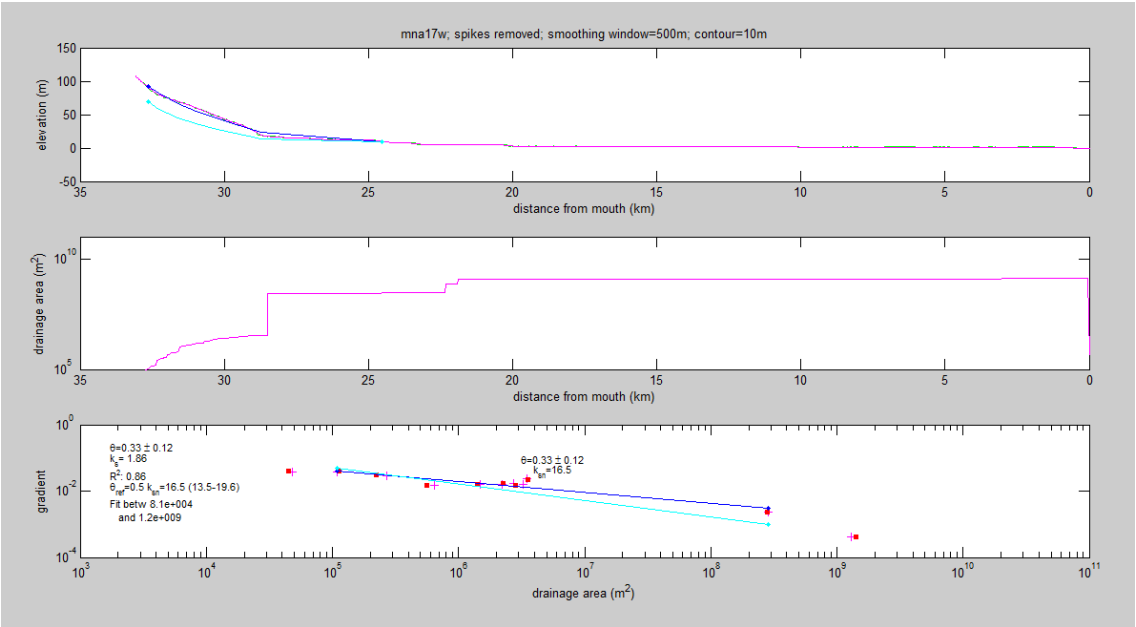
mna17w; spikes removed; smoothing window=500m; contour=10m
elevation (m)
distance from mouth (km)
drainage area (m²)
distance from mouth (km)
gradient
θ=0.33 ± 0.12
k_s= 1.86
R²: 0.86
θ_ref=0.5 k_sn=16.5 (13.5-19.6)
Fit betw 8.1e+004
and 1.2e+009
θ=0.33 ± 0.12
k_sn=16.5
drainage area (m²)

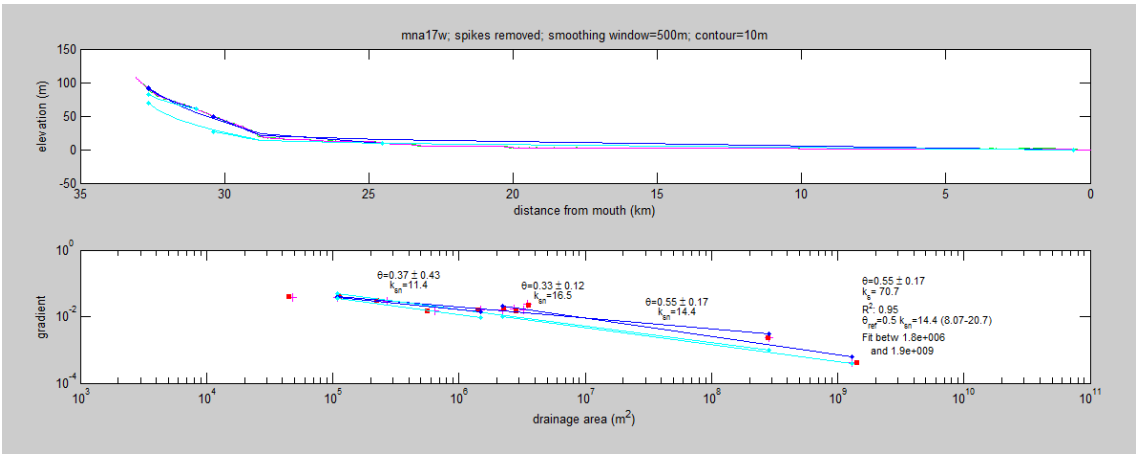
mna17w; spikes removed; smoothing window=500m; contour=10m
elevation (m)
distance from mouth (km)
gradient
θ=0.37 ± 0.43
k_sn=11.4
θ=0.33 ± 0.12
k_sn=16.5
θ=0.55 ± 0.17
k_sn=14.4
θ=0.55 ± 0.17
k_s= 70.7
R²: 0.95
θ_ref=0.5 k_sn=14.4 (8.07-20.7)
Fit betw 1.8e+006
and 1.9e+009
drainage area (m²)

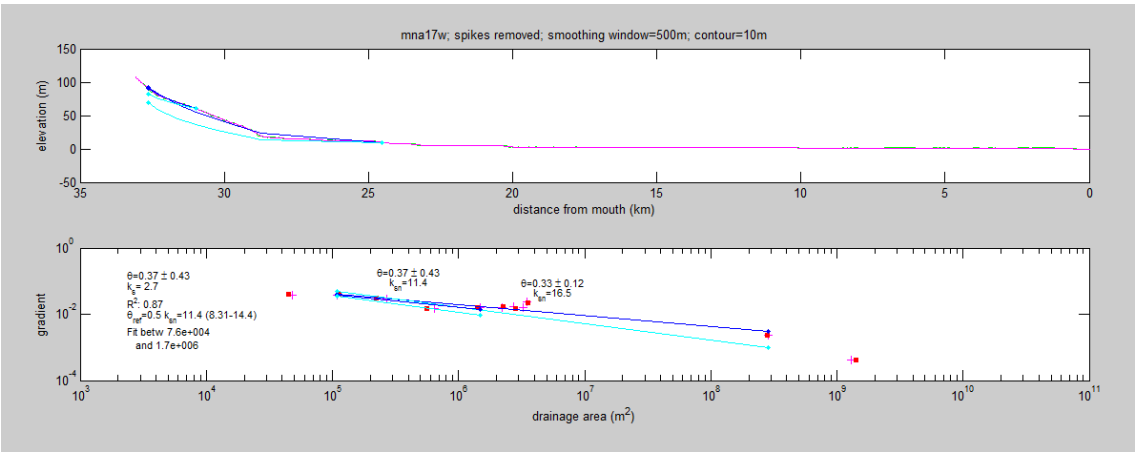
mna17w; spikes removed; smoothing window=500m; contour=10m
elevation (m)
distance from mouth (km)
gradient
θ=0.37 ± 0.43
k_s= 2.7
R²: 0.87
θ_ref=0.5 k_sn=11.4 (8.31-14.4)
Fit betw 7.6e+004
and 1.7e+006
θ=0.37 ± 0.43
k_sn=11.4
θ=0.33 ± 0.12
k_sn=16.5
drainage area (m²)

Longitudinal profile, area- length relationship, gradient-area relationship and values of concavity and Ksn obtained for channel 17w.

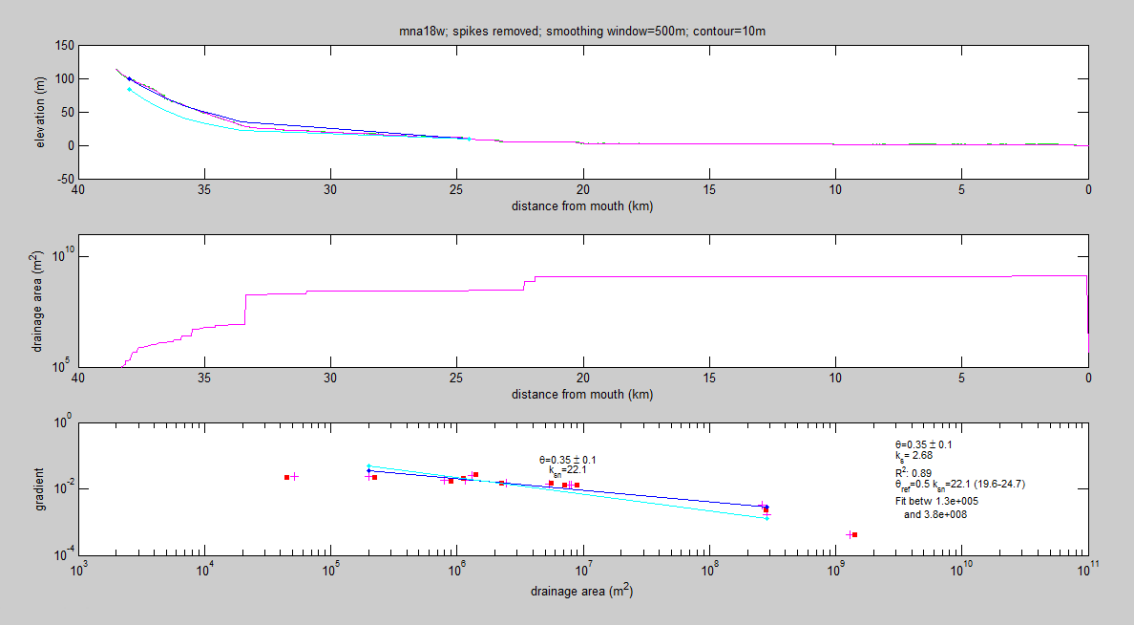

Longitudinal profile, area- length relationship, gradient-area relationship and values of concavity and Ksn obtained for channel 18w.

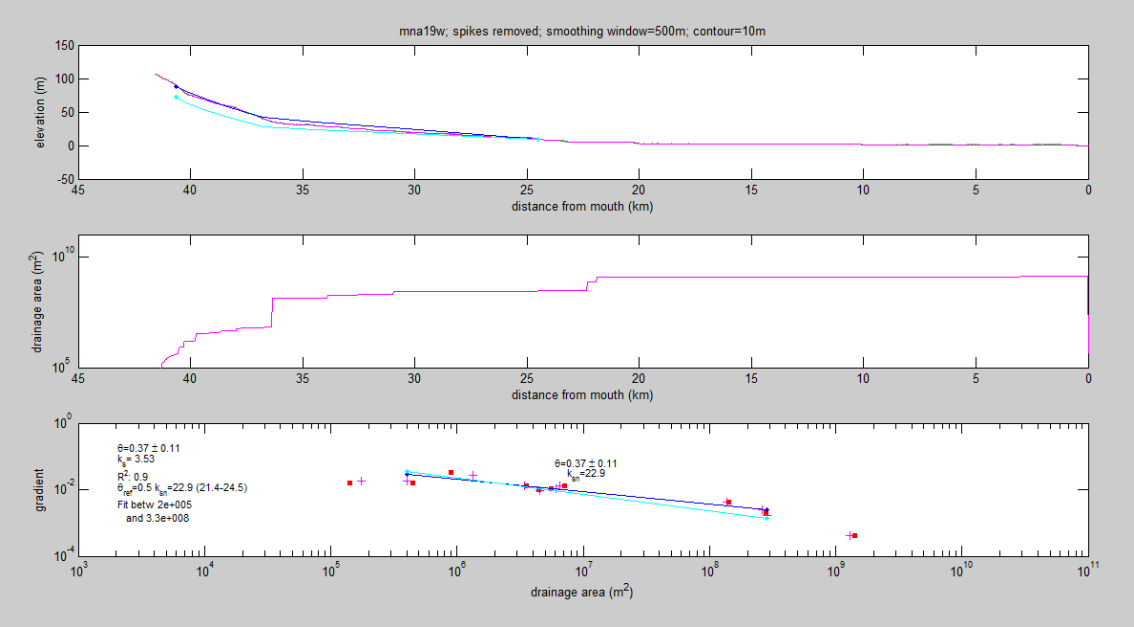

Longitudinal profile, area- length relationship, gradient-area relationship and values of concavity and Ksn obtained for channel 19w.

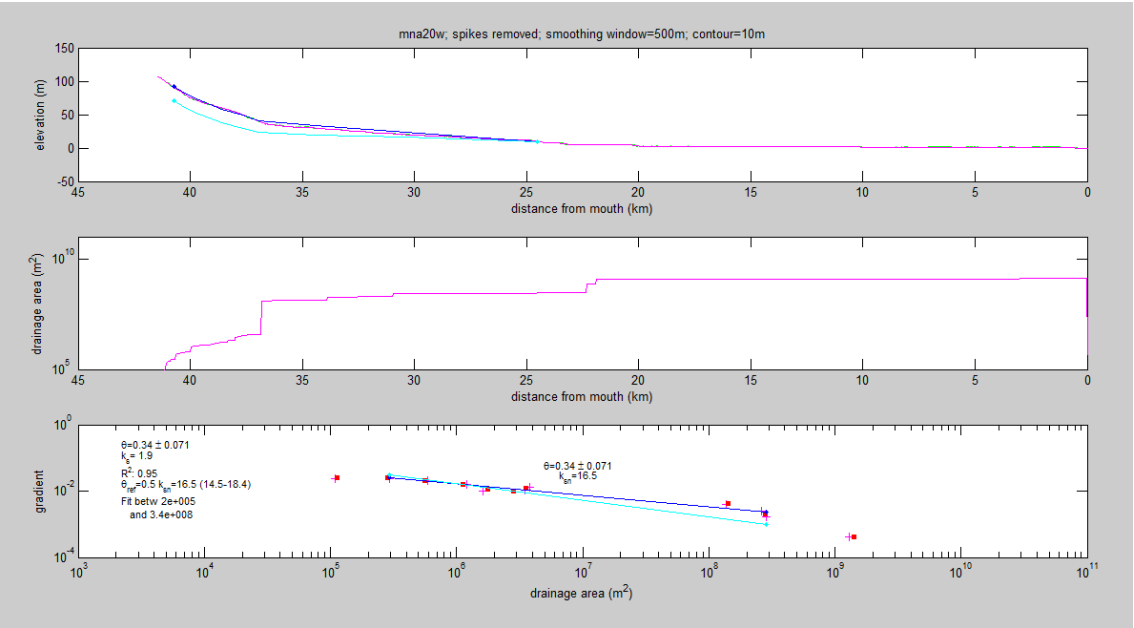

Longitudinal profile, area- length relationship, gradient-area relationship and values of concavity and Ksn obtained for channel 20w.

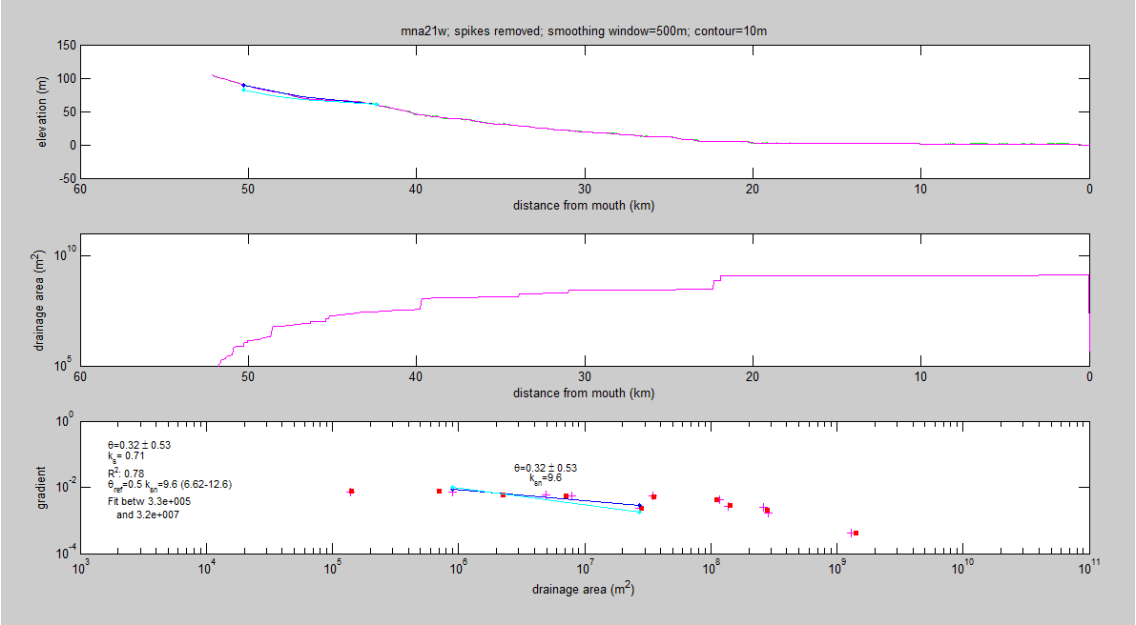
mna21w; spikes removed; smoothing window=500m; contour=10m
elevation (m)
distance from mouth (km)
drainage area (m²)
distance from mouth (km)
gradient
θ=0.32 ± 0.53
k_s= 0.71
R²: 0.78
θ_ref=0.5 k_sn=9.6 (6.62-12.6)
Fit betw 3.3e+005
and 3.2e+007
θ=0.32 ± 0.53
k_sn=9.6
drainage area (m²)

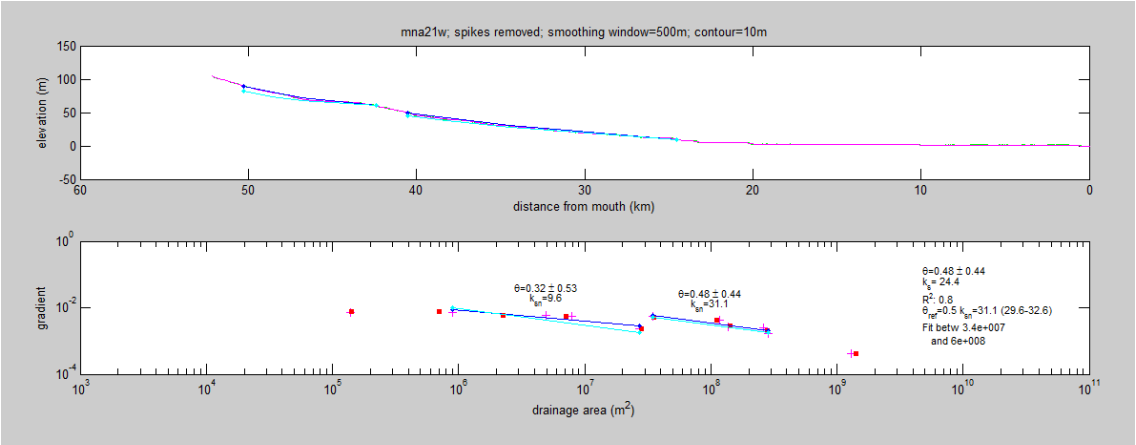

Longitudinal profile, area- length relationship, gradient-area relationship and values of concavity and Ksn obtained for channel 21w.

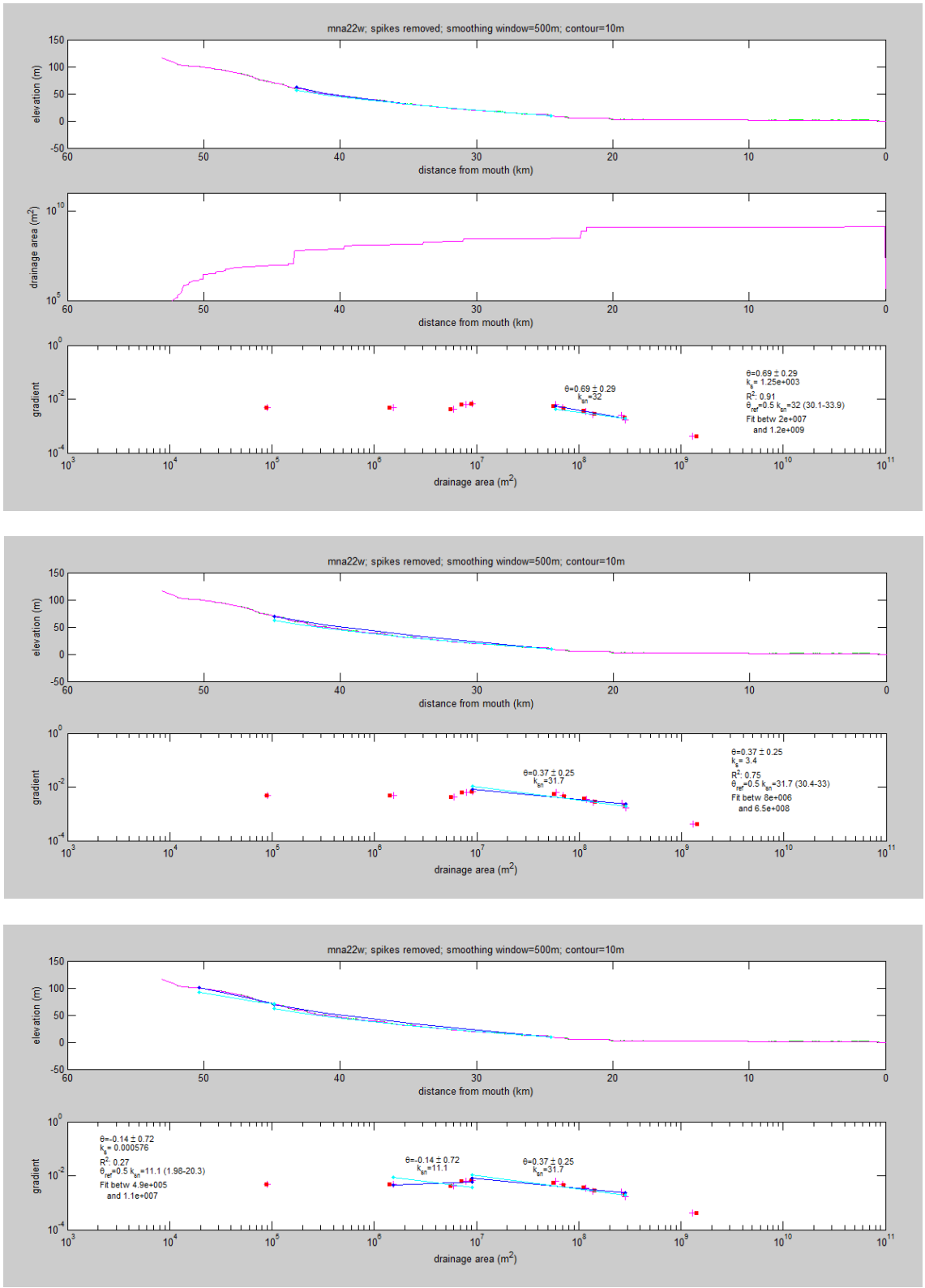

Longitudinal profile, area- length relationship, gradient-area relationship and values of concavity and Ksn obtained for channel 22w.

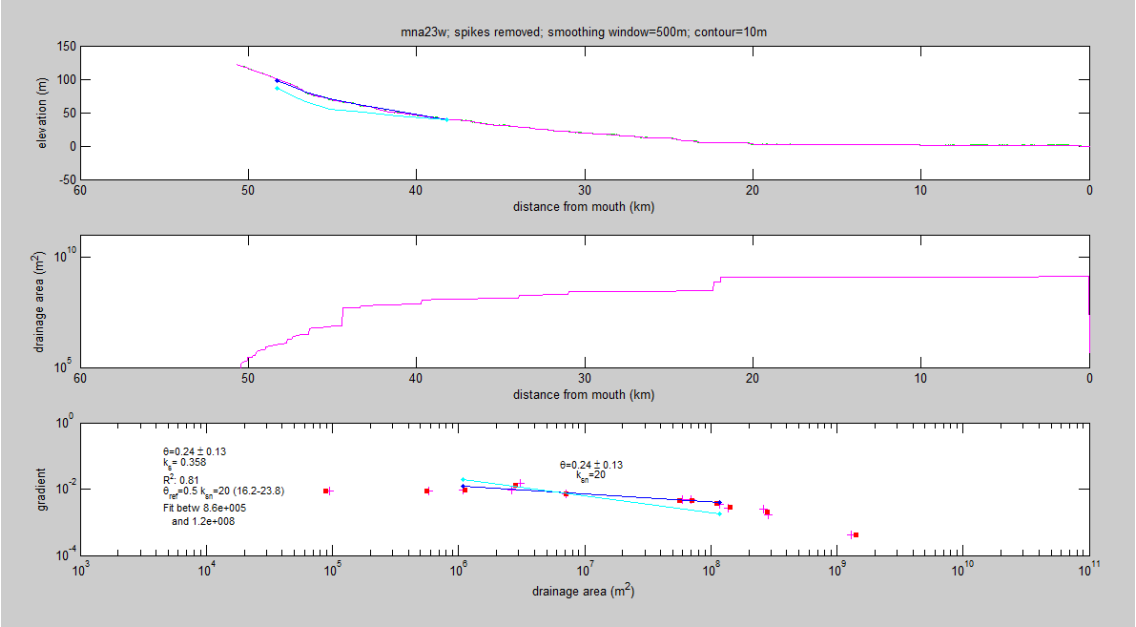

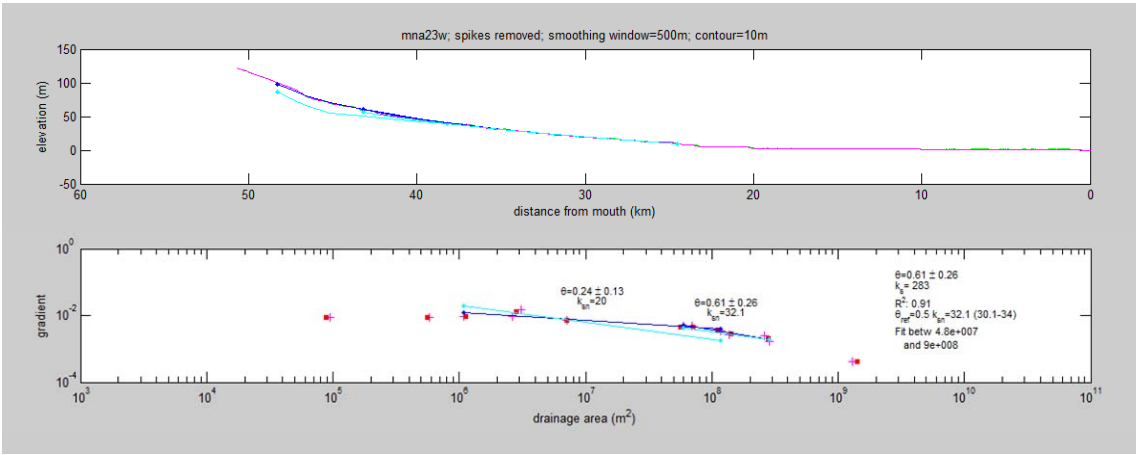

Longitudinal profile, area- length relationship, gradient-area relationship and values of concavity and Ksn obtained for channel 23w.

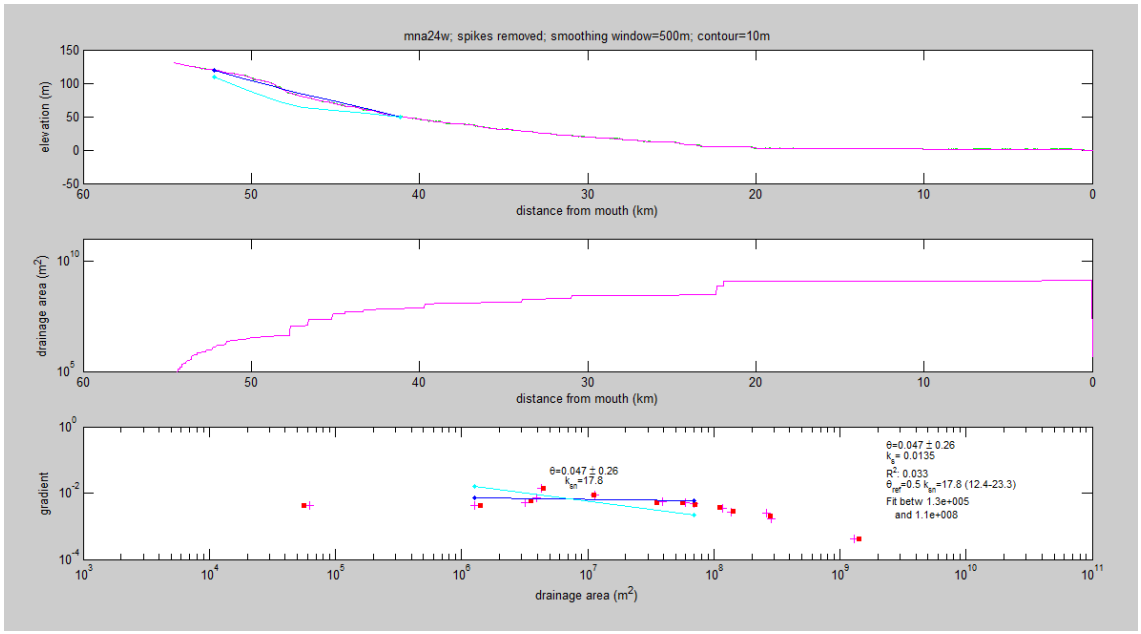

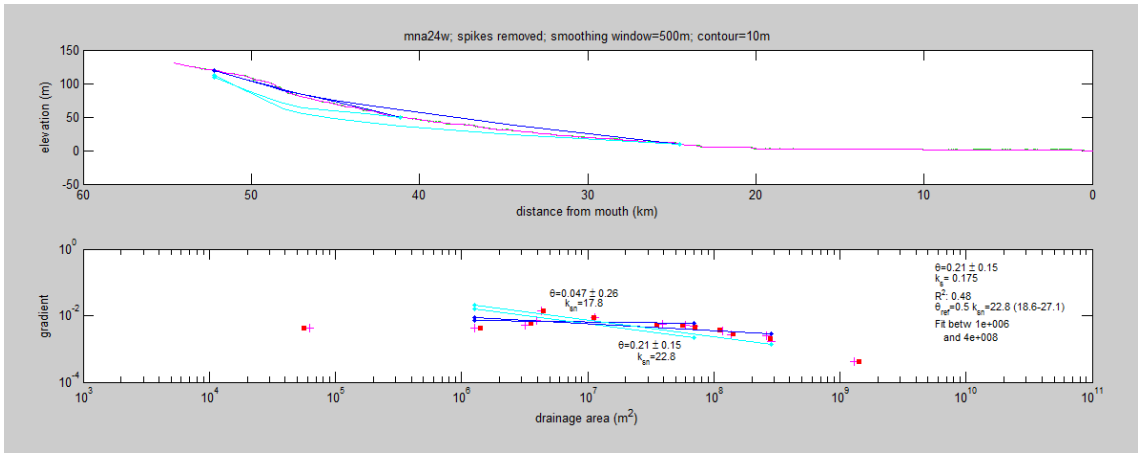

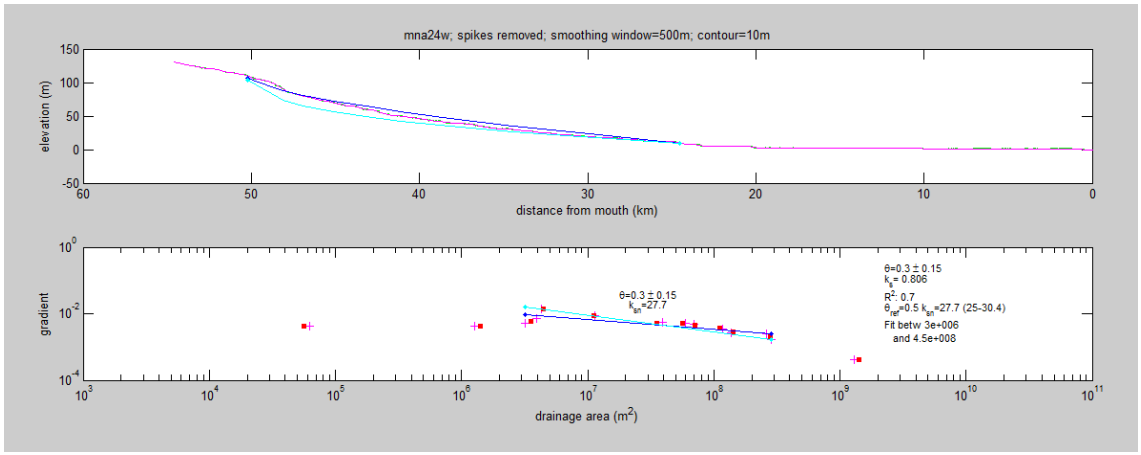

Longitudinal profile, area- length relationship, gradient-area relationship and values of concavity and Ksn obtained for channel 24w.

Annex III

Longitudinal Profiles for Tributary Drainages

(Aljezur River Basin)

Annex III

Longitudinal Profiles for Tributary Drainages (Aljezur River Basin)

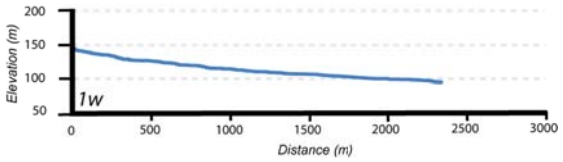

Longitudinal drainage profile for basin 1w (Vertical exaggeration 5x)

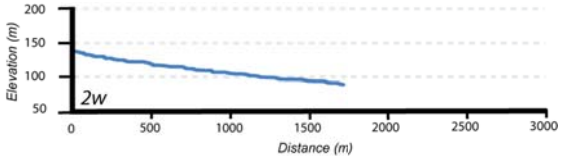

Longitudinal drainage profile for basin 2w (Vertical exaggeration 5x)

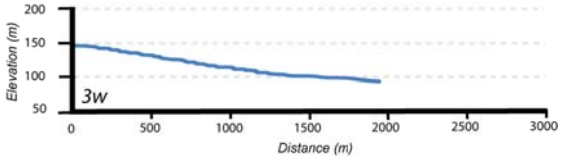

Longitudinal drainage profile for basin 3w (Vertical exaggeration 5x)

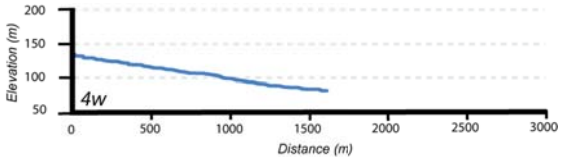

Longitudinal drainage profile for basin 4w (Vertical exaggeration 5x)

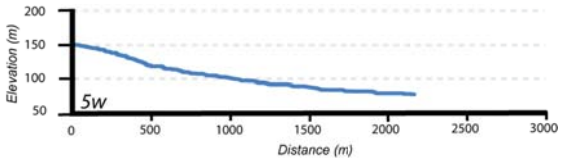

Longitudinal drainage profile for basin 5w (Vertical exaggeration 5x)

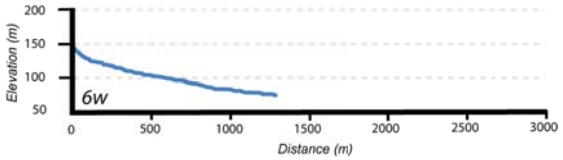

Longitudinal drainage profile for basin 6w (Vertical exaggeration 5x)

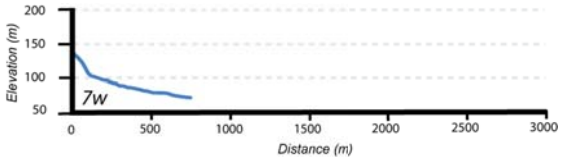

Longitudinal drainage profile for basin 7w (Vertical exaggeration 5x)

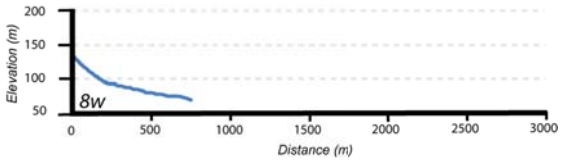

Longitudinal drainage profile for basin 8w (Vertical exaggeration 5x)

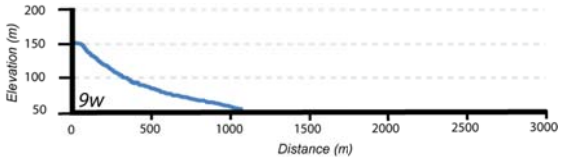

Longitudinal drainage profile for basin 9w (Vertical exaggeration 5x)

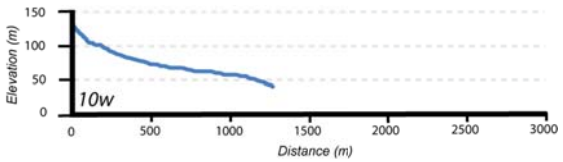

Longitudinal drainage profile for basin 10w (Vertical exaggeration 5x)

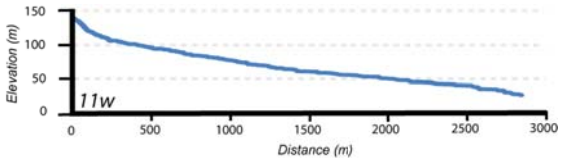

Longitudinal drainage profile for basin 11w (Vertical exaggeration 5x)

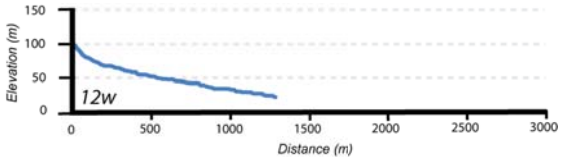

Longitudinal drainage profile for basin 12w (Vertical exaggeration 5x)

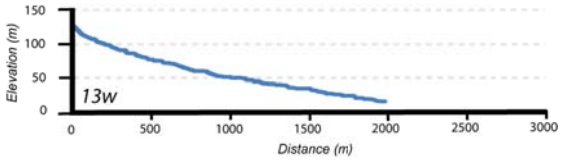

Longitudinal drainage profile for basin 13w (Vertical exaggeration 5x)

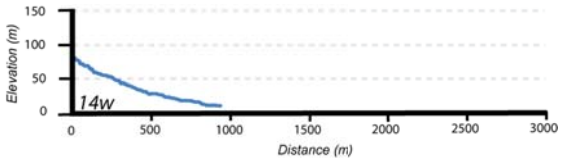

Longitudinal drainage profile for basin 14w (Vertical exaggeration 5x)

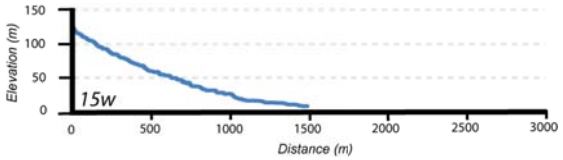

Longitudinal drainage profile for basin 15w (Vertical exaggeration 5x)

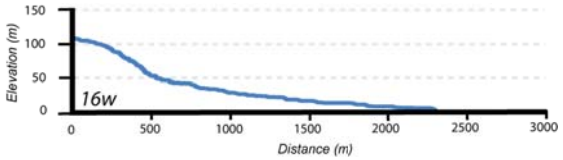

Longitudinal drainage profile for basin 16w (Vertical exaggeration 5x)

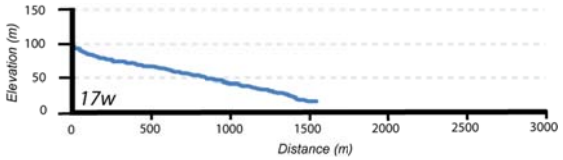

Longitudinal drainage profile for basin 17w (Vertical exaggeration 5x)

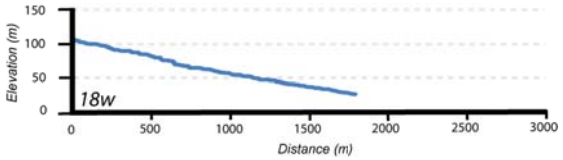

Longitudinal drainage profile for basin 18w (Vertical exaggeration 5x)

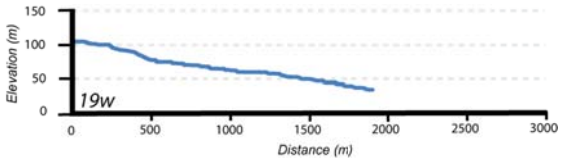

Longitudinal drainage profile for basin 19w (Vertical exaggeration 5x)

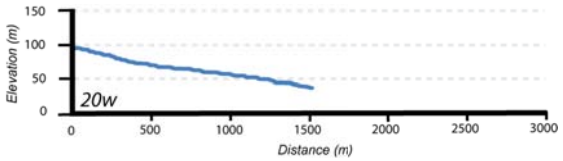

Longitudinal drainage profile for basin 20w (Vertical exaggeration 5x)

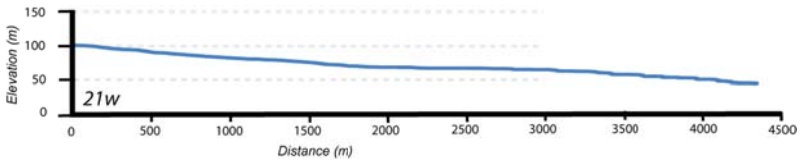

Longitudinal drainage profile for basin 21w (Vertical exaggeration 5x)

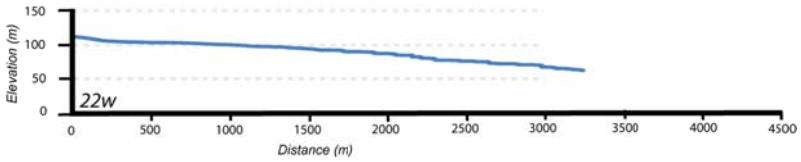

Longitudinal drainage profile for basin 22w (Vertical exaggeration 5x)

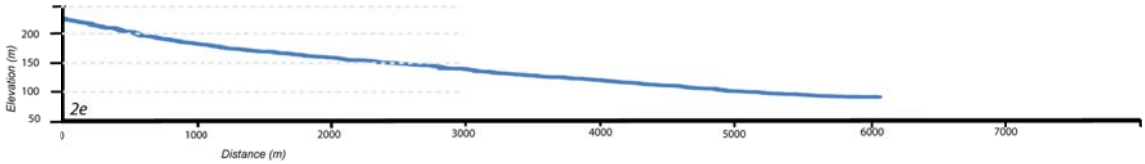

Longitudinal drainage profile for basin 2e (Vertical exaggeration 5x)

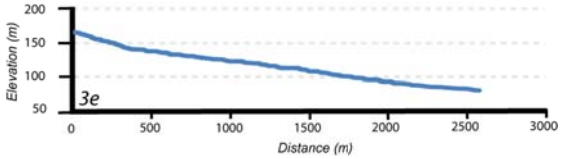

Longitudinal drainage profile for basin 3e (Vertical exaggeration 5x)

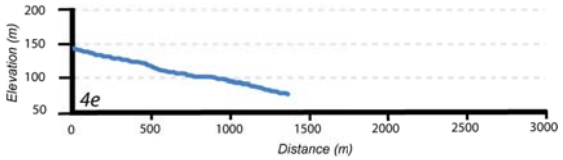

Longitudinal drainage profile for basin 4e (Vertical exaggeration 5x)

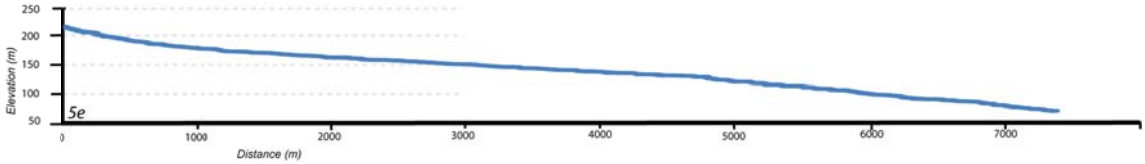

Longitudinal drainage profile for basin 5e (Vertical exaggeration 5x)

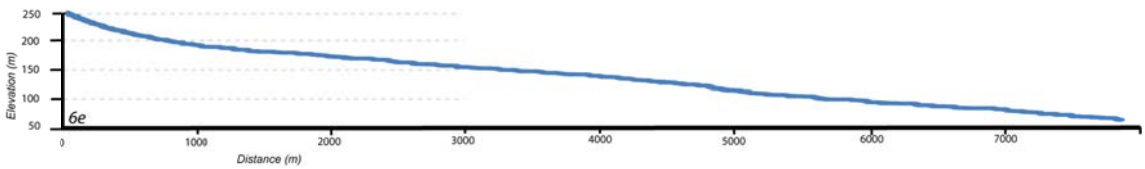

Longitudinal drainage profile for basin 6e (Vertical exaggeration 5x)

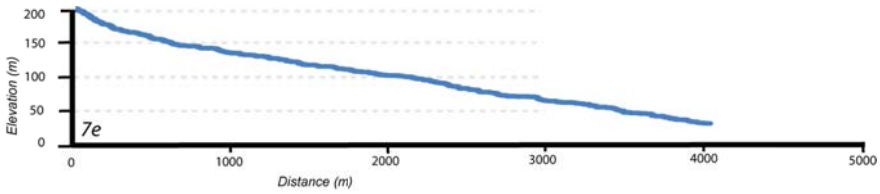

Longitudinal drainage profile for basin 7e (Vertical exaggeration 5x)

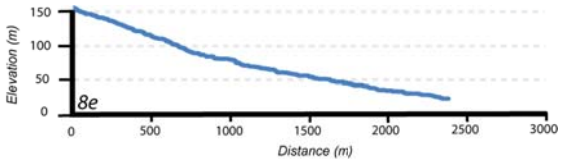

Longitudinal drainage profile for basin 8e (Vertical exaggeration 5x)

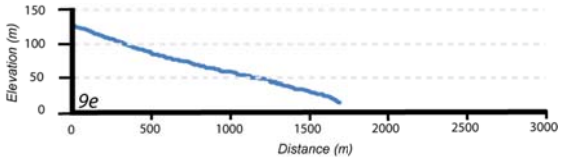

Longitudinal drainage profile for basin 9e (Vertical exaggeration 5x)

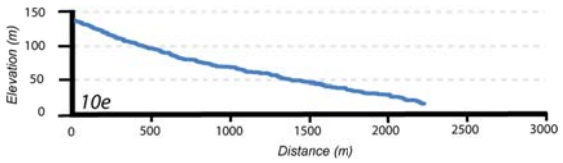

Longitudinal drainage profile for basin 10e (Vertical exaggeration 5x)

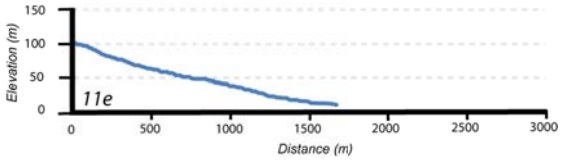

Longitudinal drainage profile for basin 11e (Vertical exaggeration 5x)

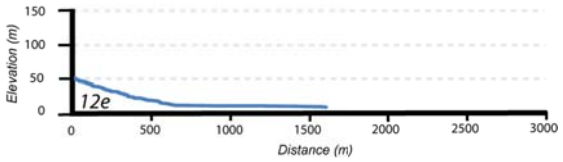

Longitudinal drainage profile for basin 12e (Vertical exaggeration 5x)

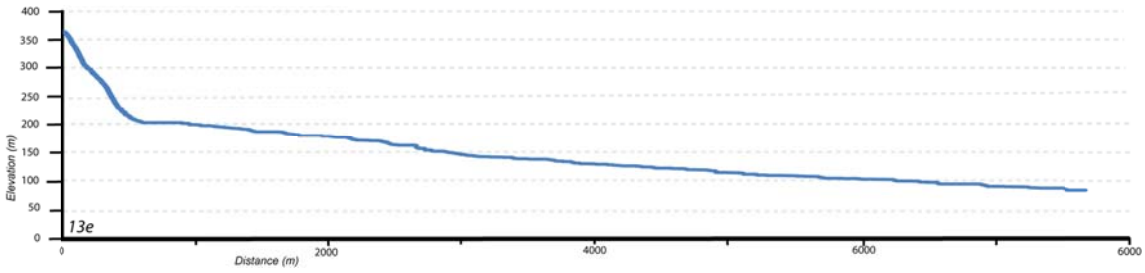

Longitudinal drainage profile for basin 13e (Vertical exaggeration 5x)

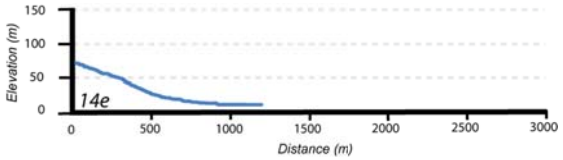

Longitudinal drainage profile for basin 14e (Vertical exaggeration 5x)

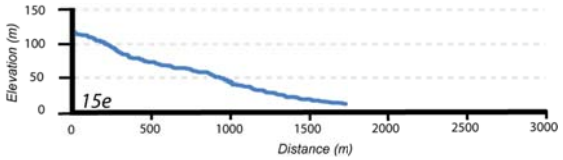

Longitudinal drainage profile for basin 15e (Vertical exaggeration 5x)

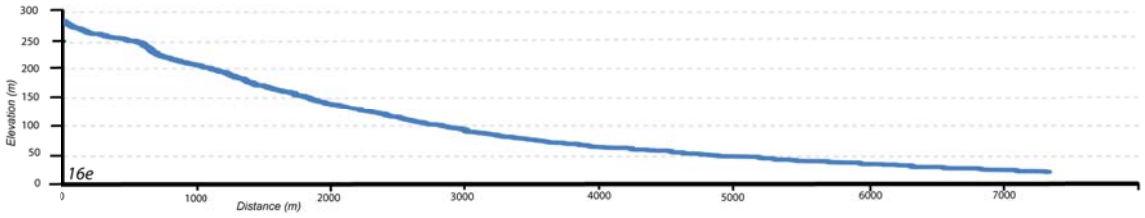

Longitudinal drainage profile for basin 16e (Vertical exaggeration 5x)

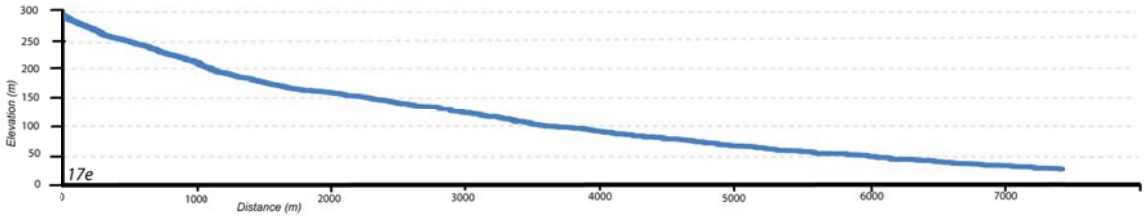

Longitudinal drainage profile for basin 17e (Vertical exaggeration 5x)

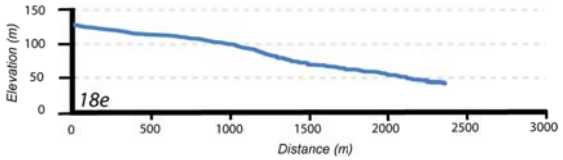

Longitudinal drainage profile for basin 18e (Vertical exaggeration 5x)

Annex IV

Dating Results

Annex IV

Dating Results

OSL – pIRIR dating results

Dating Summary
Site: Portugal
Contact: Pedro Cunha

pIRIR290 results

Risø no.	Your No.	Site	Depth, cm	Age , ka	Dose , Gy	(n)	Dose rate, Gy/ka	w.c. %
10 22 22	SW Castelejo 1	JoÔo Cabral algarve	1300	98 ± 6	155 ± 6	6	1.59 ± 0.07	5
10 22 23	Telheiro 1	JoÔo Cabral algarve	300	> 300	> 1000	3	3.58 ± 0.13	12
10 22 24	A1F-BV	JoÔo Cabral algarve	300	> 300	> 1000	3	3.37 ± 0.12	15

OSL- pIRIR results for the basal aeolianite at Castelejo beach

Dating Summary
Site: Portugal
Contact: Pedro Cunha

pIRIR290 results

Risø no.	Your No.	Site	Depth, cm	Age , ka	Dose , Gy	(n)	Dose rate, Gy/ka	w.c. %
11 22 35	AP-1	Castelejo beach	400	112 ± 7	156 ± 4	18	1.39 ± 0.07	10

OSL – PIRIR results for sample AP1, the beach sand layer at Castelejo beach

Dating Summary
Site: 0
Contact: 0

pIRIR290

Risø no.	Your No.	Site	Depth, cm	Age , ka	Dose , Gy	(n)	Dose rate, Gy/ka	w.c. %
12 22 06	AP2	Castelejo beach	275	110 ± 5	163 ± 3	18	1.48 ± 0.06	10

OSL – PIRIR results for sample AP2, the beach sand layer at Castelejo beach

Cosmogenic Nuclide Dating

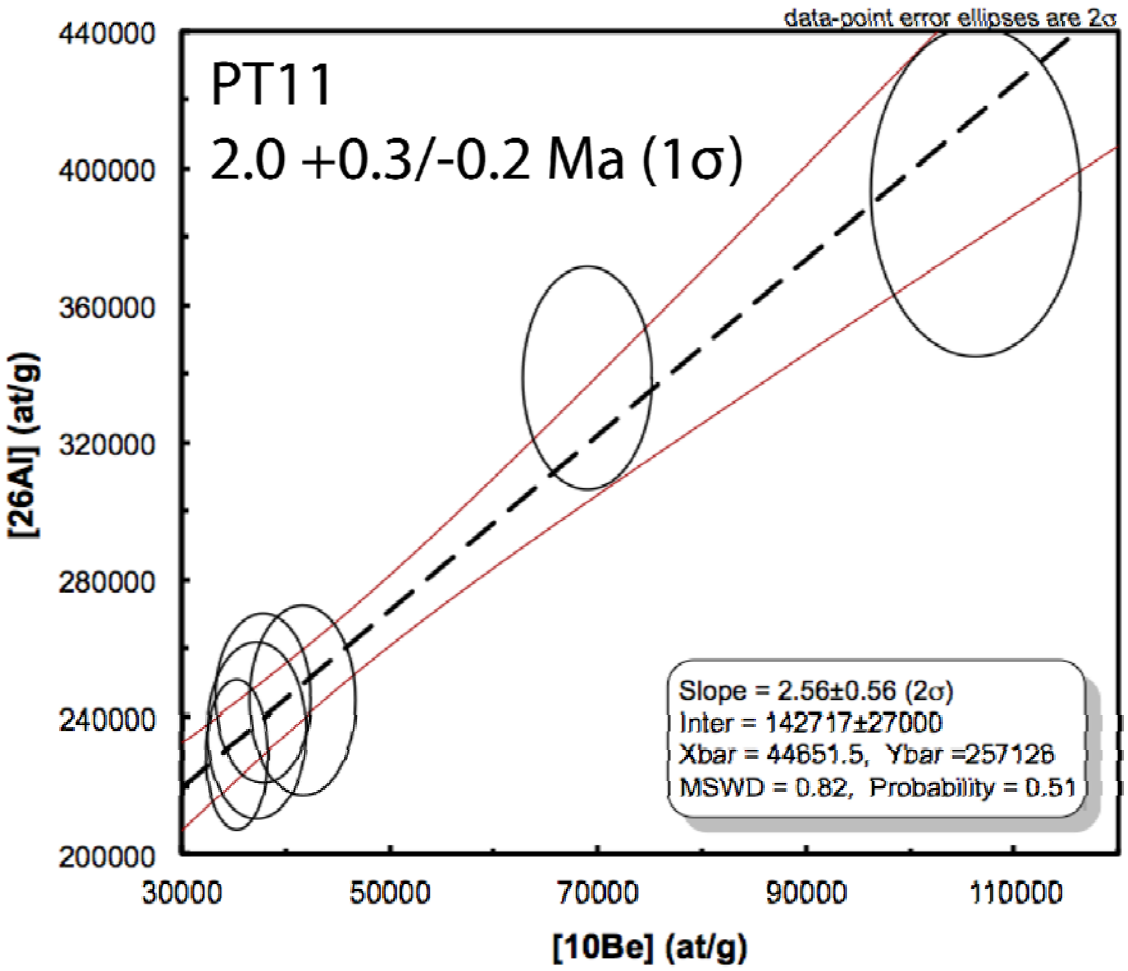

Preliminary results for Telheiro marine terrace